UNIVERSIDAD AUTÓNOMA DE MADRID
FACULTAD DE CIENCIAS
DEPARTAMENTO DE QUÍMICA-FÍSICA

TESIS DOCTORAL INTERNACIONAL

Nuevas Arquitecturas de Polipropileno Isotáctico: Síntesis y Caracterización Molecular, Competencia entre Polimorfos (monoclínico/ ortorrómbico / mesomórfico / trigonal), y Evaluación de Propiedades

Alberto García Peñas

Directores:
Dra. María Luisa Cerrada García
Dr. José Manuel Gómez-Elvira González
Dr. Ernesto Pérez Tabernero
Tutor:
Dra. María del Pilar Herrasti González

INSTITUTO DE CIENCIA Y TECNOLOGÍA DE POLÍMEROS (ICTP-CSIC)
Madrid, 2015

UNIVERSIDAD AUTÓNOMA DE MADRID
FACULTAD DE CIENCIAS
DEPARTAMENTO DE QUÍMICA-FÍSICA

INTERNATIONAL Ph. D. THESIS

New Architectures based on Isotactic Polypropylene: Synthesis and Molecular Characterization, Competition between Polymorphs (monoclinic / orthorhombic / mesomorphic / trigonal), and Properties Evaluation

Alberto García Peñas

Supervisors:
Dr. María Luisa Cerrada García
Dr. José Manuel Gómez-Elvira González
Dr. Ernesto Pérez Tabernero
Supervisor at UAM:
Dr. María del Pilar Herrasti González

INSTITUTO DE CIENCIA Y TECNOLOGÍA DE POLÍMEROS (ICTP-CSIC)
Madrid, 2015

“Con un profundo sentimiento de gratitud culmina una etapa maravillosa de mi vida, en la que he contado siempre con el apoyo incondicional de mi amada familia. Muy especialmente, quiero agradecer la inestimable ayuda de mi madre a la que dedico este trabajo, no sólo a lo largo de este tiempo sino a lo largo de toda mi vida.”

¡Gracias de corazón!

"Exsultabo et laetabor"

Madrid, Septiembre de 2015

En primer lugar, deseo expresar mi agradecimiento al actual Ministerio de Economía y Competitividad por la concesión de la financiación predoctoral FPI con la que he podido llevar a cabo la presente tesis doctoral. Asimismo, al Instituto de Ciencia y Tecnología de Polímeros (ICTP-CSIC) que ha sido mi casa durante este periodo.

Esta memoria ha sido dirigida por la Dra. María Luisa Cerrada García, el Dr. José Manuel Gómez-Elvira González y el Dr. Ernesto Pérez Tabernero a los que agradezco de corazón su implicación constante, su dedicación y la enorme paciencia que han tenido para conmigo durante estos cuatro años.

Todo el trabajo de síntesis hubiera sido muy complicado de realizar sin la ayuda del Dr. Gómez-Elvira. En su calidad de codirector ha supuesto para mí no sólo un apoyo desde el punto de vista científico sino un referente: en él la caridad y el servicio dejan de ser valores para convertirse en una forma de vida.

El Prof. Pérez, con un profundo y extenso conocimiento en polimorfismo, ha sido todo un ejemplo de rigor científico, no sólo por su brillantez indudable, sino por la sencillez y humildad que me ha transmitido siempre y que, sin duda, lo convierten en un ejemplo a seguir.

La Dra. Cerrada es todo un modelo de lo que significa el compromiso, la honradez y la sinceridad, valores que están presentes en su vida, y que siempre me ha demostrado. Su implicación en mi trabajo ha superado cualquier expectativa profesional, y me ha mostrado que además de ser una gran científica es, sobre todo,

una gran persona. Siento profundo respeto, admiración y gratitud hacia ella. Ha sido todo un regalo trabajar con ella estos años. ¡Gracias de corazón Malú!

Así mismo, hago extensivo mi agradecimiento al Dr. Vicente Lorenzo y a la Dra. María Ulagares de la Orden, de la Universidad Politécnica de Madrid y la Universidad Complutense de Madrid, respectivamente. Con ellos he tenido la oportunidad de colaborar y obtener grandes resultados.

Tengo muy presente a todas las personas, sin excepción, del Departamento de Química-Física, a los que agradezco su apoyo, su ayuda y su amistad. También al grupo de Ingeniería Macromolecular, encabezado por la Dra. Fernández, con los que he podido compartir grandes momentos.

Quiero tener un recuerdo muy especial hacia las personas que durante este tiempo he visitado en la Residencia de las Hermanitas de los Pobres, y que he desatendido en esta última etapa de la tesis. Gracias a vosotros especialmente, por demostrarme que todos somos personas.

Igualmente, debo de dar las gracias a todas las personas que forman parte de mi vida, y que me han acompañado especialmente estos años. No puedo dejar de nombrar a mi otra querida familia de la que forman parte Lourdes, Mª Carmen, P. Felipe, Antonio, Simonetta, y especialmente, Luis, que tanto me ha ayudado.

Gracias a todos los que formáis parte de mi vida, en las alegrías y en las dificultades, espero que el amor gobierne definitivamente nuestras vidas. Para todos vosotros mi más sincera gratitud con el corazón abierto. ¡Muchas gracias!

Alberto García Peñas, de Pedrezuela

RESUMEN

Nuevas Arquitecturas de Polipropileno Isotáctico: Síntesis y Caracterización Molecular, Competencia entre Polimorfos (monoclínico/ ortorrómbico / mesomórfico / trigonal), y Evaluación de Propiedades

El polipropileno isotáctico se encuentra presente en una enorme variedad de aplicaciones, que lo sitúan en la segunda posición de los polímeros con mayor demanda mundial, los denominados “commodities”. Las necesidades del mercado, la expansión de su uso así como nuevas políticas, medioambientales entre otras, están detrás de los numerosos esfuerzos que se llevan a cabo a diario para mejorar las arquitecturas existentes y diseñar otras nuevas basadas en ellas, con objeto de optimizar y ampliar su espectro de propiedades.

El presente trabajo de investigación tiene, por tanto, el propósito último de incidir en las posibilidades que ofrecen los copolímeros y terpolímeros de propileno con alfa-olefinas de longitudes intermedias como comonómeros (1-penteno, 1-hexeno y 1-hepteno), motivado por el hallazgo en 2005 de una nueva estructura cristalina (celdilla trigonal) en copolímeros de propileno con 1-penteno y 1-hexeno a elevados contenidos. Para ello, se han sintetizado diferentes familias de copolímeros de propileno-*co*-1-penteno, propileno-*co*-1-hexeno y propileno-*co*-1-hepteno en intervalos amplios de composición de los comonómeros, así como terpolímeros de propileno-*co*-1-penteno-*co*-1-hexeno y propileno-*co*-1-penteno-*co*-1-hepteno, en los que, además, se varió el ratio entre comonómeros a una composición global dada. Se han preparado también los homopolímeros correspondientes, es decir, el polipropileno isotáctico, el poli(1-penteno), el poli(1-hexeno) y el poli(1-hepteno).

Los numerosos materiales obtenidos presentan pesos moleculares suficientemente elevados así como una alta isotacticidad, características que garantizan unas buenas prestaciones mecánicas, como se ha comprobado. Un entendimiento adecuado de las estructuras cristalinas que pueden generarse y, consecuentemente, de las propiedades finales que pueden manifestar estos materiales, ha requerido una minuciosa evaluación de su microestructura. De ella se ha deducido que la inserción de los monómeros durante la polimerización se produce al azar.

A continuación, se ha realizado un estudio pormenorizado sobre las diferentes estructuras cristalinas existentes, la competencia entre los diversos polimorfos y sus

transiciones de fase, para cada una de las familias sintetizadas, en función de la composición, la velocidad de cristalización y el ratio entre comonómeros. Se ha prestado especial atención a las condiciones para obtener la mesofase y la nueva modificación trigonal.

Finalmente, se ha procedido al estudio de algunas propiedades que se han considerado de interés para futuras posibles aplicaciones, haciendo incidencia en su comportamiento mecánico, su caracterización óptica y sus propiedades de transporte. Además, se ha realizado un estudio pionero sobre la estabilidad térmica de los copolímeros de propileno con 1-penteno y 1-hexeno.

En general, las propiedades han resultado ser muy sensibles tanto a la cristalinidad total como a la naturaleza de las diversas fases presentes, lo que ha permitido obtener materiales polímeros en un extenso espectro de propiedades, que se pueden modular a voluntad en un amplio intervalo.

SUMMARY

New Architectures based on Isotactic Polypropylene: Synthesis and Molecular Characterization, Competition between Polymorphs (monoclinic / orthorhombic / mesomorphic / trigonal), and Properties Evaluation

Isotactic polypropylene can be found in an enormous variety of applications, and, consequently, its demand is extraordinary high between those polymers denominated as “commodities”. Requirements of markets joined to expansion of its uses and new environmental policies, among others factors, are underneath the numerous efforts that are being carried out in order to enhance the existing architectures and to design new ones, aiming optimization and expansion of its properties range.

The present research work has the final purpose of exploring the possibilities offered by copolymers and terpolymers based on propylene and alpha-olefins of different lengths as comonomers (1-pentene, 1-hexene, and 1-heptene), primarily motivated by the discovery in 2005 of a new crystalline structure (trigonal lattice) in propylene copolymers at high contents of 1-pentene or 1-hexene. For that, different families of propylene-*co*-1-pentene, propylene-*co*-1-hexene and propylene-*co*-1-heptene copolymers have been synthesized in a wide range of comonomer compositions, as well as propylene-*co*-1-pentene-*co*-1-hexene and propylene-*co*-1-pentene-*co*-1-heptene terpolymers, where the ratio between comonomers has been additionally varied at a given global composition. Moreover, the corresponding homopolymers have been also prepared, namely isotactic polypropylene, poly(1-pentene), poly(1-hexene) and poly(1-heptene).

All these numerous materials prepared present sufficiently high molecular weights and high isotacticity, both features ensuring good mechanical performance, as observed. The adequate understanding of the different crystalline structures that can be developed and, consequently, of the final properties exhibited by these materials, required a detailed and thorough evaluation of the microstructure. From that, a random inclusion of the monomers during polymerization has been deduced.

In addition, the different existing crystalline lattices, the competence between the various polymorphs and their phase transitions have been studied in detail for the different materials synthesized, as function of composition, crystallization rate and

comonomers ratio. Special attention has been paid to the conditions for obtaining the mesophase and the new trigonal modification.

Finally, some properties of interest for possible future applications have been studied, especially the mechanical behavior, optical response, and transport properties. In addition, a pioneer study on the thermal stability of propylene copolymers with 1-pentene and 1-hexene has been performed.

In general, properties have turned out very sensitive both to the global crystallinity and to the nature of the phases involved, so that polymer materials covering a broad spectra of properties have been obtained and their ultimate performance can be widely tailored.

ÍNDICE

Capítulo 1. Introducción

Terpolímeros de propileno-co-1-penteno-co-1-hexeno

Capítulo 2. Isotactic Poly(propylene-*co*-1-pentene-*co*-1-hexene) Terpolymers: Synthesis, Molecular Characterization and Evidence of the Trigonal Polymorph

Capítulo 4. Synthesis, Molecular Characterization, Evaluation of Polymorphic Behavior and Indentation Response in isotactic Poly(propylene-*co*-1-heptene) Copolymers

Capítulo 5. Mesophase features in isotactic poly(propylene-*co*-1-heptene) copolymers

Capítulo 6. Mechanical and transport properties of poly(propylene-*co*-1-heptene) copolymers and their dependence on monoclinic and/or mesomorphic polymorphs

Terpolímeros de propileno-co-1-penteno-co-1-hepteno

Capítulo 7. Trigonal δ form as a tool for tuning mechanical behavior in poly(propylene-*co*-1-pentene-*co*-1-heptene) terpolymers

Capítulo 8. Microstructure and thermal stability in metallocene iPP-materials: 1-pentene and 1-hexene copolymers

Capítulo 9. Conclusiones

Anexos

CAPÍTULO 1

Introducción

1.1. Antecedentes

Los materiales polímeros forman parte de nuestra vida cotidiana encontrándose, por tanto, presentes en gran parte de nuestro entorno y en la mayoría de objetos y/o productos comerciales e industriales. De todos los polímeros de gran consumo (denominados en medios especializados como "commodities"), el polipropileno isotáctico, iPP, es el segundo en consumo y demanda mundial ya que exhibe múltiples ventajas, entre las que destacan su baja densidad respecto a la exhibida por otros polímeros así como un excelente balance de propiedades. A estas características se le suman, entre otras, su relativo bajo coste y su buena procesabilidad, resistencia química, dureza y rigidez [1].

La autoría de los investigadores que realizaron la síntesis inicial del iPP fue controvertida debido al hecho que en la época había muchos grupos de investigación trabajando en su obtención de forma casi simultánea [1,2]. En 1950, el profesor Evering de Standard Oil, preparó una mezcla de polipropileno y etileno cuyas características no resultaron satisfactorias. Un año más tarde, Hogan y Banks de Phillips Petroleum obtuvieron un polipropileno cuyas propiedades no sobresalían respecto a las exhibidas por otros materiales poliméricos [3]. En 1954, el doctor Baxter produjo una pequeña cantidad de polipropileno al que la compañía DuPont no encontró utilidad específica [4]. Sin embargo, ese mismo año el científico Guilio Natta, con el patrocinio de la compañía italiana Montecatini, sintetizó y describió la estructura del polipropileno isotáctico [2,5]. Dicha empresa, Montecatini, comenzó a producirlo a escala industrial en 1957, aunque con algunas dificultades, entre las que se encontraba la denuncia de Ziegler a Natta por el empleo de sus catalizadores para la síntesis del mencionado polipropileno isotáctico sin su consentimiento. Esta complicación, unida a diversos contenciosos relativos a los derechos de la propiedad intelectual entre Montecatini y las multinacionales Phillips, DuPont y Standard Oil, paralizaron inicialmente la expansión de la industria del polipropileno isotáctico [4]. En

cualquier caso, algunas de sus primeras aplicaciones comprendían la preparación de fibras, filmes y objetos moldeados por inyección, y su implementación en el mercado fue muy rápida dada la gran aceptación por parte de los consumidores [1,5]. Años después, en 1963, a los investigadores Ziegler y Natta se les concedió conjuntamente el Premio Nóbel de Química.

A pesar de las múltiples ventajas que se admitían para el polipropileno en comparación con otros polímeros conocidos en la época [3], también presentaba algunos inconvenientes en su producción y comercialización a gran escala. Sus deficientes características reológicas, su baja resistencia a la oxidación por efecto de la temperatura y de la luz, así como su extremada fragilidad a baja temperatura supusieron sus mayores impedimentos [5]. Sin embargo, su notable potencial se convirtió en su mejor aliado y la industria rápidamente encontró soluciones factibles para subsanar dichas deficiencias, promoviendo el desarrollo de nuevos antioxidantes, nuevos sistemas catalíticos y nuevas formulaciones, siendo, por tanto, solventadas dichas deficiencias en gran medida.

En los años sesenta, la fabricación de copolímeros constituyó la apuesta para resolver algunas de las limitaciones comentadas que presentaba el homopolímero. En esa década, el polipropileno isotáctico se encontraba aún en desarrollo y su comercialización estaba todavía bastante limitada [5].

A partir de los setenta, la industria del polipropileno inicia una rápida expansión como consecuencia de la caducidad de algunas de sus patentes. El crecimiento de su mercado abarató sensiblemente los costes de producción y su demanda comercial se incrementó exponencialmente. En esa década comenzaron a estudiarse mezclas de diferentes polipropilenos que mejoraban significativamente sus propiedades de impacto y, por tanto, el número de sus aplicaciones se amplió notablemente [5].

La industria del polipropileno registró su primer máximo en 1983, convirtiéndose en el tercer polímero más demandado, sólo superado en la época por el polietileno, PE, y el poli(cloruro de vinilo), PVC [5]. Su industria continuó creciendo a un ritmo extremadamente rápido [1] fomentado, entre otros aspectos, por la resolución final en 1989 de todos los problemas de propiedad intelectual entre Montecatini y las compañías Phillips, DuPont y Standard Oil [3]. Además, en ese mismo período se comenzó a trabajar en la fabricación de materiales compuestos mediante la incorporación de diferentes cargas y en el desarrollo de grados de reología controlada [5].

Los años noventa fueron también especialmente dinámicos en el área del polipropileno isotáctico. Su campo de aplicaciones se desarrolló considerablemente como consecuencia de la implementación de nuevas tecnologías, la obtención de materiales mejorados y de novedosas arquitecturas de base propilénica. La posibilidad de sintetizar poliolefinas, en general, y, consecuentemente, polipropileno en particular mediante catalizadores metalocénicos despertó un gran interés en la industria del sector [5]. El potencial de estos sistemas catalíticos era incluso superior en el caso del polipropileno dado que permitían, dependiendo de la geometría y las propiedades electrónicas del catalizador, el diseño “a medida” de la microestructura resultante, incluyendo su tacticidad, la modulación de su peso molecular y la incorporación uniforme de counidades alifáticas y aromáticas. Este descubrimiento supuso un enorme abanico de nuevas posibilidades para el polipropileno ya que las propiedades que manifiesta están íntimamente relacionadas con la microestructura molecular de sus macrocadenas. En efecto, tanto la composición como la tacticidad condicionan la conformación de las cadenas y, consecuentemente, las interacciones que establecen entre ellas para configurar un ordenamiento cristalino característico [6]. La disposición ordenada de las cadenas del polipropileno resulta relativamente sencilla, permitiendo la generación de numerosas y distintas formas cristalinas según sea su configuración isotáctica o sindiotáctica [6]. En concreto para el polipropileno isotáctico, las variables fundamentales que condicionan las estructuras cristalinas y su grado de cristalinidad

comprenden el peso molecular, los errores de las macrocadenas (estereo y regioerrores), las condiciones de cristalización y la presencia o ausencia de agentes nucleantes [7]. La formación de una u otra celdilla cristalina así como la coexistencia de varios polimorfos en un objeto final dado que condicionará en gran medida todo su espectro de propiedades y, por tanto, su aplicación última.

A pesar de las atractivas características encontradas en los polipropilenos sintetizados con catalizadores tipo metaloceno, es necesario mencionar que, incluso en la actualidad, la mayor parte del polipropileno producido a escala industrial se obtiene con catalizadores Ziegler-Natta [3]. Éstos, por supuesto, no son exactamente idénticos a los iniciales de mediados del siglo XX sino que han ido evolucionando a lo largo de las décadas con la finalidad de optimizar los procesos productivos, habiéndose dedicado grandes esfuerzos a la eliminación de las etapas de separación de restos catalíticos y de la fracción de polipropileno atáctico. Estos hitos implicaron la aparición de nuevas familias de catalizadores, clasificadas en las llamadas generaciones de catalizadores Ziegler-Natta según su impacto en los procesos. Uno de los motivos principales para que la producción industrial continúe utilizando estos catalizadores en vez de los metalocénicos, radica en que el proceso de polimerización con los sistemas catalíticos basados en estos últimos se lleva a cabo en condiciones homogéneas, mientras que los catalizadores Ziegler-Natta se inmovilizan (o heterogeinizan) sobre un soporte. Esta inmovilización tiene implicaciones prácticas importantes y, por tanto, resulta altamente interesante desde un punto de vista industrial ya que requiere cantidades de disolvente sensiblemente inferiores, reduce significativamente la cantidad de polímero adherido a las paredes del reactor y, por tanto, su ensuciamiento, y conduce a una mejora substancial de la morfología y tamaño de las partículas del polímero obtenido, favoreciendo además la procesabilidad del material resultante y, por consiguiente, sus propiedades últimas [6].

Estas ventajas son las responsables del interés que ha surgido en los últimos años en la inmovilización de los sistemas catalíticos metalocenos sobre diversos tipos

de soportes. Por ello, se ha comenzado a trabajar intensamente para intentar minimizar las deficiencias que supone la polimerización en medio homogéneo en el proceso productivo a gran escala.

La preparación de copolímeros de propileno ha supuesto desde los años sesenta, como ya se ha indicado, una metodología para solventar la insuficiente resistencia al impacto que exhibe el polipropileno isotáctico a temperaturas relativamente bajas. Su propósito último ha consistido básicamente en encontrar el balance óptimo entre el mantenimiento de las excelentes características del polipropileno isotáctico homopolímero y el aumento del contenido de cadenas macromoleculares en estado amorfo, siendo éstas capaces de absorber y disipar la energía de un impacto sin provocar la ruptura del material, debido a sus conformaciones desordenadas. En las últimas dos décadas, su producción ha cobrado un gran interés comercial y se ha llevado a cabo, principalmente, a través de dos vías sintéticas diferentes, que han conducido a la obtención de copolímeros al azar [8-10] y de copolímeros heterofásicos [11]. Éstos últimos presentaban, inicialmente, problemas de homogeneidad debido a la formación de fases e interfases. Sin embargo, la evolución de los métodos sintéticos ha contribuido a la mejora de sus propiedades [12,13] y, con ello, de sus perspectivas de futuro. El impulso de los reactores de tecnología de granulado [14] ha posibilitado, además, la generación de polímeros heterofásicos con un buen balance entre la rigidez y el impacto [15].

En relación con los copolímeros al azar, los más estudiados han sido, principalmente, los de etileno insertado de forma aleatoria en las cadenas poliméricas. En ellos se observa una disminución de la cristalinidad con el contenido en etileno y, por consiguiente, una modificación de sus propiedades físicas [16,17]. Estos materiales se utilizan en multitud de aplicaciones industriales, como productos de inyección, tuberías, fibras y filmes. Además del etileno, el 1-buteno ha sido otro comonómero muy utilizado, ya que ambas unidades presentan, entre otras ventajas, su bajo coste. La utilización industrial de counidades α-olefínicas de mayor longitud, como el 1-

penteno, 1-hexeno, 1-octeno, etcétera, no se ha explorado intensivamente, salvo en copolímeros con pequeños contenidos de 1-hexeno, debido principalmente a motivos económicos. Sin embargo, sí han demostrado tener interés desde un punto de vista académico (sobre todo desde el advenimiento de los sistemas metalocénicos) y numerosos grupos de investigación han dedicado esfuerzos considerables a su síntesis y caracterización exhaustiva [8,10,15,18-31], evaluándose amplios intervalos de composiciones, competencias entre distintas estructuras cristalinas y balance de sus propiedades. Esta insistencia científico-académica condujo al descubrimiento en 2005 de una nueva forma cristalina en copolímeros de propileno con altos contenidos en 1-hexeno [10,27,28], descrita también poco tiempo después en los análogos de 1-penteno [25].

La ingeniería ha mostrado un gran interés en los últimos años por el empleo de distintas arquitecturas de polipropileno para muchas de sus aplicaciones específicas, reconociendo su potencial, su excelente balance de propiedades, su gran versatilidad y los precios moderados que los nuevos desarrollos basados en polipropileno suponen respecto a los relativos a otros polímeros [5]. Dichas aplicaciones específicas comprenden, entre otros, el sector de automoción y aeroespacial [32]; el área del envasado y embalaje donde la mejora de la transparencia [33,34] y la obtención de polipropilenos con actividad biocida [35-37] pueden seguir contribuyendo a su expansión; el sector textil con un amplia variedad de tipos de tejidos y fibras; y el área de salud en forma de dispositivos desechables [38].

La Figura 1 representa una comparación de datos correspondientes al año 2013 entre diferentes materiales polímeros dependiendo del sector de su aplicación industrial. En ella se evidencia cuantitativamente la gran relevancia de los materiales basados en polipropileno.

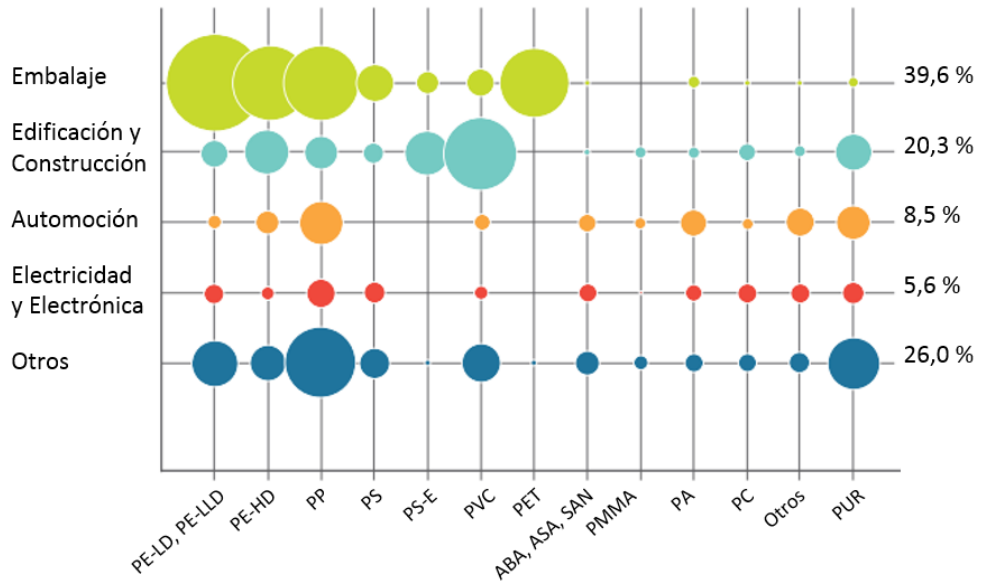

Figura 1. Demanda europea de los diferentes materiales poliméricos en función al sector de aplicación industrial. (*European plastics demand* by segment polymer 2013, PlasticEurope (PEMRG) / Consultic /ECEBD *EU-27+NO/CH*)

Las características y propiedades intrínsecas de los materiales plásticos existentes proporcionan, consecuentemente, respuestas a las diferentes necesidades del mercado en múltiples aplicaciones como se observa en la Figura 2, cuyo crecimiento ha desplazado a materiales clásicos en muchos sectores. Las poliolefinas (polietileno de alta densidad, PE-HD; polietileno de baja densidad, PE-LD; polietileno lineal de baja densidad, PE-LLD; y polipropileno, PP) representan casi el 50 % de la demanda, de ahí el interés tecnológico-científico por parte de las empresas y del mundo académico en una búsqueda continuada, eficiente y medioambientalmente viable de nuevos catalizadores para su producción a partir de procesos menos contaminantes; de su posterior aprovechamiento mediante el reciclado u otros métodos de recuperación después de su ciclo de vida útil; o del desarrollo de aditivos que posibiliten su descomposición en tiempos más cortos y en fracciones de menor tamaño.

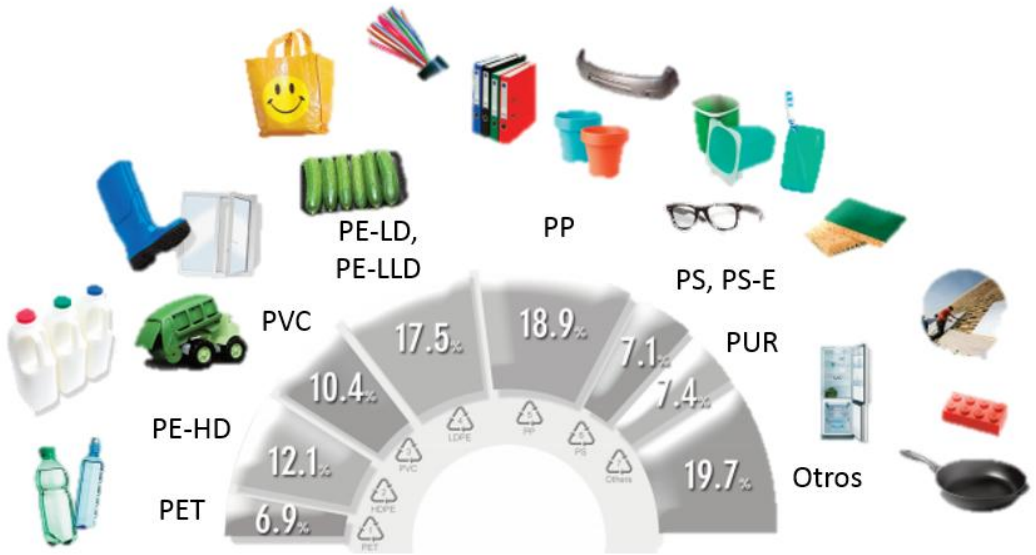

Figura 2. Demanda comercial de polímeros en la industria y algunas de sus aplicaciones. (*European plastics demand* by polymer 2013, PlasticEurope (PEMRG) / Consultic /ECEBD *EU-27+NO/CH*)

A pesar del continuado crecimiento del consumo de los materiales poliméricos, en general, y, específicamente, de los basados en polipropileno en la segunda mitad del siglo XX, la crisis mundial iniciada en el segundo lustro del siglo XXI ha afectado considerablemente al mercado de los plásticos, sobre todo en sectores como la construcción y la automoción, observándose una caída significativa de la producción mundial, como se representa en la Figura 3. Transcurrida casi una década desde el comienzo de la crisis, se vislumbra actualmente una reactivación del mercado y el pronóstico para los años futuros es prometedor y se predice un aumento de la demanda. La previsión de expansión en los próximos 10 años para el polipropileno, en particular, recogida en la Figura 4, augura un incremento del 8 % en la India, y un 6 % en Asia y China. Sin embargo, en Europa, Norteamérica y Japón el supuesto crecimiento es menor, ya que el uso del polipropileno se encuentra ya implementado en los diversos sectores comerciales. Además, han de tenerse en consideración las

políticas de reciclaje puestas en marcha en Europa, Norteamérica y Japón desde hace años.

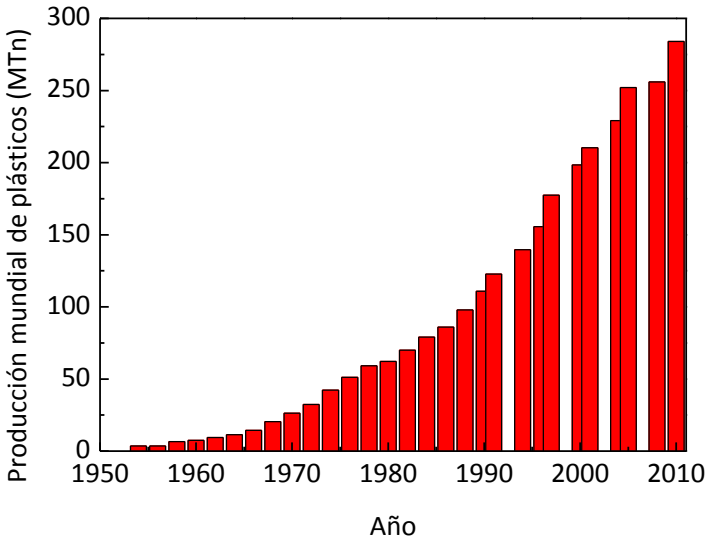

Figura 3. Evolución de la producción mundial de materiales plásticos (Mt/año). (*Datos extraídos de ""World plastic production" by Quartz"*)

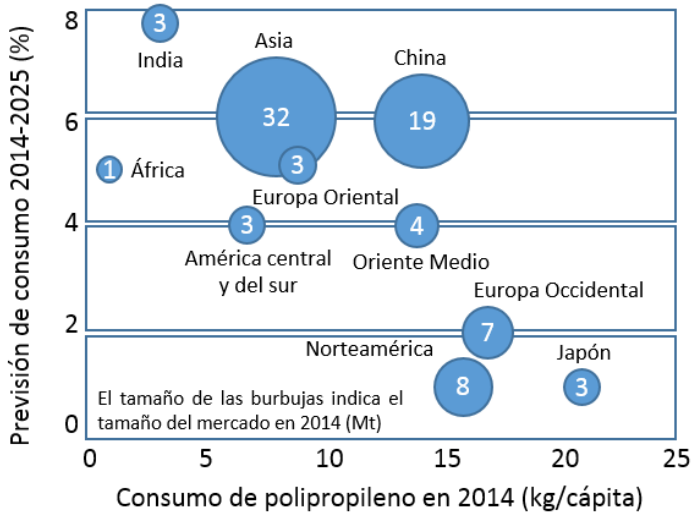

Figura 4. Mercado del polipropileno en el año 2014 y previsiones de demanda para la próxima década (2014-2025). (*Fuente: "Platts"*)

1.2. Síntesis y microestructura de arquitecturas de polipropileno

1.2.1. Tipos de síntesis y catalizadores

Los procesos sintéticos para la obtención de polímeros pueden clasificarse en función a su mecanismo de reacción, tal y como describió Flory en 1953. Se dividen, principalmente, en dos tipos de reacciones: en cadena y en etapas. Sus principales características se recogen en la Tabla 1.

Tabla 1. Características de la polimerización en cadena y en etapas.

	Polimerización en cadena	**Polimerización en etapas**
Reacción	Sólo entre los monómeros y las especies propagantes.	Todas las especies presentes pueden reaccionan entre si.
Cinética	Varios procesos.	Un proceso.
Consumo de monómeros	Paulatino durante el avance de la reacción.	Instantáneo al inicio de la reacción.
Velocidad	Aumenta hasta un valor máximo que mantiene hasta el final.	Máxima al inicio de la reacción y disminuye con el tiempo.
Peso Molecular	Altos pesos desde el inicio de la reacción.	Requiere largo tiempo para obtener elevados pesos moleculares.
Composición química de productos	Similar a la de partida.	Diferente a la de partida.

La polimerización de α-olefinas transcurre mediante un proceso en cadena en el que el iniciador es un catalizador de tipo organometálico. Sin embargo, este proceso tiene ciertas peculiaridades, como son que los monómeros son apolares y se coordinan al centro activo, previamente a su inserción en la cadena y que los polímeros así obtenidos son, en algunas ocasiones, altamente estereorregulares. Este proceso se conoce específicamente como polimerización por coordinación [39].

Existe una amplia gama de catalizadores para llevar a cabo las reacciones de polimerización de olefinas, como muestra la Tabla 2, pudiéndose éstos clasificar en función de los centros activos, su naturaleza o el estado físico, entre otras cualidades.

Tabla 2. Catalizadores para la síntesis de poliolefinas.

Centro activo	Estado físico	Catalizador	Ejemplos
Múltiples	Homogéneo	Ziegler-Natta	VCl_4
	Heterogéneo	Ziegler-Natta	$TiCl_3$
		Philips	CrO_3/SiO_2
		Ziegler-Natta (1ª Generación)	$TiCl_4/AlEt_3$
		Ziegler-Natta (2ª Generación)	$TiCl_4/AlRCl_2$
		Ziegler-Natta (3ª Generación)	$TiCl_4$/Éster/$MgCl_2$ + TEAl/Éster
		Ziegler-Natta (4ª Generación)*	$TiCl_4$/Diéster/$MgCl_2$ + TEAl/Silano
		Ziegler-Natta (5ª Generación)*	$TiCl_4$/Diéter/$MgCl_2$ + TEAl
Único	Homogéneo	Metalocenos	Cp_2ZrCl_2
		No metalocenos	Eisen
			Brookhart
			Gibson-Brookhart
	Heterogéneo	Metalocenos soportados	Cp_2ZrCl_2/SiO_2

*Algunos científicos sostienen que no existe cuarta y quinta generación de estos catalizadores, sino que son una mejora de los anteriores.

Los catalizadores de **centros activos múltiples** pueden clasificarse en homogéneos y heterogéneos. Los catalizadores Ziegler-Natta homogéneos presentan una baja actividad y estabilidad en la polimerización, lo que ha limitado su utilización en la industria. Sin embargo, los catalizadores Ziegler-Natta heterogéneos se emplean generalmente en los procesos industriales de producción de poliolefinas [40,41], como se ha comentado en el anterior apartado. Este tipo de sistemas presentan distintos tipos de centros activos y diferencias de tipo estérico o electrónico que dificultan el estudio de su mecanismo cinético e influyen directamente sobre las características de

las macrocadenas, produciendo poliolefinas con distribuciones anchas de pesos moleculares. Existen cinco generaciones de catalizadores Ziegler-Natta heterogéneos, diferenciados sensiblemente por la actividad de los mismos y su complejidad química. No obstante, la cuarta y quinta generación de catalizadores han generado un debate científico sobre si realmente suponen una novedad o si son, exclusivamente, una mejora de los anteriores.

Los catalizadores Phillips han estado generalmente destinados a la síntesis de polietileno de alta densidad, y cuando se emplean en las reacciones de polimerización el control del peso molecular de las cadenas poliméricas se realiza mediante la incorporación de hidrógeno.

Los catalizadores de **centro activo único** más conocidos son los complejos organometálicos. Su origen en 1952 está asociado a la descripción de la estructura de ferroceno [42,43], que despertó un gran interés científico. Natta y Breslow descubrieron posteriormente la posibilidad de polimerizar α-olefinas empleando metalocenos de metales de transición con alquilos de aluminio [44-45]. Inicialmente, estos sistemas presentaban una actividad muy baja, que se mejoró increíblemente en sistemas titanoceno con $AlEt_2Cl$ añadiendo pequeñas cantidades de agua [46,47].

Décadas más tarde, el profesor Kaminsky y sus colaboradores [48,49] observaron que el sistema $Cp_2TiMe_2/AlMe_3$ inactivo en polimerización se tornaba altamente activo al introducir pequeñas trazas de agua. Las siguientes investigaciones concluyeron que el cocatalizador responsable de la activación era el metilaluminoxano (MAO) [50]. A partir de estos descubrimientos, los sistemas catalíticos metalocenos de centro activo único revolucionaron el mundo de la catálisis de poliolefinas desde un punto de vista académico e industrial, aunque el interés a gran escala ha decaído con el transcurso del tiempo. Los polímeros obtenidos presentan diferencias muy significativas en relación con los sintetizados mediante catalizadores heterogéneos Ziegler-Natta, como se resume en la Tabla 3.

Tabla 3. Diferencias entre los catalizadores Ziegler-Natta heterogéneos y los metalocénicos homogéneos.

	Catalizador	
Propiedad	**Ziegler-Natta**	**Metalocénico**
Estado físico	Heterogéneo	Homogéneo
Centro activo	Múltiple	Único
Actividad	Alta	Muy alta (hasta 100 veces superior)
Distribución de pesos moleculares	Ancha	Estrecha
Estereoselectividad resultante	No uniforme	Uniforme
Distribución resultante de comonómeros en copolímeros	No uniforme	Uniforme

Actualmente, se está trabajando en la búsqueda de nuevos catalizadores para la síntesis de poliolefinas que se encuentran aún en fase experimental. Como ejemplo mencionar los catalizadores de Eisen que presentan una preparación muy sencilla en comparación con los metalocénicos, además de exhibir actividades muy elevadas. Otros catalizadores prometedores fueron los de Brookhart [51-53] y Gibson-Brookhart [54-57]; éstos últimos son altamente activos y permiten obtener polietilenos altamente lineales.

Resulta indicado comentar en este punto que la temática de la presente investigación se centra en nuevas arquitecturas basadas en propileno, y por ello a partir de ahora las características sintéticas se particularizarán para polipropilenos y se obviarán los detalles relativos a otro tipo de poliolefinas. Además, el catalizador utilizado para su preparación es de origen metaloceno, de ahí que se insista mayoritariamente en sus particularidades específicas y no las exhibidas por otros tipos de sistemas catalíticos.

Los procesos de producción industrial de polipropileno emplean principalmente catalizadores de tipo Ziegler-Natta [3], aunque existe un pequeño sector específico que utiliza los catalizadores metalocénicos. Los catalizadores metalocénicos no han tenido definitivamente el impacto previsto a principio de la década de los 90 en la industria por los problemas de adhesión de polímeros a las paredes del reactor, de su peor procesabilidad y de las deficiencias en la morfología y tamaño de las partículas del polímero obtenido, comentados en el apartado anterior.

Los catalizadores metalocénicos permiten controlar la orientación del metilo del propileno que se coordina al centro activo [49,50,58-62], ya que el propileno es un monómero pro-quiral con dos enantiocaras (R y S), [63,64] (Figura 5). Esta estereoespecificidad es la que determina la estereorregularidad de la cadena que se forma.

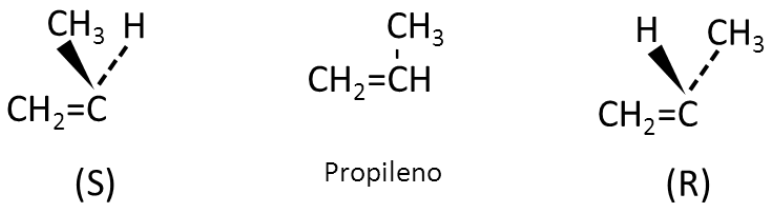

Figura 5. Enantiocaras del propileno R y S.

La tacticidad, o estereorregularidad del PP se define como el ordenamiento espacial relativo de los grupos metilo, según éstos se dispongan respecto del plano definido por la cadena principal, dispuesta en una conformación exclusivamente *trans*. Dicha disposición puede ser hacia un mismo lado del plano (isotáctica), alternante (sindiotáctica) o aleatoria (atáctica), como se representa en la Figura 6.

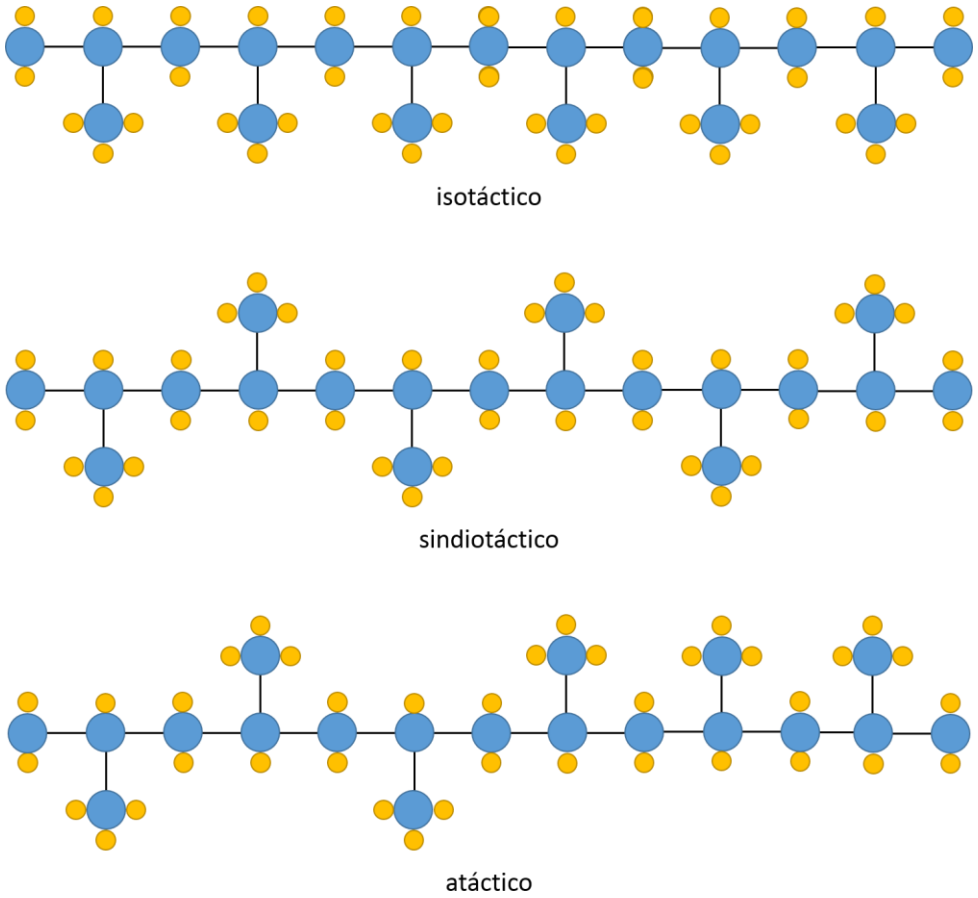

Figura 6. Diferentes tacticidades que pueden generarse en el polipropileno, PP.

El polipropileno isotáctico ha sido el estereoisómero más explotado comercialmente en el polipropileno, presenta elevadas cristalinidades y excelentes prestaciones mecánicas. El polipropileno sindiotáctico es más flexible y tenaz que su análogo isotáctico y, por ello, su resistencia a la tracción es menor. Su mayor inconveniente radica en que presenta una cristalización mucho más lenta pudiendo ésta prolongarse durante la vida útil de los objetos con él producidos y afectar a su estabilidad dimensional. La configuración atáctica dispone los grupos metilo al azar, dando lugar a un material totalmente amorfo.

La geometría y la composición química del precursor metalocénico influyen directamente en la tacticidad y el peso molecular de las cadenas poliméricas resultantes, así como sobre la actividad del mismo. Estos complejos presentan un metal de transición en el centro de su estructura, perteneciendo éste generalmente al grupo IVB de la tabla periódica, es decir, titanio, zirconio y hafnio (Ti, Zr y Hf). El átomo metálico lleva unido dos ligandos de tipo ciclopentadienilo (Cp) y otros dos grupos, normalmente cloruros o alquilos. La presencia de grupos voluminosos en el catalizador dificulta la coordinación del centro activo y, por tanto, disminuye la velocidad de propagación de la reacción de polimerización. Este hecho afecta, además, a la orientación del monómero en la cadena, favoreciendo su inserción donde la repulsión entre los sustituyentes y el mismo es mínima [65-67].

Existe una gama de catalizadores selectivos de tipo metalocénico que permiten controlar la estereoquímica de las cadenas (ver Tabla 4), de acuerdo a las conocidas como “reglas de Ewen”, que establecen la relación de cada una de las configuraciones de los catalizadores sobre la estereorregularidad del polímero resultante. Estos catalizadores poseen un centro activo con dos posiciones de coordinación, que pueden discriminar entre las enantiocaras del monómero proquiral (R y S, Figura 5) [68].La orientación del grupo metilo del propileno que se inserta depende entonces del entorno que establece la configuración estérica del centro activo, es decir de la simetría y del tipo de ligando.

Uno de los aspectos más relevantes del empleo de catalizadores metalocénicos en la síntesis de arquitecturas de polipropileno es la estrecha distribución de pesos moleculares que se obtiene, siendo la polidispersidad, M_w/M_n, en torno a 2, [69]. Esta característica se relaciona con la presencia de centros catalíticos muy similares, con cinéticas de polimerización y reacciones de terminación análogas.

La catálisis metalocénica permite también obtener una elevada homogeneidad en la distribución de las unidades comonoméricas al azar [70,71] en los

copolímeros o terpolímeros de base propilénica, incluso para altas composiciones en comonómeros [72].

Tabla 4. Catalizadores selectivos de tipo metalocénico que permiten controlar la estereoquímica.

Estereorregularidad	Simetría del catalizador	Posiciones de coordinación	Ejemplo
Isotáctico	C_2	 Idénticas	
Sindiotáctico	C_S Pro-quiral	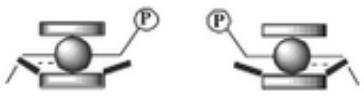 Imágenes especulares	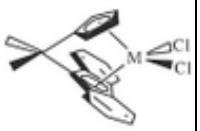
Atáctico	C_1 Aquiral	 Una isoespecífica, otra no selectiva	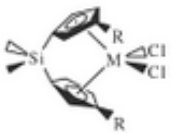

Los copolímeros al azar, presentan una distribución estadística de los monómeros a lo largo de las cadenas poliméricas. Éstos son los más empleados comercialmente dado que presentan algunas ventajas en sus propiedades, por ejemplo en la flexibilidad, la resistencia el impacto, la trasparencia o el procesado.

1.2.2. Catálisis metalocénica: Mecanismos de reacción

La elección de un precursor metalocénico responde a diferentes criterios dependiendo del tipo de polímero que se desee sintetizar [73]. Las principales razones son las siguientes:

- La estereorregularidad que se desee obtener (isotáctico, sindiotáctico y atáctico), y el grado de pureza del polímero. La industria relativa al

polipropileno tiene preferencia por el balance de propiedades presentadas por el isotáctico.

- El peso molecular que se persigue es generalmente alto, ya que el material producido exhibe buenas propiedades y, por tanto, mejores prestaciones.

- Los errores presentes en las cadenas. Un catalizador puede inducir diferentes tipos de errores de acuerdo a su estructura y a las condiciones en las que se lleve a cabo la reacción de polimerización.

- El control del grado de homogeneidad del comonómero en la cadena así como el tipo de distribución deseada en el caso de copolímeros o terpolímeros. A nivel industrial se prefieren distribuciones al azar debido a que los polímeros resultantes muestran unas propiedades más versátiles.

En función a los criterios anteriores, un precursor metalocénico para la producción de polipropileno debe, entre otros aspectos, garantizar una buena actividad, ser estable, conducir a una tacticidad elevada y pesos moleculares convenientes, y presentar una distribución homogénea de los comonómeros [73]. Un ejemplo de este tipo de catalizadores es el dicloruro de *rac*-dimetilsilil-bis(1-indenil) zirconio, cuya estructura aparece representada en la Figura 7.

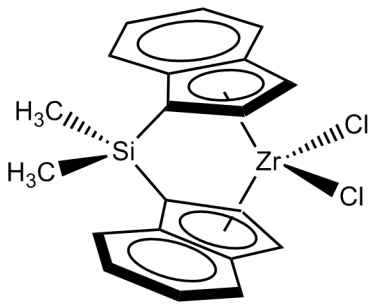

Figura 7. Estructura del dicloruro de *rac*-dimetilsilil-bis(1-indenil) zirconio. ($C_{20}H_{18}Cl_2SiZr$, 448,53 g/mol)

La activación del precursor metalocénico requiere la presencia de un cocatalizador, que es un alquil derivado de aluminio. Los complejos metalocenos suelen emplear, mayoritariamente, el metilaluminoxano (MAO) como cocatalizador. El MAO se define como un oligómero (n= 5-20), soluble en tolueno, obtenido por hidrólisis controlada de trimetilaluminio (TMA), cuya composición y estructura aún no está completamente aclarada [74]. El MAO parece estar constituido por cadenas lineales, cíclicas y, seguramente "clusters" [3,75], como se puede observar en la Figura 8.

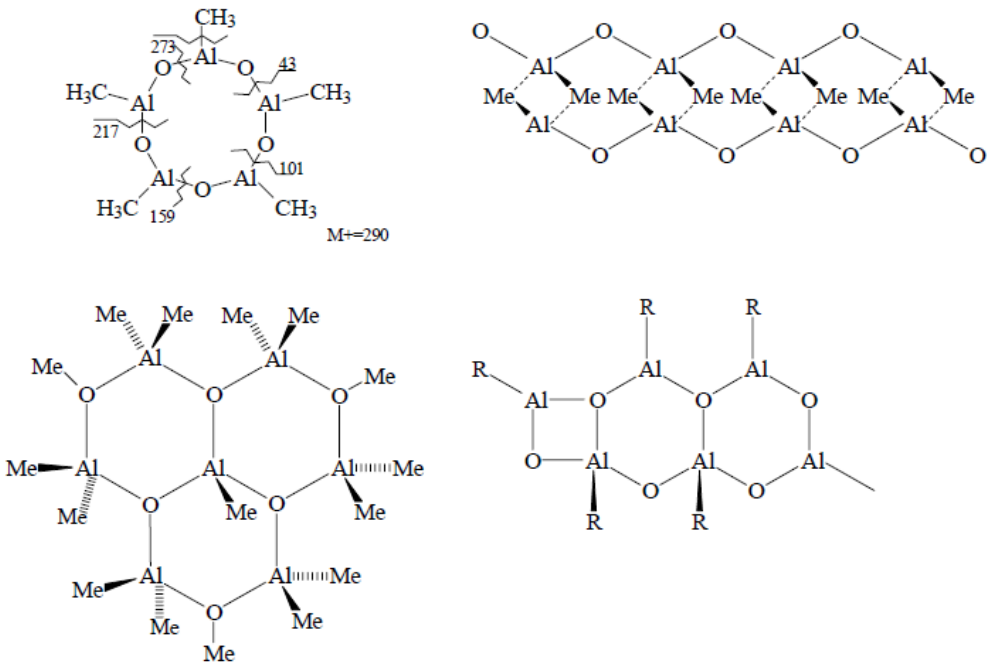

Figura 8. Posibles estructuras del MAO. [75]

El mecanismo de activación del complejo metalocénico, descrito en el Figura 9, parte de la monoalquilación producida tras el encuentro del precursor metaloceno, en este caso el dicloruro de *rac*-dimetilsilil-bis(1-indenil) zirconio, con el cocatalizador formando la especie I. Al interaccionar con el MAO, la estructura I promueve una

forma inactiva denominada II, a través de que se genera la especie activa III responsable de la polimerización. Los centros desactivados se pueden reactivar con MAO mediante una abstracción de metano (IV). No obstante, también puede ocurrir que se forme otra especie irreversible V [76].

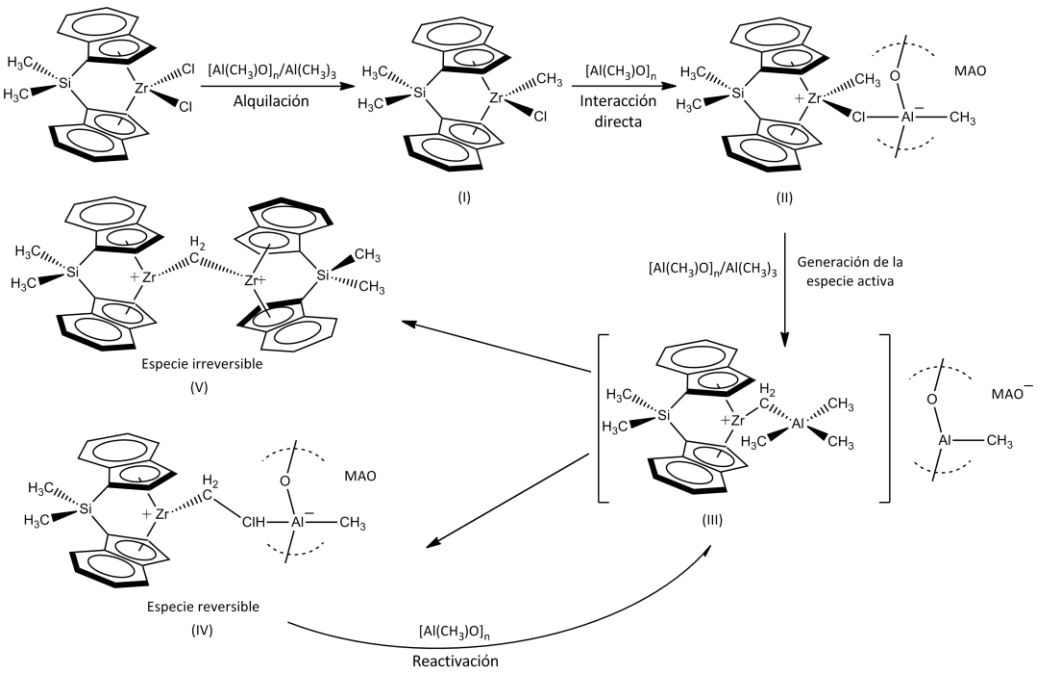

Figura 9. Mecanismo más aceptado de activación del sistema metalocénico.

La experiencia evidencia la necesidad de trabajar con enormes cantidades de cocatalizador relativas a la del complejo organometálico para garantizar elevadas actividades y perfiles cinéticos estables (independientemente de requerirse una mayor concentración de MAO para la reactivación de los centros activos). Sin embargo, la relación óptima entre dichas especies es aún desconocida en la actualidad. De ahí que la relación entre Al/Zr aparece definida en el intervalo de 1000 a 10000 a lo largo de la literatura [64], y se observan problemas en el proceso catalítico para relaciones inferiores a 100 en la mayor parte de los sistemas.

La primera etapa del mecanismo de polimerización es la coordinación del monómero a través del orbital vacío del átomo del metal de transición, como se puede apreciar en la Figura 10. La inserción del monómero ocurre entre el enlace del metal de transición y el carbono de la especie deficiente en electrones. Para facilitar el proceso de inserción del monómero en la cadena y aumentar la velocidad de polimerización es necesario que el contra-ión MAO se encuentre lo más alejado posible de la especie catiónica. La consiguiente inserción de monómero ocurre en el sitio opuesto al inicial, y así sucesivamente [75].

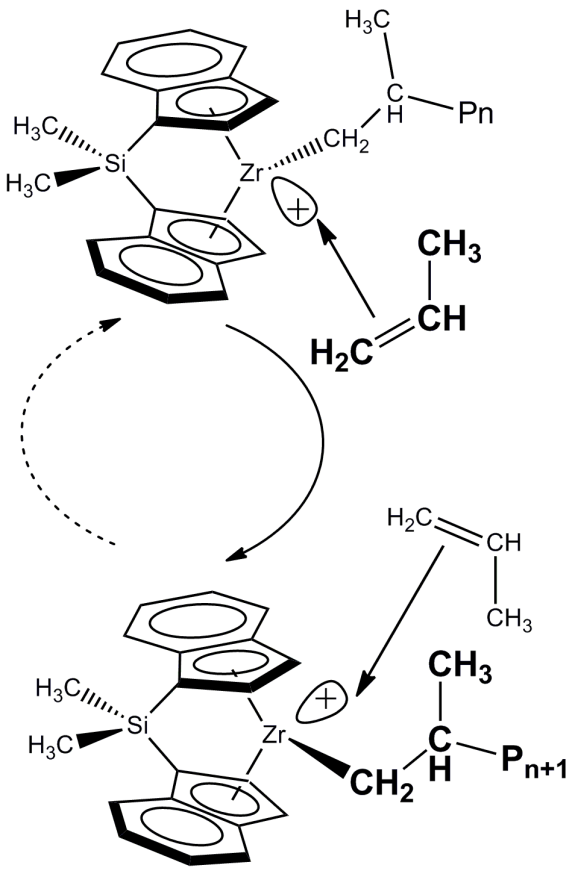

Figura 10. Mecanismo de propagación. [70]

Sin embargo, los catalizadores metalocénicos generan estereo y regioerrores, siendo éstos últimos principalmente de tipo 1,2 y 1,3 en la cadena principal [77], como se describen en la Figura 11. El más común es el 1,2 y se produce por inserciones cabeza-cabeza o cola-cola. La incorporación de errores durante el proceso sintético va a condicionar la microestructura, que está íntimamente relacionada con las estructuras cristalinas que se podrán generar durante el procesado y, por ello, con las propiedades últimas que van a manifestar los materiales sintetizados.

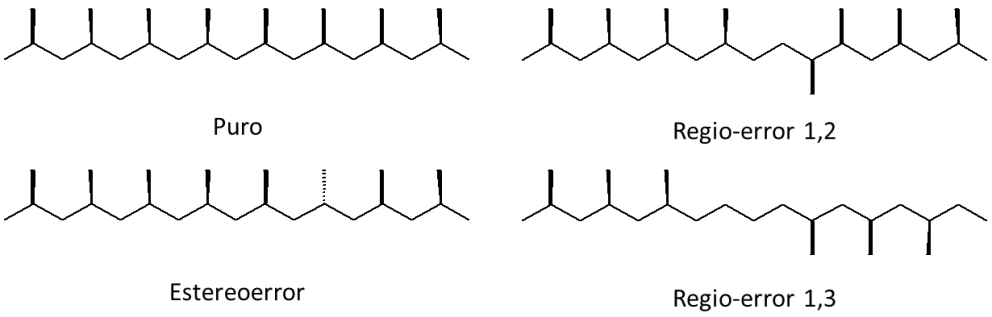

Figura 11. Tipos de defectos del polipropileno isotáctico.

El final de las cadenas de polipropileno producidas con catalizadores zirconoceno está compuesto por grupos *n*-propilo sobre el metal y 2-propenilo en el polímero, según los estudios de resonancia magnética nuclear. Éstos últimos se producen como consecuencia de la transferencia de un átomo de hidrógeno-β de la cadena polimérica al centro metálico. El enlace metal-hidrógeno generado puede entonces reaccionar con un propileno formando un *n*-propilo a través del que puede comenzar a crecer una nueva cadena de polímero. La terminación también puede darse por la transferencia de cadena bien al monómero o al MAO [78,79].

1.2.3. Variables del proceso sintético

La microestructura y el peso molecular del polipropileno isotáctico pueden modificarse a través de diferentes parámetros de síntesis: catalizador (descrito en el apartado anterior), temperatura, presión, disolvente, y las concentraciones de catalizador, de cocatalizador y de monómeros.

La **temperatura** a la que se lleva a cabo la reacción afecta de manera significativa la actividad del catalizador, la tacticidad y el peso molecular [64] de la estructura propilénica resultante. No obstante, existe un intervalo de temperaturas apropiado para el control de las diferentes variables durante el proceso sintético. El aumento de la temperatura conlleva la reducción de la estereoselectividad del catalizador como consecuencia de la promoción de distorsiones en los ligandos, y, por tanto, del peso molecular, ya que se favorecen los procesos de transferencia de cadena.

La **presión** a la que se realiza la polimerización está relacionada con la concentración de monómero gas en el medio de reacción, es decir, del propileno en nuestro estudio. La solubilidad del medio aumenta con la presión a una temperatura de trabajo establecida, y con ello la cantidad de propileno disuelta. Por ello, se requiere una presión mayor en el medio de reacción para aumentar la concentración de monómero a una temperatura dada.

La concentración de **monómeros** en el interior del reactor afecta a la regioselectividad y estereoselectividad [64,80] del catalizador. Además, altas concentraciones de monómero en la reacción promueven una mayor productividad del catalizador [83]. Por el contrario, a bajas concentraciones de monómero se produce un descenso del peso molecular y de la isotacticidad, como consecuencia de los factores cinéticos involucrados del proceso.

La concentración de **catalizador** frente a la de **cocatalizador** tiene influencia directa sobre la actividad del sistema catalítico. La concentración de MAO alrededor

del centro activo afecta a la estructura del catalizador y, por tanto, a la tacticidad de la cadena polimérica [81]. Asimismo, el peso molecular puede aumentar con la concentración de MAO [82].

La polaridad del **disolvente** afecta a la actividad del proceso catalítico [83], de forma que la actividad mejora excepcionalmente con la polaridad del disolvente [84] ya que se produce un incremento de la constante dieléctrica, por lo que mejora la disociación del par iónico (catalizador/MAO).

1.3. Polimorfismo en polipropileno isotáctico

1.3.1. Polipropileno homopolímero

El polipropileno isotáctico se caracteriza por exhibir un comportamiento polimorfo muy interesante. Sus cadenas al cristalizar desde el estado fundido se disponen en una conformación helicoidal 3_1, de modo que en cada vuelta de hélice se encuentran tres unidades de monómero. El diferente ordenamiento/empaquetamiento de estas cadenas en dicha conformación origina las diversas celdillas cristalinas que se pueden generar y que van a condicionar significativamente muchas de las propiedades finales exhibidas y requeridas para una aplicación específica.

La generación de un polimorfo u otro va a depender de características intrínsecas y extrínsecas de las cadenas propilénicas. Las primeras comprenden la **microestructura** molecular que se genera durante el proceso de síntesis, mientras que entre las segundas se encuentran todas aquellas variables que afectan al proceso de transformación del material. La promoción de una celdilla cristalina concreta está sujeta a las características moleculares y estructurales de la misma, de manera que dependiendo de cómo sea la longitud de la cadena, su conformación, la tacticidad, la presencia y distribución de defectos, se pueden generar unos polimorfos u otros en diferente proporción, cantidad, perfección y tamaño.

La microestructura depende de si la polimerización del propileno se ha llevado a cabo empleando un catalizador Ziegler-Natta o de tipo metaloceno, de modo que el primero conduce a una arquitectura polipropilénica en la que la celdilla cristalina desarrollada casi por completo es la monoclínica (ver más adelante). En cambio, si se emplean los sistemas catalíticos metalocénicos se puede observar la coexistencia de cristales monoclínicos y ortorrómbicos [85,86], ya que generan regioerrores capaces de actuar como defectos. Además, estos sistemas catalíticos permiten en el caso de sintetizar copolímeros o terpolímeros al azar, obtener una alta homogeneidad en la distribución de las unidades comonoméricas. Desde este punto de vista, el empleo de estos sistemas catalíticos aporta una elevada homogeneidad en la microestructura e isotacticidad para poder evaluar el comportamiento cristalino y el balance de sus propiedades.

Los parámetros extrínsecos que van a condicionar la formación de uno u otro polimorfo en el polipropileno isotáctico comprenden: el estado a partir del que se parte (disolución o fundido); la velocidad de cristalización, la aplicación de presión, la inducción de una orientación preferente durante la transformación, y, la incorporación de aditivos específicos, entre otros.

El tratamiento térmico al que se someta el polímero tiene una influencia importante sobre la formación de unas estructuras cristalinas u otras. Una velocidad lenta de enfriamiento desde el fundido del polipropileno isotáctico va a favorecer la formación de unas determinadas estructuras cristalinas de gran perfección y con cristalitos de tamaños considerables. Sin embargo, a nivel industrial se aplican enfriamientos mucho más enérgicos que involucran velocidades lo más rápidas posibles para abaratar los costes de producción. Se puede generar el mismo tipo de celdilla que bajo condiciones de cristalización más lentas pero, obviamente, menos perfecta y con cristales más pequeños. Además, se puede inducir el desarrollo de otros polimorfos, que pueden coexistir en proporciones relativas variables. Estos tratamientos responden a los criterios de producción del mercado, ya que tiempos

largos de cristalización reducen drásticamente la eficiencia de la cadena productiva y con ello los beneficios obtenidos.

La presencia de aditivos y/o agentes nucleantes en los polímeros condicionan también el desarrollo de los polimorfos. De forma general, los agentes nucleantes reducen el tiempo de cristalización, e incluso el subenfriamiento pues actúan como núcleos de crecimiento de los cristalitos. De la misma manera, la simple presencia de estos agentes nucleantes en el material pueden alterar algunas de las propiedades del mismo, entre otras ópticas o mecánicas. Existe una gran variedad de agentes nucleantes destinados a la promoción de la celdilla monoclínica como las sales organofosfatadas [87,88], el benzoato sódico [88,89] y el talco [90]. En el caso de la entidad hexagonal se emplean también agentes nucleantes específicos [91-93].

Los diversos polimorfos del iPP se conocen desde hace mucho tiempo [94,95]. Sus difractogramas característicos son los representados en la Figura 12. De izquierda a derecha se observa el perfil de difracción de las celdillas: monoclínica o α; ortorrómbica o γ; hexagonal o β; y mesomórfica, respectivamente.

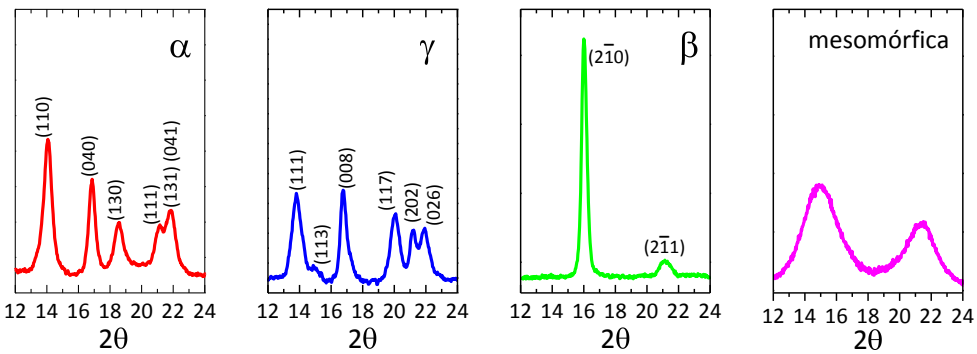

Figura 12. Perfiles de difracción para las diferentes formas cristalinas: de izquierda a derecha, monoclínica, ortorrómbica, hexagonal y mesomórfica.

Los **cristales monoclínicos** (también denominados como α) se han estudiado ampliamente, ya que son la forma cristalina más común encontrada en el

polipropileno isotáctico. Su morfología presenta la mejor relación entre los criterios cinéticos y termodinámicos, apareciendo en las condiciones más habituales de procesado [96]. Este polimorfo cristalino fue descrito inicialmente por Natta y Corradini [97] y se genera tanto si la cristalización tiene lugar desde el estado fundido como a partir de disolución [95]. Su estructura viene definida por las cadenas dispuestas paralelamente y empaquetadas en una celdilla monoclínica en las que se alternan capas de hélices con giro a la derecha y capas de hélices con giro a la izquierda. Su perfil de difracción muestra cinco picos característicos a diferentes valores de 2θ, concretamente para radiación CuKα a 14.1, 16.9, 18.4, 21.1 y 28.5°, que corresponden a las reflexiones (110), (040), (130), (111) y (041, 131) de la unidad cristalina [15]. Cuatro de estas difracciones aparecen en posiciones semejantes a las correspondientes al polimorfo ortorrómbico. Sin embargo, su identificación inequívoca resulta sencilla a partir de su reflexión (130) que aparece en torno a 18.4 ° en 2θ.

La entidad **ortorrómbica**, también conocida como γ, presenta numerosas difracciones a ángulos similares a los de las correspondientes a la celdilla monoclínica, como se ha indicado en el párrafo anterior. No obstante, los cristalitos γ presentan una reflexión distintiva característica, la (117), localizada a 19.9 ° en 2θ (CuKα) [15]. La celdilla γ inicialmente se confundió con una estructura hexagonal [98,99], hasta que estudios cristalográficos posteriores dedujeron que la celdilla ordenada de menor tamaño era de tipo ortorrómbico [86]. Esta entidad se desarrolla cuando la cristalización se produce bajo presión [7] generalmente en polipropilenos de bajos pesos moleculares. Además, la forma γ se favorece con la utilización de catalizadores metalocénicos [8,100-102], dado que éstos promueven la concurrencia de ciertos regiodefectos y estereodefectos, es decir, ciertas interrupciones en las cadenas poliméricas [15,103,104], que inducen la formación de la celdilla ortorrómbica [105].

La forma **hexagonal**, (o cristalitos β) del polipropileno isotáctico es termodinámicamente menos estable que la celdilla monoclínica y la forma ortorrómbica, aunque su velocidad de cristalización es mayor. Su aparición está unida

a la cinética de cristalización y, por tanto, al tratamiento térmico aplicado. Estos cristales son de mayor volumen y densidad que los monoclínicos, pero su temperatura de fusión es menor. La formación de estas entidades en el iPP metalocénico se favorece a través de condiciones específicas como elevados sub-enfriamientos o bajas temperaturas de cristalización. Además, se puede promover su formación con el empleo de agentes nucleantes específicos o bajo deformación [7]. Esta entidad presenta las reflexiones características (210) y (211), aunque el pico identificativo corresponde a su primera difracción, la situada a unos 16 ° en 2θ.

Existe, además, en el polipropileno isotáctico otra forma ordenada, denominada **mesomórfica,** con una disposición intermedia entre el estado amorfo y el cristalino. La naturaleza de este ordenamiento no está aún consensuada en la actualidad. Algunos autores la describen como una forma hexagonal con una conformación helicoidal semejante a la exhibida por el polimorfo monoclínico [106]. Otros la refieren como paracristalina, o formada por microcristalitos e incluso integrada por nanocristalitos. El supuesto más aceptado [107] es el de un cristal conformacionalmente desordenado, basado en una disposición de tipo líquido congelado. Se genera cuando se aplican enfriamientos extremadamente rápidos [7,8,13,100-109]. Es estable a temperatura ambiente pero si se la somete a un proceso de templado en el intervalo 70-90 °C experimenta una transformación a la fase monoclínica [110,111], y lo mismo sucede cuando se calienta a velocidades típicas de DSC [13,112,113]. Esta forma subenfriada del polipropileno isotáctico se caracteriza por dos difracciones anchas en su perfil de rayos X, como inicialmente describieron Natta y Corradini [95]. La mesofase mejora sensiblemente la transparencia del polipropileno [13,114], y se ha estudiado su formación en diversos tipos de copolímeros [115,116,117].

1.3.2. Copolímeros al azar de propileno isotáctico con α-olefinas

La introducción de una unidad comonómera α-olefínica distribuida al azar en las cadenas propilénicas es considerada, en principio, como un defecto que tiende a

ser expulsado por los cristales en crecimiento. La presencia de las counidades, dependiendo de su longitud y su contenido, puede conducir a materiales polímeros con una menor cristalinidad, perfección y tamaño de las entidades formadas y, por tanto, con un espectro muy distinto de propiedades respecto a las exhibidas por el homopolímero.

La entidad **monoclínica** interpreta la presencia del comonómero en las cadenas poliméricas como un defecto no deseable para su formación, ya que esta celdilla se encuentra asociada a la longitud de las secuencias isotácticas de las macrocadenas [118-122]. A medida que aumenta el contenido de counidades en las cadenas disminuye el tamaño de las secuencias propilénicas isotácticas y se producen diversos fenómenos. En el caso del 1-buteno como counidad se ha observado que copolímeros con altas proporciones del mismo incluyen el comonómero en la celdilla monoclínica [123]. Igualmente, el etileno es capaz de incluirse parcialmente. En general, los difractogramas muestran picos de difracción algo más anchos, cuya localización se desplaza a ángulos más bajos como consecuencia de que la presencia de estas counidades reduce la perfección cristalina y el tamaño de los cristalitos monoclínicos.

La celdilla **ortorrómbica** se encuentra, como en el caso de la entidad monoclínica, muy ligada al tamaño de las secuencias propilénicas isotácticas. Sin embargo, las inserciones de comonómero y su distribución en las cadenas favorecen la cristalización de la forma γ [29,116,117,124]. El tipo de counidad α-olefínica empleada en el copolímero está relacionada con la proporción de cristales ortorrómbicos generados, ya que el comonómero se va a distribuir de forma diferente entre la fase amorfa y cristalina, circunstancia que modifica la capacidad de cristalización de las secuencias propilénicas [100]. Algunas counidades se introducen con relativa facilidad en las celdillas ortorrómbicas, aunque ésta desaparece a elevados contenidos de comonómeros como consecuencia del grado de inclusión del defecto en el cristal, por lo que la concentración y el tipo de monómero contribuyen a favorecer o entorpecer

la generación de los cristales ortorrómbicos [123]. Si el etileno es la counidad, el contenido de las estructuras ortorrómbicas es proporcional a la composición de etileno [124]. Además, se justifica la inclusión de las counidades en los cristales con la consecuente disminución de la temperatura de fusión de los mismos. Sin embargo, para el 1-buteno no se obtiene tanta cantidad de esta celdilla comparada con la generada cuando la counidad es el etileno. En cualquier caso, dicho efecto se explica asumiendo que los comonómeros se acomodan en los cristales ortorrómbicos en función a su longitud, generando menor cantidad de los mismos debido a que son secuencias más largas [23,100,118,119].

La formación de las entidades **mesomórficas** requiere, para copolímeros con una counidad dada, velocidades de enfriamiento más bajas a medida que aumenta el contenido de comonómero. También se han observado diferencias dependiendo de la longitud del tipo de counidad empleada [125-128]. Su formación se ha evaluado en copolímeros con diferentes α-olefinas, desde el etileno hasta el 1-octadeceno, aunque algunos de los estudios se han llevado a cabo en copolímeros con intervalos de composiciones muy limitadas. Como consecuencia, en ciertos copolímeros los resultados descritos no son del todo concluyentes dada la falta de datos experimentales. Los copolímeros con etileno y 1-buteno parecen mostrar un comportamiento distinto en función de las velocidades de cristalización [129] para la formación de la fase mesomórfica al exhibido por otros copolímeros [116,125,128], como los de 1-penteno, 1-hexeno y 1-octeno, cuyas características para la formación de las entidades mesomórficas son muy similares.

Adicionalmente a las diferentes celdillas cristalinas comentadas, en 2005 se describió por primera vez en la literatura un nuevo polimorfo **trigonal** en copolímeros de polipropileno isotáctico con elevados contenidos (superiores al 10 % molar) [130] de 1-penteno o 1-hexeno como comonómeros [10,28,131]. Esta celdilla trigonal o δ presenta tres reflexiones características (110), (300) y (220+211) correspondientes a

las difracciones que aparecen alrededor de 10.3, 17.7 y 20.6 ° en una escala de 2θ, como se puede observar en el difractograma de la Figura 13.

Esta nueva celdilla cristalina es muy similar a la forma I del poli-1-buteno isotáctico [28]. Asimismo, el nuevo polimorfo comparte la conformación helicoidal 3_1 al igual que las otras celdillas del polipropileno y la simetría romboédrica, con desorden en el posicionamiento de los grupos laterales, como ocurre en el caso del poli-1-buteno isotáctico o el poliestireno isotáctico [27,28]. La inclusión de 1-penteno o 1-hexeno en la celdilla cristalina puede producir un incremento de masa y del número de entidades cristalinas, llegando a alcanzar una densidad tan alta como la de la forma I del poli-1-buteno isotáctico. Esta circunstancia apunta a la inclusión completa del comonómero (1-penteno y/o 1-hexeno) en los cristales trigonales.

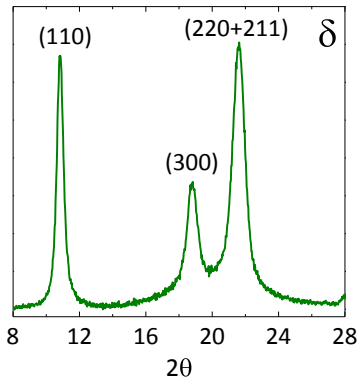

Figura 13. Difracciones características de la forma trigonal δ.

Los copolímeros con un 10 % molar en 1-penteno y/o 1-hexeno son tremendamente interesantes porque en ellos puede haber competencia entre cuatro polimorfos diferentes: forma monoclínica, ortorrómbica, mesomórfica y trigonal, dependiendo principalmente del tratamiento térmico aplicado. Estas peculiaridades se determinaron a través del estudio de los materiales mediante difracción de rayos-X [26,116,125,128,131]. Además, se describió que los picos de difracción de rayos-X se ensanchaban indicando cristales menos perfectos, por lo que la counidad actúa como

defecto y disminuye la temperatura de fusión de los mismos. Conviene destacar que las dimensiones de la celdilla trigonal para los copolímeros de 1-hexeno son mayores que las encontradas para los copolímeros de 1-penteno (Figura 14, izquierda) como consecuencia de la inclusión parcial de las unidades comonoméricas en las celdillas cristalinas. Este factor está asociado a que la composición molecular tiene presente que la longitud del 1-hexeno es mayor que la de 1-penteno. De ahí que si el contenido en comonómero se expresa en % en peso, la variación de las dimensiones es coincidente para los copolímeros de 1-penteno y 1-hexeno (Figura 14, derecha). Este hecho confirma que la formación de la celdilla trigonal responde a los criterios de densidad cristalina. Por ello, se requiere una densidad mínima para la cristalización de la forma trigonal (0,89 g/cm^3), que se produce en el entorno del 10 % molar en comonómero [130].

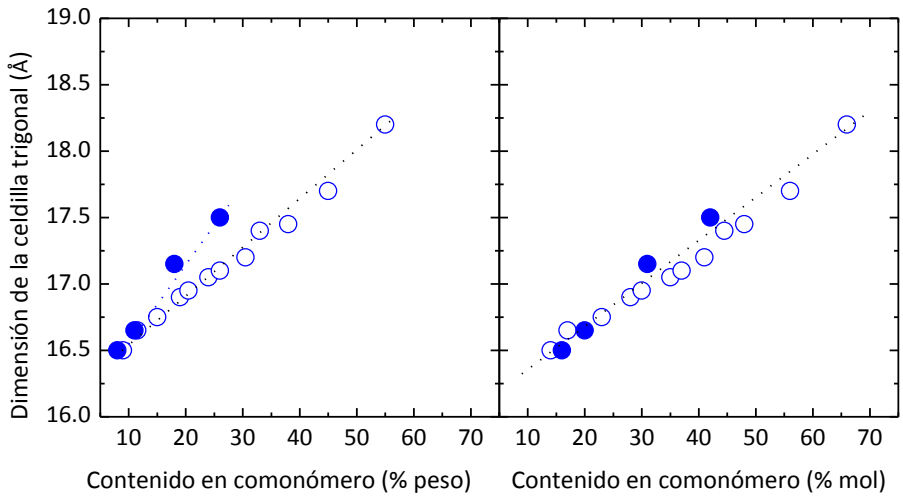

Figura 14. Variación de las dimensiones de la celda unidad de la forma trigonal observada en copolímeros con 1-penteno (símbolos vacíos) y 1-hexeno (símbolos rellenos) en función del contenido en comonómero expresado en % molar (izquierda) o % en peso (derecha). [130]

Sin embargo, la velocidad de cristalización de ambas counidades es muy diferente, de tal modo que la cristalización desde el fundido a velocidades relativamente rápidas de los copolímeros con 1-penteno conduce a la formación de la

estructura trigonal mientras que la de los copolímeros con 1-hexeno conduce al estado amorfo y la cristalización de la forma trigonal en estos copolímeros se inicia desde el amorfo mediante un proceso de cristalización en frío [130]. Para muestras con elevado contenido en 1-hexeno se requieren tiempos relativamente largos de permanencia a una temperatura dada para la formación de la cedillas trigonal en condiciones normales a partir del amorfo [26]. El hecho de que la cinética de cristalización de la forma trigonal en copolímeros de 1-penteno sea mucho más rápida que para los correspondientes con 1-hexeno se justifica por su menor longitud de cadena lateral, de modo que el acoplamiento de las cadenas en las entidades cristalinas resulta más sencillo y se lleva a cabo en tiempos más cortos.

Los copolímeros con composiciones superiores al 15 % molar en comonómero (1-penteno y/o 1-hexeno) son capaces de cristalizar exclusivamente en la forma trigonal. Las celdillas pueden acomodar las cadenas del comonómero hasta un cierto límite a partir del cual no se produce la cristalización porque el contenido en propileno en las cadenas es demasiado bajo para poder formar los cristales [26]. El intervalo de composiciones en el que se genera la forma δ es más extenso [23] si el comonómero empleado es 1-penteno en vez del 1-hexeno, circunstancia que parece indicar que una gran cantidad de unidades de comonómero pueden incorporarse perfectamente en la celdilla cristalina [130].

1.4. Propiedades físicas del iPP y sus derivados

El excelente balance de propiedades exhibido por el polipropileno isotáctico es el responsable de su enorme versatilidad que ha permitido su extraordinaria aplicabilidad en numerosos sectores y el desarrollo de una amplia variedad de productos comerciales. Algunas de sus características más destacadas se resumen a continuación:

- Baja densidad: Es el polímero comercial de menor densidad, lo que resulta interesante desde el punto de vista de los costes de producción, de transporte

y de reemplazamiento de piezas o elementos pesados por otros más ligeros con las mismas o mejores propiedades.

- Elevada cristalinidad (hasta un ~ 85 %).
- Buena resistencia química.
- Buen aislante eléctrico.
- Excelente procesabilidad.
- Temperatura de fusión relativamente superior a la exhibida por otras poliolefinas.
- Elevada rigidez que resulta significativamente superior a la manifestada por el resto de poliolefinas.
- Posibilidad de reciclado dado que es un polímero termoplástico en el que no existe entrecruzamiento químico.

La mejora de algunas de las propiedades del homopolímero, así como la búsqueda de otras nuevas, puede llevarse a cabo mediante la introducción de uno o más comonómeros en sus cadenas. Por consiguiente, la preparación de copolímeros o terpolímeros aparece como una vía factible para resolver algunas de sus deficiencias y ampliar el ámbito de sus prestaciones. Inicialmente estos trabajos estuvieron exclusivamente enfocados en la mejora de algunas de las limitaciones presentes en el polipropileno isotáctico, como su resistencia al impacto. En este sentido, los copolímeros con el etileno responden a esta necesidad concreta [132] y son los que actualmente se producen a nivel industrial. No obstante, dichos estudios demostraron que aparte de potenciar algunas de sus prestaciones, la introducción de α-olefinas abría un nuevo espectro de propiedades, como la sensible mejora de la transparencia. Desde entonces, la industria ha demostrado un enorme interés por este nuevo tipo de materiales capaces de ampliar el ya enorme espectro de aplicaciones de los materiales basados en el polipropileno isotáctico.

En general, las propiedades físicas comentadas para el polipropileno isotáctico dependen de diversos factores que van a modificarse por la presencia de una o varias unidades comonómeras:

- **Microestructura**. Las características moleculares asociadas al polímero, es decir su composición y su configuración, determinan las propiedades finales de los materiales, ya que condicionan decisivamente las características de la morfología semicristalina. [133]. La inserción de unidades de comonómero en las cadenas del iPP disminuye la tacticidad propilénica global y, con ella, la perfección y tamaño de los cristales. En el caso de las α-olefinas, la relación rigidez/tenacidad y la transparencia se mejoran para algunos intervalos de composiciones óptimas en comonómero.
- **Pesos moleculares** y su distribución. Las propiedades mecánicas del iPP, en particular la resistencia a la tracción, mejoran cuando los pesos moleculares son elevados [134], dado que dicho aumento involucra unas mayores longitudes de las cadenas poliméricas que favorece un mayor enmarañamiento de las mismas y, por tanto, una mayor resistencia del material [135]. En los copolímeros o terpolímeros la presencia de los comonómeros tiende a reducir significativamente los pesos moleculares.
- **Cristalinidad**. Las propiedades del polipropileno isotáctico, entre otras su respuesta mecánica, están muy vinculadas a la cristalinidad del mismo. De forma general, una elevada cristalinidad en el polímero se relaciona con una rigidez y dureza más elevadas, una mayor resistencia a la tracción y a la flexión, así como un esfuerzo superior en el punto de fluencia. Grados de cristalinidad inferiores favorecen una mayor tenacidad y resistencia al impacto del polímero. La presencia del comonómero disminuye la longitud media de las secuencias de polipropileno isotáctico capaz de cristalizar y, consecuentemente modifica considerablemente la morfología cristalina, como se comentó en apartados previos.

- **Aditivos, Cargas y Refuerzos**. Los aditivos permiten mejorar algunas de las limitaciones del iPP. El uso de algunos agentes de refuerzo favorece el aumento de la rigidez y dureza, así como de la resistencia al impacto del mismo [136,137].
- **Condiciones de procesado**. La velocidad de cristalización del polímero desde el fundido, la presión aplicada y la inducción de orientaciones preferentes mediante cizalla son algunas de las variables de procesado que influyen en las prestaciones finales del iPP. Estas condiciones están también directamente relacionadas con las propiedades de impacto del polipropileno isotáctico [133].

De forma general, se puede prever que la copolimerización con α-olefinas conducirá a materiales con menor cristalinidad, rigidez y fragilidad, además de con una mayor flexibilidad, resistencia al impacto y elasticidad. No obstante, no se conoce con precisión cuál será su efecto sobre otras propiedades como, por ejemplo, la estabilidad térmica. En cualquier caso, es fundamental llevar a cabo un estudio exhaustivo de la microestructura molecular de estos materiales para conocer la influencia de los factores que controlan el tipo de polimorfo así como el crecimiento y la evolución de las entidades cristalinas bajo distintas condiciones. Las principales características microestructurales son, como se ha mencionado previamente, la longitud de cadena (peso molecular), la homogeneidad en el tamaño de las cadenas (polidispersidad), el contenido de counidades en las cadenas poliméricas así como su distribución y, finalmente, su disposición en el espacio (tacticidad).

Desde el punto de vista comercial, los copolímeros de propileno con etileno han resultado hasta la fecha los más comercializados, dado el bajo coste del comonómero y su fácil incorporación a las cadenas. La introducción de estas counidades al azar conduce a una disminución de la cristalinidad que involucra una variación de las propiedades físicas del material [16,17]. En este sentido la **caracterización mecánica**, mediante el estudio del comportamiento viscoelástico,

resulta fundamental en los materiales poliméricos sintetizados en el presente trabajo para dilucidar convenientemente la posible aplicación de los mismos. Los ensayos mecanodinámicos permiten conocer las contribuciones elástica y plástica de la respuesta a una solicitación mecánica, en un amplio rango de frecuencia y temperatura.

Otra de las propiedades estudiadas de forma general en los materiales de base propilénica es su resistencia a la indentación. Este ensayo de **dureza** se emplea habitualmente en la caracterización del polipropileno isotáctico o sus copolímeros para la industria del automóvil, dado que los coches se encuentran muy expuestos a este tipo de situaciones. En este sentido, los copolímeros de propileno con etileno mantienen unos valores aceptables de la dureza que garantizan la durabilidad del material [138].

El estudio de las **propiedades térmicas** de las arquitecturas de polipropileno es imprescindible para la evaluación de la estabilidad de los materiales y, por tanto, para la determinación de sus posibles aplicaciones [139-141]. Además, desde el punto de vista científico, la comparación de algunas arquitecturas de polipropileno como copolímeros puede aportar interesantes prestaciones y ventajas respecto al homopolímero de referencia.

Principalmente los materiales cuya base es el polipropileno isotáctico sufren un proceso de degradación oxidativa durante todo su ciclo de vida, que incluye el procesado, el tiempo de uso y el recomendado reciclado final. La introducción de unidades de α-olefina en la cadena isotáctica del PP disminuye su capacidad de cristalización en sus polimorfos característicos y conlleva, consecuentemente, un aumento de la fracción amorfa del material susceptible de oxidarse en condiciones ambientales por acción de la luz y el calor. Este hecho, unido a una concentración más elevada de dobles enlaces terminales, derivada de la disminución del peso molecular asociada a la copolimerización, permitiría inferir una disminución de la resistencia a la oxidación de estos materiales. No obstante, el efecto que pueda tener tanto la mayor

flexibilidad de las cadenas como la presencia de ramas largas sobre la energía de activación de la oxidación, no es evidente y requiere de un estudio detallado.

Actualmente, las políticas medioambientales invitan al **reciclaje** para intentar prevenir el exceso en el consumo de materias primas y la acumulación innecesaria de cantidades ingentes de residuos, difíciles de degradar en los vertederos aparte de ser contaminantes en muchos casos. De entre las posibles vías de reciclado de los materiales termoplásticos, el reciclado químico ha despertado un gran interés ya que constituye una fuente potencial de recuperación de productos químicos así como de producción de otros nuevos. Debido a que estos procesos son pirolíticos, los estudios de estabilidad térmica en atmósfera inerte resultan fundamentales para determinar los parámetros cinéticos que permiten su control y aprovechamiento. Aunque los procesos de pirólisis se han estudiado generalmente a altas temperaturas y en presencia de catalizadores, para obtener fracciones volátiles de bajo peso molecular, la posibilidad de usar reactores de lecho fluidizado puede hacer necesaria una etapa previa de pre-pirólisis a más baja temperatura que disminuya el peso molecular convenientemente. En este caso, cobra interés también la caracterización de la cinética de la pirólisis a baja temperatura, como un proceso que, por una parte contribuye a la sostenibilidad de la producción del polipropileno isotáctico y, por otra, permite la obtención de productos oligómeros con un gran valor añadido.

Conviene destacar que, aunque se conoce el mecanismo de pirólisis del polipropileno [142,143], la energía de activación del proceso está íntimamente relacionada con la estereorregularidad del material, es decir con la rigidez de las cadenas poliméricas [144]. Por tanto, en el caso de los copolímeros de polipropileno, la presencia de unidades de comonómero puede ser determinante en la magnitud de los parámetros cinéticos, en virtud de su influencia en la flexibilidad de las cadenas. Éste es un aspecto que no se ha estudiado suficientemente y que puede ser esencial para la rentabilidad de su reciclaje. Así, un material con una energía de activación baja

implica un craqueo más rápido y, por consiguiente, un volumen mayor de residuos tratados y un menor coste del proceso [145].

Desde el punto de vista de otras propiedades conviene tener presente que los copolímeros de etileno son empleados en mezclas para la fabricación de envases y filmes generalmente destinados a la industria alimentaria. Dicho interés surge tras conocer las excelentes propiedades de barrera al agua presentes en el polipropileno, pese a su relativa elevada **permeabilidad** al oxígeno. Este tipo de envases deben proteger el alimento de la entrada de oxígeno, humedad, y otros aromas, asegurando por un tiempo las correctas condiciones de consumo [146-148]. El análisis de las propiedades barrera mediante ensayos de permeación son clave para estudiar las posibilidades que ofrecen los copolímeros con α-olefinas en el campo de la industria del envasado y embalaje [148].

Se conoce desde hace tiempo que al emplear 1-buteno como comonómero del propileno, se pueden obtener buenos comportamientos mecánicos. Estos copolímeros se han destinado esencialmente a la producción de filmes con elevada resistencia a la tracción, así como de productos que combinan unas buenas propiedades mecánicas con una gran transparencia. Resulta enormemente atractiva la idea de conjugar un excelente balance de propiedades junto con una elevada transparencia.

Las aplicaciones de los copolímeros con 1-penteno y 1-hexeno no se han planteado hasta la fecha en el mercado como consecuencia del elevado coste de estas counidades. No obstante, la obtención de materiales cristalinos (estructura trigonal) para elevados contenidos en comonómero puede darles una oportunidad comercial si manifiestan algún tipo de propiedades de interés, entre las que podrían encontrarse su respuesta mecánica.

Por último, comentar que se ha observado un excelente comportamiento de sellado en los terpolímeros basados en polipropileno [149], circunstancia que ha despertado un gran interés comercial por los mismos.

1.5. Motivación

El crecimiento de la demanda de polipropileno frente a otros materiales poliméricos responde, principalmente, a su baja densidad y a su enorme versatilidad en relación con los requerimientos comerciales demandados y el cumplimiento de calidad exigido por las normativas y regulaciones actuales en áreas de sostenibilidad energética, medioambiental, sanitaria e higiénica, entre otras. Estas características han posibilitado su expansión masiva en sectores de producción como el textil, la automoción, el envasado alimentario y de dispositivos clínicos, entre otros, como se ha indicado en secciones previas.

La clave de su éxito se adscribe a que los materiales resultantes de su modificación parcial (por copolimerización, mezclado con otros polímeros, incorporación de aditivos de bajo peso molecular y de refuerzos micro y nanométricos) se procesan a partir de las técnicas convencionales de transformación de polímeros y manifiestan unas prestaciones generales y específicas adecuadas a la aplicación final para las que han sido diseñados y similares a las exhibidas por polímeros de mayor precio. Además, los objetos obtenidos requieren una cantidad inferior de material y suponen, por ello, un menor coste económico a igualdad de otras consideraciones. Por otra parte, finalizada su vida útil pueden entrar a formar parte de la correspondiente cadena de reciclado. Todo lo comentado implica que, aún en la actualidad, el polipropileno sea un material con un enorme potencial de expansión, de ahí que se continúen realizando grandes esfuerzos científicos y de investigación aplicada para, en base a las nuevas tecnologías y metodologías, actualizar los sistemas catalíticos empleados durante su obtención con objeto de optimizar los procesos sintéticos ya existentes, así como para desarrollar arquitecturas

noveles basadas en propileno, y, además, actualizar su caracterización con las nuevas técnicas hoy disponibles que puedan proporcionar información adicional hasta ahora ignorada por la falta de los métodos adecuados. Todos estos progresos tecnológicos pueden permitir la producción de materiales derivados del iPP con nuevas propiedades.

Una de las hipótesis que verifica que no todo está descubierto y que esa potencialidad de futuro existe y es real, se relaciona con el hallazgo en 2005 de un nuevo polimorfo en derivados isotácticos de propileno. Esta forma cristalina trigonal observada en copolímeros de propileno con 1-penteno y 1-hexeno con elevados contenidos molares de counidades (superiores al 10 %) es clara evidencia de la existencia de espacio para llevar a cabo investigaciones punteras relacionadas con el iPP que es el segundo polímero más producido, comercializado y utilizado a nivel mundial.

La motivación última de este trabajo de investigación es, por tanto, adquirir nuevos conocimientos científicos y profundizar en los ya existentes relativos a las arquitecturas basadas en iPP que puedan desarrollar esta celdilla cristalina trigonal. Su reciente hallazgo genera multitud de incógnitas que conciernen la síntesis de estas nuevas macroestructuras poliméricas, sus características moleculares, el efecto de las condiciones de cristalización en su desarrollo, la competencia que pueda existir con los otros polimorfos en los intervalos de composición donde sea posible su formación y, obviamente, las propiedades que manifiesten los polímeros que la contengan. Éstas, es decir, sus prestaciones últimas serán sus valedoras para la posterior búsqueda de un posible nicho de mercado y de su producción a gran escala o para ser interesantes únicamente desde un punto de vista académico.

Esta motivación científica se completa con la labor formativa que ha supuesto su desarrollo en el campo de los polímeros, de su síntesis, su caracterización y estudio de propiedades. La investigación planteada conlleva una labor sintética muy considerable dado que involucra la obtención de otras arquitecturas distintas de los

copolímeros de 1-penteno y/o 1-hexeno en las que se genere esta nueva fase δ trigonal. La adquisición de ese conocimiento fundamental y de las diferentes variables que puedan afectar al desarrollo de la nueva celdilla requiere la preparación de familias de derivados de polipropileno en intervalos de composición amplios, no sólo aquéllos de contenidos elevados. La primera posibilidad a explorar contempla la incorporación de ambas counidades (1-penteno y 1-hexeno) en una misma cadena polimérica, es decir, terpolímeros propileno-*co*-1-penteno-*co*-1-hexeno. La segunda se corresponde con la sustitución de esos comonómeros por el siguiente superior en longitud, es decir, por el 1-hepteno y evaluar copolímeros de propileno-*co*-1-hepteno. Y, por último, una tercera alternativa que se baraja, dependiendo de los resultados derivados de las dos precedentes, es la combinación de 1-penteno/1-hepteno y/o 1-hexeno/1-hepteno como counidades en terpolímeros propileno-*co*-1-penteno-*co*-1-hepteno y/o terpolímeros propileno-*co*-1-hexeno-*co*-1-hepteno.

El trabajo de caracterización molecular y estructural previsto es también extenso debido a la síntesis de diferentes familias con distintos contenidos y en los terpolímeros, adicionalmente, con varias proporciones de los comonómeros involucrados. Asimismo, la información que se pretende obtener a ambos niveles es diversa, dado que es relativa al peso molecular y su distribución, composición en comonómero, contenido en defectos, tacticidad, composición de las cadenas poliméricas, estructuras cristalinas posibles y su dependencia con el contenido en counidad y variables de cristalización. Diferentes técnicas son necesarias, incluyendo: cromatografía por exclusión de tamaños, viscosimetría, resonancia magnética nuclear de protón y carbono; difracción de rayos X con radiación convencional y sincrotrón; calorimetría diferencial de barrido, entre otras posibles.

Las propiedades manifestadas por las diferentes familias estarán condicionadas por la correlación microestructura molecular-estructura cristalina existente en cada una de ellas. Esta investigación contempla el conocimiento de las prestaciones mecánicas, en general, y otras de tipo más específico como propiedades

de transporte de gases, ópticas y de estabilidad térmica. Distintas técnicas se han utilizado: indentación instrumentada; análisis mecanodinámico; deformación uniaxial; células de permeación; espectroscopia ultravioleta-visible; análisis termogravimétrico.

1.6. Objetivos

1.6.1. Objetivo general

El objetivo final de la presente investigación lo constituye la síntesis y posterior elucidación de las arquitecturas basadas en iPP que puedan desarrollar el nuevo polimorfo trigonal, la evaluación del efecto de las condiciones de cristalización en su desarrollo, el estudio de la competencia que pueda existir con otras estructuras cristalinas en los intervalos de composición dónde sea posible su formación así como la evaluación de ciertas propiedades en algunas de las familias de polímeros sintetizadas.

1.6.2. Secuencia de Objetivos

La consecución del objetivo general de la presente tesis doctoral ha sido posible mediante el planteamiento y secuencia de hitos u objetivos específicos afrontados cronológicamente desde su inicio. Todos ellos tienen como propósito último conocer qué arquitecturas son capaces de formar el nuevo polimorfo, dilucidar las variables que afectan su formación así como su posible competencia con otras estructuras ordenadas y las propiedades que se derivan de su presencia. Entre estas estructuras, se ha prestado también especial atención a la obtención y competencia con la fase mesomórfica, la cual presenta propiedades bien diferenciadas de las otras formas cristalinas.

Los **terpolímeros propileno-*co*-1-penteno-*co*-1-hexeno** se consideraron las primeras arquitecturas distintas a los copolímeros de 1-penteno y/o 1-hexeno en las que se podría desarrollar esta nueva fase δ trigonal. Los dos primeros artículos [150,151] recogidos en la presente Tesis se centran, por tanto, en el estudio de dichos

terpolímeros. En el primero se describe la síntesis de estos terpolímeros con diferentes composiciones globales comprendidas en un amplio intervalo y tres ratios distintos de 1-penteno/1-hexeno a un contenido dado. Además, se realiza un estudio de la microestructura de estos terpolímeros haciendo especial hincapié en la isotacticidad y otras secuencias estereoselectivas. Adicionalmente, se verificó la formación del polimorfo δ trigonal en los terpolímeros de mayores contenidos globales, procesados en condiciones similares a las aplicadas industrialmente. Se observó también que el desarrollo de esta celdilla se ralentiza a medida que aumenta el contenido de 1-hexeno en la serie de terpolímeros con la composición global superior.

El segundo artículo dedicado a estos mismos **terpolímeros de propileno-*co*-1-penteno-*co*-1-hexeno** tiene por objeto caracterizar en profundidad su microestructura comparándola con la encontrada en **copolímeros propileno-*co*-1-penteno** y **propileno-*co*-1-hexeno** sintetizados en idénticas condiciones. Se evalúan las relaciones de reactividad de ambas counidades y se observa cómo se produce la incorporación simultánea de ambos comonómeros en las cadenas poliméricas en unos escenarios de trabajo específicos.

Una vez conocido que, además de los copolímeros de 1-penteno y/o 1-hexeno, la combinación de ambas counidades en una misma macrocadena conduce a materiales que también son capaces de generar la estructura δ, el siguiente planteamiento involucra el incrementar la longitud de la unidad comonómera, es decir, a los **copolímeros propileno-*co*-1-hepteno**. La literatura los describe muy poco, siendo sólo pinceladas relativas a su síntesis no existiendo nada relacionado con sus propiedades físicas. El primer artículo de esta investigación que les hace referencia [152], describe su síntesis en un intervalo de composiciones suficientemente amplio, su caracterización molecular así como su respuesta mecánica mediante medidas de indentación instrumentada. El análisis preliminar de sus estructuras cristalinas en muestras procesadas bajo dos tratamientos térmicos pone en evidencia que la

ramificación del 1-hepteno es ya demasiado larga y es incapaz de desarrollar la celdilla trigonal. A continuación, se ha realizado un estudio pormenorizado (artículo enviado) sobre las diferentes estructuras cristalinas observadas en función de la composición mediante calorimetría diferencial de barrido y difracción de rayos X. Se ha evaluado, por tanto, la competencia entre los diversos polimorfos y sus transiciones de fase identificándolas inequívocamente. Además, se ha analizado la influencia de las estructuras cristalinas en las propiedades ópticas resultantes en la región del visible.

Un tercer artículo (actualmente bajo revisión) relativo a estos copolímeros evalúa sus propiedades de transporte a diferentes gases y distintas temperaturas, sus procesos de relajación, así como la correlación del módulo de elasticidad estimado por medidas mecanodinámicas con el obtenido por los ensayos de indentación. Se observan dependencias diferentes en función de los polimorfos coexistentes en los varios copolímeros.

Otra de las tentativas comentadas para obtener materiales capaces de desarrollar la estructura trigonal, dependiendo de los resultados obtenidos, es la síntesis de los terpolímeros propileno-*co*-1-penteno-*co*-1-hepteno y/o terpolímeros propileno-*co*-1-hexeno-*co*-1-hepteno. La limitación temporal de la investigación ha obligado a tener que seleccionar sólo una de las opciones. Como, por un lado, el 1-hexeno ralentiza la formación de la estructura trigonal y, por otro, el 1-hepteno la inhibe, los **terpolímeros propileno-*co*-1-penteno-*co*-1-hepteno** son los que se han sintetizado finalmente, con diferentes composiciones globales y tres ratios distintos de 1-penteno/1-hepteno a un contenido dado. Un primer artículo (enviado a publicar) relacionado con ellos se recoge en la presente memoria explicando su síntesis, su microestructura y la descripción preliminar de la forma trigonal en ellos generada.

El último objetivo de la presente tesis doctoral se asocia a la **estabilidad térmica** de parte de los materiales sintetizados y se recoge en otro artículo enviado para su publicación. Actualmente, no existe ningún estudio sobre el comportamiento de los copolímeros basados en propileno con otras α-olefinas en condiciones

pirolíticas. Su interés reside en el hecho que este análisis permite conocer cuál es el papel específico de la microestructura molecular de las cadenas polipropilénicas en su estabilidad térmica y, además, sirve como base para evaluar los procesos de reciclaje químico como una ruta alternativa de aprovechamiento final. Este estudio preliminar se ha realizado sobre los **copolímeros propileno-*co*-1-penteno** y **propileno-*co*-1-hexeno** en un amplio rango de composiciones.

En resumen, esta investigación expone los resultados obtenidos en siete artículos: tres de ellos ya publicados y cuatro enviados a publicar. Se ha tratado de realizar una evaluación en profundidad de los materiales que generan el nuevo polimorfo δ trigonal, que comprende desde sus procesos sintéticos, el estudio de sus microestructuras, la influencia de la composición en las diferentes formas cristalinas, y la competencia entre ellas, con especial énfasis en la nueva forma trigonal y la mesofase. La correlación estructura-propiedades se ha llevado a cabo en el comportamiento mecánico, en general, y en los procesos de transporte de gases, las características ópticas en la región del visible y en la estabilidad térmica.

1.7. Bibliografía

1. Leach, B.; “Applied Industrial Catalysis”. Elsevier 1983, Volumen 1.
2. Hogan, J.P.; Banks, R. L.; Chemists and Chemistry 1986, 7, 103-115.
3. Malpass, D.B.; Band, E.; “Introduction to Industrial Polypropylene: Properties, Catalysts Processes”. Wiley 2012, ISBN: 978-1-118-06276-0.
4. Martin, H.; “Polymers, Patents, Profits: A Classic Case Study for Patent Infighting”. Wiley-VCH 2007, ISBN: 978-3-527-31809-4.
5. Barnetson, A.; “Advances in Polymers: Market and Technical Trends : a Report from Rapra's Industry Analysis Department (Rapra Industry Analysis report series)”. Rapra Technology 1997, B001A15T7M.
6. Garrido, L.; Ibarra, L.; Marco, C.; “Ciencia y Tecnología de Materiales Poliméricos” ICTP-CSIC 2004.
7. Bruckner, S.; Meille, S.V.; Nature 1989, 340, 455-457.
8. Palza, H.; López-Majada, J. M.; Quijada, R.; Benavente, R.; Pérez, E.; Cerrada, M. L. Macromol Chem Phys 2005, 206, 1221.
9. Quijada, R.; Guevara, J. L.; Galland, G. B.; Rabagliati,F. M.; Lopez-Majada, J. M.; Polymer 2005, 46, 1567.
10. Poon, B.; Rogunova, M.; Hiltner, A.; Baer, E.;Chum, S. P.; Galeski, A.; Piorkowska, E.; Macromolecules 2005, 38, 1232.
11. Galli, P.; Vecellio, G. Prog Polym Sci 2001, 26, 1287.
12. Arranz-Andrés, J.; Benavente, R.; Peña, B.; Pérez,E.; Cerrada, M. L.; J Polym Sci Part B: Polym Phys 2002, 40, 1869.
13. Arranz-Andrés, J.; Benavente, R.; Pérez, E.; Cerrada, M. L.; Polym. J. 2003, 35, 766.
14. Galli, P.; Macromolecular Symposia 1996, 112 (1), 1–16.

15. López-Majada, J.M. ; Palza, H.; Guevara, J.L. ; Quijada, R.; Martínez, M.C. ; Benavente, R. ; Pérez, E. ; Cerrada, M.L.; J. Polym. Sci. Part B, Pol. Phys. 2006, 44, 1253.

16. Pérez, E.; Benavente, R.; Bello, A.; Polymer, 1997, 38(21), 5411-5418.

17. Galli, P.; Prog. Polym. Sci., 1994, 19, 959-974.

18. Karger-Kocsis, J.; "Polypropylene: Structure, Blends and Composites. Vol I". Chapman & Hall 1995.

19. Benavente, R.; Pereña, J.M.; Bello, A.; Pérez, E.; Locatelli, P.; Fan, Z.; Zucchi, D.; Polym. Bull. 1996, 36, 249.

20. Arranz-Andrés, J.; Guevara, J.L.; Velilla, T.; Quijada, R.; Benavente, R.; Pérez, E.; Cerrada, M.L.; Polymer 2005, 46, 12287.

21. Arnold, M.; Henschke, O.; Knorr, J.; Macromol. Chem. Phys. 1996, 197, 563.

22. Halasz, L; Vorster, O.C.; Belina, K.; Juhasz, P. ; Plast. Rubber Compos. 2004, 33, (5), 205.

23. Jeon, K.; Palza, H.; Quijada, R.; Alamo, R.G.; Polymer 2009, 50, 832.

24. Palza, H.; López-Majada, J.M.; Quijada, R.; Pereña, J.M.; Benavente, R.; Pérez, E.; Cerrada, M.L.; Macromol. Chem. Phys. 2008, 209, 2259.

25. De Rosa, C.; Auriemma, F.; Talarico, G.; Ruiz de Ballesteros, O.; Macromolecules 2007, 40, 8531.

26. De Rosa, C.; Dello Iacono, S.; Auriemma, F.; Ciaccia, E.; Resconi, L.; Macromolecules 2006, 39, 6098.

27. De Rosa, C.; Auriemma, F.; Corradini, P.; Tarallo, O.; Dello Iacono, S.; Ciaccia, E.; Resconi. L.; J. Am. Chem. Soc. 2006, 128, 80.

28. Lotz, B.; Ruan, J.; Thierry, A.; Alfonso, G.C.; Hiltner, A.; Baer, E.; Piorkowska, E.; Galeski, A. ; Macromolecules 2006, 39, 5777.

29. Guidetti, G.P.; Busi, P.; Giulianelli, I.; Eur. Polym. J. 1983, 19, (9), 757.

30. Marega, C.; Marigo, A.; Mater. Eng. 2002, 10, (3), 337.

31. Hong, S. M.; Seo, Y.; J. Phys. Chem. 2007, 111, (14), 3571.

32. <http://www.pcpiplastics.com/industries/aerospace.html> [consulta: 05/2015].

33. <http://www.totalrefiningchemicals.com/SiteCollectionDocuments/Press_releases_news/2006/75_press%20release%20pp.pdf> [consulta: 05/2015].

34. <http://www.foodproductiondaily.com/Packaging/Repsol-launches-polypropylene-copolymers-for-food-packaging> [consulta: 05/2015].

35. Kubacka, A.; Cerrada, M. L.; Serrano, C.; Fernández-García, M.; Ferrer, M.; Fernández-García, M. J. Nanosci. Nanotech. 2008, 8, 3241–3246.

36. Cerrada, M.L.; Serrano, C.; Sánchez-Chaves, M.; Fernández-García, M.; de Andrés, M.A.; Riobóo, R.J.; Fernández-Martín, F.; Kubacka, A.; Ferrer, M.; Fernández-García, M. Environ. Sci. Techn. 2009, 43, 1630–1634.

37. Kubacka, A.; Ferrer, M.; Cerrada, M.L.; Serrano, C.; Sánchez Chaves, M.; Fernández García, M.; de Andrés, A.; Jiménez Riobóo, R.J.; Fernández Martín, F.; Fernández García. M. Appl. Catal. B-Environ. 2009, 89, 441-447.

38. <http://meshmedicaldevicenewsdesk.com/what-do-we-know-about-polypropylene-2> [consulta: 05/2015].

39. Mier, J. L.; Artiaga, R.; García L.; "Síntesis de Polímeros. Pesos moleculares. Conformación y configuración." Universidade da Coruña 1997.

40. Ziegler, K.; Holzkamp, E.; Breil, H.; Martin, H.; Angew. Chem. 1955, 67, 541.

41. Natta, G.; Angew. Chem. 1956, 68, 393.

42. Wilkinson, G.; Birmingham, I. M.; J. Am. Chem. Soc. 1954, 76, 4281.

43. Fischer, E. O.; Angew Chem. 1952, 22, 620.

44. Natta, G.; Pino P.; Corradini, P.; Danusso, F.; Mantica, E.; Mazzanti, G.; Moraglio, G.; J. Am. Chem. Soc.1955, 77, 1708.

45. Breslow, D. S.; Newburg, N. R.; J. Am. Chem. Soc. 1957, 79, 5072.

46. Reichert, K. H.; Meyer, K. R.; Makromol. Chem. 1973, 169, 163.

47. Long, W. P.; Breslow, D. S.; Justus Liebigs Ann. Chem. 1975, 463.

48. Andresen, A.; Cordes, H. G.; Herwing, J.; Kaminsky, W.; Merck, A.; Mottweiler, R.; Pein, J.; Sinn, H.;Wollmer, H. J.; Angew. Chem. 1976, 88, 688.

49. Andersen, A. A.; Cordes, H. G.; Herwig, J.; Kaminsky, W.; Merck, A.; Mottweiler, R.; Pein, J.; Sinn H.; Vollmer, H. J.; Angew. Chem., Int. Ed. Engl., 1976, 15, 630.

50. Sinn, H.; Kaminsky, W.; Adv. Organomet. Chem. 1980, 18, 99.

51. Johnson, L. K.; Killian, C. M.; Brookhart, M.; J. Am. Chem. Soc. 1995, 117, 6414.

52. Johnson, L. K.; Mecking, S.; Brookhart, M.; J. Am. Chem. Soc. 1996, 118, 267.

53. Killian, C. M.; Tempel, D. J.; Johnson, L. K.; Brookhart, M.; J. Am. Chem. Soc. 1996, 118, 11664.

54. Britovsek, G. J. P.; Gibson, V. C.; Kimberley, B. S.; Maddox, P. J.; Mctavish, S. J.; Solan, G. A.; White, A. J. P.; Williams, D. J.; Chem. Commun. 1998, 849.

55. Britovsek, G. J. P; Bruce, M.; Gibson, V. C.; Kimberley, B. S.; Maddox, P. J.; Mastroniani, S.; Mctavish, S. J.; Redshaw, C.; Solan, G. A.; Strömberg, S.; White, A. J. P.; Williams, D. J.; J. Am. Chem. Soc. 1999, 121, 8728.

56. Small, B. L.; Brookhart, M.; Bennett, A. M. A.; J. Am. Chem. Soc. 1998, 120, 4049.

57. Small, B. L.;Brookhart, M.; J. Am. Chem. Soc. 1998, 120, 7143.

58. Sinn, H.; Kaminski, W.; Vollmer, H.J.; Woldt, R. ; Angew. Chem., Int. Ed. Engl. 1980, 19, 390.

59. Kaminsky, W.; Kuper, K.; Brintzinger, H.H.; FRWP Wild. Angew. Chem. Int. Ed. Engl. 1985, 24, 507.

60. Ewen, J.A.; Jones, R.L.; Racazi, A.; Ferrara, J.D.; J. Am. Chem. Soc. 1988, 110, 6255.

61. Kaminsky, W.; Miri, M.; Sinn, H.; Woldt, R.; Makromol. Chem. Rapid. Commun. 1983, 4, 417.

62. Herwing, J.; Kaminsky, W.; Polym. Bull. 1983, 9, 464.

63. Caporaso, l.; Izzo, l.; Zappile, S.; Oliva L.; Macromolecules 2000, 33(20), 7275-7282.

64. Resconi, L.; Cavallo, L.; Fait, A.; Piemontesi, F.; Chemical Reviews 2000, 100(4), 1253-1346.

65. Spalek, W.; Kiiber, F.; Winter, A.; Rohrmann, J.; Bachmann, B.; Antberg, M.; Dolle, V.; Psulus, E. F.; Organometallics 1994, 13, 954.

66. Mise, T.; Miya, S.; Yamakazi, H.; Chem. Lett. 1989, 10, 1853.

67. Ravazi, A.; Atwood, J. L. J. Am. Chem. Soc. 1993, 11, 7529.

68. Fajardo González, M.; Polo Cerón, D.; Gómez Ruiz, S.; Prasha, S.; "Aplicaciones de nuevos complejos metaloceno en polimerización de olefinas" Dykinson 2010, ISBN: 978-84-9982-018-7.

69. Kaminsky, W.; Miri, M.; Sinn, H.; Woldt R. Makromol. Chem. Rapid Commun. 1983, 4, 225.

70. Mülhaupt, R.; Duschek, T.; Rieger, B. Makromol. Chem. Macromol. Symp. 1991, 48-49, 317-332.

71. Mansel, S.; Pérez, E.; Benavente, R.; Pereña, J.M.; Bello, A.; Röll, W.; Kirsten, R.; Beck, S.; Brintzinger, H-H. Macromol. Chem. Phys. 1999, 200, 1292-1297.

72. Kaminsky, W. Catal. Today 1994, 20, 257-271.

73. Shamiri, A.; Chakrabarti, M.H.; Jahan, S.; Hussain, M.A.; Kaminsky, W.; Aravind, P.V.; Yehye, W.A.; Materials 2014, 7, 5069-5108.

74. Negureanu, L. ; Hall, R. W.; Butler, L. G.; Simeral, L. A.;J. Am. Chem. Soc. 2006, 128, 168.

75. Marques M.; Junior, P.; Guimarães, M.J.; Coutinho, F.; Polímeros: Ciência e Tecnologia 98, 26-40.

76. Bochmann, M.; Cuenca, T.; Ardí, D.T.; J.Organomet. Chem. 1994, 484, 10.

77. Nifant'ev, L. E.; Guidotti, S; Camurati, I.; De Rosa, C.; Auriemma, F.; Laishevtsev, I.P.; Resconi, L.; Di Capua, A.; Journal of the American Chemical Society 2004, 126 (51), 17040-17049.

78. Resconi, L.; Camurati, I.; Sudmeijer, O.; Topics Catal 1999., 7, 145.

79. Böhm, L. L.; Angew. Chem. Int. E. 2003, 42, 5010.

80. Junglin, S.; Mülhaupt, R.; Stehling, U.; Brintzinger, H-H.; Fisher, D.;J. Polym., Polym. Chem. 1995, 33, 1305.

81. Zurek, E.; Ziegler, T.; Prog. Polym. Sci. 2004, 29, 107.

82. Fischer, D.; Dissertation, Universität Freiburg, 1992.

83. Forlini, F.; Tritto, I.; Locatelli, P.; Sacchi, M.C.; Piemontesi, F.; Macromolecular Chemistry and Physics 2000, 201 (4), 401–408.

84. Longo, P.; Oliva, A.; Grassi, C; Pellecchia, C.; Macromol. Chem. 1989, 190, 2357.

85. Fischer, D.; Mulhaupt, R.; Macromol. Chem. Phys. 1994, 195, 1433.

86. Suhm, J.; J. Mat. Chem. 1998, 8, 553.

87. Marco, C.; Gómez, M.A.; Ellis, G.; Arribas, J.M.; J. Appl. Polym. Sci. 2002, 84, 1669.

88. Nagasawa, S.; Fujimori, A.; Masuko, T.; Iguchi, M.; Polymer 2005, 46, 5241.

89. Jang, G.S.; Cho, W.J.; Ha, C.S.; Kim, W.; Kim, H.K.; Colloid Polym. Sci. 2002, 280, 424.

90. Marco, C.; Ellis, G.; Gómez, M. ; Arribas, J.M.; J. Appl. Polym. Sci. 2002, 1, 587.

91. Varga, J.; J. Macromol. Sci. Phys. 2002, 41, 1121.

92. Jacoby, P.; Bersted, B.H.; Kissel, W.J.; Smith, C.E.; J. Polym. Sci. B, Pol. Phys. 1986, 24, 461.

93. Mubarak, Y.; Martin, P. J.; Harkin-Jones, E.; Plast. Rubber Compos. 2000, 29, (7), 307.

94. Turner Jones, A.; Aizlewood, J.M.; Beckett, D.R.; Makromol. Chem. 1964, 75, 134.

95. Natta, G.; Corradini, P.; Nuovo Cimento Suppl. 1960, 15, 40.

96. Meille, S.V.; Ferro, D.R.; Brückner, S.; Macromol. Symp. 1995, 89, 499.

97. Thomann, R.; Wang, C.; Macromolecules 1996, 29, 8425.

98. Pérez, E.; Zucchi, D.; Sacchi, M.C.; Forlini, F.; Bello, A.; Polymer 1999, 41, 341.

99. Lovinger. A.J.; J. Polym. Phys. 1983, 21 (1), 97.

100. Hosier, I. L.; Alamo, R. G.; Esteso, P.; Isasi, J. R.; Mandelkern, L.; Macromolecules 2003, 36, 5623.

101. De Rosa, C.; Aurienma, F.; Paolillo, M.; Resconi, L.; Camurati, I.; Macromolecules 2005, 38, 9143.

102. Arranz-Andrés, J.; Peña, B.; Benavente, R.; Pérez, E., Cerrada, M. L.; Eur. Polym. J. 2007, 43, 2357-2370.

103. Brückner, S.; Meille, S. V.; Petraccone, V.; Pirozzi, B. Prog. Polym. Sci. 1991, 16, 361.

104. Phillips, P. J.; Mezghani, K.; Salamone, J.C.; Ed. CRC Press: Boca Raton 1996, 9, 6637.

105. Kalay, G.; Bevis, M.; Journal of Polymer Science Part B 1996. 35(2), 265-291.

106. Coccorullo, I.; Pantani, R.;Titomanlio, G.; Polymer 2003. 44, 307-310.

107. Grebowicz, J.; Lau, S.-F.; Wunderlich, B.; Journal of Polymer Science: Polymer Symposia, 71 (1), 19–37.

108. Slichter, W. P.; Mandell, E. R.; J. Appl. Phys. 1958, 29, 1438.

109. Corradini, P.; de Rosa, C.; Guerra, G.; Petraccone, V. Polym. Commun. 1989, 30, 281.

110. Corradini, P.; Petraccone, V.; De Rosa, C.; Guerra, G.; Macromolecules 1986, 19, 2699-2703.

111. Ferrer-Balas, D.; Maspoch, M.L.; Martínez, A.B.; Polymer 2001, 42(4), 1697-1705.

112. Vittoria, V. J. Macromol. Sci-Phys. 1989, B28, 489-502.

113. Okane, W.J.; Young, R.J.; Ryan, A.J.; Bras, W.; Derbyshire, G.E.; Mant, G.R. Polymer 1994, 35, 1352-1358.

114. Mileva, D.; Androsch, R. H.; J. Radusch. Polym. Bull. 2009, 62, 561.

115. Mileva, D.; Cavallo, D.; Gardella, L.; Alfonso, G.C.; Portale, G.; Balzano, L.; Androsch, R.; Polym. Bull. 2011, 67, 497.

116. Cerrada, M.L.; Polo-Corpa, M.J.; Benavente, R.; Pérez, E.; Velilla, T.; Quijada, R.; Macromolecules, 2009, 42 (3), 702.

117. Mezghani, K.; Philips, P.J.; Polymer 1998, 39, 3735.

118. Alamo, R.G.; Kim, M.H.; Galante, M.J.; Isasi, J.R.; Mandelkern, L.; Macromolecules 1999, 32, 4050.

119. De Rosa, C.; Auriemma, F.; Circelli, T.; Wymouth, R.M.; Macromolecules 2002, 35, 3622.

120. De Rosa, C.; Auriemma, F.; Macromolecules 2002, 35, 9057.

121. Turner-Jones, A.; Polymer 1966, 7, 23.

122. Turner-Jones, A.; Polymer 1971, 12, 487.

123. De Rosa, C.; Auriemma, F.; Ruiz de Ballesteros, O.; Resconni, L.; Camurati, I.; Macromolecules 2007, 40, 6600.

124. Laihonen, S.; Gedde, U.W.; Werner, P.E.; Martínez-Salazar, J.; Polymer 1997, 3, 361.

125. Pérez, E.; Gómez-Elvira, J.M.; Benavente, R.; Cerrada, M.L.; Macromolecules 2012, 45, 6481.

126. Polo-Corpa, M.J.; Benavente, R.; Velilla, T.; Quijada, R.; Pérez, E.; Cerrada, M.L.; Eur. Polym. J. 2010, 46, 1345.

127. Mileva, D.; Androsch, R.; Cavallo, D.; Alfonso, G.C.; Eur. Polym. J. 2012, 48, 1082.

128. J. Arranz-Andrés, J.; Parrilla, R.; Cerrada, M.L.; Pérez, E.; Macromolecules 2013, 46, 8557.

129. Mileva, D.;, Androsch, R.; Radusch, H-J. Polym. Bull. 2008, 61, 643–654.

130. De Rosa, C.; Ruiz de Ballesteros, O.; Auriemma, F.; Di Caprio, M.R.; Macromolecules 2012, 45 (6), 2749–2763.

131. Pérez, E.; Cerrada, M.L.; Benavente, R.; Gómez-Elvira, J.M.; Macromol. Res. 2011, 19, 1179.

132. van Reenen, A.J.; Basson, N.C. Express Polym. Lett. 2012, 6, 427-436.

133. Li, R.; Zhang, X.; Zhao, Y.; Polymer 2009, 50, 5124-5133.

134. Fayolle, B.; Tcharkhtchi, A.; Verdu, J.; Polymer Testing 2004, 23, 939-947.

135. Fan, Y.; Zhang, C.; Xue, Y.; Polymer 2011, 52, 557-563.

136. Bartczak, Z.; Argon, A.S.; Cohen, R.E.; Polymer 1999, 40, 2347.

137. Weon, J-I.; Sue, H.-J.; J. Mater. Sci. 2006, 41, 2291-2300.

138. Karger-Kocsis, J. Prefacio. Polypropylene Structure, Blends and Composites: Copolymers and Blends (1ªEd). London (UK): Ed. Chapman & Hall 1995.

139. Day, M.; Cooney, J. D.; Klein, C.; Fox, J.; Polym. Prepr. Am. Chem. Soc., Div. Polym. Chem. 1993, 34, 123−124.

140. Fouhy, K.; Kim, I.; Moore, S.; Culp, E. Chem. Eng. 1993, 100, 30−33.

141. Scott, D. S.; Majerski, P.; Piskorz, J.; Radlein, D.; Barnickel, M. Can. J. Chem. Eng. 1999, 77, 1021−1027.

142. Gómez-Elvira, J.M., Benavente, R., Martínez, M.C. Polym. Degrad. Stab. 2015, 117, 46-57.

143. Kumar R., Madras G. J. Appl. Polym. Sci. 2003, 90, 2206-2213.

144. Thompson, M.R. ,Part A 1997, 35, 3083-3086 / Sawaguchi, 1995, 28, 7973-7978.

145. Aguado, J.; Sotelo, J.L.; Serrano, D.P.; “Feedstock Recycling of Plastic waste”, RSC 1999, Cambridge.

146. Faisant, J.B.; Ait-Kodi, A.; Bousmina, M.; Desoheues, L. Polymer. 1998, 39, 533-545.

147. Demarquette, N.R.; Kamal, M.R. J. Appl.Polym. Sci. 1998, 70, 75-87.

148. Abad, M.J.; Ares, A.; Barral, L.; Cano, J.; Díez, F.J.; García-Garabal, S.; López, J.; C. Ramírez, J. Appl. Polym. Sci. 2004, 94, 1763-1770.

149. <http://www.ineos.com/Global/Olefins%20and%20Polymers%20Europe/Brochures/flyer_PP_film.pdf>[consulta: 08/2015]

150. García-Peñas, A.; Gómez-Elvira, J.M.; Pérez, E.; Cerrada, M.L. J. Polymer Sci. Polymer Chem. 2013, 51, 3251-3259.

151. García-Peñas, A.; Gómez-Elvira, J.M.; Pérez, E.; Cerrada, M.L. J. Polymer Sci. Polymer Chem. 2014, 52, 2537-2547.

152. García-Peñas, A.; Gómez-Elvira, J.M.; Lorenzo, V.; Pérez, E.; Cerrada, M.L. Eur. Polym. J. 2015, 64, 52-61.

CAPÍTULO 2

Isotactic Poly(propylene-*co*-1-pentene-*co*-1-hexene) Terpolymers: Synthesis, Molecular Characterization and Evidence of the Trigonal Polymorph

Alberto García-Peñas, José M. Gómez-Elvira, Ernesto Pérez and María L. Cerrada.

Journal of Polymer Science Part A: Polymer Chemistry, 2013. 51 (15), 3251–3259.

2.1. Abstract

Terpolymers based on propylene with 1-pentene and 1-hexene as comonomeric units are satisfactorily synthesized using a metallocene catalyst. Thus, several terpolymers are prepared with distinct overall compositions in comonomers as well as three different 1-pentene/1-hexene ratios at a given composition to evaluate the influence on polymerization activity, intrinsic viscosity and microstructural details. The new trigonal δ polymorph is observed in those quenched terpolymers with a global content in comonomers of about 14 mol %, independently of the ratio between both comonomers. However, preliminary results indicate a profound influence of that ratio on the crystallization rate.

2.2. Introduction

The use of metallocene catalysts from the late 1980s for the olefin polymerization introduced important changes as their single-site characteristics [1,2] leaded to produce polymers with nearly the same chain architecture, [3,4] that is polyolefins with narrower molecular weight distributions rather than those synthesized using Ziegler-Natta catalysts and, consequently, with new properties. There are a variety of materials that, for the first time, could be prepared with high activity by these metallocene catalysts such as long chain-branched polyethylene [5], polypropylenes with low amounts of oligomers and different tacticities [6] (atactic, isotactic, isoblock, stereoblock, and syndiotactic), copolymers based on ethylene or propylene with a high proportion (5-30%) of long chain α-olefins [7-14]; elastomers made of ethylene, propene, and dienes (EPDM) [15,16], syndiotactic polystyrene [17,18] with a high melting point, homo- and copolymerization of cyclo-olefins [19-22]; and polymerization in the presence of fillers [23,24], filled polyolefins [25-27], or blends [28-30].

In fact, a new polymorphic form has been recently reported [31-37] in the case of metallocene isotactic copolymers of propylene with high contents of 1-hexene (isotactic propylene-1-hexene copolymers, iPPHe) or 1-pentene (isotactic propylene-1-pentene copolymers, iPPPe) as comonomers. The structure of this trigonal form in these iPPHe and iPPPe copolymers represents the fulfillment of the principles of polymer crystallography and indicates that the packing of polymer molecules is mainly driven by density (principle of entropy−density-driven phase formation in polymers) [38]. In specimens slowly or isothermally crystallized, both types of copolymers (iPPHe and iPPPe) develop the α and/or γ forms of isotactic polypropylene (iPP) for comonomer concentrations lower than about 10 mol %, whereas they crystallize in the new trigonal form at higher 1-hexene and 1-pentene concentrations. In fast cooled samples, the scenario is somehow different. Then, the monoclinic (and/or orthorhombic) crystallites are not the only competitors of this new trigonal phase but

the mesomorphic form [34] is also playing a primary role in this composition range: at low comonomer contents, the monoclinic form is primarily developed (gathered with a reduced and variable amount of the iPP orthorhombic polymorph, depending on the copolymer microstructural details); copolymers with molar compositions ranging around 5-10 are able to generate easily the mesomorphic structure. This form is already well-known in the iPP [39] for decades; the great difference is, however, that these mesomorphic entities can be developed in much milder conditions in these copolymers with intermediate comonomer contents than those necessary ones for their achievement in the iPP homopolymer. Moreover, its formation is even easier when the comonomer content is increased [14,40]. Nevertheless, at higher compositions the new trigonal polymorph is the only one able to crystallize although there are kinetic differences between using 1-hexene or 1-pentene as comonomers [34,40]. The obtainment of this trigonal δ polymorph only in propene-based copolymers using 1-hexene or 1-pentene as comonomers triggers the following question: what does it occur if both counits are involved, that is, if terpolymers are synthesized instead of iPPHe or iPPPe copolymers? To the best of our knowledge, up to now, there exists no investigation that is reported in open literature, concerning the preparation and characterization of terpolymers based on propylene and both 1-pentene and 1-hexene comonomers in a broad composition interval. Accordingly, the aim of this article is to describe the synthesis of these propylene-*co*-1-pentene-*co*-1-hexene terpolymers at different global compositions in comonomers (1-pentene or 1-hexene) and at three distinct 1-pentene/1-hexene ratios at a given total composition, as well as to perform a thorough and complete molecular characterization. Furthermore, the crystalline structure generated at the different compositions will be checked by applying the regular industrial processing conditions, that is, a rapid cooling from the molten state. Finally, a preliminary analysis of the influence of the comonomer ratio on the crystallization rate is also performed.

2.3. Experimental

2.3.1. Materials

Toluene (Merck) and the comonomers 1-pentene and 1-hexene (Acros) have been previously refluxed over sodium, distilled and kept under N_2 to avoid the presence of traces of water and oxygen. Both propylene (Praxair 2.5) and nitrogen (Praxair 3X) were passed through oxygen-trap columns and molecular sieves before their use. The catalyst *rac*-dimethylsilyl*bis*(1-indenyl) zirconium dichloride (Strem) and the cocatalyst methylaluminoxane (MAO) (10 wt % solution in toluene, from Aldrich) were used as received. The activated catalyst was prepared by dissolving 15 mg of the metallocene in 3 mL of MAO solution. A volume of 0.125 mL containing 1.39 X 10^{-6} mol of the active complex was used in each polymerization. Ethanol (Acros, 96%) and HCl (VWR, 37%) were used for the precipitation of the polymers.

2.3.2. Synthesis of the poly(propylene-*co*-1-pentene-*co*-1-hexene) terpolymers

The terpolymerization of propylene with 1-pentene and 1-hexene was carried out in a 250-mL stainless steel autoclave at -5 °C in toluene (90 mL) by using *rac*-dimethylsilylbis(1-indenyl)zirconium dichloride/MAO as the catalyst/cocatalyst system ([Al]/[Zr]= 3648). The initial propylene pressure was 0.35 bar, the catalyst amount was 1.39 X 10^{-6} mol, and the starting comonomers/propylene molar ratio ranging from 0 to 0.905. In addition, three 1-pentene/1-hexene ratios (75:25; 50:50; 25:75) were studied for every single comonomer/propylene feeding. The polymerization was stopped by adding 5 mL of ethanol and enabling the unreacted propylene out from the reactor. The polymer was obtained as a powder by pouring the reaction batch on a mixture of ethanol/HCl (30:1). The precipitated was stirred thoroughly overnight, filtrated, washed again with ethanol and, afterwards, dried under vacuum at room temperature. Table 1 summarizes the four series of terpolymerization runs carried out. They are referred as T followed by the total content of comonomers and the relative proportion of 1-pentene and 1-hexene used in the feeding being indicated

next. Thus, for example, T4-75Pe-25He stands for a run that yields a total composition in comonomers around 4 mol % and with a 1-pentene/1-hexene mole ratio of 75:25.

Table 1. Data of terpolymerization runs.

Sample	Composition (mol %)	$(C_6+C_5)/C^a$ (mole ratio)	Activity (Kg mol^{-1}(prop) mol^{-1}(cat) h^{-1})
iPP	0	0	443
T4-75Pe-25He	4.3	0.245	3496
T4-50Pe-50He	4.0	0.245	566
T4-25Pe-75He	3.7	0.245	4939
T7-75Pe-25He	7.1	0.423	5571
T7-50Pe-50He	6.7	0.423	5398
T7-25Pe-75He	6.6	0.423	8608
T10-75Pe-25He	10.3	0.579	6392
T10-50Pe-50He	9.2	0.579	6367
T10-25Pe-75He	9.6	0.579	5581
T14-75Pe-25He	13.7	0.905	10826
T14-50Pe-50He	14.5	0.905	8863
T14-25Pe-75He	13.5	0.905	11188

[a] The mole content of propylene in the reaction medium was estimated by means of the relationship given by Ferreira et al.[41] from a propylene pressure of 0.35 bar at -5 ºC in a volume of 90 mL of toluene.

2.3.3. Synthesis of the poly(1-pentene), poly(1-hexene) and poly(1-hexene-*co*-1-pentene) copolymers

The homopolymerization of every comonomer has been carried out in the bulk at room temperature by adding 5.6 X 10^{-7} mol of the activated metallocene ([MAO]/[Zr]=3246) to 5 mL of the comonomer under N_2. The same procedure has been employed in the case of the copolymerization of both comonomers, but at 0 °C. The polymers were precipitated with acidified ethanol (ethanol/HCl, 30:1), washed with ethanol, and dried under vacuum at 100 °C.

2.3.4. Viscosimetry

The intrinsic viscosity values were determined in decalin stabilized with Irganox 1010 (1 g·L^{-1}) at 135 °C.

2.3.5. Nuclear magnetic resonance characterization

The composition in comonomers as well as the tacticity of the samples were determined by carbon nuclear magnetic resonance, ^{13}C NMR, analysis from a solution of the polymers in 1,1,2,2-tetrachloroethane-*d4* (70 mg/1 mL) at 80 °C, using an Innova 400 spectrometer (100 MHz). In the case of the samples of the T4 series, the ^{13}C NMR spectra were obtained from 1,2,4-trichlorebenzene solutions in a Bruker Avance DPX-300 (75 MHz) at 100 °C, using deuterated *o*-dichlorobenzene as an internal reference. A minimum of 8000 scans were recorded with broad band proton decoupling and using an acquisition time of 1 s, a relaxation delay of 4 s, and a pulse angle of 45°.

2.3.6. Diffraction profiles

Wide-Angle X-Ray diffraction patterns were recorded in the reflection mode by using a Bruker D8 Advance diffractometer provided with a PSD Vantec detector (from Bruker, Madison, WI). Cu Kα radiation (λ = 0.1542 nm) was used, operating at 40 kV and 40 mA. The parallel beam optics was adjusted by a parabolic Göbel mirror with

horizontal grazing incidence Soller slit of 0.12° and LiF monochromator. The equipment was calibrated with different standards. A step scanning mode was employed for the detector. The diffraction scans were collected with a 2θ step of 0.024° and 0.2 s per step.

2.3.7. DSC analysis of the crystallization rate

A preliminary analysis of the crystallization rate has been performed on T14 terpolymers by using a Perkin-Elmer DSC-7 calorimeter connected to a cooling system and calibrated with different standards. The sample weight was around 2 mg.

2.4. Results

2.4.1. Catalyst activity

The apparent activity of the catalyst/cocatalyst system used has been estimated as the weight of polymer obtained during the whole polymerization time per mole of both propylene and Zr. The results summarized in Table 1 can be fitted roughly into a straight line when they are plotted as a function of the total comonomer content in the feeding (Fig. 1). In this fit, the two runs showing strong deviations from the standard average findings have been neglected. As it has been profusely reported in the literature [42-48], an increasingly ratio of the α-olefin enhances the activity of metallocene catalyst centers in ethylene or propylene polymerization. Among the factors causing this observed rate enlargement, a positive effect in the polymer solubility, [49] an enhanced chain transfer activity, [50] and a modification of the active center quality [50] have been claimed to play a significant role as a consequence of the comonomer presence. Moreover, the growth of the activity is concomitant with a decrease in molecular weight as Figure 2 clearly shows from the viscosity variation on overall comonomer composition.

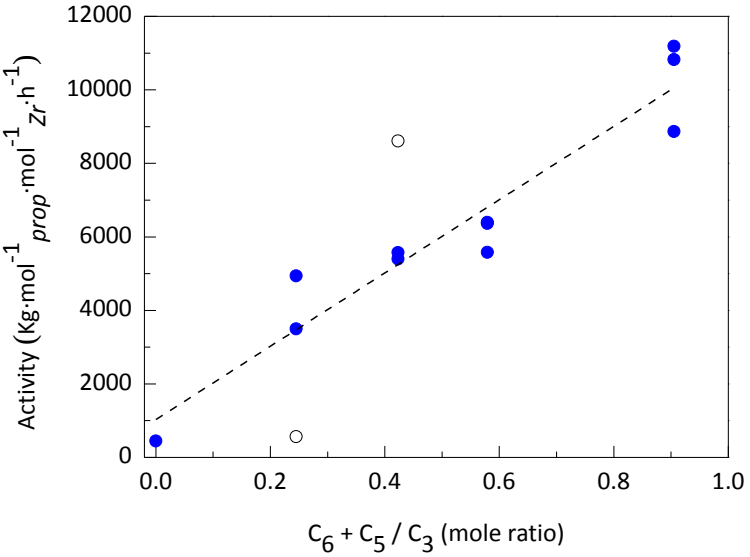

Figure 1. Evolution of catalytic activity as a function of the global feed ratio of comonomers (white circles correspond to runs that do not fit the average findings).

2.4.2. Determination of intrinsic viscosity

It is well known that the molar mass of either ethylene or propylene-based copolymers decreases remarkably upon addition of α-olefins in the feeding. [48,50,51] In this particular case, where propylene-based terpolymers have been synthesized, the intrinsic viscosity has been taken as a magnitude directly related to the molar mass, and its variation shown in Figure 2 undoubtedly shows the expected trend, that is, the higher is the comonomer composition in the copolymer, the smaller is the intrinsic viscosity obtained. It is worth noticing that the viscosity values fit a straight line regardless of the three different 1-pentene/1-hexene ratios used. This fact allows inferring that the role of both comonomers as chain-transfer agents in the polymerization must be quite similar.

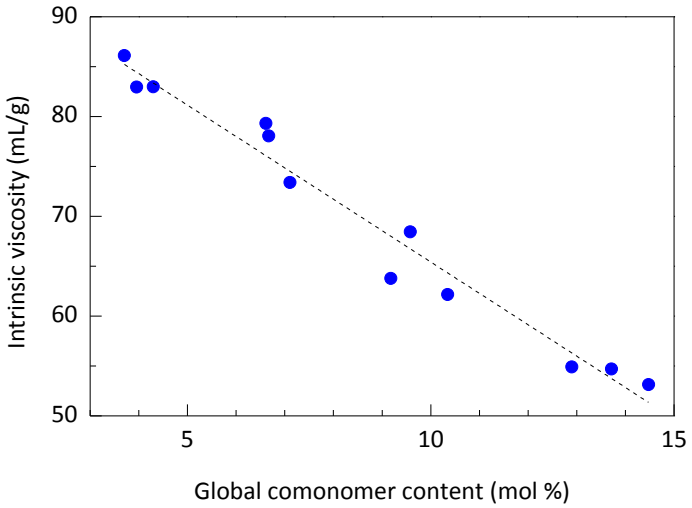

Figure 2. Variation of the intrinsic viscosity in decaline at 135 °C as a function of the global comonomer content.

2.4.3. Evaluation of microstructure

The characteristic ^{13}C NMR peaks of the terpolymers under study are assigned in Figure 3 which shows the spectrum of T10-25Pe-75He together with those of the reference homopolymers as well as with that of the (90/10) poly(1-hexene-*co*-1-pentene) copolymer (HA 90/10 copolymer). These signals can be undoubtedly assigned from the data reported in the literature about the iPP copolymers with 1-pentene and 1-hexene. [46,52,53] Table 2 summarizes their respective chemical shifts in 1,1,2,2-tetrachloroethane-*d4* at 80 °C and the carbon nuclei that are related to. The different carbon nuclei have been named as P, A, and H as belonging to propylene, 1-pentene, and 1-hexene, respectively, for the purpose of making the identification easier [46] (X refers to a comonomeric unit independently of being 1-pentene or 1-hexene). In addition, a superscript that denotes the carbon position in the corresponding monomer, according to Scheme I, is also used.

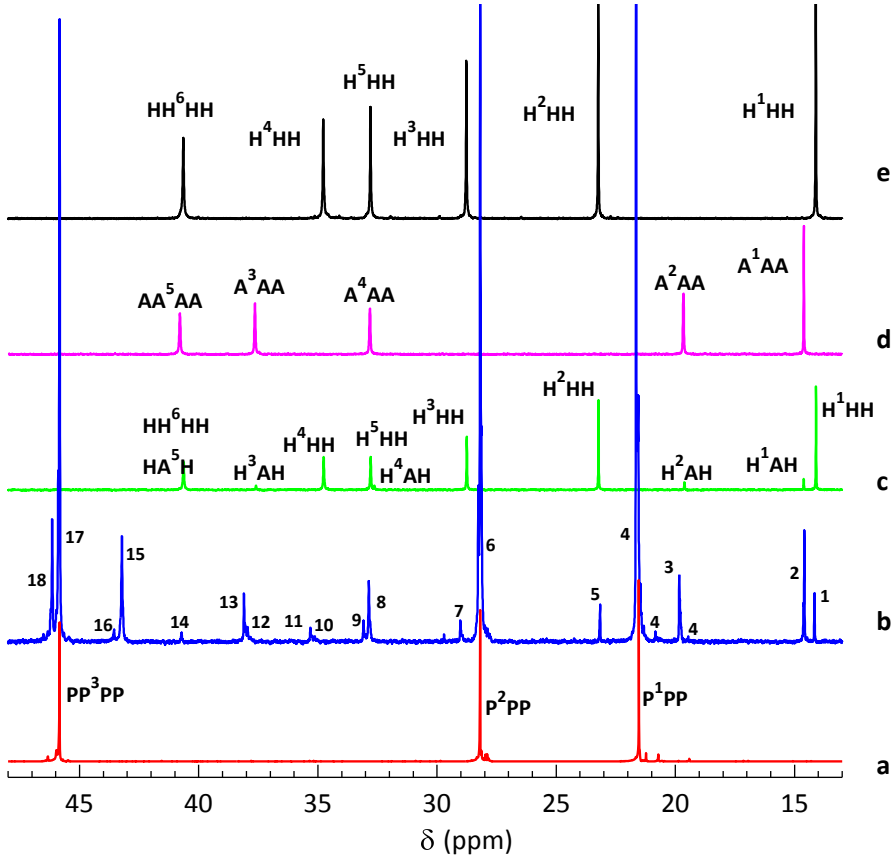

Figure 3. ^{13}C NMR spectra of (a) Ipp, (b) T10-25Pe-75He, (c) the (90/10) poly(1-hexene-*co*-1-pentene), (HA 90/10 copolymer), (d) Poly(1-pentene), and (e) Poly(1-hexene).

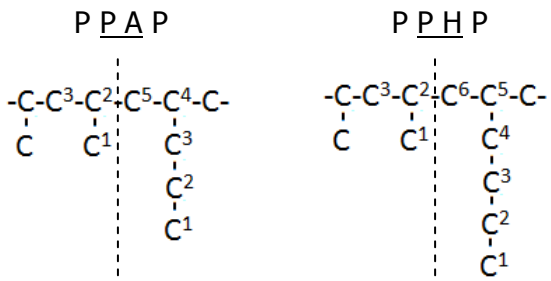

Scheme 1. Numeration of carbons belonging to propylene (P), 1-pentene (A), and 1-hexene (H) in the polymer chain.

Table 2. Experimental chemical shifts and assignments (Scheme 1) of the ^{13}C NMR peaks of poly(propene-*co*-1-pentene-*co*-1-hexene) terpolymers observed in 1,1,2,2-tetrachloroethane-*d4* at 80 ºC.

Peak	Chemical Shift (ppm)[a]	Carbon Nucleus: P=propylene; A=1-pentene; H=1-hexene
1	14.16	^{1}H
2	14.58	^{1}A
3	19.83	^{2}A
4	19.4-22.0	^{1}P ($P^{1}PP+P^{1}PX$)
5	23.16	^{2}H
6	27.6-28.6	^{2}P ($P^{2}PP+P^{2}PX$)
7	29.02	^{3}H
8	32.86	^{4}A
9	33.09	^{5}H
10	35.12	$X^{4}HP$
11	35.31	$P^{4}HP$
12	37.94	$X^{3}AP$
13	38.10	$P^{3}AP$
14	40.72	$PX^{5,6}XP$
15	43.22	$PP^{5,6}XP+PP^{5,6}XX$
16	43.54	$XP^{5,6}XX+XP^{5,6}XP$
17	45.84	$PP^{3}PP$
18	46.15	$PP^{3}PX$

[a] Chemical shifts are referenced to $C_4D_2Cl_4$ (74.00 ppm). X is related to comonomeric unit independently of being 1-pentene or 1-hexene.

The molar content in every comonomer for the different terpolymers is listed in Table 3. It was estimated from the relative intensities of the methyl signals at 14.58 ppm (1-pentene), 14.16 ppm (1-hexene) and 19.4-22.0 ppm (propene) in the ^{13}C NMR spectra. The methyl window of the T4-25Pe-75He sample is shown in Figure 4 as an example. In this particular case, the comonomers are exclusively present as isolated units and the assignation of the comonomer side-chain carbons can be made at the compositional triad level.

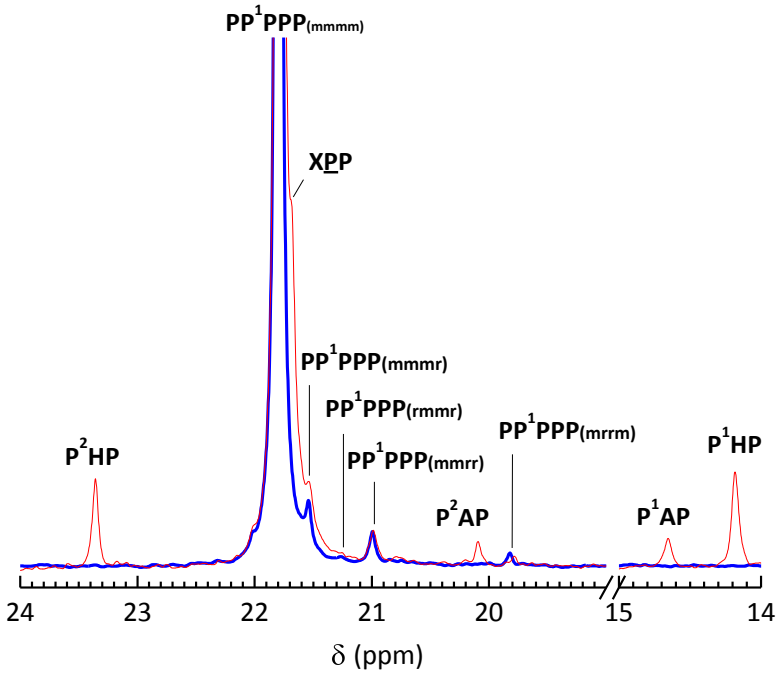

Figure 4. Methyl ^{13}C NMR spectral window of T4-25Pe-75He (thin line) and iPP (thick line) obtained in *o*-dochlorobencene at 100 °C.

The C_2-symetric *ansa* metallocene used leads only to *mrrm* stereodefects. This fact allows an accurately measure of the propene methyl area because, although the side-chain β-methylene carbon of the 1-pentene unit (P^2AP in Fig. 4) appears inside the region of syndiotactic methyls, this signal overlaps with the nonexistent *mrrr* misinsertion, and not with the *mrrm* one. However, the so-obtained compositions of the terpolymers have been compared with those ones deduced from the methine carbons, and no appreciable differences have been found. Moreover, the propylene tacticity can be estimated from the methyl region at the pentad level. The results are summarized in Table 3 and show a decrease in the content of *mmmm* propylene units as comonomer composition is increased. The quality of the isotacticity seems to be subtly deteriorated in the case of the T4 series. A small content of the stereodefective sequences *mmrm+rmrr* is actually detected; however, this feature cannot be related to some distortion in the *iso*-selective control of the insertion but to the error in the

mrrm pentad is absent in the other series despite the fact that associated *mmrr* pentad appears necessarily.

It has been widely assumed, on one hand, that no comonomer sequences longer than 2 units are formed in propylene based co- and terpolymers in the composition range studied here and, on the other hand, that most of the comonomers are present as isolated entities disrupting the PPP segments. [46,47,52] This fact is supported by the low intensity of the band at 40.72 ppm in Figure 3. This signal is attributed to $X^{5,6}X$ methylenes and can be considered as exclusively produced by $PX^{5,6}XP$ tetrads. A confirmation is shown in Figure 5 in which it can be checked that this peak does not fit the resonance of a XX methylene carbon inserted in a longer sequence of comonomers, either the characteristic $HH^{6}HH$ or $AA^{5}AA$ signals in poly(1-hexene) and poly(1-pentene), respectively. Additional evidence is supported by those signals that are sensitive enough to composition, as it is the case, for example, of ^{3}A and ^{4}H signals, which is also shown in Figure 5. It can be verified that the bands of $X^{3}AP$ and $X^{4}HP$ carbons in the terpolymer do not correspond with neither those ones of the same nuclei in the homopolymers of poly(1-pentene) and poly(1-hexene) (AAA and HHH triads), nor in the 1-pentene/1-hexene copolymer ($X^{3}AH$ and $A^{4}HX$ sequences).

Some other important features of the ^{13}C NMR spectra of the terpolymers are, first, that methyl and methine carbons (^{1}P and ^{2}P) of propylene units in PPX triads appear at the same chemical shift regardless of the nature of the comonomer X, either A or H. It is also the case for main-chain methylene carbons in the middle of XX and PX diads (peaks 14, 15 and 16 at 40.72, 43.22 and 43.54 ppm, respectively), and for methylene carbons in $P\underline{P^{3}P}X$ sequences (peak 18 at 46.15 ppm). On the contrary, methyl, methine, and side-chain methylene carbons of 1-pentene and 1-hexene units yield distinctive signals (peaks of *n*A and *n*H with *n*=1-4 and *n*=1-5, respectively, in Table 2).

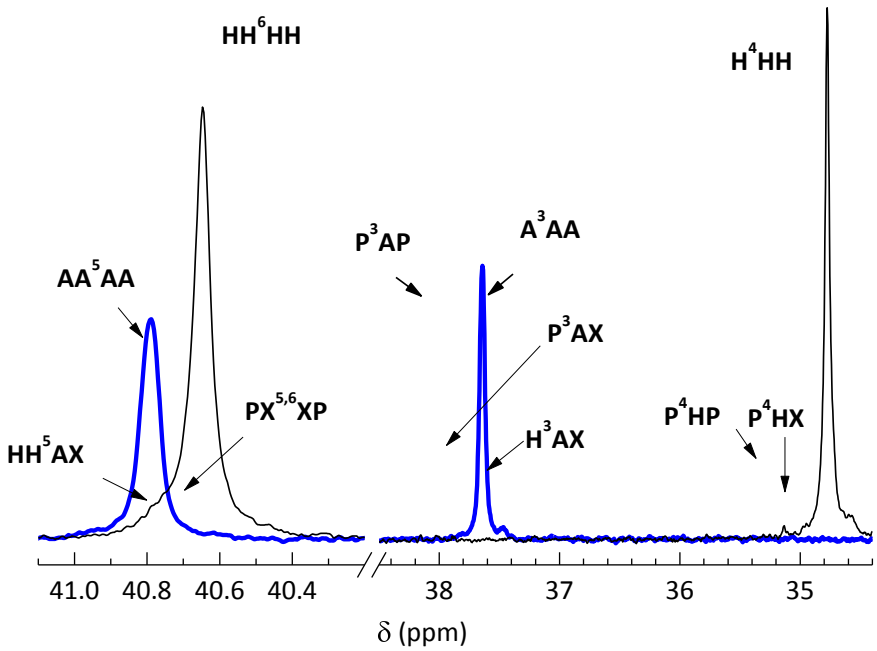

Figure 5. Spectral window of the T10-75Pe-25He (circles), poly(1-pentene) (thick solid line), poly(1-hexene) (thin solid line), and poly(1-hexene-*co*-1-pentene) copolymer (dashed line).

Estimation of the content for PAA, PHH and PAH sequences is not possible owing to the fact that neither main-chain $X^{5,6}X$ methylenes (peak 14) nor side branched X^4HP and X^3AP methylenes (peaks 10 and 12) are sensitive enough to the nature of X. However, a global analysis of the compositional distribution in terms of PXP and PXX has been considered to be accurate enough for the purpose of this study as it provides a detailed description of the chain microstructure, that is, the comonomer content, the propylene average length, and the nature of interruptions, which are, in principle, the main driving factors in the final balance of the different polymorphs produced under given processing conditions. The distribution of the composition from the ^{13}C NMR spectra is then obtained at the triad level by using the following relationships:

$$[PPP] = K\cdot(I_6 - I_{15} - \tfrac{1}{2}\cdot I_{16})$$

$$[PPX] = K\cdot I_{15}$$

$$[XPX] = K\cdot\tfrac{1}{2}\cdot I_{16}$$

(The relationship [XPX] = ½· ([XPXP] + [XXPX]) is applied taking [XXPX]= 0 [47])

$$[PXP] = K\cdot(I_1 + I_2 - 2\cdot I_{14})$$

$$[XXP] = K\cdot 2\cdot I_{14}$$

$$[XXX] = 0$$

where K is a normalization constant and I_n corresponds to the intensity of peak n tabulated in Table 2. The relative content of the different triad sequences is listed in Table 4. It is immediately apparent that comonomer units are mostly isolated and that the content of those ones belonging to XX diads grows from zero in the T4 series to more than 25% of the total composition in the T14 series. Finally, a small but not negligible value of XPX triads denotes the presence of some isolated X units in alternating sequences (XPXP).

From the triad content, the average propylene length has been calculated according to the expression [54]:

$$n_p = ([PPP] + [PPX] + [XPX]) / ([XPX] + \tfrac{1}{2}\bullet[PPX])$$

As summarized in Table 4, the values of n_p change from 24 units in the T4 series to 8 units in the T14 series.

Table 3. Comonomer content of the terpolymers and propylene tacticity at the pentad level.

Sample	Global comonomer (mol %)	A	H	[*mmmm*]	[*mmmr*]	[*rmmr*]	[*mmrr*]	[*mmrm+ rmrr*]	[*mrmr*]	[*rrrr*]	[*rrrm*]	[*mrrm*]
T4-75Pe-25He	4.3	74.7	25.2	86.6	4.5	1.3	2.1	1.4	0.0	0.0	0.0	1.0
T4-50Pe-50He	3.9	54.8	45.1	87.4	4.9	0.9	2.0	1.2	0.0	0.0	0.0	0.8
T4-25Pe-75He	3.7	22.7	77.2	90.2	4.0	0.3	1.7	0.5	0.0	0.0	0.0	0.3
T7-75Pe-25He	7.1	75.3	24.6	90.8	1.0	0.0	1.2	0.0	0.0	0.0	0.0	0.0
T7-50Pe-50He	6.6	52.5	47.4	90.0	1.5	0.0	1.3	0.0	0.0	0.0	0.0	0.0
T7-25Pe-75He	6.6	28.1	71.8	91.5	1.0	0.0	1.0	0.0	0.0	0.0	0.0	0.0
T10-75Pe-25He	10.3	76.8	23.1	87.3	2.3	0.0	0.7	0.0	0.0	0.0	0.0	0.0
T10-50Pe-50He	9.2	52.4	47.5	88.8	1.4	0.0	1.1	0.0	0.0	0.0	0.0	0.0
T10-25Pe-75He	9.6	30.3	69.6	88.1	1.3	0.0	0.7	0.0	0.0	0.0	0.0	0.0
T14-75Pe-25He	13.7	75.3	24.7	83.8	2.3	0.0	1.1	0.0	0.0	0.0	0.0	0.0
T14-50Pe-50He	14.4	50.4	49.5	82.6	3.2	0.0	1.3	0.0	0.0	0.0	0.0	0.0
T14-25Pe-75He	13.5	25.2	74.8	82.2	3.1	0.0	0.8	0.0	0.0	0.0	0.0	0.0

Table 4. Relative content of triads and average propylene length, n_p.

Sample	PPP	PPX	XPX	PXP	XXP	XXX	[XXP]/[PXP+XXP] (x10^2)	n_p
T4-75Pe-25He	87.5	8.0	0.0	4.4	0.0	0.0	0	24
T4-50Pe-50He	87.6	8.0	0.0	4.4	0.0	0.0	0	24
T4-25Pe-75He	87.9	7.7	0.0	4.4	0.0	0.0	0	25
T7-75Pe-25He	80.1	11.9	0.6	6.3	1.1	0.0	14.9	14
T7-50Pe-50He	80.2	11.9	0.5	6.4	0.9	0.0	12.3	14
T7-25Pe-75He	80.7	11.4	0.7	6.0	1.1	0.0	15.5	14
T10-75Pe-25He	72.2	15.7	1.0	9.7	1.4	0.0	12.6	10
T10-50Pe-50He	74.1	15.0	1.0	8.4	1.5	0.0	15.1	11
T10-25Pe-75He	75.2	14.3	0.8	7.6	2.0	0.0	20.8	11
T14-75Pe-25He	64.3	19.7	1.4	10.7	3.8	0.0	26.2	8
T14-50Pe-50He	63.0	19.3	1.8	11.4	4.5	0.0	28.3	7
T14-25Pe-75He	66.2	18.2	1.6	10.3	3.7	0.0	26.4	8

2.4.4. Crystalline structure

As described in the **Introduction** section, this is the first time that the synthesis and characterization of terpolymers based on propylene with 1-pentene and 1-hexene as comonomeric units are reported, whose compositions are ranging up to about 14 mol %. At this initial stage, one of the primary interests for obtaining these terpolymers is directly related to their capability for the formation of the new trigonal form, previously found in iPPPe and iPPHe copolymers. Figure 6 shows the wide-angle X-ray scattering (WAXS) profiles found in rapidly cooled films of the terpolymers with different global composition at a given ratio of 1-pentene/1-hexene (75:25). The variation of the crystalline structure with the overall content in comonomers is clearly seen. Thus, T4-75Pe-25He exhibits the diffractions that characterize the monoclinic α lattice. There is not evidence of the (117) reflection stemming from the orthorhombic

cell, most probably because of the high cooling rate used during the film processing. The increase of composition in both comonomers, T7-75Pe-25He terpolymer, leads to the development of a minor amount of defective monoclinic crystallites in addition to a majority of mesomorphic entities. The situation is somehow different in the T10-75Pe-25He terpolymer where the macromolecular chains are only able to be ordered into mesomorphic entities.

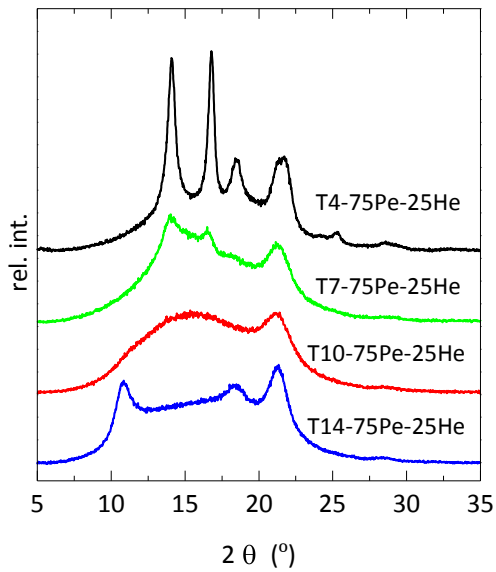

Figure 6. X-ray diffractograms, at room temperature, for the terpolymers (rapidly cooled from the melt) at different overall compositions and identical 1-pentene/1-hexene ratio (75:25). From top to bottom: T4-75Pe-25He, T7-75Pe-25He, T10-75Pe-25He, and T14-75Pe-25He, respectively.

The two broad diffraction characteristic of this intermediate ordering are, then, clearly observed in the WAXS pattern. If content in comonomers is further raised, T14-75Pe-25He terpolymer, a diffraction located at around 10.5° is noticed, this being characteristic from presence of the trigonal δ polymorph. These δ crystals are rather imperfect, as deduced from the considerable width of their reflections owing to the thermal treatment applied during film preparation.

Figure 7 shows the WAXS profiles found in the T14 terpolymers with nearly identical overall composition and distinct 1-pentene/1-hexene ratios. All of them are able to generate the trigonal lattice, and it appears that T14-50Pe-50He is the

terpolymer with somewhat higher crystallinity and more perfect crystallites. These features can be ascribed to the fact that this terpolymer presents a slightly higher overall composition (Table 3), and this parameter has a key role in the formation of the new trigonal polymorph.

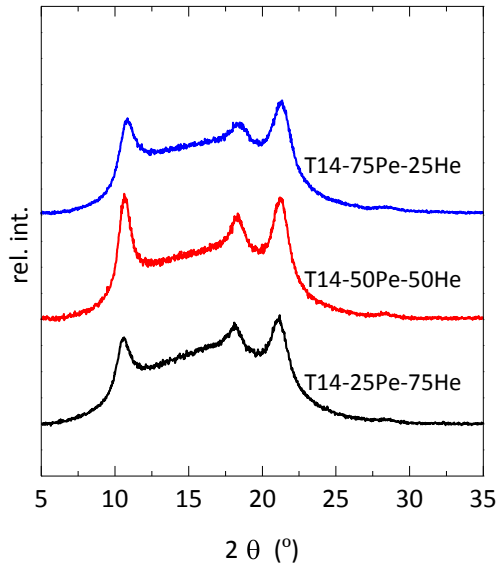

Figure 7. X-ray diffractograms, at room temperature, for the terpolymers (rapidly cooled from the melt) at a given overall composition and different 1-pentene/1-hexene ratios. From top to bottom: T14-75Pe-25He, T14-50Pe-50He, and T14-25Pe-75He, respectively.

More interesting is the behavior of the crystallization rate in these T14 terpolymers. A preliminary analysis of that rate has been performed by means of differential scanning calorimetry (DSC) experiments. Thus, the upper frame of Figure 8 shows the DSC curves of the three T14 terpolymers on cooling from the melt at 4 °C/min. It can be clearly observed that the enthalpy involved in the crystallization exotherm changes very much with the ratio of 1-pentene/1-hexene in the terpolymer, and that enthalpy decreases with increasing 1-hexene counits. Moreover, the exotherm peak temperature is also dependent on that ratio, and lower values are found with rising 1-hexene content, those values being very close to the glass transition temperature. Both facts can be interpreted by a considerably slower crystallization rate when the 1-hexene proportion is enlarged. This is clearly

ascertained in the subsequent heating ramps shown in the lower frame of Figure 8. Thus, the melting curve for terpolymer T14-75Pe-25He shows the glass transition at around -15 °C, followed by the main melting endotherm at 64 °C. On the contrary, the other two samples show a clear cold crystallization on heating, which increases with the 1-hexene proportion, indicating that crystallization was not completed on cooling at 4 °C min^{-1}. Moreover, the melting temperature seems to be dependent on 1-pentene/1-hexene ratio and, thus, it is shifted to higher temperatures as 1-pentene content increases. This fact can be associated with a smaller tolerance of the 1-hexene units within the crystal structure because of their longer pendant branches. However, it is also important to note that crystallization temperature [(Fig. 8(a)] decreases as 1-hexene content rises. Therefore, the lower melting temperature found in T14-25Pe-75He can also be explained owing to its inferior crystallization temperature.

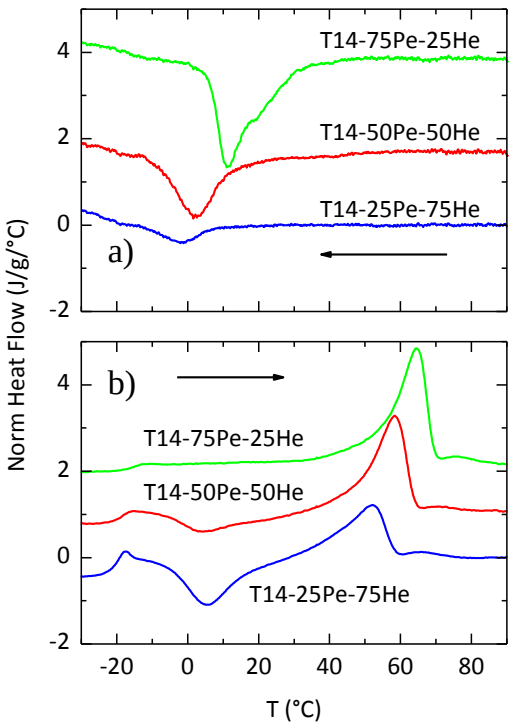

Figure 8. DSC curves (normalized to the scanning rate) for terpolymers T14 with different 1-pentene/1-hexene ratios: (a) cooling curves at 4 °C/min, (b) subsequent heating curves at 10 °C/min. From top to bottom: T14-75Pe-25He, T14-50Pe-50He, and T14-25Pe-75He, respectively.

Additional experiments are being planned (by means of DSC and real-time synchrotron X-ray diffraction) to obtain a better picture of the effect of the 1-pentene/1-hexene proportion in the terpolymers on the final crystallization rate (and on the crystal forms obtained as well as on their properties).

2.5. Conclusions

Different terpolymers, based on propylene with 1-pentene and 1-hexene as comonomeric units, have been synthesized at several global compositions in comonomers (ranging from around 4 to 14 mol %) and three 1-pentene/1-hexene ratios at a given composition. Intrinsic viscosity decreases as comonomer content is increased, pointing out a reduction in molecular weight with increasing composition in comonomers.

Both comonomeric units are randomly incorporated into the macrochains, although isotacticity is lowered as comonomer composition is raised in the terpolymers. Nevertheless, the quality of this isotacticity is most deteriorated in the T4 series. In fact, the content of the *mmmm* pentad is lower than in the T7 series and the content of the *mmmr* and *rmmr* pentads is relatively high. Furthermore, some other stereodefective sequences (*mmrm* + *rmrr*), not-present in the other series, appear in T4 terpolymers. These features could be associated with a change in the polymerization mechanism compared with that occurring at higher compositions.

The new trigonal δ polymorph is clearly observed in rapidly cooled films prepared from those terpolymers with a global content in comonomers of about 14 mol %, independently of the ratio between both comonomers. However, preliminary results indicate a profound influence of that ratio on the crystallization rate.

A competition between monoclinic crystallites, mesomorphic entities, and trigonal crystals takes place within the composition interval analyzed here. A deeper study is now under progress to elucidate the exact effect of each comonomeric unit in the kinetic aspects of development of the different ordered forms. The full

understanding of the relationships between these crystalline structures and properties could allow tailoring different polypropylenes having desired physical properties.

2.6. References

1. H. Sinn, W. Kaminsky, H.J. Vollmer, R. Woldt, Angew. Chem. Int. Ed. 1980, 19, 390.
2. H.H. Brintzinger, D. Fischer, R. Mulhaupt, B. Rieger, R.M. Waymouth, Angew. Chem. Int. Ed. 1995, 34, 1143.
3. V.K. Gupta. In: Cheremisinoff NP, editor. Handbook of Engineering Polymeric Materials, New York: Marcel Dekker, 1997. p. 155–165. Chap 12.
4. R. Mulhaupt, Macromol. Chem. Phys. 2003, 204, 289.
5. R. Quijada, A. Narvaez, R. Rojas, F.M. Rabagliati, G.B. Galland, R.S. Mauler, R. Benavente, E. Pérez, J.M. Pereña, A. Bello, Macromol. Chem. Phys. 1999, 200, 1306.
6. W. Kaminsky, Catalysis Today 1994, 20, 257.
7. M.L. Cerrada, R. Benavente, E. Pérez. J. Mater. Res. 2001, 16, 1103.
8. M.L. Cerrada, R. Benavente, E. Pérez, J. Moniz-Santos, M.R. Ribeiro, Polymer 2001, 42, 7197.
9. M.F. Laguna, M.L. Cerrada, R. Benavente, E. Pérez, R. Quijada. J. Polym. Sci., Part B: Polym. Phys. 2003, 41, 2174.
10. M.L. Cerrada, E. Pérez, J.M. Pereña, R. Benavente, M. Misheva, T. Grigorov, Macromolecules 2005, 38, 8430.
11. J.M. López Majada, H. Palza, J.L. Guevara, R. Quijada, M.C. Martínez, R. Benavente, J.M. Pereña, E. Pérez, M.L. Cerrada, J. Polym. Sci., Part B: Polym. Phys. 2006, 44, 1253.
12. J. Arranz Andrés, J.L. Guevara, T. Velilla, R. Quijada, R. Benavente, E. Pérez, M.L. Cerrada, Polymer 2005, 46, 12287.

13. H. Palza, J.M. López-Majada, R. Quijada, J.M. Pereña, R. Benavente, E. Pérez, M. L. Cerrada, Macromol. Chem. Phys. 2008, 209, 2259.

14. M.J. Polo-Corpa, R. Benavente, T. Velilla, R. Quijada, E. Pérez, M.L. Cerrada, Eur. Polym. J. 2010, 46, 1345.

15. A.O. Starzewski, N. Steinhauser, B.S. Xin, Macromolecules 2008, 41, 4095.

16. S. Ahmadjo, H. Arabi, M. Nekoomanesh, G.H. Zohuri, M.M. Mortazavi, G. Naderi, Macromol. React. Eng. 2010, 4, 707.

17. B.T. Gall, J. McCahill, D.W. Stephan, R. Mulhaupt, Macromol. Rapid Comm. 2008, 29, 1549.

18. C.L. Huang, Y.C. Chen, T.J. Hsiao, J.C. Tsai, C. Wang, Macromolecules 2011, 44, 6155.

19. W. Kaminsky, A. Bark, R. Spielh, N. Muller-Lindenhof, S. Niedoda, in: Transition Metals and Organometallics as Catalysts for Olefin Polymerization, W. Kaminsky, H. Sinn, Eds., Springer, Berlin 1988, p. 291.

20. J. Forsyth, J.M. Perena, R.Benavente, E. Pérez, I. Tritto, L. Boggioni, H.H. Brintzinger, Macromol. Chem. Phys. 2001, 202, 614.

21. I. Tritto, L. Boggioni, J.C. Jansen, K.Thorshaug, M.C. Sacchi, D.R. Ferro, Macromolecules 2002, 35, 616.

22. T. Hasan, T. Ikeda, T. Shiono, Macromolecules 2004, 37, 8503.

23. A.A. Kovalchuk, V.G. Shevchenko, A.N. Shchegolikhin, P.M. Nedorezova, A.N. Klyamkina, A.M. Aladyshev, J. Materials Sci. 2008, 43, 7132.

24. A. Bento, J. P. Lourenço, A. Fernandes, M. L. Cerrada, M. Rosário Ribeiro, ChemCatChem (DOI:10.1002/cctc.201200639)

25. M.L. Cerrada, R. Benavente, E.Perez, Macromol. Chem. Phys. 2002, 203, 718.

26. M.L. Cerrada, C. Serrano, M. Sánchez-Chaves, M. Fernández-García, M.A. de Andrés, R.J. Riobóo, F. Fernández-Martín, A. Kubacka, M. Ferrer, M. Fernández-García, Environ. Sci. Techn. 2009, 43, 1630.

27. C. Serrano, M.L. Cerrada, M. Fernández-García, J. Ressia, E.M. Vallés. Eur. Polym. J. 2012, 48, 586.

28. O. Prieto, J. M. Pereña, R. Benavente, M. L. Cerrada, E. Pérez. Macromol. Chem. Phys. 2002, 203, 1844.

29. M.L. Cerrada, M.F. Laguna, R. Benavente, E. Pérez, Polymer 2004, 45, 171.

30. M.F. Laguna, M.L. Cerrada, R. Benavente, E. Pérez, J. Polym. Sci., Part B: Polym. Phys. 2004, 42, 3766.

31. B. Poon, M. Rogunova, A. Hiltner, E. Baer, S.P. Chum, A. Galeski, E. Piorkowska, Macromolecules 2005, 38, 1232.

32. B. Lotz, J. Ruan, A. Thierry, G.C. Alfonso, A. Hiltner, E. Baer, E. Piorkowska, A. Galeski, Macromolecules 2006, 39, 5777.

33. C. De Rosa, S. Dello Iacono, F. Auriemma, E. Ciaccia, L. Resconi, Macromolecules 2006, 39, 6098.

34. M.L. Cerrada, M.J. Polo-Corpa, R. Benavente, E. Pérez, T. Velilla, R. Quijada, Macromolecules 2009, 42, 702.

35. P. Stagnaro, L. Boragno, M. Canetti, F. Forlini, F. Azzurri, G.C. Alfonso, Polymer 2009, 50, 5242.

36. E. Pérez, M.L. Cerrada, R. Benavente, J.M. Gómez-Elvira, Macromol. Res. 2011, 19, 1179.

37. C. De Rosa, O.R. de Ballesteros, F. Auriemma, M.R. Di Caprio, Macromolecules 2012, 45, 2749.

38. C. De Rosa, F. Auriemma, P. Corradini, O. Tarallo, S. Dello Iacono, E. Ciaccia, L. Resconi, J. Am. Chem. Soc. 2006, 128, 80.

39. (A) W.P. Slichter, E.R. Mandell, J. Appl. Phys. 1958, 29, 1438; (B) R. Hosemann, W. Wilke, Makromol. Chem. 1968, 118, 230; (C) J. Grebowicz, J.F. Lau, B.J. Wunderlich, Polym. Sci., Polym. Symp. 1984, 71, 19; (D) P. Corradini, C. de Rosa, G. Guerra, V. Petraccone, Polym. Commun. 1989, 30, 281; (E) J. Arranz-Andrés, R. Benavente, E. Pérez, M.L. Cerrada, Polymer J. 2003, 35, 766.

40. E. Pérez, J.M. Gómez-Elvira, R. Benavente, M.L. Cerrada, Macromolecules 2012, 45, 6481.

41. M.A. Villar, M.L. Ferreira, J. Polym. Sci., Part A: Polym. Chem. 2001, 39, 1136.

42. W. Kaminsky, H. Hahnsen, Polymerization of olefins with a homogeneous zirconium/alumoxane catalyat. In Advances in Polyolefins, R.B. Seymour, T. Cheng, Eds., Plenum Press: New York, 1987, pp.361-371

43. A. Akimoto, A. Yano, New Developments in the production of Metallocene LLDPE by High-pressure Polymerization. In Metallocene-Based Polyolefins, J. Scheirs, W. Kaminsky Eds., John Wiley & Sons: Chichester, 2000, pp.287-308

44. T. Tsutsui, T. Kashiwa, Polym. Commun. 1988, 29, 180

45. J.C.W. Chien, T. Nozaki, J. Polym. Sci., Part A: Polym. Chem. 1993, 31, 227.

46. M.A. Da Silva, G.B. Galland, J. Polym. Sci., Part A: Polym. Chem. 2008, 46, 947.

47. F. Forlini, I. Tritto, P. Locatelli, MC. Sacchi, F. Piemontesi, Macromol. Chem. Phys. 2000, 201, 401.

48. R. Quijada, Macromol. Chem. Phys. 1996, 197, 3091.

49. H.F. Herrmann, L.L. Böhm, Polym. Commun. 1991, 32, 58.

50. J. Koivumäki, J.V. Seppälä, Macromolecules 1993, 26, 5535

51. K. Heiland, W. Kaminsky, Makromol. Chem. 1992, 193, 601.

52. F.F.N. Escher, G.B. Galland, J. Polym. Sci., Part A: Polym. Chem. 2004, 42, 2474.

53. U.M. Wahner, I. Tincul, D.J. Joubert, E.R. Sadiku, F. Forlini, S. Losio, I. Tritto, M.C. Sacchi, Macromol. Chem. Phys. 2003, 204, 1738.

54. J.C. Randall, J. Macromol.Sci.-Rev. Macromol. Chem. Phys. 1989, C29, 201.

CAPÍTULO 3

Microstructure of Metallocene Isotactic Propylene-*co*-1-Pentene-*co*-1-Hexene Terpolymers

Alberto García-Peñas, José M. Gómez-Elvira, Ernesto Pérez and María L. Cerrada.

Journal of Polymer Science Part A: Polymer Chemistry, 2014. 52 (17), 2537–2547.

3.1. Abstract

This study aims at characterizing in depth the microstructure of propylene-*co*-1-pentene-*co*-1-hexene terpolymers, which have been recently reported to develop the isotactic polypropylene δ trigonal polymorph when the total comonomer content is high enough. Such a specific crystalline form had been only reported so far in the analogous copolymers containing either 1-pentene or 1-hexene. A comparative ^{13}C NMR study in solution of the aforementioned terpolymers and copolymers allows asserting the random insertion of both comonomers during chain growth under the polymerization conditions used. The reaction parameters, mainly catalyst and temperature, have been chosen for the purpose of assuring relatively high molar mass polymers.

3.2. Introduction

The use of single site catalysts (SSC) has greatly widened the range of service properties of ethylene and propylene-based polyolefins. Current SSC co-poly-α-olefins are indeed able to cover the gap existing in mechanical properties between highly-crystalline rigid PP and elastic rubbers. [1-3] These copolymers are known as polyolefin plastomers or elastomers, depending on whether the distinctive mechanical response is flexible or elastic-like, respectively.

The versatility of these also called branched polyolefins (SCB or LCB depending on the length of the side branch) lies on the fact that they can be produced either as low or as high-conversion copolyolefins, which additionally show the characteristic advantages of the SSC-based materials, namely, an uniform insertion of the comonomer in the chains, narrow molecular weight distributions and low content of extractable fractions. All these features allow them exhibiting well-defined morphologies in which both the total crystalline content and the quality of the crystallite entities can be accurately controlled.

In the case of PE-based co-poly-α-olefins, an increasing content of side branches simply drives the appearance of fringed micelles as new crystalline entities, at the expense of the quality and the population of typical PE lamellae, [4-11] while in the case of isotactic propylene (iPP)-based co-poly-α-olefins it can additionally exert a profound effect on the polymorph type in which the crystalline associations are permitted to grow. [12-19] On the basis of these effects, SSC catalysis has proven to be a suitable manner to afford polyolefins, having appropriate morphologies for lots of practical requirements. [20]

In the particular case of isotactic poly(propylene-*co*-α-olefins), the coexistence of polymorphs can be conveniently modulated by tailoring the chain microstructure at both the compositional and the configurational level. Recently, such a potentiality is even more broadened since the discovery of a new polymorph, the trigonal form,

about which some works have been focused on lately. This new crystalline lattice has been found to be formed in iPP copolymers with 1-pentene or 1-hexene [21-27] of high enough co-unit content, as well as in the terpolymers with both comonomers in recent works. [19,28]

To exploit in depth the advantages in service applications offered by iPP-based co-poly-α-olefins, in which the presence of the trigonal form poses a new scenario in the balance between mesophase, amorphous fraction, and the other crystalline polymorphs, it is mandatory, first, to characterize in detail the primary structure of these materials. Some preliminary work on this respect was first put forward on isotactic poly(propylene-*co*-1-pentene-*co*-1-hexene) terpolymers. [19] As an step forward, we present here a study focused on the analysis of the comonomer distribution with the purpose of furnishing a thorough description of these terpolymers' chain microstructure. The corresponding ^{13}C NMR results are compared with the equivalent ones in the analogous 1-pentene and 1-hexene copolymers, in the conversion range where the contribution of the trigonal form starts to be the largest share of the crystalline phase (up to 14 mol. %). The study has been restricted exclusively to such a conversion range, because of the enormous interest existing in improving the technical performance of iPP, but without sacrificing entirely the advantages offered by the pristine propylene crystallinity. However, the extension of the study to a wider composition range would imply the use of relatively large volumes of liquid α-olefins, whose effect on the propylene solubility should be taken into account.

This analysis aims not only at ensuring an unambiguous elucidation of the comonomer distribution, but also at enlarging the family of α-olefin-containing terpolymers, whose ^{13}C NMR characterization has been reported. To the best of our knowledge, only ethylene-based specimens have been studied. [29-35]

3.3. Experimental

3.3.1. Materials

Oxygen and water free solvent (toluene-Merck) and comonomers (1-pentene, 1-hexene-Acros) were obtained by refluxing over metallic sodium and further distillation under N_2. Both propylene (Praxair 2.5) and nitrogen (Praxair 3X) were purified by flowing through oxygen-trap columns and molecular sieves before using. The catalyst *rac*-dimethyl-silylbis(1-indenyl) zirconium dichloride (Strem) and the co-catalyst methylaluminoxane (MAO-Aldrich, 10 wt % solution in toluene) were used as received. Ethanol (Aroca, 96%) and HCl (VWR, 37%) were used for the precipitation and purification of the copolymers and terpolymers. Stabilized decaline (Panreac; 1g/L Irganox 1010) and 1,1,2,2-tetrachloroethane-d_2 (Aldrich) were used for viscosimetry and NMR analysis respectively.

3.3.2. Synthesis of the poly(propylene-*co*-1-pentene) and poly(propylene-*co*-1-hexene) copolymers and of the poly(propylene-*co*-1-pentene-*co*-1-hexene) terpolymers

Propylene co and ter-polymerizations with 1-pentene and 1-hexene were carried out in a 250 mL stainless steel autoclave at -5°C in 90 mL of toluene. The reactions were run in closed batch mode from an initial propylene pressure between 0.35 and 0.40 bar. The starting comonomers/propylene molar ratios ranged from 0.2 to 0.9. In the particular case of ter-polymerizations, three 1-pentene/1-hexene molar ratios (75:25, 50:50, 25:75) were studied for every single comonomer/propylene feeding ratio.

After equilibrating the system, the reactions were started by injecting a volume of 0.125 mL containing 1.39 X 10^{-6} moles of the activated catalyst ([Al]/[Zr]=3648). The propylene pressure was monitored all along the process in order to control the diminution of the propylene content in the bulk. The system was quenched at a 5 mol% conversion of propylene by adding 5mL of ethanol, and finally degassed. The polymers were obtained as powders by pouring the reaction bulk onto

a mixture of acidified ethanol (HCl, 4% vol.). The so-precipitated polymers were stirred overnight, filtrated, washed with ethanol and, finally, dried under vacuum at room temperature.

Table 1 summarizes the three series of samples synthesized. In the case of the terpolymers, they are referred as T followed by the total content of comonomers and the relative proportion of 1-pentene and 1-hexene used in the feed. CPPe and CPHe stand for the 1-pentene and 1-hexene copolymers respectively, being the molar co-unit content indicated next.

Table 1. Composition of the samples and data of their corresponding runs.

Sample	Comonomer content (mol%)			$[C_5+C_6]/[C_3]$ feeding molar ratio	Polymerization time (min)	Activity ($Kg \cdot mol^{-1}(C_3) \cdot mol^{-1} \cdot (Zr)\ h^{-1}$)
	total	Pe	He			
iPP	0	0	0	0	166	443
T4-75Pe-25He	4.1	3.1	1.0	0.204	25	3614
T4-50Pe-50He	4.0	2.2	1.8	0.245	299	566
T4-25Pe-75He	4.2	1.0	3.2	0.220	22	4502
T7-75Pe-25He	7.1	5.4	1.7	0.423	19	5571
T7-50Pe-50He	6.7	3.5	3.2	0.423	12	5398
T7-25Pe-75He	6.8	2.0	4.8	0.361	21	5125
T9-75Pe-25He	8.7	6.5	2.2	0.479	22	6282
T9-50Pe-50He	8.8	4.5	4.3	0.493	27	7180
T9-25Pe-75He	8.8	2.4	6.4	0.504	23	4946
T13-75Pe-	13.2	9.9	3.3	0.773	20	6498
T13-50Pe-	12.1	6.2	5.9	0.767	44	3683
T13-25Pe-	12.9	3.9	9.0	0.905	41	4725
CPPe4	4.0	4.0	-	0.204	42	2663
CPPe7	6.9	6.9	-	0.343	8	7293
CPPe9	9.0	9.0	-	0.538	13	7997
CPPe15	15.4	15.4	-	0.733	15	12989
CPHe6	6.1	-	6.1	0.320	23	4307
CPHe10	9.8	-	9.8	0.565	20	6503
CPHe12	11.8	-	11.8	0.759	21	6987
CPHe14	14.2	-	14.2	0.888	22	5743

3.3.3. Viscosimetry

An indirect assessment of the molecular mass evolution with conversion was performed by measuring the intrinsic viscosity in stabilized decaline, at 135 °C based on unpublished results that show a linear relationship between average molecular weights obtained by GPC and intrinsic viscosity of propene copolymers, either with 1-pentene or 1-heptene as comonomers, in the conversion range here presented.

3.3.4. Nuclear magnetic resonance characterization

Microstructure of samples was studied in detail by ^{13}C NMR analysis of sample solutions in $C_2D_2Cl_4$ (10% wt/vol), at 80°C, using an Inova 400 spectrometer (100 MHz). In the case of the less soluble samples, that is, T4, CPPe4 and CPHe6 specimens, the ^{13}C NMR spectra were obtained from 1,2,4-trichlorobenzene solutions in a Bruker Avance DPX-300 (75 MHz) at 100°C, using deuterated *o*-dichlorobenzene as internal reference. A minimum of 8000 scans were recorded with broad band proton decoupling, an acquisition time of 1 s, a relaxation delay of 4 s and a pulse angle of 45°.

3.4. Results and discussion

3.4.1. Conversion range

The evolution of the conversion as a function of the comonomer/propylene molar ratio, shown in figure 1, makes clear that no significant difference can be found in the global composition of the polymer obtained, depending on whether 1-pentene, 1-hexene or a mixture of both are used in the polymerization. Thus, the three series of polyolefins can be fitted into a unique straight line intercepting point zero, in the conversion range here studied. Even more, in the case of the terpolymers, the fact that the relative ratio between the two α-olefins integrating the terpolymer corresponds to the original relative proportion in the feeding (Table 1), allows us to definitively assume that there is no preferential insertion of one of them under the

experimental conditions used, i.e. no significantly different reactivity ratios against propylene must be expected and, then, the terpolymerization can be treated as a copolymerization. This matter will be discussed later.

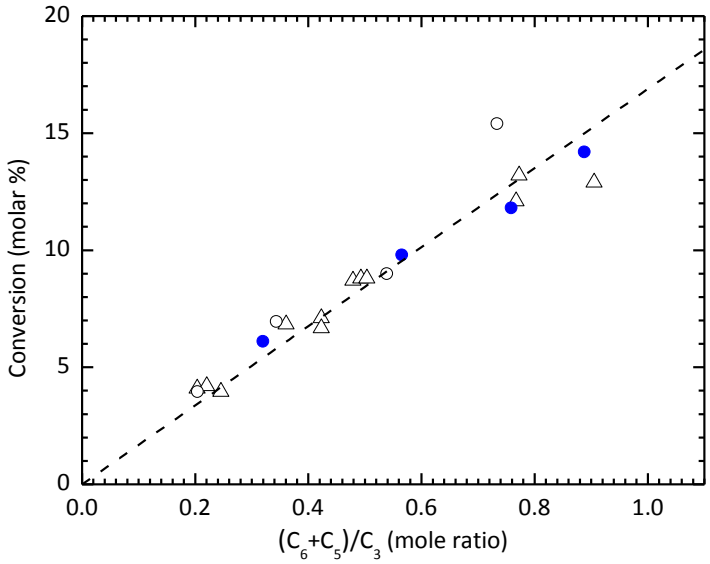

Figure 1. Relationship between total comonomer conversion and total feed ratio of comonomers: (△) T samples; (○) CPPe samples; (●) CPHe samples.

3.4.2. Catalyst activity

The evolution of the apparent activity in the three series of copolymerizations follows an initial upward trend, as shown in Figure 2. This is a well-known effect attributed to the comonomer presence, [36-42] which has been set out in the literature on the basis of different factors, mainly an enhanced solubility of chains in the medium, [43] a larger chain transfer activity [44] and a modification of the active center quality. [44] At high molar feeding ratios, however, the activity eventually decreases, in agreement with other authors' results. [41] The activity average trend has been traced without taking into account the values corresponding to samples T4-50Pe-50He and CPPe15, which are respectively very much under and over the average activity curve.

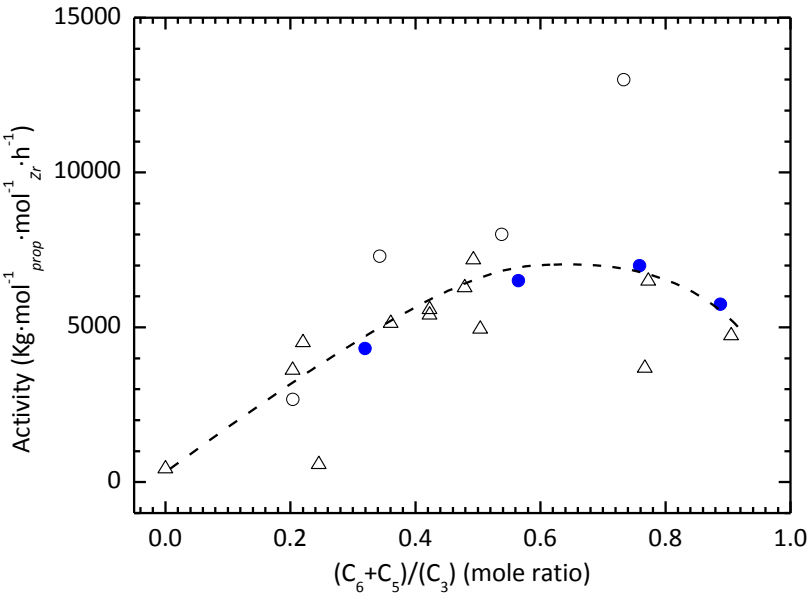

Figure 2. Evolution of the catalytic activity as a function of the global feed ratio of comonomers: (△) T samples; (○) CPPe samples; (●) CPHe samples.

It seems from the results in Table 1 and Figure 2 that the activity of CPPe samples is somewhat higher than the one for CPHe copolymers; however, this difference is not confirmed by the terpolymerization data, which should show two trends depending on weather the feeding is richer in 1-pentene or 1-hexene. Consequently, this difference must be considered inside the experimental error. Anyway, it is clear that the activity seems not to depend on the comonomer used, and such a lack of dependence spreads over the higher molar feeding ratios with decreasing activity.

3.4.3. Evolution of the intrinsic viscosity

One of the expected effects of a feeding richer and richer in comonomers is chain molecular weight diminution [42,44,45]. Such a variation can be indirectly monitored by means of the intrinsic viscosity, since a straight relationship between this parameter and average molecular weight, as obtained by GPC, has been found to

exist in this kind of copolyolefins. In particular, it has been checked for both propylene-*co*-1-pentene and propylene-*co*-1-heptene-copolymers. [46]

The variation of intrinsic viscosity against conversion is plotted in Figure 3. It is then directly related to the molar mass variation and support the fact that the conditions used are not sensitive to the comonomer nature since, once again, all samples fit a sole trend. Consequently, a similar role of both comonomers as chain transfer agents in the copolymerization must be inferred.

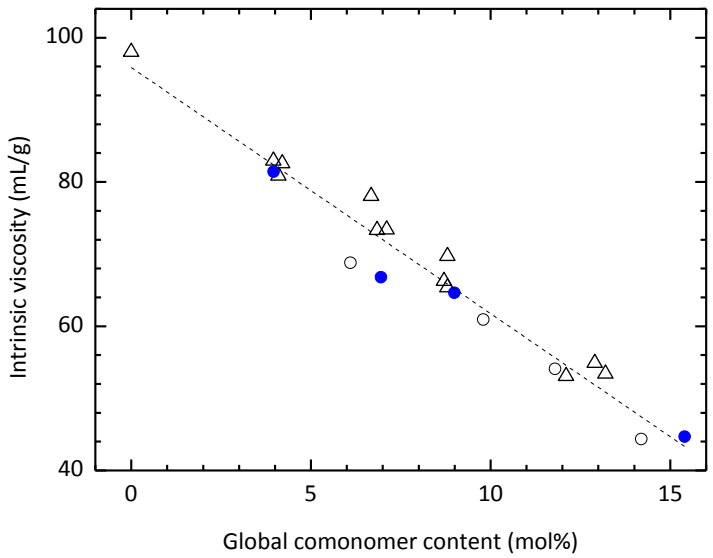

Figure 3. Evolution of the intrinsic viscosity in decaline at 135°C as a function of the conversion (global comonomer content): (△) T samples; (○) CPPe samples; (●) CPHe samples.

3.4.4. Evaluation of the microstructure in composition and configuration

Figure 4 shows, as an example, the ^{13}C NMR spectra of the CPPe9 and CPHe10 samples together with that one for the terpolymer T9-50Pe-50He. The assignments for all the bands are collected in Table 2, where identification numbers are associated with their corresponding carbon nuclei, according to the nomenclature proposed in a

previous work [19] and shown in Scheme 1. While P, Pe, and He stand for carbon nuclei belonging to propylene, 1-pentene, and 1-hexene respectively, X stand for carbon nuclei of any of the comonomer units (1-pentene or 1-hexene). The superscript denotes the carbon position in the monomer, as depicted in Scheme 1. It should be noted that some of the bands numbered in Figure 4 appear in Table 2 with subindexes "*a*" and "*b*". This notation has been used to specify, when possible, whether a specific carbon nucleus belongs to an isolated comonomer unit or not, for example, to P**X**P or P**X**X sequences respectively, since X**X**X triads are not generated. The chemical shift of every carbon is reported for the three series of materials since small differences are found in some cases.

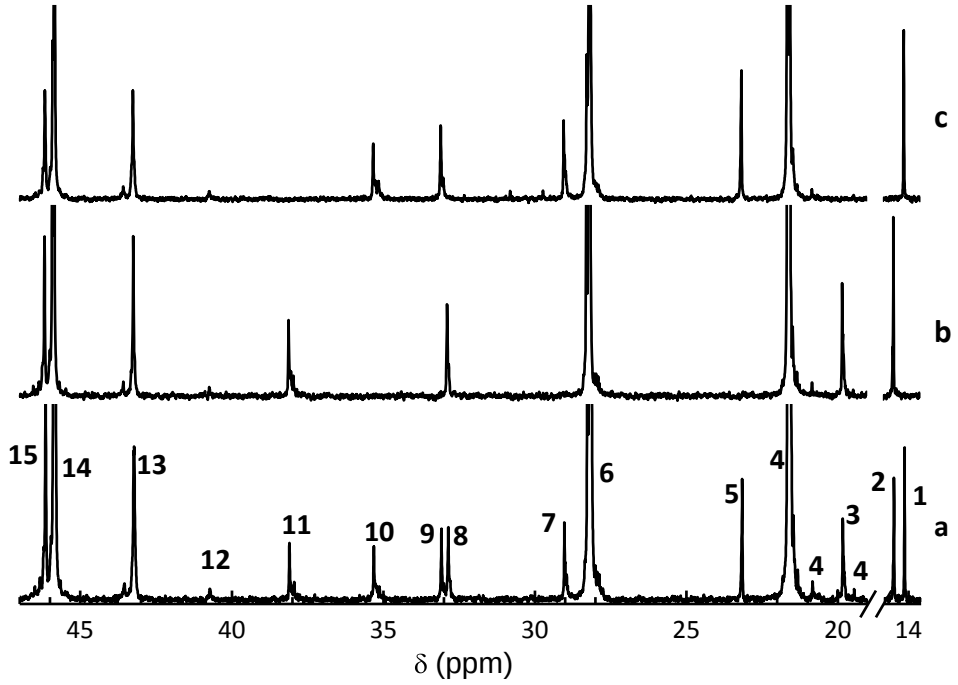

Figure 4. ^{13}C NMR spectra of a) T9-50Pe-50He, b) CPPe9, c) CPHe10.

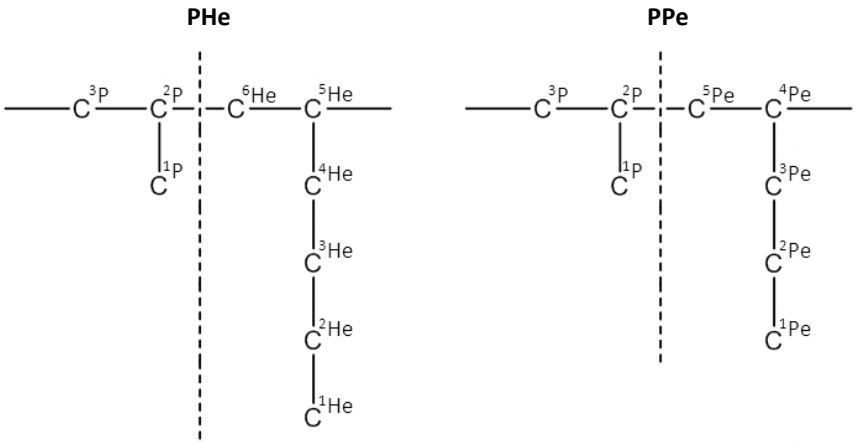

Scheme 1. Numeration of carbons belonging to propylene (P), 1-pentene (Pe), and 1-hexene (He) in the polymer chain.

Such a detailed assignment can be inferred from the evolution of the spectrum signals with the conversion degree. This is shown in Figures 5 and 6 for the CPPe and CPHe copolymers, respectively. In these figures, the characteristic bands of the side-chain carbons of both comonomers are tracked with conversion, using the 40.72 ppm signal (peak 12), attributed to $PX^{5,6}XP$ carbons, as an indicative for the presence of comonomer diads. In both cases, it is clear that no comonomer diads are formed in the low conversion samples, that is, CPPe4 and CPHe6, but new signals associated with side chain carbons are increasingly apparent for higher comonomer contents, concurrently with the growth of peak 12. These new peaks must be reasonably associated with the presence of contiguous comonomers in PXXP sequences. As a matter of fact, related results in the literature have excluded the formation of comonomer sequences longer than 2 in the conversion range studied here. [29,30,41] It is worth noticing that the ^{1}He signal at 14.16 ppm is the only carbon not sensitive to whether the adjacent unit is propylene or comonomer. All other carbon nuclei for both comonomers are sensitive to the compositional environment and can be distinguished at the triad level.

Table 2. Experimental chemical shifts and assignments (see Scheme 1) of the ^{13}C NMR peaks of poly(propene-*co*-1-pentene-*co*-1-hexene) terpolymers observed in 1,1,2,2-tetrachloroethane-*d4* at 80°C.

Peak		Carbon Nucleus (P=propylene, Pe=1-pentene, He=1-hexene)	Chemical Shift (ppm)[a]		
			poly(propene-*co*-1-pentene)	poly(propene-*co*-1-hexene)	poly(propene-*co*-1-pentene-*co*-1-hexene)
1		$P^1\underline{He}P$, $P^1\underline{He}X$	-	14.16	14.16
2	2a	$P^1\underline{Pe}P$	14.58	-	14.59
	2b	$\mathbf{P^1\underline{Pe}X}$	14.61	-	14.62
3	3a	$P^2\underline{Pe}X$	19.80	-	19.81
	3b	$P^2\underline{Pe}P$	19.83	-	19.83
4		$\mathbf{^1P}$ ($P^1\underline{P}P+P^1\underline{P}X+$	19.4-22.0	19.4-22.0	19.4-22.0
5	5a	$P^2\underline{He}P$	-	23.15	23.16
	5b	$P^2\underline{He}X$		23.17	23.17
6	6	$\mathbf{^2P}$ ($P^2\underline{P}P+P^2\underline{P}X+X^2\underline{P}X$)	27.6-28.6	27.6-28.6	27.6-28.6
7	7a	$P^3\underline{He}X$	-	28.95	28.95
	7b	$P^3\underline{He}P$	-	29.02	29.02
8	8a	$P^4\underline{Pe}X$	32.81	-	32.81
	8b	$P^4\underline{Pe}P$	32.87	-	32.86
9	9a	$P^5\underline{He}X$	-	33.00	33.01
	9b	$P^5\underline{He}P$	-	33.08	33.09
10	10a	$X^4\underline{He}P$	-	35.12	35.12
	10b	$P^4\underline{He}P$	-	35.31	35.31
11	11a	$X^3\underline{Pe}P$	37.94	-	37.94
	11b	$P^3\underline{Pe}P$	38.10	-	38.10
12		$PX^{5,6}\underline{X}P$	40.72	40.72	40.72
13	13a	$PP^{5,6}\underline{X}P+PP^{5,6}\underline{X}X$	43.22	43.22	43.22
	13b	$XP^{5,6}\underline{X}X+XP^{5,6}\underline{X}P$	43.55	43.55	43.54
14		$PP^3\underline{P}P$	45.84	45.84	45.84
15		$PP^3\underline{P}X$	46.15	46.15	46.15

[a] Chemical shifts are referenced to $C_4D_2Cl_4$ (74.00 ppm). X stands for a comonomeric unit either 1-pentene or 1-hexene.

The analysis of the terpolymer series provides the same evidence about the variation of the compositional microstructure of chains with conversion, that is, shorter and shorter propylene sequences linked either by isolated comonomer units or by an increasing amount of comonomer diads that, in this case, may correspond to

any of the XX pairs. Signals ascribed to two selected terpolymer samples are shown for comparison in Figures 5 and 6.

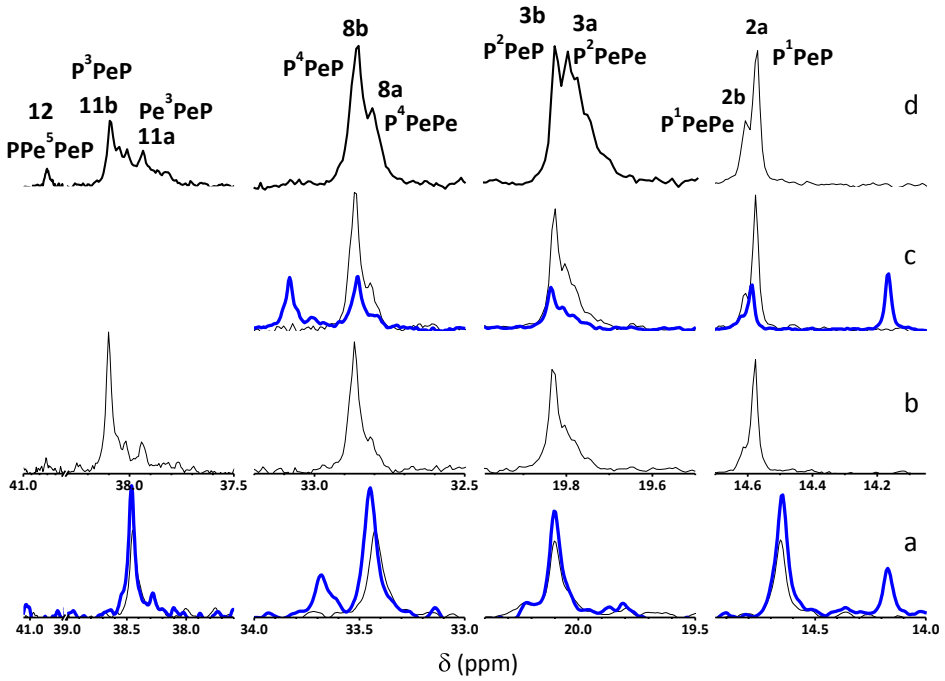

Figure 5. Detailed assignment of ^{n}Pe carbons (n=1-5) in the ^{13}C NMR spectra of CPPe samples (black lines): (a) CPPe4; (b) CPPe7; (c) CPPe9; (d) CPPe15. The bands of T4-75Pe-25He and T9-50Pe-50He terpolymes are compared in figures (a) and (c) respectively (blue lines). The ppm scales in figures (a) and (b) correspond to the spectra obtained in 1,2,4-trichlorobenzene + ortho-dichlorobenzene-d_4 at 100°C and 1,1,2,2- tetrachloroethane-d_2 at 80°C, respectively.

The molar content in each comonomer for the different series was estimated from the relative intensities of the methyl signals 1 and 2 versus 4, and is shown in Table 3. This table also collects the compositional distribution at the triad level.

The estimation has been performed by using the relationships reported previously. [19] In the general case of a terpolymer, these expressions are:

$$[PPP] = K\cdot(I_6 - I_{13a} - \tfrac{1}{2}\cdot I_{13b})$$

$$[PPX] = K\cdot I_{13a}$$

$$[XPX] = K\cdot\tfrac{1}{2}\cdot I_{13b}$$

(The relationship [XPX]= ½·([XPXP]+[XXPX]) is applied [47])

$$[PXP] = K\cdot(I_1+I_2-2\cdot I_{12})$$

$$[XXP] = K\cdot 2\cdot I_{12}$$

$$[XXX] = 0$$

where K is the normalization constant and I_n corresponds to the intensity of peak n, according to the tabulation shown in Table 2.

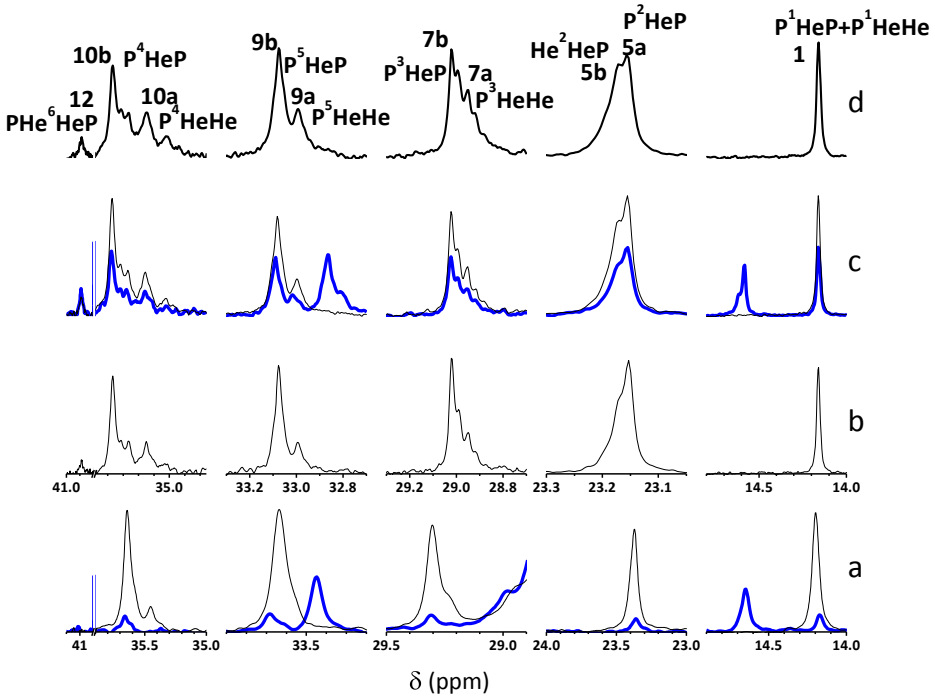

Figure 6. Detailed assignment of ^{n}He carbons (n=1- 6) in the ^{13}C NMR spectra of CPHe samples (black lines): (a) CPHe6; (b) CPHe10; (c) CPHe12; (d) CPHe14. The bands of T4-75Pe-25He and T9-50Pe-50He terpolymes are compared in figures (a) and (c), respectively (blue lines). The ppm scales in figures a) and b) corresponds to the spectra obtained in 1,2,4-trichlorobenzene + ortho-dichlorobenzene-d_4 at 100°C and 1,1,2,2- tetrachloroethane-d_2 at 80°C.

Additionally, the average propylene sequence length and the relative contribution of XXP triads to the total of interruptions are also given in Table 3. It should be remarked the similar variation of these two characteristics with conversion in the three series of materials.

The estimation of the content for the different comonomer diads (PePe, HeHe, and PeHe) in the terpolymer series is not possible due to the lack of sensitivity of any

of the comonomer carbons to the length of the adjacent diad partner. Consequently, only the content of XX can be considered in this case for the calculus of global reactivity ratios.

Table 3. Relative content of triads and average propylene length (*np*).

Sample	PPP	PPX	XPX	PXP	XXP	XXX	$\frac{[XXP]}{[PXP+XXP]}\cdot 10^2$	$^{a}n_p$
T4-75Pe-25He	87.8	7.4	0	4.8	0	0	0	26
T4-50Pe-50He	87.3	8.2	0	4.5	0	0	0	23
T4-25Pe-75He	87.5	8.1	0	4.4	0	0	0	24
T7-75Pe-25He	80.1	11.	0.6	6.3	1.1	0	14.9	14
T7-50Pe-50He	80.2	11.	0.6	6.4	0.9	0	12.3	14
T7-25Pe-75He	81.2	11.	0.5	6.3	1.0	0	13.7	15
T9-75Pe-25He	75.9	13.	0.8	8.1	1.3	0	13.8	12
T9-50Pe-50He	75.4	14.	0.9	7.8	1.6	0	17.0	11
T9-25Pe-75He	75.7	14.	0.8	7.4	1.9	0	20.4	11
T13-75Pe-25He	66.2	18.	1.6	10.	3.7	0	26.4	8
T13-50Pe-50He	65.5	19.	1.5	10.	3.9	0	27.9	8
T13-25Pe-75He	67.0	18.	1.6	9.6	3.4	0	26.1	8
CPPe4	87.3	8.7	0	4.0	0	0	0	22
CPPe7	81.2	11.	0.4	6.6	0.8	0	11.3	16
CPPe9	75.3	14.	0.7	9.0	0.7	0	7.2	11
CPPe15	60.6	20.	2.1	12.	4.3	0	25.1	7
CPHe6	82.8	11.	0	6.0	0	0	0	17
CPHe10	72.5	15.	1.2	7.8	2.8	0	26.4	10
CPHe12	66.9	18.	1.5	9.7	3.2	0	24.8	8
CPHe14	61.3	21.	2.2	10.	4.8	0	31.2	7

$$^{a}\,np = \frac{[PPP] + [PPX] + [XPX]}{[XPX] + \frac{1}{2}[PPX]}$$

The tacticity distribution of the propylene sequences has been calculated at the pentad level from ^{1}P signals (band 4 in Table 2). As reported in the previous work, [19] the isoselective control of the catalyst used allows the sole production of *mrrm* sequences as syndiotactic defects. This fact makes it possible to accurately assess the evolution of configuration all along the conversion range studied by using the ^{1}P window since, if the *mrrm* signal is apparent, it does not overlap with the ^{2}Pe signal at 19.83 ppm and can be also estimated. The results for the configurational

microstructure of the three series are summarized in Table 4. The most remarking finding is the fact that the propylene isotacticity decreases with conversion in the three series.

Table 4. Propylene tacticity at the pentad level.

Sample	*mmmm*	*mmmr*	*rmmr*	*mmrr*	*mmrm+ rmrr*	*mrmr*	*rrrr*	*rrrm*	*mrrm*
T4-75Pe-25He	89.5	4.6	0.0	2.4	0.0	0	0	0	0
T4-50Pe-50He	87.4	4.9	0.9	2.0	1.2	0	0	0	0.8
T4-25Pe-75He	90.3	3.9	0.0	1.8	0.0	0	0	0	0
T7-75Pe-25He	90.8	1.0	0.0	1.2	0	0	0	0	0
T7-50Pe-50He	90.0	1.5	0.0	1.3	0	0	0	0	0
T7-25Pe-75He	89.8	2.1	0.0	1.2	0	0	0	0	0
T9-75Pe-25He	87.9	2.6	0.0	0.9	0	0	0	0	0
T9-50Pe-50He	90.0	1.2	0.0	0.3	0	0	0	0	0
T9-25Pe-75He	87.5	2.9	0.0	1.0	0	0	0	0	0
T13-75Pe-25He	83.8	2.6	0.0	0.9	0	0	0	0	0
T13-50Pe-50He	84.5	2.7	0.0	0.9	0	0	0	0	0
T13-25Pe-75He	82.2	3.1	0.0	0.8	0	0	0	0	0
CPPe4	89.5	4.0	0.0	2.2	0	0	0	0	0
CPPe7	88.9	3.0	0.0	1.9	0	0	0	0	0
CPPe9	87.9	2.8	0.0	0.7	0	0	0	0	0
CPPe15	79.1	4.1	0.0	1.6	0	0	0	0	0
CPHe6	86.8	4.3	0.0	2.3	0	0	0	0	0.4
CPHe10	87.3	1.4	0.0	1.1	0	0	0	0	0
CPHe12	85.3	1.7	0.0	1.0	0	0	0	0	0
CPHe14	82.1	2.2	0.0	1.1	0	0	0	0	0

As a certain check of the self-consistency of the different calculations, the last column of Table 5 shows the product of the total comonomer content by n_p. It can be observed that the values of this product are in all cases close to 100. For a statistical random propylene copolymer (or terpolymer) of sufficiently high molecular weight, it is evident that the average value of propylene sequences [48] will be exactly 100 divided by the total comonomer content expressed in mol %. The conclusion is, therefore, that the preceding calculations appear to be self-consistent.

Table 5. Checking of the value given by the product: [comonomer molar %] n_p

Sample	Comonomer molar %	n_p	Product
T4-75Pe-25He	4.1	25.7	105.5
T4-50Pe-50He	4.0	23.3	93.2
T4-25Pe-75He	4.2	23.6	99.1
T7-75Pe-25He	7.1	14.1	100.4
T7-50Pe-50He	6.7	14.2	94.8
T7-25Pe-75He	6.8	15.5	105.1
T9-75Pe-25He	8.7	11.7	101.7
T9-50Pe-50He	8.8	11.3	99.0
T9-25Pe-75He	8.8	11.5	101.0
T13-75Pe-25He	13.2	8	106.1
T13-50Pe-50He	12.1	7.8	94.6
T13-25Pe-75He	12.9	8.1	103.9
CPPe4	4.0	22.1	88.3
CPPe7	6.9	15.7	108.3
CPPe9	9.0	11.5	103.5
CPPe15	15.4	6.8	104.6
CPHe6	6.1	16.8	102.4
CPHe10	9.8	9.9	96.8
CPHe12	11.8	8	94.7
CPHe14	14.2	6.6	94.2

3.4.5. Evaluation of the Reactivity Ratios

On account of the fact that an unique conversion trend can be tracked in Figure 1 for all three series of materials and that the relative content of both comonomers in the terpolymer series coincides with that one used in the feed, 1-pentene and 1-hexene have been considered as the same comonomer in terms of the

reactivity ratio analysis, under these specific synthesis conditions. This global analysis is supported by the fact that chain features, like molar mass and distribution of both configuration and composition, evolve with conversion in a similar way for the two comonomers.

The monomer reactivity ratios r_p and r_x (with P= propylene and X= 1-pentene or 1-hexene) have been estimated by applying both the Fineman-Ross and the Kelen-Tüdos linearization methods of the Lewis-Mayo equation, [49,50] on the one hand, and from the ^{13}C NMR spectra, on the other, by using the following relationships proposed by Uozumi and Soga. [51]

$$r_p = \frac{2[PP]}{[PX]R_P} \qquad r_X = \frac{2[XX]R_P}{[PX]}$$

[PP], [PX] and [XX] stand in these equations for the relative content of the different diads in composition and R_p stands for the propylene/comonomer molar ratio in the feed. The results are summarized in Tables 6 and 7. The ^{13}C NMR reactivity ratios shown in Table 7 correspond to the average values calculated from data collected in Table 6.

The most apparent feature is that, even though the value obtained for the propylene reactivity ratio (r_p) does not depend on the method of calculus (Table 7), the r_x value calculated from the ^{13}C NMR spectra is an order of magnitude higher than the one obtained from the Fineman-Ross and the Kelen-Tüdos method. If these reactivity ratio values are considered, it should be concluded that the co- and terpolymerization processes are alternating-like, as for $r_p \cdot r_x$ is close to zero (Table 7). On the contrary, these processes would be random if r_p and r_x derived from ^{13}C NMR data are taken, as it is deduced from values of the reactivity ratio product, which is around one in all runs (Table 6). In these cases, the smallest conversion in every series is excluded because the low concentration of the α-olefins in the feed makes the likelihood of producing XX diads to be zero.

Table 6. Monomer reactivity ratios calculated from the ^{13}C NMR spectra of the different samples.

Sample	From ^{13}C NMR		
	r_p	r_x	$r_p \cdot r_x$
T4-75Pe-25He	4.39	-	-
T4-50Pe-50He	5.18	-	-
T4-25Pe-75He	4.78	-	-
T7-75Pe-25He	5.41	0.19	1.04
T7-50Pe-50He	5.45	0.16	0.86
T7-25Pe-75He	4.88	0.22	1.08
T9-75Pe-25He	4.82	0.17	0.80
T9-50Pe-50He	4.90	0.18	0.90
T9-25Pe-75He	5.12	0.24	1.21
T13-75Pe-25He	5.03	0.22	1.10
T13-50Pe-50He	5.29	0.20	1.05
T13-25Pe-75He	5.98	0.18	1.07
CPPe4	4.46	-	-
CPPe7	4.64	0.19	0.87
CPPe9	5.18	0.07	0.39
CPPe15	3.82	0.21	0.82
CPHe6	4.88	-	-
CPHe10	4.99	0.26	1.31
CPHe12	5.22	0.19	0.99
CPHe14	4.96	0.21	1.06

Table 7. Monomer reactivity ratios calculated by the different methods used.

	Fineman-Ross	Kelen-Tüdos	^{13}C-NMR[a] (average values)
r_p	4.763	4.777	4.977
r_x	0.020	0.025	0.193
$r_p \cdot r_x$	0.095	0.119	0.960

[a] Average reactivity ratios from data shown in Table 6.

In spite of this difference, the Lewis-Mayo function, yields indeed quite similar composition diagrams for R_p values under 0.5, when any of the reactivity ratios pairs (r_p and r_x) are used (Fig. 7). The Fineman-Ross and the Kelen-Tüdos methods have been shown to be very simple and useful, but it has been demonstrated that they

provide reactivity ratios with some lack of reliability. [52] According to Sarzotti et al., [53] it is recommended to widen the conversion range to get more reliable values of the reactivity ratios by applying methods that imply the linearization of the Lewis-Mayo equation. A further study to a large conversion range is, however; beyond our purpose in this work. Then, an expected consequence is that the reactivity ratios derived from these approaches, with such a restricted number of points, are not reliable at all.

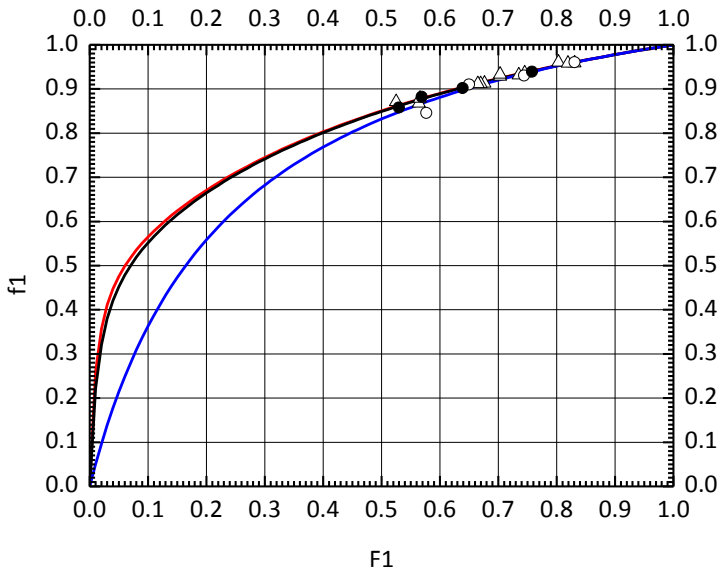

Figure 8. Composition diagram for the copolymerization and terpolymerization reactions: (△) T samples; (○) CPPe samples; (●) CPHe samples. The lines correspond to the Lewis-Mayo function ($f_1=[r_1F_1^2+F_1F_2]/[r_1F_1^2+F_1F_2+r_2F_2^2]$) by using the r_p,r_x pairs (r_1, r_2, respectively) obtained from: the Fineman-Ross method (red line); the Kelen-Tudos method (black line), and from the ^{13}C NMR spectra (blue line).

In the conversion range studied, the comparison of the actual microstructure distribution of the three series of samples with the ones predicted by the Lewis-Mayo equation, by using the different reactivity ratio pairs obtained, serves us to confirm which one among them is the right one. This is shown at the triad level in Figure 8, where it is clear that the average value of the reactivity ratios obtained from the ^{13}C NMR data provide a good fit of the actual microstructure distribution [Fig. 8(a)].

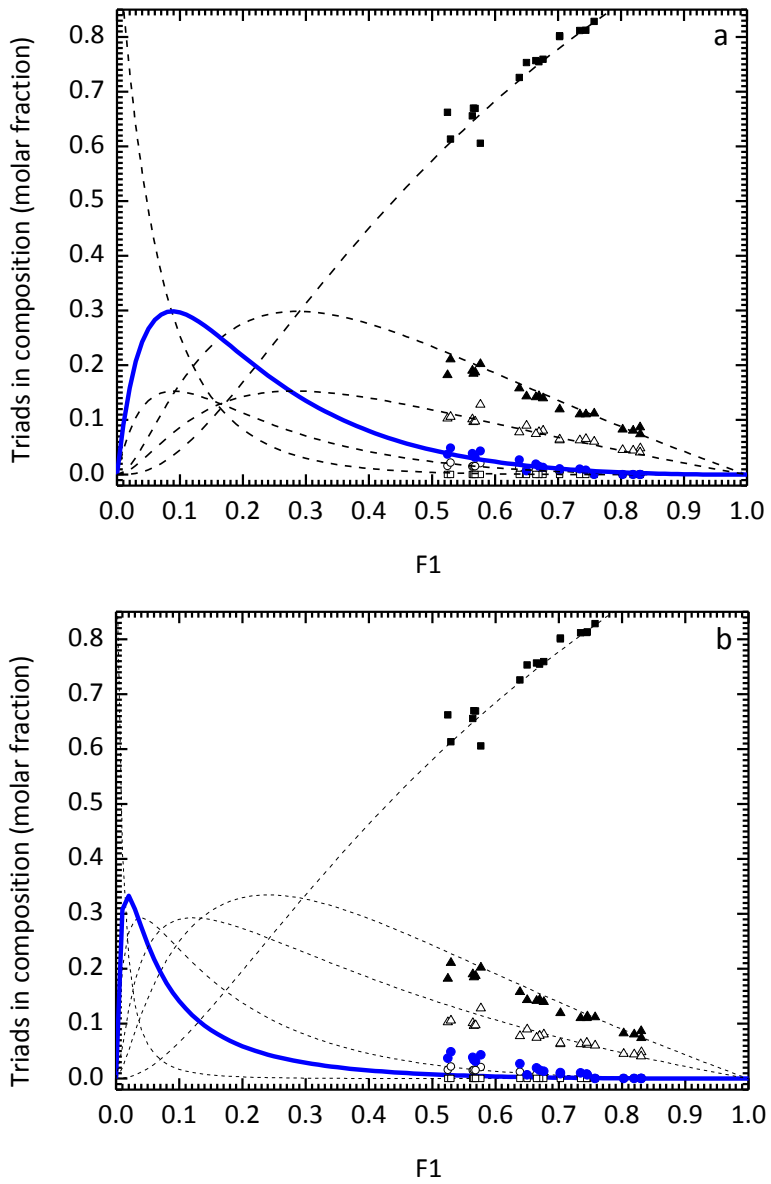

Figure 8. Triad distribution versus propylene/comonomer feeding molar ratio. Experimental data: (■) PPP; (▲) PPX; (○) XPX; (□) XXX; (●) XXP; (△) PXP. Lines correspond to predicted data by running the Lewis-Mayo equation with: (a) r_p and r_x from ^{13}C NMR spectra and (b) r_p and r_x calculated from the Kelen-Tüdos procedure. The blue lines correspond to the evolution of XXP triads.

This is not the case if the Lewis-Mayo equation is considered by taking the reactivity ratios provided by any of both linearizations. Figure 8(b) shows only the Kelen-Tüdos prediction as an example. In this case, a conspicuous deviation is apparent between predicted and experimental values for the content of (PXX) triads in the conversion range analyzed. Consequently, r_p and r_x values derived from ^{13}C NMR seem to describe better the polymerization systems under study. These reactivity ratio values are, additionally, in agreement with literature data, which report the metallocene copolymerization of propene with α-olefins to be also a random process at higher polymerization temperatures. [41,51,54-57]

3.5. Conclusions

The synthesis of propylene copolymers with either 1-pentene or 1-hexene, as well as of terpolymers with both comonomers, up to 14 molar % and under the reaction conditions described, yielded propylene co-poly-α-olefins showing, on the one hand, a single conversion build-up with comonomer feeding and, on the other, an unique molecular weight variation with comonomer content.

Both copolymers and terpolymers can be coherently fitted into a singular composition diagram trend that can be described through the Lewis Mayo equation. The comonomer and propylene reactivity ratios associated with such a variation must be calculated from the compositional distribution furnished by the ^{13}C NMR spectra, rather than using the Fineman-Ross or the Kelen-Tüdos methods, due to the fact that these approaches are not reliable if the conversion range under study is not wide enough. As a matter of fact, the comparison of the experimental and predicted triad evolutions with feeding composition allows discarding these Lewis-Mayos' linearization procedures. The so-estimated $r_p \cdot r_x$ value is around unity, and therefore, it can be concluded that the synthesis carried out provided random propylene copolymers and terpolymers.

3.6. References

1. Y. Imanishi, N. Naga. Prog. Polym. Sci. 2001, 26, 1147-1198.
2. Metallocene–Based Polyolefins: Preparation, Properties and Technology Vol.2, PART III, Plastomers and Elastomers; J. Scheirs, W. Kaminsky, Eds.; John Wiley and Son, Ltd.: Chichester, 2000; p.161-267
3. H. H. Brintzinger, D. Fischer, R. Mülhaupt, B. Rieger, R. Waymouth, Angew. Chem. Int. Ed. Engl. 1995, 34, 1143-1170.
4. T. Ho, J. M. Martin in Structure, Properties and Applications of Polyolefin Elastomers Produced by Constrained Geometry Catalysts. Metallocene–Based Polyolefins: Preparation, Properties and Technology Vol.2, J. Scheirs and W. Kaminsky, Eds.; John Wiley and Son, Ltd.: Chichester, 2000; p.175-203.
5. Encyclopedia of materials: science and technology; K. H. J. Buschow, R. N. Cahn, M. Flemings, B. Ilschner, E. Kramer, S. Mahajan, P. Veyssiere Eds.; Elsevier: Oxford, 2001; Vol. 10.
6. T. Cho, E. Shin, W. Jeong, B. Heck, R. Graf, G. Strobl, H. W. Spiess, D. Y. Yoon, Macromol. Rapid Commun. 2006, 27, 322–327.
7. M. L. Cerrada, R. Benavente, and E. Pérez, J. Mater. Res. 2001, 16, 1103-1111.
8. M. F. Laguna, M. L. Cerrada, R. Benavente, E. Pérez, R. Quijada, J. Polym. Sci. Part B: Polym. Phys. 2003, 41, 2174–2184.
9. E. Perez, R. Benavente, R. Quijada, A. Narvaez, G. B. Galland, J. Polym. Sci. Part B: Polym. Phys. 2000, 38, 1440-1448.
10. R. Benavente, E. Pérez, M. Yazdani-Pedram, R. Quijada, Polymer, 2002, 43, 6821-6828.
11. M. L. Cerrada, E. Pérez, J.M. Pereña, R. Benavente, M. Misheva, T. Grigorov, Macromolecules 2005, 38, 8430-8439.
12. K. Jeon, H. Palza, R. Quijada, R.G. Alamo, Polymer 2008, 50, 832–844.

13. J. M. López Majada, H. Palza, J. L. Guevara, R. Quijada, M. C. Martínez, R. Benavente, J. M. Pereña, E. Pérez, M. L. Cerrada, J. Polym. Sci. Part B: Polym. Phys. 2006, 44, 1253–1267.

14. H. Palza, J.M. López-Majada, R. Quijada, R. Benavente, E. Pérez, M.L. Cerrada, Macromol. Chem. Phys. 2005, 206, 1221-1230

15. H. Palza, J.M. López-Majada, R. Quijada, J.M. Pereña, R. Benavente, E. Pérez, M. L. Cerrada, Macromol. Chem. Phys. 2008, 209, 2259-2267.

16. J. Arranz-Andres, R. Benavente, E. Pérez, M.L. Cerrada, Polymer Journal 2003, 35, 766-777.

17. H. Palza, J. M. López-Majada, R. Quijada, J. M. Pereña, R. Benavente, E. Pérez, M. L. Cerrada, Macromol. Chem. Phys. 2008, 209, 2259–2267.

18. M. J. Polo-Corpa, R. Benavente, T. Velilla, R. Quijada, E. Pérez, M. L. Cerrada, Eur. Polym. J. 2010, 46, 1345–1354.

19. A. García-Peñas, J. M. Gómez-Elvira, E. Pérez, M. L. Cerrada. J. Polym. Sci. PartA: Polym. Chem. 2013, 51, 3251-3259.

20. Metallocene–Based Polyolefins: Preparation, Properties and Technology Vol.2, PART VII, Aplications of Metallocene-based Polyolefins, J. Scheirs and W. Kaminsky, Eds.; John Wiley and Son, Ltd.: Chichester, 2000; p.463-555.

21. B. Poon, M. Rogunova, A. Hiltner, E. Baer, S. P. Chum, A.Galeski, E. Piorkowska, Macromolecules 2005, 38, 1232–1243.

22. B. Lotz, J. Ruan, A. Thierry, G. C. Alfonso, A. Hiltner, E. Baer, E. Piorkowska, A. Galeski, Macromolecules 2006, 39, 5777–5781.

23. C. De Rosa, S. Dello Iacono, F. Auriemma, E. Ciaccia, L. Resconi, Macromolecules 2006, 39, 6098–6109.

24. M. L. Cerrada, M. J. Polo-Corpa, R. Benavente, E. Perez, T. Velilla, R. Quijada, Macromolecules 2009, 42, 702–708.

25. P. Stagnaro, L. Boragno, M. Canetti, F. Forlini, F. Azzurri, G.C. Alfonso, Polymer 2009, 50, 5242–5249.

26. E. Pérez, M. L. Cerrada, R. Benavente, J. M. Gomez-Elvira, Macromol. Res. 2011, 19, 1179–1185.

27. C. De Rosa, O. R. de Ballesteros, F. Auriemma, M. R. Di Caprio, Macromolecules 2012, 45, 2749–2763.

28. L. Boragno, P. Staganaro, F. Forlini, F. Azzurri, G. C. Alfonso, Polymer, 2013, 54, 1656-1662.

29. F. F. N. Escher, G. B. Galland, J. Polym. Sci. Part A: Polym. Chem. 2004, 42, 2474-2482.

30. M. A. daSilva, G. B. Galland, J. Polym. Sci. Part A: Polym. Chem. 2008, 46, 947-957.

31. F. F. N. Escher, G. B. Galland, Polymer, 2006, 47, 2634–2642.

32. A. A. S. Filho, G. B. Galland, J. Appl. Polym. Sci. 2001, 80, 1880–1890.

33. G. B. Galland, J. H. Z. doSantos, M. Dall'Agnol, R. Bisatto, Macromol. Symp. 2006, 245–246, 42–50.

34. M. A. Villar, M. L. Ferreira, J. Polym.Sci. Part A: Polym.Chem. 2001, 39, 1136-1148.

35. L. Sun, S. Lin, J. Polym. Sci. Part A: Polym.Chem. 1990, 28, 1237-1254.

36. W. Kaminsky, H. Hahnsen, In Advances in Polyolefins; R. B. Seymour, T. Cheng, Eds.; Plenum Press: New York, 1987; pp 361–371.

37. A. Akimoto, A. Yano, In Metallocene-Based Polyolefins; J. Scheirs, W. Kaminsky Eds.; John Wiley & Sons: Chichester, 2000; pp 287–308.

38. T. Tsutsui, T. Kashiwa, Polym. Commun. 1988, 29, 180–183.

39. J. C. W. Chien, T. Nozaki, J. Polym. Sci. Part A: Polym. Chem. 1993, 31, 227–237.

40. M. A. Da Silva, G. B. Galland, J. Polym. Sci. Part A: Polym. Chem. 2008, 46, 947–957.

41. F. Forlini, I. Tritto, P. Locatelli, M. C. Sacchi, F. Piemontesi, Macromol. Chem. Phys. 2000, 201, 401–408.

42. R. Quijada, Macromol. Chem. Phys. 1996, 197, 3091–3098.

43. H. F. Herrmann, L. L. Böhm, Polym. Commun. 1991, 32, 58–61.

44. J. Koivumäki, J. V. Seppälä, Macromolecules 1993, 26, 5535–5538.

45. K. Heiland, W. Kaminsky, Makromol. Chem. 1992, 193, 601–610.

46. A.García-Peñas, J.M.Gómez-Elvira, E.Pérez, M.L.Cerrada, Unpublished results

47. J.C.Randall, J. Macromol. Chem. Rev. Macromol. Chem. Phys. 1989, C29 (2,3), 201-317.

48. Obviously, this value of n_p represents the average propylene length free of comonomeric units, although it may include some stereo and regio defects. A somewhat smaller value is obtained for n_{iso}, representing the average value of isotactic propylene sequences free of any kind of defect.

49. M. Fineman, S.D. Ross, J.Polym.Sci. 1949, 5, 259-265.

50. T. Kelen, F. Tüdos, J. Macromol. Sci. Part A: Chem. 1975, 9, 1-27.

51. T. Uozumi, K. Soga, Makromol. Chem. 1992, 193, 823-831.

52. K. F. Driscoll, P.M. Reilly, Makromol.Chem. Macromol.Symp. 1987, 10/11, 355-374.

53. D. M. Sarzotti, J. B. P. Soares, A. Penlidi, J. Polym. Sci. Part B: Polym. Phys. 2002, 40, 2595-2611.

54. U. M. Wahner, I. Tincul, D. J. Joubert, E. R. Sadiku, F. Forlini, S. Losio, I. Tritto, M. C. Sachi, Macromol. Chem. Phys. 2003, 204, 1738-1746.

55. J. T. Xu, Y. B. Zhu, Z. Q. Fan, L. X. Feng, J. Polym. Sci.: Polym. Chem. 2001, 39, 3294-3303.

56. P. M. Nedorezova, A. V. Chapurina, A. A. Koval'chuk, A. N. Klyamkina, A. M. Aldyshev, A. O. Baranov, B. F. Shklyaruk, Polymer Science Series B, 2012, 54 (1-2), 1-14.

57. L. A. Risina, N. M. Galashina, P. M. Nedorezova, A. N. Klyamkina, A. M. Aladysev, V. I. Tsvetkova, A. O. Baranov, V. A. Optov, Yu. V. Kissin, Polymer Science Series A, 2004, 46 (9), 911-920.

CAPÍTULO 4

Synthesis, Molecular Characterization, Evaluation of Polymorphic Behavior and Indentation Response in isotactic Poly(propylene-*co*-1-heptene) Copolymers

Alberto García-Peñas, José M. Gómez-Elvira, Vicente Lorenzo,
Ernesto Pérez and María L. Cerrada.
European Polymer Journal, 2015. 64 (17), 52–61

4.1. Abstract

Different polymorphs are developed in isotactic poly(propylene-*co*-1-heptene) copolymers depending on 1-heptene molar content and thermal history: monoclinic and orthorhombic crystallites as well as mesomorphic entities. Indentation hardness values and deformability are found to be related to those variables as well as to crystallinity degree. Consequently, mechanical behavior can be tailored mainly by varying all of these parameters and a range from rigid to soft and more easily deformable materials is attained by synthesis of copolymers based on isotactic propylene with 1-heptene as comonomeric unit. Evaluation of the influence of molecular weight, intrinsic viscosity and microstructural details is also performed.

4.2. Introduction

Isotactic polypropylene, iPP, is one of most versatile polymers currently produced at industrial level primarily because of its relatively low manufacturing cost and its rather interesting properties, both as a plastic and as a fiber. Therefore, iPP is used in a variety of applications, including packaging, textiles, plastic parts and reusable containers of various types, laboratory equipment, automotive components, and polymer banknotes, among others. The good inherent properties and the fact that iPP is reasonably economical, make it competitive to other more expensive engineering plastics. Incorporation of specific fillers or other polymers can allow spreading out even more its application fields. This addition can be performed either by direct blending of the different components, filled polypropylenes [1-6] or blends [7,8], or by polymerization in the presence of fillers [9-11].

Another approach to vary structure and, then, the ultimate performance of iPP is by incorporation of comonomers during its synthetic stage. Metallocene catalysts have constituted a great tool from mid 90s to synthesize polypropylenes with low amounts of oligomers and different tacticities [12] (atactic, isotactic, isoblock, stereoblock, syndiotactic), and also copolymers with ethylene, 1-butene and longer chain α-olefins [13-16] with high comonomeric proportions. Consequently, properties could be tunable depending on the ultimate practical requirements.

The interest on those copolymers allowed finding a new polymorphic form [17] in 2005 for metallocene isotactic copolymers of propylene with high contents of 1-hexene (cPHe) or 1-pentene (cPPe) as comonomers [18-23]. This structure shows a trigonal cell and indicates that the packing of polymer molecules is mainly driven by density (principle of entropy–density driven phase formation in polymers) [24]. At contents lower than 14 mol%, this polymorph competes with the other ones that can be developed (α and γ forms as well as the mesomorphic phase), depending on rate

applied during the crystallization process and/or on supercooling from the isotropic melt before ordering.

The mesomorphic form is already well-known in iPP [25-29] for decades, obtained by very fast cooling from the melt. In the copolymers, however, these mesomorphic entities can be attained under much milder conditions than those necessary ones for their achievement in the iPP homopolymer. Consequently, there exists a reduction in the rate of mesophase formation that depends upon comonomer content at a given counit and upon length of the chain branches at a specific content. Mesomorphic entities formation is, then, easier as the comonomer content increases and as the length within branches is enlarged [16,30,31].

On the other hand, it is important to remark that the trigonal δ polymorph has been exclusively attained using 1-hexene or 1-pentene as comonomers in propene based copolymers and, very recently, in propylene terpolymers containing both 1-pentene and 1-hexene as comonomeric units [32,33]. Furthermore, the new trigonal polymorph is the only one able to crystallize at compositions higher than 14 mol% (up to a limit for 1-hexene copolymers of around 30% of hexene units [17b]), although there are kinetic differences between using 1-hexene or 1-pentene as comonomers [20,30].

The following question can be, then, addressed: what does it occur in random isotactic copolymers if chain-branching length within counit is slightly enlarged, i.e., if 1-heptene, Hp, is incorporated as comonomer? It should be said that these propene-*co*-1-heptene copolymers (cPHp) have been barely referred in open literature. There are few investigations [34,35] that compare some aspects of their copolymerization kinetics and microstructure with those exhibited by others olefinic counits, but to the best of our knowledge there are not other investigations concerning either structural studies or properties evaluation in these cPHp copolymers. Although there was not yet experimental support, Lotz et al.[17b] established as hypothesis from the analysis of the relative intensity of 110 and 300 reflections of the 1-hexene based copolymers that “folded” conformations of the hexene side chains were favored instead of those

stretched ones. Their reasoning also suggested that copolymers of propene with olefins different from hexene may possibly crystallize in a similar form-I-type poly(1-butene) crystal structure when the average side-chain material approaches that of poly(1-butene). Additionally, de Rosa et al. [18] proposed, from the crystal structures obtained for 1-hexene based copolymers and the principle of density (entropy)-driven phase formation, that copolymers of propylene with olefins different from hexene might crystallize in a similar trigonal form, the form I-type poly(1-butene) crystal structure, when the crystal density and the average composition of the copolymer approach those of poly(1-butene), if distribution of the comonomer was random. The crystallization of the trigonal form would be probably dependent on comonomer type, in such a way that in the case of smaller comonomer as, for instance, pentene, it could be developed at higher comonomer concentrations and in the case of bigger comonomers, as heptene at lower comonomer contents.

All of these preliminary investigations point out the importance of evaluating propene-*co*-1-heptene copolymers to fill out the existing gap. Therefore, the aim of this article is, firstly, to describe the synthesis (using a metallocene catalyst) of these propylene-*co*-1-heptene copolymers at different comonomer contents in a broad composition interval as well as to perform their complete molecular characterization. Secondly, to evaluate the crystalline structure generated as function of both composition and crystallization conditions (type of polymorph, competition between lattices, and crystallinity) and correlate these structural features with their mechanical response examined by indentation measurements.

4.3. Experimental

4.3.1. Materials

Toluene (Merck) and the comonomer 1-heptene (TCI Tokyo Kasei) have been previously refluxed over sodium, distilled and kept under N_2 to avoid the presence of traces of water and oxygen. Both propylene (Praxair 2.5) and nitrogen (Praxair 3X) were passed through oxygen-trap columns and molecular sieves before their use. The

catalyst *rac*-dimethylsilylbis(1-indenyl) zirconium dichloride (Strem) and the cocatalyst methylaluminoxane (MAO) (10 wt.% solution in toluene, from Aldrich) were used as received. The activated catalyst was prepared by dissolving 15 mg of the metallocene in 3 mL of MAO solution. A volume of 0.125 mL containing $1.39 \cdot 10^{-6}$ moles of the active complex was used in each polymerization. Ethanol (Aroca, 96%) and HCl (VWR, 37%) were used for the precipitation of the polymers.

4.3.2. Synthesis of poly(propylene-*co*-1-heptene) copolymers

The copolymerization of propylene with 1-heptene was carried out in a 500 mL Büchi glass ecoclave at -5 °C in toluene (250 mL) for 30 min by using *rac*-dimethylsilylbis(1-indenyl) zirconium dichloride/MAO as the catalyst/cocatalyst system ([Al]/[Zr] = 3648). The initial propylene pressure was 0.40 bar, the catalyst amount was $1.39 \cdot 10^{-6}$ mol and the starting comonomer/propylene molar ratio ranging from 0 to 0.893. The copolymerization reaction was stopped after 30 min of reaction time by adding 5 mL of ethanol and enabling the unreacted propylene out from the reactor. The polymer was obtained as a powder by pouring the reaction batch on a mixture of ethanol/HCl (30:1). The precipitated solid was stirred thoroughly overnight, filtrated, washed again with ethanol and, afterwards, dried under vacuum at room temperature. Table 1 shows the different copolymers attained, which are referred as cPHp followed by the closest integer value of the 1- heptene mol % content in the copolymer.

Film samples of the different copolymers were obtained by compression molding in a Collin press between hot plates (at a temperature of 30 °C above the melting point) with a pressure of 2.5 MPa for 3 min, and subsequently cooled down to room temperature under two different thermal treatments: the first one consisted of a relatively rapid cooling between plates refrigerated with cold water after the melting of the material in the press (Q samples, using a cooling rate around 80-100 °C min^{-1}). The second one was a slow cooling process at the inherent cooling rate of the press,

after the power was switched off (S samples, cooling rate around 0.5-1 °C min^{-1}). Pressure was maintained constant at 2.5 MPa along both cooling treatments.

Table 1. Comonomer ratio in the feed and molecular characterization of the different copolymers (1-heptene content, weight-average molecular weight and polydispersity).

Sample	C_7/C_3 [a] (mole ratio)	Hp content (mol %)	M_w (g/mol)	M_w/M_n
iPP	0.000	0.0	140900	2.27
cPHp3	0.179	3.0	135300	2.05
cPHp6	0.406	6.5	102700	2.05
cPHp10	0.534	10.1	83400	2.43
cPHp12	0.816	12.3	76900	2.05
cPHp14	0.892	13.9	74000	2.04
cPHp21	0.920	21.4	-	-

4.3.3. Size exclusion chromatography

The molecular weights were evaluated by size exclusion chromatography (SEC) in a Waters GPC/V 2000 equipment with both refractive index and viscosimeter detectors. A set of three columns of the PL Gel type was used with 1,2,4-trichlorobenzene as the solvent. The analyses were calibrated with narrow molecular mass distribution standards of polystyrene.

Moreover, the intrinsic viscosity values were determined in decaline stabilized with Irganox 1010 (1 g/L^{-1}) at 135 °C.

4.3.4. Nuclear Magnetic Resonance Characterization

The comonomer composition and tacticity were determined at 80 °C by carbon nuclear magnetic resonance, ^{13}C NMR, using 1,1,2,2-tetrachloroethane-d_4 (70 mg 1 $mL^{-1)}$ as solvent, using an Innova 400 spectrometer (100 MHz). A minimum of 8000 scans were recorded with broad band proton decoupling and using an acquisition time of 1s, a relaxation delay of 4 s and a pulse angle of 45°. The homopolymer was characterized in a Bruker Avance DPX-300 (75 MHz) spectrometer,

from solutions in 1,2,4-trichlorebenzene at 100 °C, using deuterated *o*-dichlorobenzene as an internal reference.

4.3.5. Diffraction profiles

Wide-Angle X-ray Diffraction (WAXD) patterns were recorded in the reflection mode by using a Bruker D8 Advance diffractometer provided with a PSD Vantec detector (from Bruker, Madison, Wisconsin). Cu Kα radiation (λ = 0.1542 nm) was used, operating at 40 kV and 40 mA. The parallel beam optics was adjusted by a parabolic Göbel mirror with horizontal grazing incidence Soller slit of 0.12° and LiF monochromator. The equipment was calibrated with different standards: Al_2O_3 (Corundum) and Cr_2O_3. A step scanning mode was employed for the detector. The diffraction scans were collected with a 2θ step of 0.024° and 0.2 s per step.

4.3.6. Mechanical response

Depth Sensing Indentation, DSI, experiments were performed at room temperature with a Shimadzu tester (model DUH211S) equipped with a Berkovich type diamond indenter. In all copolymers, at least 10 indentations were performed at different regions of the specimen surface. The experimental protocol consisted in: (a) the application of a load of 10 mN at a loading speed of 1.46 mN s^{-1}; (b) the maintenance of this constant load for 5 s, and (c) the release of the load at an unloading speed equal than the one used along the loading stage. Finally, indentation depth was registered, additionally, for 5 s after reaching the minimum load (0.1 mN). Martens hardness, HMs, and indentation hardness, Hit, were calculated according to Oliver-Pharr method [36]. These hardness values are related to the ratio of the maximum load to the contact area under load and after releasing the indentor, respectively. Consequently, HMs is related to elastic, viscoelastic and permanent strains, whereas Hit only depends on viscoelastic and plastic strains.

4.4. Results and discussion

4.4.1. Molecular characterization

The molar mass of either ethylene or propylene-based copolymers decreases remarkably upon addition of α-olefins in the feeding because of the existence of transfer reactions with the comonomer, as reported in literature [33,37,38] Fig. 1 does verify this assumption in the present case, where propylene based 1-heptene copolymers have been synthesized (see also data in Table 1). This tendency is observed analyzing the dependence on 1-heptene content of either the weight-average molecular weight or the intrinsic viscosity. Thus, the higher is the comonomer composition in the copolymer, the smaller are either the molecular weights or the intrinsic viscosities.

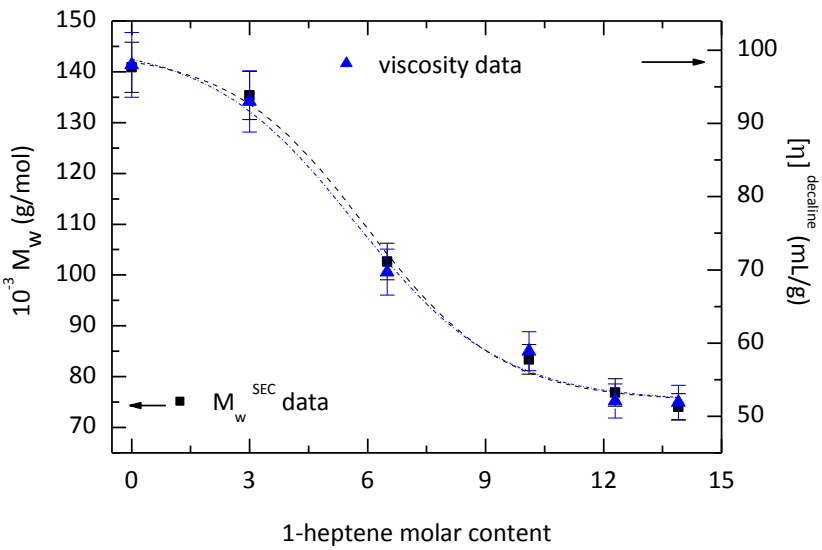

Figure 1. Variation of the weight-average molecular weight determined by SEC measurements (left axis) and of the intrinsic viscosity in decaline at 135 °C (right axis) as a function of the 1-heptene content.

Regarding the microstructural details, the characteristic ^{13}C NMR peaks of the cPHp copolymers under study are detailed in Fig. 2, which shows the spectrum exhibited by the cPHp12 copolymer. These signals can be undoubtedly assigned from the data reported in the literature about the iPP copolymers with 1-heptene [34,35]. Table 2 collects their respective chemical shifts in 1,1,2,2-tetrachloroethane-d_4 at 80 °C and the carbon nuclei that are related to. The different carbon nuclei have been named as P and Hp as belonging to propylene and 1-heptene, respectively, for the purpose of making easier their identification [35]. In addition, a superscript that denotes the carbon position in the corresponding monomer, according to Scheme I, is also used.

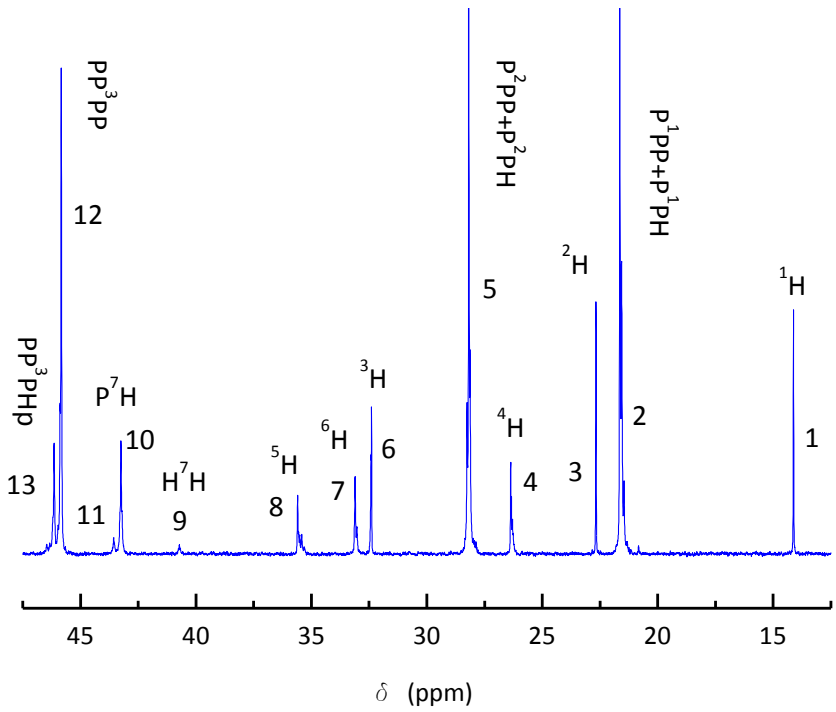

Figure 2. ^{13}C NMR spectra of the cPHp12 copolymer and the peak assignations related to carbons belonging to propylene (P) and 1-heptene (Hp) units, as detailed in Scheme 1.

Table 2. Experimental chemical shifts and assignments (see Scheme 1) of the ^{13}C NMR peaks of copolymers observed in 1,1,2,2-tetrachloroethane-d_4 at 80 °C.

Peak	Chemical Shift (ppm)[a]	Carbon Nucleus: (P= propylene; Hp= 1-heptene)
1	14.11	^{1}Hp
2	22.00-19.40	^{1}P($P^{1}PP$+$P^{1}PHp$)
3	22.65	^{2}Hp
4	26.36	^{4}Hp
5	28.60-27.70	^{2}P($P^{2}PP$+$P^{2}PHp$)
6	32.42	^{3}Hp
7	33.11	^{6}Hp
8	35.59	^{5}Hp
9	40.72	PHp^{7}HpP
10	43.25	PP^{7}HpP+PP^{7}HpHp
11	43.56	HpP^{7}HpHp+HpP^{7}HpP
12	45.84	PP^{3}PP
13	46.15	PP^{3}PHp

[a] Chemical shifts are referenced to $C_4D_2Cl_4$ (74.00 ppm).

Scheme 1. Numeration of carbons belonging to propylene (P) and 1-heptene (Hp) in the polymer chain

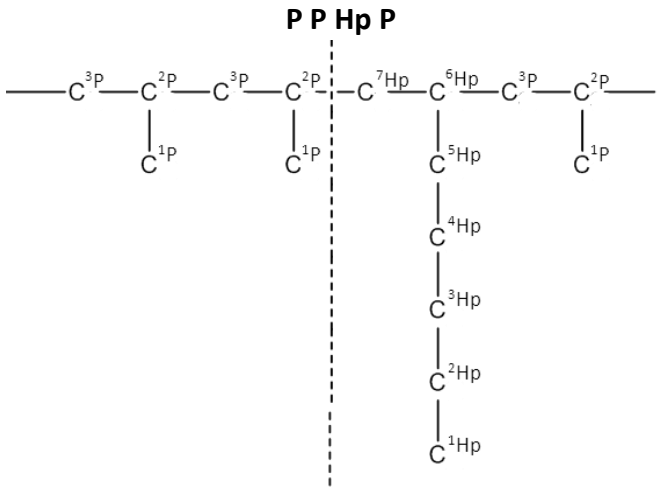

The molar content in 1-heptene comonomer for the different copolymers is shown in Table 3. It was estimated from the relative intensities of the methyl signals at 14.11 ppm (^{1}Hp) and 22.00-19.40 ppm (^{1}P) in the ^{13}C NMR spectra. The so-obtained composition in the copolymers has been compared with that one deduced from the methine carbons and non-significant differences have been found.

Table 3. Comonomer content of the copolymers and propylene tacticity at the pentad level.

Sample	Comonomer content (mol %)	[*mmmm*]	[*mmmr*]	[*rmmr*]	[*mmrr*]	[*mmrm+ rmrr*]	[*mrmr*]	[*rrrr*]	[*rrrm*]	[*mrrm*]
cPHp3	3.0	94.2	1.8	0.0	1.1	0.0	0.0	0.0	0.0	0.0
cPHp6	6.5	89.7	2.1	0.0	1.0	0.0	0.0	0.0	0.0	0.0
cPHp10	10.1	86.9	1.7	0.0	0.4	0.0	0.0	0.0	0.0	0.0
cPHp12	12.3	84.4	2.0	0.0	0.6	0.0	0.0	0.0	0.0	0.0
cPHp14	13.9	83.2	1.6	0.0	0.3	0.0	0.0	0.0	0.0	0.0
cPHp21	21.4	73.6	0.8	0.0	0.3	0.0	0.0	0.0	0.0	0.0

In addition, the propylene tacticity can be estimated from the methyl region at the pentad level. The results are collected for the different specimens in Table 3 (and depicted in Fig 3 for iPP homopolymer as well as for the cPHp3 and cPHp12 copolymers). Besides the main *mmmm* pentads, the minor *mmmr* and *mmrr* pentads are detected. These pentads correspond to isolated steric errors [35], allowing a diagnosis of the enantiomorphic site control run by the isospecific metallocene catalyst [34]. A clear decrease is observed in the content of *mmmm* propylene units as comonomer composition increases. It is also worth remarking that the *mrrm* pentad cannot be detected even though the necessarily associated *mmrr* pentad appears [33]. The absence of the *mrrm* pentad is likely due to the fact that its content is under the detection limit of the NMR measurement.

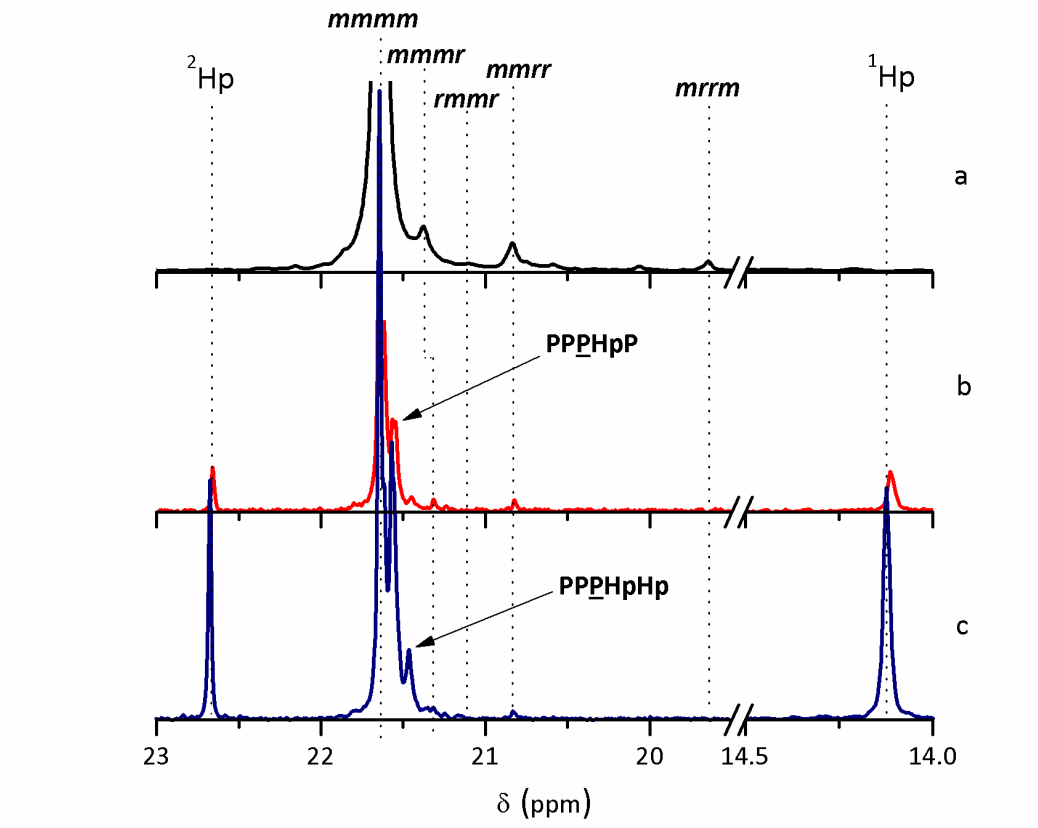

Figure 3. Methyl ^{13}C NMR spectral window of (a) iPP homopolymer (b) cPHp3 copolymer and (c) cPHp12 copolymer.

It has been widely assumed, on one hand, that no comonomer sequences longer than 2 units are formed in propylene based copolymers in the composition range studied here and, on the other hand, that most of the comonomers are present as isolated entities disrupting the PPP segments [34,40-42]. This fact is supported by the low intensity of the band at 40.72 ppm in Fig. 2. This signal is attributed to Hp7Hp methylenes and can be considered as exclusively produced by PHp^{7}HpP tetrads [33].

The methyl window of the cPHp3 and cPHp12 samples (and that of the homopolymer) is shown in Fig. 3, as examples. In the cPHp3 copolymer, the 1-heptene comonomer is exclusively present as isolated units, as a matter of fact the PPPHpP peak at 21.57 ppm is the only new band appearing, whereas 1-heptene comonomer appears in the rest of the copolymer series either as isolated units or diads, as it can

be inferred from the PPPHpHp peak at 21.46 ppm [43] (Fig. 3). The assignment of the comonomer side-chain carbons can be made at the compositional triad level. Some other important features from the ^{13}C NMR spectra of the copolymers are, first, that methyl and methine carbons (^{1}P and ^{2}P) of propylene units in PPHp triads appear well identified. It is also the case for main chain methylene carbons in the middle of HpHp and PHp diads (peaks 9, 10 and 11 at 40.72 ppm, 43.25 and 43.56 ppm respectively), and for methylene carbons in PP^{3}PHp sequences (peak 13 at 46.15 ppm).

The global analysis of the compositional distribution provides a detailed description of the chain microstructure, i.e., the 1-heptene content, the propylene average length and the nature of interruptions, which are, in principle, the main driving factors on the final balance of the different polymorphs produced at given processing conditions. The distribution of the composition from the ^{13}C NMR spectra is then obtained at the triad level by using the following relationships:

$$[PPP] = K\cdot (I_5 - I_{10} - \tfrac{1}{2}\cdot I_{11})$$

$$[PPHp] = K\cdot I_{10}$$

$$[HpPHp] = K\cdot \tfrac{1}{2}\cdot I_{11}$$

(The relationship [HpPHp] = ½· ([HpPHpP] + [HpHpPHp]) is applied taking into consideration that [44] [HpHpPHp]= 0)

$$[PHpP] = K\cdot (I_1 - 2\cdot I_9)$$

$$[HpHpP] = K\cdot 2\cdot I_9$$

$$[HpHpHp] = 0$$

where K is a normalization constant and I_n corresponds to the intensity of peak n tabulated in Table 2. The relative content of the different triad sequences obtained with this procedure is shown in Table 4. It is immediately apparent that 1-heptene units are mostly isolated and that the content of those ones belonging to HpHp diads grows from zero in cPHp3 to more than 10% of the total composition in cPHp14. Finally, a small but not negligible value of HpPHp triads denotes the presence of some isolated Hp units in alternating sequences (HpPHpP).

Table 4. Relative content of triads and average propylene length, n_p.

Sample	PPP	PPHp	HpPHp	PHpP	HpHpP	HpHpHp	[HpHpP]/ [PHpP+HpHpP] x 10^2	n_p
cPHp3	90.8	5.7	0.0	3.5	0.0	0.0	0.0	33.9
cPHp6	81.0	11.2	0.4	6.6	0.8	0.0	6.4	15.4
cPHp10	72.4	15.9	0.6	8.8	2.3	0.0	6.3	10.4
cPHp12	67.2	18.1	1.5	10.0	3.2	0.0	12.8	8.2
cPHp14	65.2	18.3	1.8	11.4	3.3	0.0	13.6	7.8
cPHp21	47.5	25.1	3.8	13.8	9.8	traces	21.6	4.7

From the triad content (see Table 4), the average propylene length has been calculated according to the expression [44]:

$$n_p = ([PPP] + [PPHp] + [HpPHp]) / ([HpPHp] + ½ \cdot [PPHp])$$

It can be observed in Table 4 that the values of n_p change from around 34 units in cPHp3 to around 5 units in cPHp21. Obviously, this important reduction will have a profound influence on both the crystallinity and on the crystal thickness, as shown below.

4.4.2. Characterization of crystalline lattices

Fig. 4 shows the great importance that 1-heptene composition and cooling rate have in the crystalline structure developed by these metallocene cPHp copolymers. This is not a remarkable feature by itself since it is a common characteristic for metallocenic iPP homopolymers and copolymers with distinct microstructural details (i.e., comonomeric units, isotacticity, molecular weight, additives) [45-48]. What is new, to the best of our knowledge as commented in the Introduction, is to perform the crystalline structural characterization using 1-heptene as comonomer. As aforementioned, our interest has been focused on cPHp copolymers in order to learn if the trigonal crystalline lattice (exclusively obtained up

to now in metallocene isotactic copolymers of propylene with high contents of 1-hexene or 1-pentene as comonomers as well as in propene based terpolymers at high contents of both counits) is triggered as length of lateral chain is slightly increased (i.e., 1-heptene instead of 1-pentene or 1-hexene). Looking at Fig. 4, it is clearly noticeable that the trigonal cell is not developed in these cPHp copolymers at similar contents and crystallization rates than those required in cPPe, cPHe copolymers and the corresponding terpolymers. Thus, the most characteristic [17] narrow reflection of the trigonal form, at around 10° in the 2θ scale, does not appear.

There are, however, several similarities with the polymorphic behavior exhibited by those cPPe and cPHe copolymers at comonomer contents lower than 12-14 mol %. Firstly, focusing the attention on the rapidly cooled specimens, the X-ray profiles point out that iPP and the copolymer cPHp3 develop only the monoclinic phase. No evidence of the γ polymorph is detected since a fast cooling rate was applied. Nevertheless, the diminishment in intensity of diffraction peaks is clear, which is ascribed to a crystallinity reduction because of incorporation of 1-heptene along propylene macrochains.

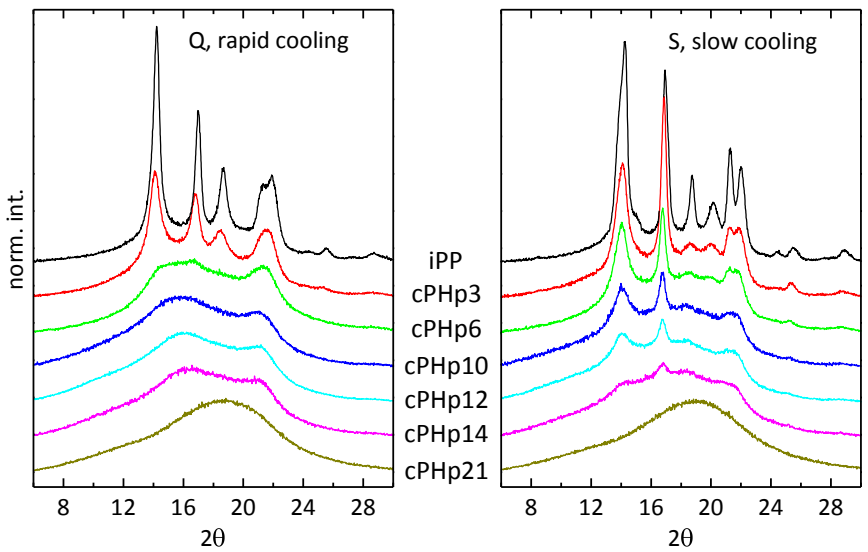

Figure 4. X-ray profiles, at room temperature, for the different rapidly cooled (left) and slowly cooled (right) samples.

A larger loss of regularity, because of a further increase in 1-heptene composition in the copolymer cPHp6, leads to the X-ray pattern characteristic of the iPP mesomorphic modification [25-29] with a very minor amount of α crystals. Moreover, those mesomorphic entities are the only ordered form developed in the rapidly cooled cPHp10, cPHp12 and cPH14 specimens. As already reported for other propylene based copolymers, the formation rate of this mesophase can be easily tailored by varying either comonomer composition or length of counit at a given mol content [16,30,31]. Thus, the mesomorphic phase in iPP homopolymer is obtained under very fast quenching conditions [30,49,50] (i.e. cooling rates higher than 100 °C/s) and from the stretching of the γ polymorph [51] in metallocene iPP, whereas the cooling rate is becoming much smaller when either comonomer content increases at a given copolymer or length in chain branching is enlarged at an almost constant molar content [30,31].

Finally, it is interesting to remark that the diffractogram for copolymer cPHp21 is indicative of a completely amorphous sample.

A somehow different scenario, compared with that one just commented, is observed in specimens slowly crystallized from the melt. The homopolymer and copolymers with the lowest 1-heptene contents (cPHp3 and cPHp6) show an obvious coexistence of monoclinic and orthorhombic (α and γ, respectively) crystallites. Incorporation of higher amounts of comonomer promotes a progressive noticeable decrease in crystallinity. Accordingly, a very small number of crystallites is deduced from the profile of copolymer cPHp14. On the other hand, the cPHp21 copolymer appears to be completely amorphous, even under these conditions of slow cooling rate.

It can be also observed that the ratio between orthorhombic to monoclinic entities is firstly increased in copolymer cPHp3 respect with that found in the homopolymer, but this ratio seems to diminish at higher comonomer content. Anyway, at concentration higher than 10 mol% it is rather difficult to determine this ratio between the two kinds of lattices (monoclinic or orthorhombic).

The degree of crystallinity, f_c^{WAXD}, can be estimated from these diffractograms, if the one related to the amorphous component is known at a particular composition. The amorphous halo corresponding to the homopolymer (at room temperature) can be obtained from an elastomeric, completely amorphous, polypropylene [52]. This profile, labeled as amPP, is shown in Fig. 5a. On the other hand, copolymer cPHp21 is also completely amorphous at room temperature, as aforementioned. With these two profiles, simulation of the amorphous component of any other copolymer at a given comonomer composition is possible just by taking the corresponding weighted average of amPP and cPHp21. For instance, the simulated amorphous profile for cPHp6 is shown in Fig. 5a. And the next step is to scale that amorphous simulated profile in order to account for the degree of crystallinity of the actual sample. Thus, Fig. 5b shows the procedure for specimen cPHp6-S, where an amorphous component of 0.64 is obtained, so that a degree of crystallinity of 0.36 is deduced. The pure crystalline profile of cPHp6-S is also shown in Fig. 5b.

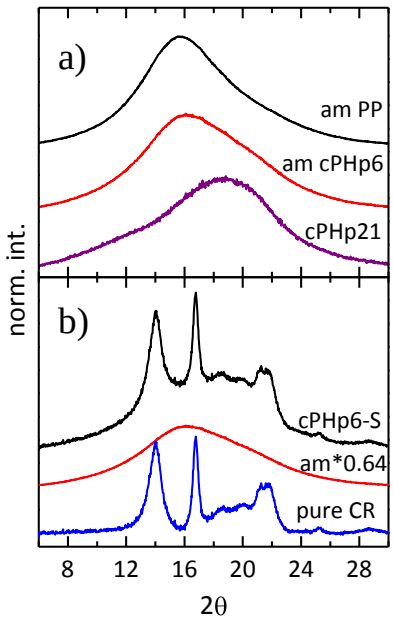

Figure 5. (a) Pure amorphous experimental X-ray profiles, at room temperature, for polypropylene [52] and copolymer cPHp21, and simulated amorphous profile (see text) for copolymer cPHp6. (b) Evaluation of the crystallinity and pure crystal profile for the specimen cPHp6-S.

Following this procedure, the degree of crystallinity has been estimated at the different compositions and thermal treatments. The corresponding results for the total crystallinity (including the mesophase content when it is developed) are plotted in Fig. 6. It can be observed that at the region of low comonomer contents, the degree of crystallinity of the slowly cooled specimens is around 0.08 units higher than the corresponding values for the rapidly cooled samples. However, that difference is getting smaller as the comonomer content increases, in such a way that it seems that the crystallinity of the Q samples is equal or even higher than that found in the S specimens at contents above 10 mol%. It has to be considered, however, that the estimated error of the present determination is around ±0.04 units, so that the differences at those high comonomer contents are practically inside the experimental error. Anyway, it is unexpected that higher crystallinities can be obtained at higher cooling rates.

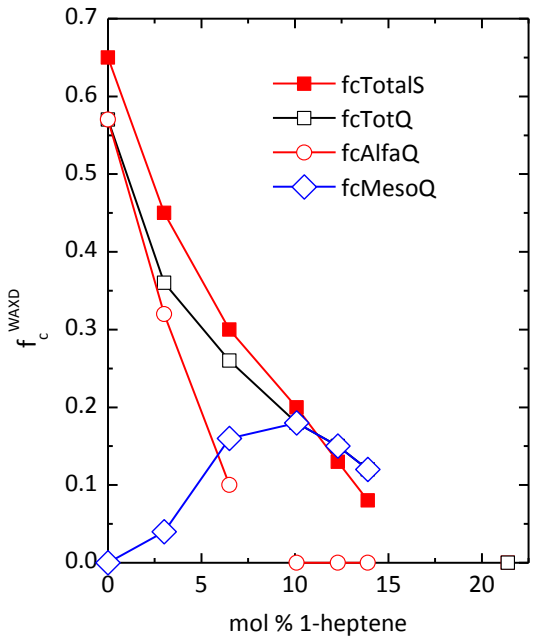

Figure 6. Variation of the WAXD degree of crystallinity with comonomer content for the two thermal treatments. The meso and α proportions are also indicated for the rapidly cooled Q specimens. Estimated errors: ± 0.04 units.

The content in mesophase (which is clearly present in most of the Q specimens) can be easily determined from the previous results, since it coincides with the total degree of crystallinity at comonomer contents higher than around 10 mol%. Estimation is not so straightforward at the lower contents, when monoclinic α phase is also present, due to the overlapping of the diffractions for these two ordered phases. An approach to the problem has been made [30], based on the fact that the diffraction plane [040] (appearing at around 17°) involves about 13% of the total monoclinic intensity. That approximation allowed obtaining a major proportion of mesophase in specimen cPHp6-Q (well evident from its diffractogram) but also a minor amount (inside the experimental error) is deduced for sample cPHp3-Q. The corresponding results are plotted in Fig. 6, indicating that the mesophase reaches a maximum amount at a comonomer content around 8–10 mol% while the monoclinic crystallites are vanished at approximately that content.

As a final comment from Fig. 6, it seems that completely amorphous samples are obtained at contents above around 17-20 mol% of 1-heptene. Considering the results for the average propylene lengths reported in Table 4, it follows that no crystallinity is detected (at room temperature) for n_p values smaller than around 6 units.

4.4.3. Mechanical performance

The versatility shown by polypropylenic derivatives and, consequently, their large application fields lie in the possibility of tuning their properties, primarily their ultimate mechanical performance, by varying their crystalline structure through approaches as crystallization rate, copolymerization, blending or incorporation of filler and/or additives. The interesting polymorphic behavior displayed by these cPHp copolymers, dependent on 1-heptene content and cooling rate, allows us analyzing the influence of structural differences on the response of these materials. Depth Sensing Indentation, DSI, experiments have been chosen to preliminary check their mechanical behavior.

The hardness of a material can be defined as a measurement of the resistance to a permanent deformation or damage. The deformation of a polymer under the action of the indenter is basically ruled by the viscoelastic and plastic components that also govern the mechanical properties of the material. Hardness indentation involves a complex combination of properties (elastic modulus, yield strength, strain hardening, toughness), and thus it can be also expected that hardness values rely on structural parameters, since mechanical properties are structure-dependent. These relationships allow hardness measurements being used as a reliable non-destructive testing technique [53].

The equipment used for this study is able to perform and monitor loading-maintenance-unloading processes, as seen in Fig. 7 for all of the samples at the two crystallization rates. Important variations are observed depending on 1-heptene composition, both on the shape of curves and on the indentation depth reached. The iPP homopolymer is the hardest material, and, consequently, the indenter cannot penetrate too much in its surface (see Fig. 7). Copolymers become progressively softer since crystallinity decreases as 1-heptene content is increased, as deduced from Figs. 4 and 6, and then, their hardness values are reduced. Accordingly, indenter can go more deeply into the material at a given load program, and depth attained is significantly enlarged (clearly seen in Fig. 7). An analogous decrease in hardness has been also found in other olefin copolymers [13-15,54].

The influence of crystallization rate on loading-maintenance-unloading processes and hardness values is also dependent on 1-heptene content. Two distinct trends can be observed as function of the amorphous fraction, as clearly shown in Fig. 8. On one hand, Hit is higher in the slowly crystallized iPP, cPHp3 and cPHp6 (and indenter depth is shorter, as depicted in Fig. 7). Therefore, these S specimens are more rigid and less deformable compared with their corresponding Q counterparts. This fact can be ascribed to the higher global crystallinity (and, consequently, lower amorphous fraction) developed in the slowly crystallized materials. The cPHp10 copolymer acts as an inflection point and, then, the Hit achieved is analogous in both

Q and S samples in spite of their significant structural differences. It is noticeable that amorphous content is very similar (~80%) for both cPHp10-S and cPHp10-Q samples, but the 20% amount of crystalline regions are monoclinic crystallites in the former specimen whereas that percentage consists of mesomorphic entities in the cPHp10-Q sample.

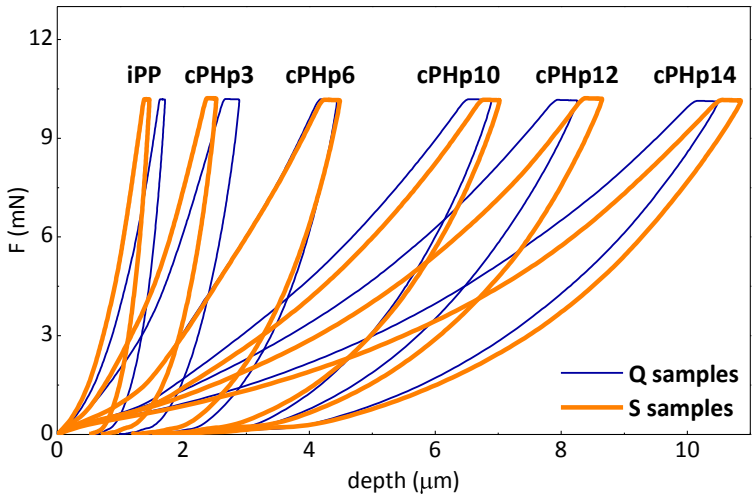

Figure 7. Load-maintenance-unload *vs*. depth curves for the Q rapidly cooled and the S slowly cooled samples.

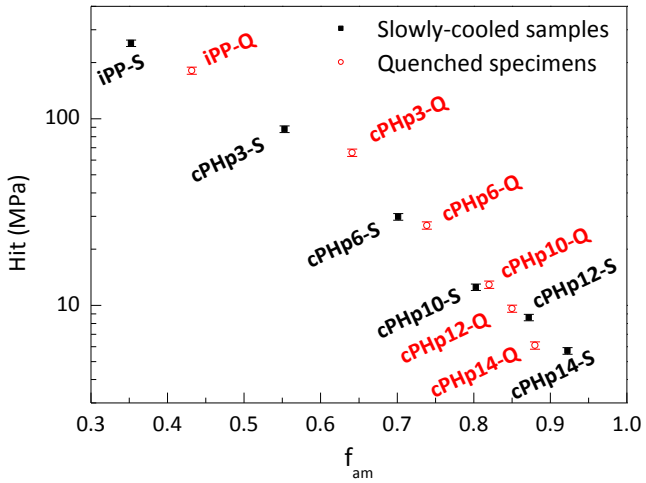

Figure 8. Dependence of indentation hardness, Hit, on the amorphous phase content for the homopolymer and the different copolymers at both thermal treatments (standard error bars are shown).

On the other extreme, the penetration depth of the indenter is smaller and Hit is slightly higher in rapidly cooled cPHp12 and cPHp14 compared with their slowly cooled S samples, as observed in Figs 7 and 8. Therefore, the Q specimens of these copolymers are slightly stiffer and less deformable at their surface compared with their analogous S samples. This is an unexpected behavior, but it can be explained considering that, at these high 1-heptene contents, the amount of ordered entities (i.e, the overall crystallinity represented in Fig. 6) seems to be the key structural feature for the hardness exhibited by these copolymers.

These results can be, then, interpreted by assuming, as a preliminary approach, that indentation behavior of these copolymers can be described by means of a model analogous to those explaining the mechanical properties of composite materials [55]. According to them, the hardness should increase as content of the compliant and soft amorphous phase decreases and this hardening is then related to contents in the mesomorphic and monoclinic phases. Although reinforcement effect of monoclinic crystallites could seem, at first glance, greater than that derived from mesomorphic entities, their lower amounts at these high 1-heptene contents (cPHp12 and cPHp14 copolymers) lead to the mentioned ultimate observation in Fig. 8: Hit is in the rapidly cooled Q specimens slightly higher than in the slowly crystallized S samples. Thus, it seems that the driving force at surface hardness in these cPHp copolymers is not the type of ordered entities developed under a thermal treatment at a given composition (monoclinic, orthorhombic or mesomorphic ones) but their overall amount. Accordingly, an almost linear Hit decreasing relationship is observed in Fig. 8 with content of macrochains in the amorphous state, that is, undoubtedly, the most deformable and less rigid phase from all the involved ones.

Additional information can be deduced from the depth *vs*. indentation time representation, as shown in Fig. 9. The loading-maintenance-unloading processes are clearly observed as well as their dependence on composition and thermal treatment. Then, deformability is raised and, accordingly, depth is enlarged along loading stage as 1-heptene content increases. The maintenance at a constant load for 5 s allows

learning on creep response of these materials. An increment of penetration depth is seen for all the specimens during this maximum load at 10 mN, L^{max}, i.e., during the maintenance period (see Figs. 7 and 9). It is important to remark that, although L^{max} is the same for all experiments, contact pressures are not, however, analogous in the different samples. According to the definition of HMs, this hardness is equal to the contact pressure under L^{max}. The indentation creep depth (which is defined as the difference of depth at the end of the maintenance interval at constant load in relation to that at the beginning of it, h creep) of the hardest sample is close to 0.1 µm under the action of a 186 MPa contact pressure whereas the creep depth of the softest one is close to 0.4 µm under the action of a 3 MPa contact pressure, as depicted in Fig. 10. So, these results clearly prove that copolymers become more compliant as 1-heptene content rises mainly because of the increase in the amorphous phase fraction. Fig. 10 also depicts that this behavior can be modulated by thermal treatment: the creep deformation under indentor in a quenched specimen is greater than that found in the slowly-cooled one at a given copolymer, fact that seems to point out that mesomorphic phase is able to creep more easily than the monoclinic one.

Fig. 9 also displays that the unloading process is mainly dominated by the viscoelastic recovery of the different materials. Once experiment is over, a permanent deformation (plus a small amount of delayed elastic recovery) is attained in all the specimens since they are not completely elastic. The softening process, increasingly observed as 1-heptene content does, involves a rise of the amount in the plastic deformation in the slowly crystallized samples because of the progressive decrease in crystallinity (and crystal sizes) (see Fig. 9a). On the contrary, it is interesting to indicate that this viscous and non-reversible contribution reaches a practically constant value, as noticed in Fig. 9b, for the rapidly cooled cPHp10, cPHp12 and cPHp14 specimens, where the mesomorphic form is the unique ordered structure developed.

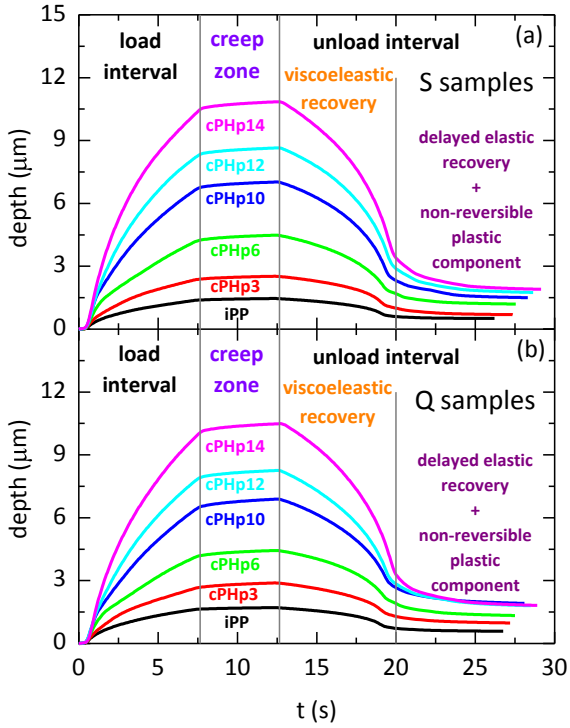

Figure 9. Indenter depth dependence on experimental time for the different copolymers and the homopolymer at the two thermal treatments: (a) S and (b) Q specimens.

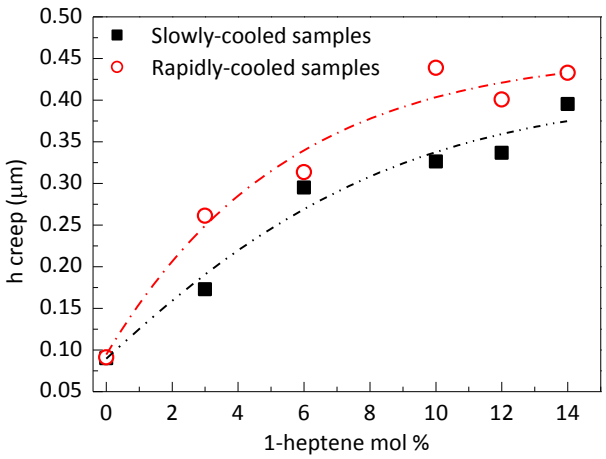

Figure 10. Indentation creep depth as a function of 1-heptene content for both thermal treatments.

4.5. Conclusions

Different copolymers, based on isotactic propylene with 1-heptene as comonomeric unit, have been synthesized at several compositions (up to a content of 21 mol %). Molecular weight and intrinsic viscosity decrease as comonomer content is increased.

The new trigonal δ polymorph (previously described in metallocene isotactic copolymers of propylene with high contents of 1-hexene or 1-pentene as comonomers as well as in propene based terpolymers at high contents of both counits) is not observed in these 1-heptene copolymers at any content, independently of crystallization rate used.

A competition between monoclinic and orthorhombic crystallites as well as mesomorphic entities takes place within the composition interval here analyzed. In rapidly cooled samples, coexistence of monoclinic and mesomorphic entities occurs at intermediate 1-heptene contents, while simultaneous presence of monoclinic and orthorhombic crystallites is seen primarily at the lowest contents in the slow cooled specimens.

Mechanical performance, evaluated through hardness measurements, is tailored mainly by varying copolymer composition and, less significantly, by changing thermal treatment. Materials become softer and more deformable as 1-heptene content increases. Moreover, the amount of non-reversible plastic deformation rises as rigidity is reduced. Even more, it has been proved that DSI technique is an adequate experimental tool to evaluate differences in the mechanical behavior of monoclinic (orthorhombic) crystallites and mesomorphic entities in propylene based copolymers.

4.6. References

1. Kubacka A, Cerrada ML, Serrano C, Fernández-García M, Ferrer M, Fernández-García M. J Nanosci Nanotech 2008;8:3241–3246.
2. Cerrada ML, Serrano C, Sánchez-Chaves M, Fernández-García M, de Andrés MA, Riobóo RJ, Fernández-Martín F, Kubacka A, Ferrer M, Fernández-García M. Environ Sci Techn 2009;43:1630–1634.
3. Gupta M, Lin Y, Deans T, Baer E, Hiltner A, Schiraldi DA. Macromolecules 2010;43:4230–4239.
4. Zhu X, Melian C, Dou Q, Peter K, Demco DE, Möller M, Anokhin DV, Le Meins J-M, Ivanov DA. Macromolecules 2010;43:6067–6074.
5. Serrano C, Cerrada ML, Fernández-García M, Ressia J, Vallés EM. Eur Polym J 2012;48:586-596.
6. Arranz-Andrés J, Pérez E, Cerrada ML. Sci Adv Mater 2013;5:1524-1532.
7. Prieto O, Pereña JM, Benavente R, Cerrada ML, Pérez E. Macromol Chem Phys 2002;203:1844-1851.
8. Álvarez C, Martínez-Gómez A, Pérez E, de la Orden MU, Urreaga JM. Polymer 2007;48:3137-3147.
9. Milani MA, González D, Quijada R, Basso NRS, Cerrada ML, Azambuja DS, Galland GB. Compos Sci Technol 2013;84:1–7.
10. Milani MA, Quijada R, Basso NRS, Graebin AP, Galland GB. J Polym Sci, Part A: Polym Chem 2012; 50:3598-3605.
11. Wan D, Zhang ZJ, Wang YJ, Xing HP, Jiang ZW, Tang T. Soft Matter 2011;7:5290-5299.
12. Kaminsky W. Catalysis Today 1994;20:257.
13. Arranz-Andrés J, Guevara JL, Velilla T, Quijada R, Benavente R, Pérez E, Cerrada ML. Polymer 2005;46:12287-12297.

14. López-Majada JM, Palza H, Guevara JL, Quijada R, Martínez MC, Benavente R, Pereña JM, Pérez E, Cerrada ML. J Polym Sci, Part B: Polym Phys 2006;44:1253-1267.

15. (a) Palza H, López-Majada JM, Quijada R, Benavente R, Pérez E, Cerrada ML. Macromol Chem Phys 2005;206:1221-1230; (b) Palza H, López-Majada JM, Quijada R, Pereña JM, Benavente R, Pérez E, Cerrada ML. Macromol Chem Phys 2008;209:2259-2267.

16. Polo-Corpa MJ, Benavente R, Velilla T, Quijada R, Pérez E, Cerrada ML. Eur Polym J 2010;46:1345-1354.

17. (a) Poon B, Rogunova M, Hiltner A, Baer E, Chum SP, Galeski A, Piorkowska E. Macromolecules 2005;38:1232; (b) Lotz B, Ruan J, Thierry A, Alfonso GC, Hiltner A, Baer E, Piorkowska E, Galeski A. Macromolecules 2006;39:5777.

18. De Rosa C, Dello Iacono S, Auriemma F, Ciaccia E, Resconi L. Macromolecules 2006;39:6098.

19. De Rosa C, Auriemma F, Talarico G, Ruiz de Ballesteros O. Macromolecules 2007;40, 8531-8532

20. Cerrada ML, Polo-Corpa MJ, Benavente R, Pérez E, Velilla T, Quijada R. Macromolecules 2009;42:702-708.

21. Stagnaro P, Boragno L, Canetti M, Forlini F, Azzurri F, Alfonso GC. Polymer 2009;50:5242.

22. Pérez E, Cerrada ML, Benavente R, Gómez-Elvira JM. Macromol Res 2011;19:1179.

23. De Rosa C, de Ballesteros OR, Auriemma F, Di Caprio MR. Macromolecules 2012;45:2749.

24. De Rosa C, Auriemma F, Corradini P, Tarallo O, Dello Iacono S, Ciaccia E, Resconi L. J Am Chem Soc 2006;128:80.

25. Slichter WP, Mandell ER. J Appl Phys 1958;29:1438.

26. Hosemann R, Wilke W. Makromol Chem 1968;118:230.

27. Grebowicz J, Lau JF, Wunderlich BJ. Polym Sci, Polym Symp 1984;71:19.

28. Corradini P, de Rosa C, Guerra G, Petraccone V. Polym Commun 1989;30:281.

29. Arranz-Andrés J, Benavente R, Pérez E, Cerrada ML. Polymer J 2003;35:766.

30. Pérez E, Gómez-Elvira JM, Benavente R, Cerrada ML. Macromolecules 2012;45:6481.

31. Arranz-Andrés J, Parrilla R, Cerrada ML, Pérez E. Macromolecules 2013;46:8557−8568.

32. Boragno L, Stagnaro P, Forlini F, Azzurri F, Alfonso GC. Polymer 2013;54:1656-1662.

33. García-Peñas A, Gómez-Elvira JM, Pérez E, Cerrada ML. J Polym Sci, Part A: Polym Chem 2013;51:3251–3259.

34. Wahner UM, Tincu I, Joubert DJ, Sadiku ER, Forlini F, Losio S, Tritto I, Sacchi MC. Macromol Chem Phys 2003;204:1738–1746.

35. Sacchi MC, Fortini F, Losio S, Tritto I, Costa G, Stagnaro P, Tincu I, Wahner UM. Macromol Symp 2004;213:57-68.

36. Oliver WC, Pharr GM. J Mater Res 1992;7:1564.

37. Heiland K, Kaminsky W. Makromol Chem 1992;193:601.

38. Quijada R. Macromol Chem Phys 1996;197:3091.

39. Villar MA, Ferreira ML. J Polym Sci, Part A: Polym Chem 2001;39:1136.

40. Da Silva MA, Galland GB. J Polym Sci, Part A: Polym Chem 2008;46:947.

41. Forlini F, Tritto I, Locatelli P, Sacchi MC, Piemontesi F. Macromol Chem Phys 2000;201:401.

42. Escher FFN, Galland GB. J Polym Sci, Part A: Polym Chem 2004;42:2474.

43. Sacchi MC, Forlini F, Losio S, Tritto I, Wahner U, Tincul I, Joubert DJ, Sadiku ER. Macromol Chem Phys 2003;204:1643-1652.

44. Randall JC. J Macromol Sci -Rev in Macromol Chem Phys 1989;C29:201–317.

45. Hosier IL, Alamo RG, Esteso P, Isasi JR, Mandelkern L. Macromolecules 2003;36:5623-5636.

46. De Rosa C, Auriemma F, Spera C, Talarico G, Tarallo O. Macromolecules 2004;37:1441-1454.

47. Arranz-Andrés J, Peña B, Benavente R, Pérez E, Cerrada ML. Eur Polym J 2007;43:2357-2370.

48. Krache R, Benavente R, López-Majada JM, Pereña JM, Cerrada ML, Pérez E. Macromolecules 2007;40:6871-6878.

49. Zia Q, Androsch R, Radusch HJ, Piccarolo S. Polymer 2006;47:8163.

50. Mileva D, Androsch R, Zhuravlev E, Schick C, Wunderlich B. Thermochim Acta 2011;522:100.

51. De Rosa C, Auriemma F, Di Capua A, Resconi L, Guidotti S, Camurati I, Nifant'ev IE, Laishevtsev IP. J Am Chem Soc.2004;126:17040–17049.

52. Mansel S, Pérez E, Benavente R, Pereña JM, Bello A, Röll W, Kirsten R, Beck S, Brintzinger H-H, Macromol Chem Phys 1999;200:1292.

53. Lorenzo V, Pereña JM. Curr Trends Polym Sci 1999;4:65.

54. Fonseca C, Pereña JM, Benavente R, Cerrada ML, Bello A, Pérez E. Polymer 1995;36:1887-1892.

55. Ward IM. In Mechanical Properties of Solids Polymers, J. Wiley & Sons, Chichester 1985, 2nd Edition.

CAPÍTULO 5

Mesophase features in isotactic poly(propylene-*co*-1-heptene) copolymers

Alberto García-Peñas, José M. Gómez-Elvira, María U. de la Orden, María L. Cerrada and *Ernesto Pérez.*

2015

5.1. Abstract

The influence of crystallization rate on the interesting polymorphism of random isotactic poly(propylene-*co*-1-heptene) copolymers has been studied, with a particular attention to the conditions for obtaining the mesomorphic phase. For that, the samples have been evaluated with differential scanning calorimetry and variable temperature X-ray diffraction. Owing to the important decrease of cooling rates involved as 1-heptene content increases, the mesophase can be clearly observed by DSC for counit contents above around 5 mol%. Furthermore, only the mesophase (or the amorphous phase) has been found for the copolymer with 13.9 mol% 1-heptene at common cooling rates of the calorimeter (above 0.5 °C/min). Finally, the copolymer with 21.4 mol% counits has been found to be completely amorphous under any thermal treatment analyzed. The results from these copolymers are compared with those found for other ones, using 1-pentene and 1-octene counits, previously reported. Variable temperature diffraction experiments have been carried out to ascertain unambiguously the nature of the phases involved. Finally, a remarkable transparency is attained (above 80 % transmittance in visible light region) at intermediate and high 1-heptene contents. Their values can be, then, tuned by appropriately choosing composition and cooling rate for these copolymers, considering that the mesomorphic entities lead to transmittance values higher than monoclinic crystals.

5.2. Introduction

Nowadays, polypropylene is one of the most important polymers worldwide manufactured. It is well known that isotactic polypropylene, iPP, exhibits an interesting polymorphic behavior together with their wide properties spectra, these facts justifying its enormous commercial applicability. These characteristics imply important technological advances, but also significant scientific developments.

The different crystalline structures found in an iPP homopolymer (monoclinic α, hexagonal β and orthorhombic γ) are related to microstructural characteristics, to the processing history applied, and also to other aspects, like the use of nucleation agents. [1-6] The control of thermal history is important for getting a specific polymorph (probably in competition with other crystalline structures), considering that thermodynamic and kinetic features are involved. Final mechanical properties are directly ascribed to the crystalline characteristics derived from the processing conditions employed [7].

Fast cooling rates, over 100°C/s (or stretching) lead additionally to a metastable mesomorphic phase [1,4,5,8-12] in iPP homopolymers. This mesophase exhibits intermediate properties between monoclinic form and amorphous phase. [13-16] When the cooling rates are lower than that value, the coexistence between mesomorphic and monoclinic forms is unfavorable for the mesophase. It has been shown, however, that the formation rate of the mesophase in random copolymers of propylene with 1-pentene or 1-octene as counits decreases progressively as comonomer content increases, [17,18] and some differences found can be related to the type of counit. Thus, the mesomorphic structure is obtained more easily as length of counit is enlarged [18,19].

An accurate evaluation of the dependence on cooling rate of the mesophase development under real time conditions in iPP homopolymer and copolymers at low comonomer content compulsorily requires the use of Fast Scanning Calorimetry, FSC,

while the mesomorphic formation for copolymers at comonomer contents high enough can be also analyzed with conventional techniques, namely DSC or X-ray diffraction. Therefore, the interest on working with copolymers is twofold: first of all, for enhancing some deficient iPP characteristics, and secondly, for tuning of new properties. Thus, copolymers with the appropriate amount of counits can contribute to enlarge the range of iPP applications, to improve its processability, [20-22] and to control of the ultimate properties. [7,19,23-28] For instance, polypropylenes, among other polyolefins, have become essential as advanced packaging materials of choice for applications in healthcare, food packaging, courier bags, flexible and rigid transport packaging, bottles, trays, large containers and pallets. Its use in this specific area requires, the most of the times, high transparency. This property is directly related to crystalline features, like type of polymorph, crystallinity degree and crystal size.

This attention to iPP copolymers allowed also the discovery of a new trigonal polymorph, obtained in copolymers at high contents (more than around 10 mol %) of 1-pentene or 1-hexene [23,29-33], or in terpolymers of both counits [34,35]. Very few investigations, however, have been dedicated to propylene-*co*-1-heptene copolymers (cPHp) and those published ones are mostly focused on several characteristics of copolymerization kinetics and of the resulting microstructure [36,37]. We have recently published an article concerning the details of the synthesis and molecular characterization of several cPHp copolymers in a broad range of compositions [38], together with preliminary results on several aspects of some structural and mechanical features.

The purpose of the present article is to extend those preliminary investigations to a more complete study about the influence of cooling rate on the interesting polymorphism of these cPHp copolymers, with a particular attention to the experimental conditions for obtaining the mesomorphic phase. This study will additionally contribute for the establishment of a global picture for formation of mesomorphic entities in propylene based copolymers with relatively long-chain branching of different length. For that, the samples have been evaluated with

differential scanning calorimetry and variable temperature X-ray diffraction. Then, results from this analysis are compared with those obtained from other copolymers previously reported in the literature. Additionally, the transmittance values in the visible light region of these samples have been evaluated.

5.3. Experimental

The polymerization reactions were performed under inert conditions after careful purification of the initial reactives: the liquid substances, toluene and 1-heptene (TCI Tokyo Kasei), were treated by refluxing over metallic sodium and further distillation under N_2 to avoid oxygen and water. In the case of gases, N_2 (Praxair 3X) and propylene (Praxair 2.5), were purified by flowing through oxygen-trap columns and molecular sieves before using.

Propylene copolymers with 1-heptene, and the corresponding homopolymer, were prepared in a Büchi glass ecoclave (500 mL) at -5 °C in 250 mL toluene (Merck) for 30 min, with an initial propylene pressure of 0.35-0.4 bar. Polymerizations were carried out at molar ratios ranging between 1-heptene/propylene from 0 to 0.893.

The reactions were started by incorporation of the catalyst, where the precursor metallocene *rac*-dimethyl-silylbis(1-indenyl) zirconium dichloride (Strem) was previously activated with co-catalyst methylaluminoxane (MAO-Aldrich, 10 wt% solution in toluene), using a [Al]/[Zr]=3648 relationship. The reaction was ended by adding 5 mL of ethanol (Aroca, 96%). Subsequently, the solutions were precipitated with a mixture of ethanol and HCl (VWR, 37%). The so-precipitated polymers were stirred overnight, filtrated, washed with ethanol and, finally, dried under vacuum at room temperature.

Molecular weights were determined by size exclusion chromatography (SEC), and compositions, tacticity and relative content of triads were assessed by carbon nuclear magnetic resonance, ^{13}C NMR. Table 1 shows some SEC and NMR data for the

different samples synthesized. Copolymers are named as cPHp followed by the mol % monomer content expressed as the closest integer number.

Table 1. Data from NMR and GPC characterization [38]: comonomer content, molecular weight and distribution, [*mmmm*] content and average propylene length, n_p.

Sample	Comonomer content		M_w (g/mol)	M_w/M_n	[*mmmm*] (%)	n_p
	mol %	w %				
iPP	0	0	140900	2.27	-	-
cPHp3	3.2	7.2	135300	2.05	94.2	33.9
cPHp6	6.5	14.0	102700	2.05	89.7	15.4
cPHp10	10.1	20.8	83400	2.43	86.9	10.4
cPHp12	12.3	24.7	76900	2.05	84.4	8.2
cPHp14	13.9	27.4	74000	2.04	83.2	7.8
cPHp21	21.4	38.8	-	-	73.6	4.7

The calorimetric analysis was performed in a PerkinElmer DSC-7 calorimeter with a connection to a cooling system. The equipment was calibrated with different standards (indium, zinc and *n*-dodecane). Sample weights ranged from 2 to 5 mg. A heating rate of 10 °C/min was used after cooling from the melt at different rates. The maximum cooling rate attained depends on the temperature interval. Thus, a rate of 20 °C/min allows controlling down to around -30 °C, while that temperature is only 80 °C for a rate of 90 °C/min. Besides the usual normalization to sample weight, the heat flows (both on heating and cooling) were also normalized to the scanning rate.

Wide-angle X-ray diffraction patterns were recorded in the reflection mode by using a Bruker D8 Advance diffractometer provided with a Goebel mirror and a PSD Vantec detector (from Bruker, Madison, Wisconsin). Cu Kα radiation (λ = 0.1542 nm) was used. The equipment was calibrated with different standards. Variable-temperature experiments were performed with an Anton-Paar TTK-450 chamber as

temperature controller (provided with a liquid nitrogen regulator and a vacuum pump). A heating rate of 4°C/min was used after cooling from the melt at different rates. Simultaneously, the diffractograms (total acquisition time of 1 min) were collected with the PSD in the step scanning mode, covering the 2θ range from 7.5 to 26°.

Film samples of the different copolymers for transmittance measurements in the visible light region were obtained by compression molding in a Collin press between hot plates (at a temperature of 30 °C above the melting point) with a pressure of 2.5 MPa for 3 min, and subsequently cooled down to room temperature under two different thermal treatments: the first one consisted of a relatively fast cooling between plates refrigerated with cold water after the melting of the material in the press (cooling rate around 80-100 °C min^{-1}). The second one was a slow cooling process at the inherent cooling rate of the press, after the power was switched off (cooling rate around 0.5-1 °C min^{-1}). Pressure was maintained constant at 2.5 MPa along both cooling treatments.

Transmittance measurements in the visible light region were determined in those films with UV-Vis spectroscopy in the visible range (400–800 nm) using a Perkin Elmer Lambda 35 at a scan rate of 480 nm/min. All visible transmittance data have been normalized to a thickness of 100 nm.

5.4. Results and discussion

The most important molecular characteristics for the different copolymers and the corresponding homopolymer are shown in Table 1. The molar mass of propylene-*co*-1-heptene based copolymers decreases remarkably upon incorporation of counit content, as observed in other copolymers [17,18]. Polydispersity values are all around 2, as usual for metallocene copolymers. All these data reported in Table 1 indicate a good monomer distribution along polymeric chains. The isotacticity of the samples decreases with 1-heptene content, as shown by the [*mmmm*] pentad fraction, and the

average propylene length, n_p, is also reduced with increasing comonomer content. Evidently, these microstructural features will have an important effect on crystalline characteristics, such as the crystallinity and crystal perfection, as shown below.

DSC experiments at different cooling rates have been performed on these propylene-*co*-1-heptene copolymers in order to obtain preliminary information about the mesophase formation. Conventional DSC exotherms on cooling from the melt for the homopolymer and the copolymer cPHp3 at different cooling rates are shown in Figure 1. As mentioned above, the mesophase development under real time conditions in iPP homopolymer and copolymers of low comonomer content has to be analyzed by Fast Scanning Calorimetry. [17,18] Thus, the exotherms in Figure 1 do not show any indication of the obtainment of the mesophase, even at the highest cooling rates attained by the conventional calorimeter. The only effects observed in Figure 1 are the expected decrease of the temperature location of the exotherms, i.e. the crystallization temperatures, and the slight reduction of the enthalpy involved, both as the cooling rate increases. More important is the decrease of temperatures and enthalpies when comparing iPP and cPHp3.

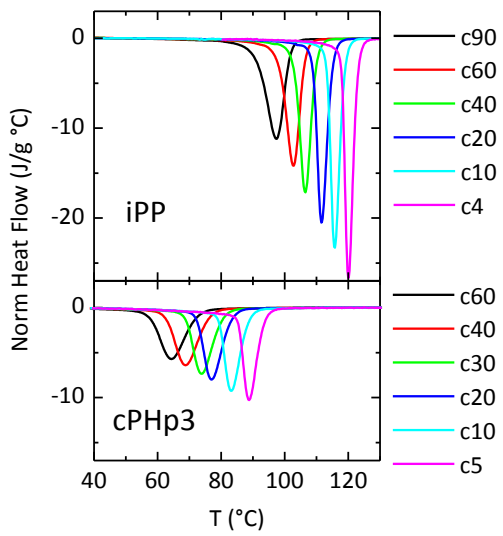

Figure 1. Normalized DSC exotherms on cooling from the melt for the homopolymer and copolymer cPHp3 at the indicated cooling rates (cx, x in °C/min).

The subsequent melting curves for the homopolymer and copolymer cPHp3 are shown in Figure 2. Again, the significant melting point depression for the copolymer in relation to the homopolymer and the great decrease of the total enthalpy are well evident. In addition, some changes in the main melting endotherm are observed, with differences in the melting-recrystallization components as function of the previous cooling rate. Moreover, there is also a clear increment of the shoulder in the low-temperature region of the main endotherm as the previous cooling rate decreases, indicative of higher amounts of orthorhombic modification. [39,40]

The behavior changes rather markedly for copolymers cPHp6 and cPHp10. Thus, the exotherms in Figure 3 show, for both copolymers, a single component at low cooling rates, but when the cooling rate increases a second low temperature peak is clearly observed, whose relative intensity is increasing for further increase of the cooling rate. According to previous results in other copolymers, that low temperature component arises from the mesophase formation. [17,18] Complementary diffraction experiments (see below) will confirm this assumption.

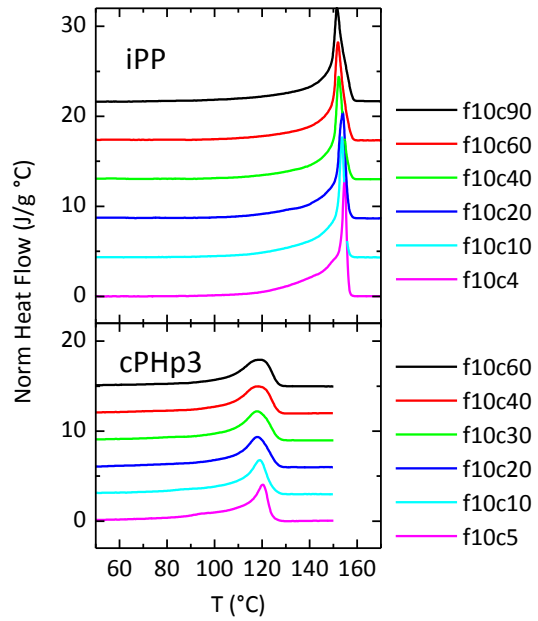

Figure 2. Normalized DSC melting curves (at 10 °C/min, f10) for the homopolymer and copolymer cPHp3 after cooling from the melt at the indicated cooling rates (cx, x in °C/min).

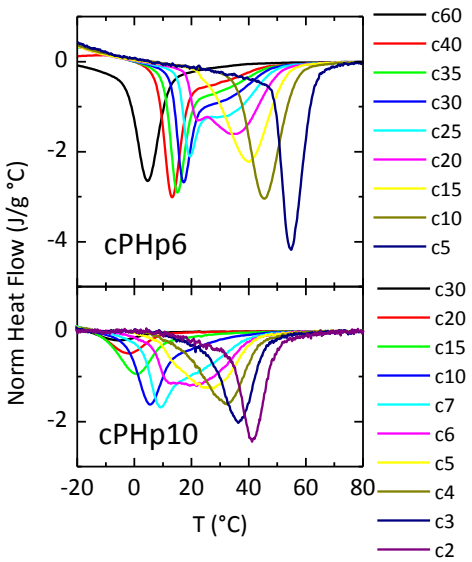

Figure 3. Normalized DSC exotherms on cooling from the melt for copolymers cPHp6 and cPHp10 at the indicated cooling rates (cx, x in °C/min).

Another important aspect from Figure 3, and especially evident for copolymer cPHp10, is the fact that at sufficiently high cooling rates the total enthalpy involved in the exotherm begins to decrease rather markedly, in such a way that at cooling rates higher than around 30 °C/min a totally amorphous sample is obtained.

This aspect is also well evident in the subsequent melting curves, as observed in Figure 4. In fact, the melting curve after cooling at 60 °C/min for copolymer cPHp6 shows a subtle cold crystallization, indicating that the ordering process was not completed in the cooling process. But the cold crystallization is especially apparent for copolymer cPHp10, after cooling rates below around 10 °C/min. Figure 4 also shows the glass transition region, this transition appearing between around -10 and -20 °C. It comes out well noticeable, therefore, the capital influence of the comonomer content on the rates required for observing the mesophase or for obtaining completely amorphous specimens (or any rate related to ordering/crystallization). The quantification of this effect is carried out below.

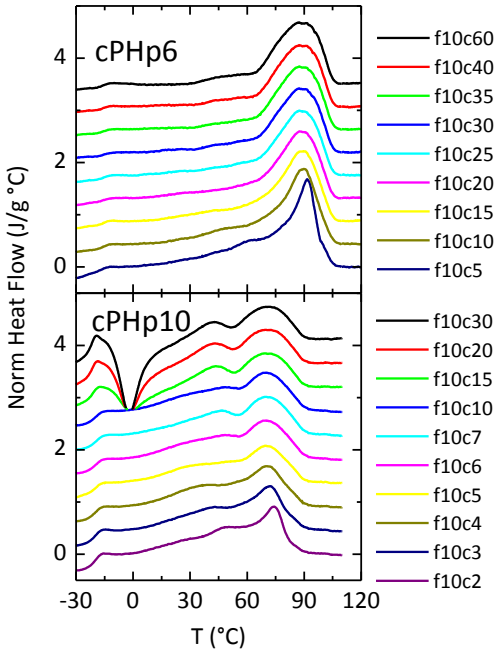

Figure 4. Normalized DSC melting curves (at 10 °C/min, f10) for copolymers cPHp6 and cPHp10 after cooling from the melt at the indicated cooling rates (cx, x in °C/min).

The cooling exotherms for copolymer cPHp12 are shown in the upper part of Figure 5. The behavior is rather similar to that of cPHp10 except for the lower cooling rates needed for the two processes (mesophase formation and total amorphous specimen). One important implication of these smaller cooling rates is that the signal-to-noise ratio is worsening rather evidently.

This problem is even worse for copolymer cPHp14 (lower part of Figure 5). In fact, the minimum cooling rate tested has been 0.5 °C/min for practical reasons of both signal-to-noise and time consumption. Comparison with other copolymers allows concluding that only the mesophase is formed in the entire range of cooling rates used (except for cooling rates higher than around 5 °C/min, when completely amorphous specimens are obtained).

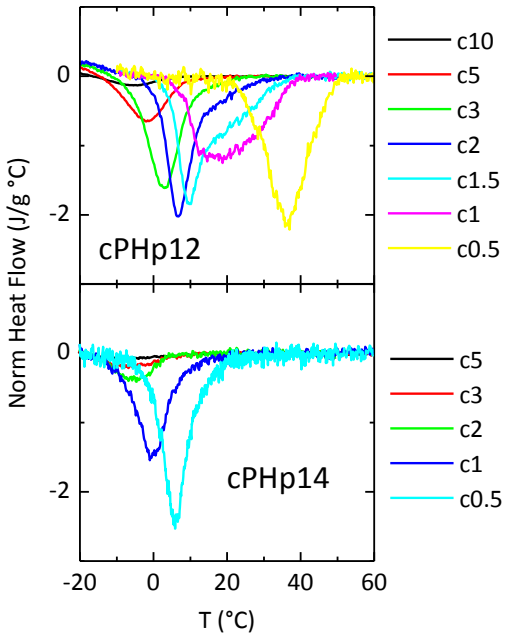

Figure 5. Normalized DSC exotherms on cooling from the melt for copolymers cPHp12 and cPHp14 at the indicated cooling rates (cx, x in °C/min).

Figure 6 shows the subsequent melting curves for copolymers cPHp12 and cPHp14. Three aspects can be highlighted from it. First, glass transition is shifted to lower temperatures as comonomer content increases. Secondly, well evident cold crystallizations are observed at the higher cooling rates. And finally, bimodal character of the melting endotherms is exhibited, the low temperature peak assigned to the melting of the mesophase and further recrystallization into the monoclinic modification, and the one at high temperature associated with the final melting of this α modification. The diffraction experiments (see below) will probe these assignments.

Finally, the DSC curves corresponding to copolymer cPHp21 are shown in Figure 7. It can be seen that the sample is completely amorphous, even after remaining a long time at room temperature, and only the glass transition is observed, centered at -28 °C in the melting curves.

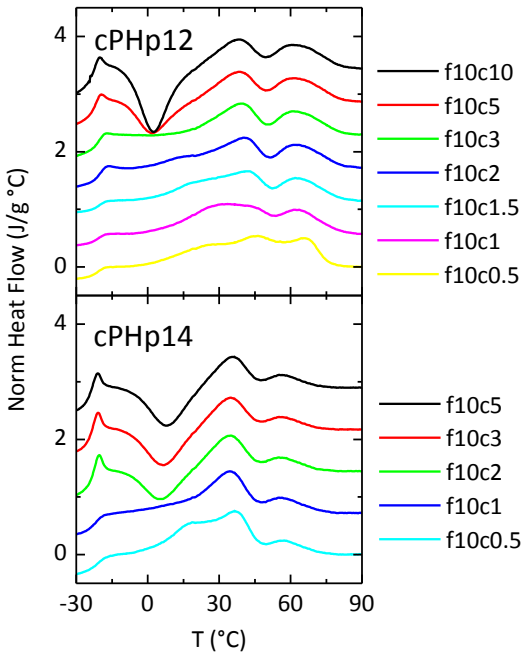

Figure 6. Normalized DSC melting curves (at 10 °C/min, f10) for copolymers cPHp12 and cPHp14 after cooling from the melt at the indicated cooling rates (cx, x in °C/min).

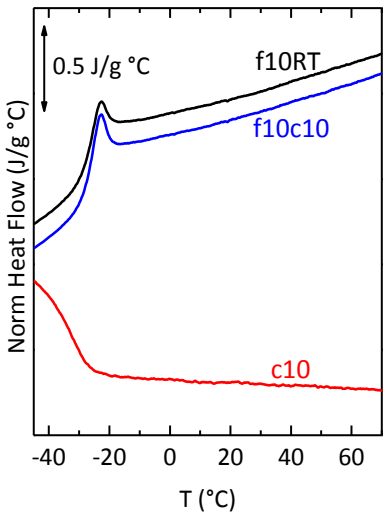

Figure 7. Normalized DSC curves for copolymer cPHp21, corresponding to: melting at 10 °C/min after long time at room temperature (f10RT), cooling at 10 °C/min (c10), and melting at 10 °C/min after cooling at the same rate (f10c10).

The quantification of the different melting experiments for the semicrystalline copolymers is shown in Figure 8, where variation of the enthalpy of melting with cooling rate for the different samples is observed (extracted from Figures 2, 4 and 6). For iPP and copolymer cPHp3 only a smooth decrease of the total enthalpy of melting with increasing cooling rates is detected in the practical range of the calorimeter. For copolymer cPHp6, a higher decrease of the enthalpy is already noticeable, up to the maximum cooling rate attained. For the other three copolymers, however, a rate where entirely amorphous samples are achieved is possible to be reached.

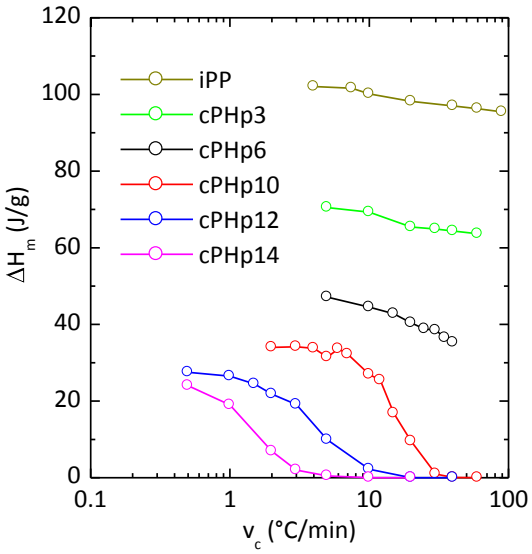

Figure 8. Variation of the enthalpy of melting with the cooling rate for the different samples.

The results for the cooling experiments, which are much more informative, are presented in Figure 9. Its upper part shows the dependence on cooling rate of the peak temperatures in the exotherms for both the α and meso, m, components. As indicated above, only the α component can be observed for iPP and cPHp3 at the rates under study, and only the mesophase one for cPHp14. For the other three copolymers where both components are obtained, it can be seen that the α peak appears at around 10-15 °C above the mesomorphic one, similarly to the results found in other iPP copolymers. [18]

The lower part of Figure 9 shows the variation with cooling rate of the total enthalpy in the exotherms, together with its deconvolution into the two components: mesomorphic and α, for copolymers cPHp6, cPHp10 and cPHp12 (derived from Figures 3 and 5). The most interesting feature is the variation of the mesomorphic enthalpy, showing a maximum at "intermediate" cooling rates, observable for cPHp10 and cPHp12. The absolute value of this maximum is approximately similar for the two copolymers, but it follows that relatively higher proportion of mesophase is obtained at the highest counit content taking into account the substantial decrease of the total enthalpy with increasing comonomer content.

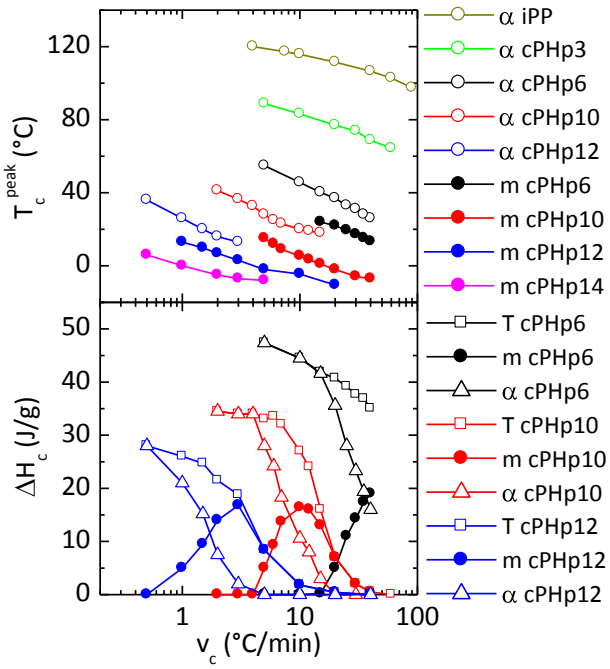

Figure 9. Variation with the cooling rate of the peak temperatures (above: α and meso, m, components) in the exotherms for the different samples, and of the enthalpy (below: total, T, meso, m, and α components) for the indicated copolymers.

Determination of the cooling rates needed for first observing the mesomorphic peak (applicable to copolymers cPHp6, cPHp10 and cPHp12) and for attaining entirely amorphous samples (applicable to cPHp10, cPHp12 and cPHp14) is also possible from these results. The values of these rates are shown in Figure 10,

compared with those reported [17, 18] for 1-pentene (cPPe) and 1-octene (cPO) copolymers (note that, since many of those reported results were obtained from FSC, the cooling rates in Figure 9 are expressed in °C/s, as usual in FSC). This representation is a certain kind of continuous cooling curve, CCC, diagram [41-43] regularly utilized in metallurgy for quenched steel. As reported before, [18] the parameters related to the rate and degree of ordering were found to depend on the comonomer content expressed in weight percentage since those parameters are interconnected to the size of the counits (while the crystallization and melting temperatures vary with the mol content of counits). It can be observed in Figure 10 that the results for the present cPHp copolymers are rather similar to those found for cPPe and cPO copolymers, regarding the values for the two boundary regions of the CCC diagram.

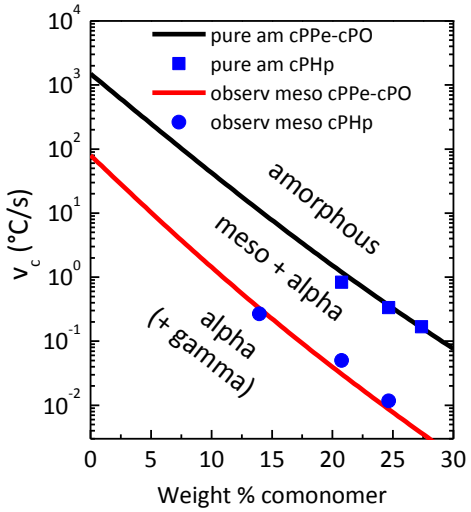

Figure 10. Variation of the cooling rates (expressed in °C/s) for the two boundary regions (entirely amorphous specimens and first observation of the mesophase) with the weight percentage of comonomer content for the present cPHp copolymers compared with the results [17, 18] reported for 1-pentene (cPPe) and 1-octene (cPO) copolymers.

This calorimetric study has been complemented by x-ray diffraction experiments in order to verify the exact character of the phases involved. Figure 11 shows, as an example, the variable-temperature X-ray diagrams for cPHp10 on cooling from the melt at different rates, ranging from 30 to 4 °C/min (since acquisition time is

always the same, the number of frames resulting from the entire temperature interval, from 100 to -20 °C, is inversely proportional to cooling rate). It can be observed that no evidence of any kind of significant order is seen when cooling takes place at 30 °C/min and, consequently, the sample remains completely amorphous. When cooling is performed at 15 °C/min the formation of the mesophase is, however, observed below around 20 °C. At a cooling rate of 10 °C/min, the mesophase is preceded by the formation of monoclinic crystals, which are the dominant ones at the lowest cooling rate (4 °C/min).

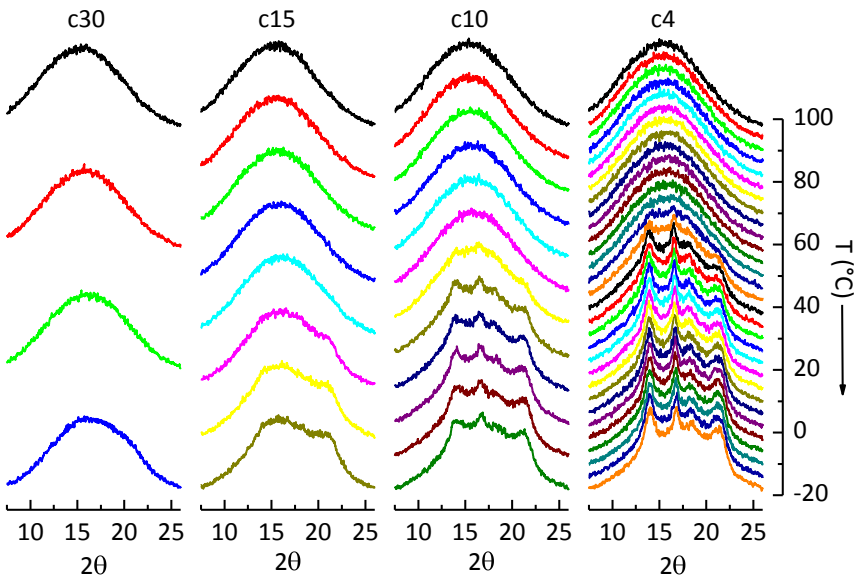

Figure 11. Variable-temperature X-ray diagrams for cPHp10 on cooling from the melt at the indicated rates (cx, x in ºC/min).

These diffraction results are in perfect agreement with the ones represented in Figure 3 and, furthermore, they confirm the previous assumption that the high-temperature component in the exotherms is due to monoclinic crystals, and the one appearing at low temperature corresponds to the mesophase.

The subsequent melting experiments are presented in Figure 12 (a melting rate of only 4 °C/min has been chosen so that the temperature resolution between

frames is good enough). Comparison of these results with the calorimetric ones depicted in the bottom plot of Figure 4 proves the assignment of the cold crystallization from an amorphous state into the mesophase (in the interval between -10 and 10 °C) when melting process after cooling is carried out at 30 °C/min, followed by the melting and recrystallization of this mesophase into monoclinic crystals (at around 40-50 °C), and its final melting (at about 80 °C). Al these X ray profiles, therefore, confirm the previous assumption related to the melting endotherms noticeable in DSC experiments.

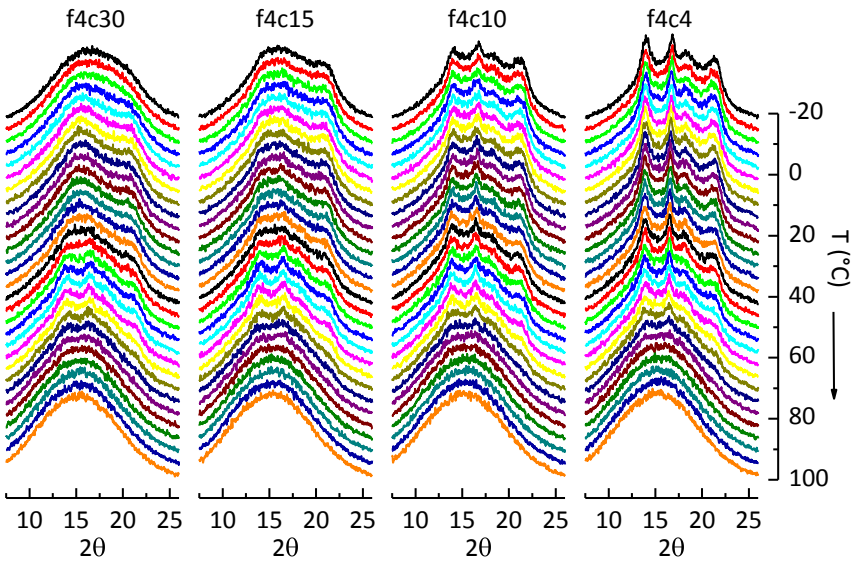

Figure 12. Variable-temperature X-ray diagrams for cPHp10 on melting at 4 °C/min (f4) after cooling from the melt at the indicated rates (cx, x in °C/min).

Obviously, if cooling is performed at rates as low as 4 °C/min where only the monoclinic form is obtained, the melting X ray diagrams show only the variations on temperature of the crystals of that modification, completely disappearing again at around 80 °C.

As a final comment on these diffraction experiments, the attention can be focused on the representative profiles observed at the lowest temperature after cooling at the different rates (inferior profiles in Figure 11 or superior ones in Figure

12). It can be deduced that an amorphous sample is obtained after cooling at 30 °C/min, a mesomorphic one for 15 °C/min, a mixture of mesomorphic and monoclinic after 10 °C/min and a typical monoclinic one after 4 °C/min, in a perfect agreement with the results in the lower part of Figure 9.

Existence of a unique crystalline lattice or competition of several polymorphs depends, as aforementioned, on cooling rate applied during processing. Knowledge of the phase transitions is, then, very important since all these structural characteristics derived from how processing occurs will determine the whole properties spectrum allowing tuning them and, consequently, their ultimate applicability. As mentioned above, an interesting application of polypropylene is as advanced packaging material, and for that use a high transparency is usually required, which depends strongly on crystalline features. Figure 13 depicts the transmittance in the visible light region determined from visible spectra, observed for the copolymers processed under two rather opposite conditions: fast (90 °C/ min) and slow (1 °C/min) cooling rates from the molten state.

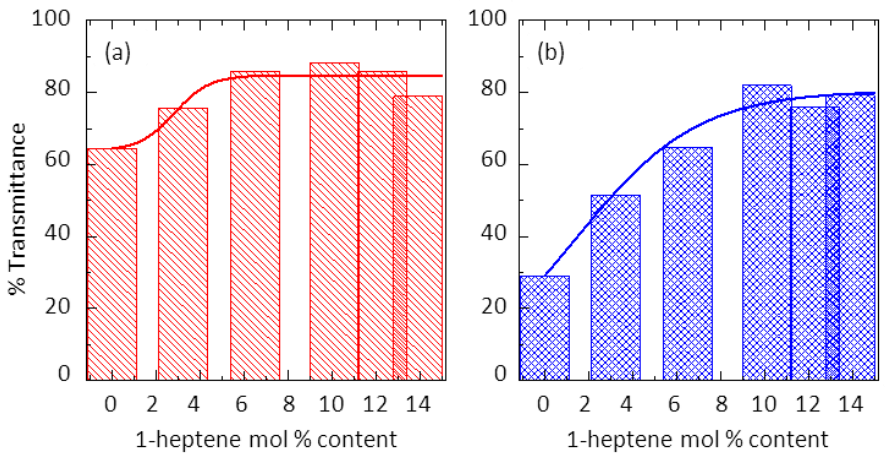

Figure 13. Dependence of visible transmittance values on 1-heptene molar content: (a) fast cooled and (b) slowly crystallized specimens, left and right respectively.

The transmittance values observed in the visible light region for the fast cooled films are remarkably high at 1-heptene contents of 6 mol % and above (an average of around 84 % of light transmission). This feature is rather significant, mainly taking into account the crystallinity values for those specimens. These ordering degrees are: 0.26, 0.18; 0.15, 0.12 for cPHp6, cPHp10, cPHp12 and cPHp14, respectively. [38]

On the other hand, the values of transmittance at contents equal or inferior than 6 mol% are considerably reduced if a slow cooling rate from the melt is applied (Figure 13b).

At higher compositions, an average value of around 80 % of light transmission is reached for cPHp10, cPHp12 and cPHp14 specimens, whose crystallinity is 0.20, 0.13 and 0.08, respectively.

The most transparent polymers, all of them completely amorphous, are: poly(methyl methacrylate) with a 92 % of transmittance, polystyrene with a value around 90 % and poly(bisphenol A carbonate), whose transmittance in the visible light region ranges from 80 to 90 %. The copolymers under study are semicrystalline and the differences found at a given sample between both thermal treatments imposed can be ascribed to the fact that crystallization at high cooling rate takes place at conditions far from the equilibrium, leading to the existence of a significant amorphous zone. These regions are at a higher extent in these copolymers because of the presence of 1-heptene, a non-crystallizable counit. Fast cooling rate, then, limits the development of crystallites and promotes the formation of mesomorphic entities at 1-heptene composition equal or higher than 6 mol %. Slow cooling is more amenable to crystallites perfection and crystallites developed in this set of copolymers under these conditions are monoclinic (and some proportion of orthorhombic) but not mesomorphic ordering. Although crystallinity values are not very distinct between fast and slow cooled samples at a specific composition, it seems that mesomorphic entities lead to transmittance values in the visible light region higher than those from monoclinic crystallites.

5.5. Conclusions

A comprehensive evaluation of the influence of cooling rates on the interesting polymorphism exhibited by isotactic poly(propylene-*co*-1-heptene) copolymers has been performed for the first time in open literature. A particular attention has been paid to those conditions for obtaining the mesomorphic phase because its industrial and scientific relevance. For that, an extensive differential scanning calorimetry and variable temperature X-ray diffraction study has been performed.

An important reduction of the cooling rates involved in the ordering process has been found as 1-heptene content increases in these copolymers, in such a way that the mesophase can be clearly observed by conventional DSC for counit contents above around 5 mol%. In this range of "intermediate" comonomer contents, two components are clearly observed in the cooling exotherms: the high temperature constituent arising from the crystallization of monoclinic entities and the low temperature peak due to mesophase formation, as it has been unambiguously ascertained from variable temperature diffraction experiments.

Furthermore, only the mesophase (or the amorphous phase) has been found for the 1-heptene copolymer with 13.9 mol% at the practical cooling rates of the calorimeter (above 0.5 °C/min), i.e, for this copolymer what is really difficult is to obtain the regular monoclinic crystallization.

Finally, the copolymer with 21.4 mol% counits has been found to be completely amorphous under any thermal treatment analyzed.

The results from this analysis are found to be rather coincident with those of other copolymers previously reported regarding the values for the two boundary regions of the continuous cooling curve diagrams: the rates needed for first observing the mesomorphic peak and the ones for attaining entirely amorphous samples.

Remarkable transmittance values in the visible light region are reached, above 80 % transmittance, at intermediate and high 1-heptene contents. Their values can be,

then, tuned by appropriately choosing composition and cooling rate for these copolymers. Mesomorphic entities lead to transmittance values in the visible light region superior than monoclinic crystals, although the ordering degrees are in the former ones even more elevated at the highest 1-heptene contents, pointing out the importance of the knowledge on the existing polymorphs and their phase transitions for final applications.

5.6. References

1. S. Brückner, S. V. Meille, V. Petraccone, B. Pirozzi, *Prog. Polym. Sci.* 1991, *16*, 361-404.
2. B. Lotz, J. C. Wittmann, A. J. Lovinger, *Polymer* 1996, *37*, 4979-4992.
3. J. Varga, *J. Mater. Sci.* 1992, *27*, 2557-2579.
4. P. J. Phillips, K. Mezghani, in The Polymeric Materials Encyclopedia, J. C. Salamone, Ed.; CRC Press: Boca Raton, 1996, Vol. 9, p. 6637.
5. G. Natta, P. Corradini, *Il Nuovo Cimento Series 10* 1960, *15*, 40-51.
6. A. Turner-Jones, J. M. Aizlewood, D. R. Beckett, *Makromol. Chem.* 1964, *75*, 134-158.
7. J. M. López-Majada, H. Palza, J. L. Guevara, R. Quijada, M. C. Martínez, R. Benavente, J. M. Pereña, E. Pérez, M. L. Cerrada, *J. Polym. Sci., Part B: Polym. Phys.* 2006, *44*, 1253-1267.
8. W. P. Slichter, E. R. Mandell, *J. Appl. Phys.* 1958, *29*, 1438-1441.
9. P. B. McAllister, T. J. Carter, R. M. Hinde, *J. Polym. Sci., Part B: Polym. Phys.* 1978, *16*, 49-57.
10. V. Vittoria, *J. Macromol. Sci., Phys.* 1989, *B28*, 489-502.
11. W. J. Okane, R. J. Young, A. J. Ryan, W. Bras, G. E. Derbyshire, G. R. Mant, *Polymer* 1994, *35*, 1352-1358.
12. J. Arranz-Andrés, R. Benavente, E. Pérez, M. L. Cerrada, *Polym. J.* 2003, *35*, 766-777.

13. V. Vittoria, *J. Polym. Sci., Part B: Polym. Phys.* 1986, *24*, 451-455.

14. R. Russo, V. Vittoria, *J. Appl. Polym. Sci.* 1996, *60*, 955-961.

15. K.-h. Nitta, K. Odaka, *Polymer* 2009, *50*, 4080-4088.

16. V. Brucato, S. Piccarolo, V. La Carrubba, *Chemical Engineering Science* 2002, *57*, 4129-4143.

17. E. Pérez, J. M. Gómez-Elvira, R. Benavente, M. L. Cerrada, *Macromolecules* 2012, *45*, 6481-6490.

18. J. Arranz-Andrés, R. Parrilla, M. L. Cerrada, E. Pérez, *Macromolecules* 2013, *46*, 8557-8568.

19. M. J. Polo-Corpa, R. Benavente, T. Velilla, R. Quijada, E. Pérez, M. L. Cerrada, *Eur. Polym. J.* 2010, *46*, 1345-1354.

20. W. Spaleck, in Metallocene-Based Polyolefins: Preparation, Properties and Technology, J. Scheirs, W. Kaminski, Eds.; Wiley: New York, 2000, Vol. 1, p. 425.

21. N. Pasquini, Polypropylene Handbook, Carl Hanser Verlag: Munich, 2005.

22. D. Mileva, R. Androsch, D. Cavallo, G. C. Alfonso, *Eur. Polym. J.* 2012, *48*, 1082-1092.

23. B. Poon, M. Rogunova, A. Hiltner, E. Baer, S. P. Chum, A. Galeski, E. Piorkowska, *Macromolecules* 2005, *38*, 1232-1243.

24. M. Gahleitner, P. Jaaskelainen, E. Ratajski, C. Paulik, J. Reussner, J. Wolfschwenger, W. Neissl, *J. Appl. Polym. Sci.* 2005, *95*, 1073-1081.

25. H. Palza, J. M. López-Majada, R. Quijada, J. M. Pereña, R. Benavente, E. Pérez, M. L. Cerrada, *Macromol. Chem. Phys.* 2008, *209*, 2259-2267.

26. J. Arranz-Andrés, B. Peña, R. Benavente, E. Pérez, M. L. Cerrada, *Eur. Polym. J.* 2007, *43*, 2357-2370.

27. B. Poon, M. Rogunova, S. P. Chum, A. Hiltner, E. Baer, *J. Polym. Sci., Part B: Polym. Phys.* 2004, *42*, 4357-4370.

28. C. De Rosa, F. Auriemma, O. R. De Ballesteros, L. Resconi, I. Carnurati, *Chem. Mater.* 2007, *19*, 5122-5130.

29. B. Lotz, J. Ruan, A. Thierry, G. C. Alfonso, A. Hiltner, E. Baer, E. Piorkowska, A. Galeski, *Macromolecules* 2006, *39*, 5777-5781.

30. C. De Rosa, S. Dello Iacono, F. Auriemma, E. Ciaccia, L. Resconi, *Macromolecules* 2006, *39*, 6098-6109.

31. C. De Rosa, F. Auriemma, G. Talarico, O. R. de Ballesteros, *Macromolecules* 2007, *40*, 8531-8532.

32. M. L. Cerrada, M. J. Polo-Corpa, R. Benavente, E. Pérez, T. Velilla, R. Quijada, *Macromolecules* 2009, *42*, 702-708.

33. E. Pérez, M. L. Cerrada, R. Benavente, J. M. Gómez-Elvira, *Macromol. Res.* 2011, *19*, 1179-1185.

34. L. Boragno, P. Stagnaro, F. Forlini, F. Azzurri, G. C. Alfonso, *Polymer* 2013, *54*, 1656-1662.

35. A. Garcia-Peñas, J. M. Gómez-Elvira, E. Pérez, M. L. Cerrada, *J. Polym. Sci., Part A: Polym. Chem.* 2013, *51*, 3251-3259.

36. U. M. Wahner, I. Tincul, D. J. Joubert, E. R. Sadiku, F. Forlini, S. Losio, I. Tritto, M. C. Sacchi, *Macromol. Chem. Phys.* 2003, *204*, 1738-1746.

37. M. C. Sacchi, F. Fortini, S. Losio, I. Tritto, G. Costa, P. Stagnaro, I. Tincul, U. M. Wahner, *Macromol. Symp.* 2004, *213*, 57-68.

38. A. Garcia-Peñas, J. M. Gómez-Elvira, V. Lorenzo, E. Pérez, M. L. Cerrada, *Eur. Polym. J.* 2015, *64*, 52-61.

39. E. Pérez, D. Zucchi, M. C. Sacchi, F. Forlini, A. Bello, *Polymer* 1999, *40*, 675-681.

40. R. G. Alamo, M. H. Kim, M. J. Galante, J. R. Isasi, L. Mandelkern, *Macromolecules* 1999, *32*, 4050-4064.

41. C. H. Choi, J. L. White, *Polym. Eng. Sci.* 2000, *40*, 645-655.

42. D. Cavallo, F. Azzurri, R. Floris, G. C. Alfonso, L. Balzano, G. W. Peters, *Macromolecules* 2010, *43*, 2890-2896.

43. D. Cavallo, G. Portale, L. Balzano, F. Azzurri, W. Bras, G. W. Peters, G. C. Alfonso, *Macromolecules* 2010, *43*, 10208-10212.

CAPÍTULO 6

Mechanical and transport properties of poly(propylene-*co*-1-heptene) copolymers and their dependence on monoclinic and/or mesomorphic polymorphs

Alberto García-Peñas, José M. Gómez-Elvira, Vicente Lorenzo, Ernesto Pérez and *María L. Cerrada.*

2015

6.1. Abstract

Poly(propylene-*co*-1-heptene) copolymers have been evaluated in a wide 1-heptene content range. Two different polymorphs can be observed in this interval under the processing conditions imposed: monoclinic crystallites and mesomorphic entities. The unique presence of one or the other lattice at specific contents or the coexistence of both of them at the intermediate composition interval is a key factor affecting some of the exhibited properties. The influence is observed in characteristics either mainly dependent on crystalline structure, like rigidity, or regarding to the amorphous regions, as location and intensity of glass transition. To get a deeper understanding, the transition from mesophase to monoclinic crystallites has been also studied by DSC and by WAXS and SAXS experiments using synchrotron radiation. It is observed that this transformation is only partial and just involves one third of the initial ordered mesomorphic entities. Permeability to different gasses is mainly dependent on amorphous content and hindrance that monoclinic or mesomorphic entities impose on those disordered regions.

6.2. Introduction

Isotactic polypropylene (iPP) is a worldwide commodity polyolefin whose field of application is continuously spreading due to its lowest density among the commodity plastics, its relatively low price, its excellent chemical resistance, the fact that if can be processed by many transformation methods, such as injection molding and extrusion, and its capability to be recycled. All these features joined to its very interesting crystalline characteristics, which are able to modulate the overall properties, allow conferring a very broad versatility. Consequently, the growth of the demand for iPP has historically exceeded that of the Gross Domestic Product, GDP. This level of growth is expected to continue due to the deeper penetration of iPP based materials into appliances, automotive, consumer films, non-woven fabrics and fiber end uses, among others ultimate applications. These final materials require, sometimes, the addition of specific fillers or other polymers to allow iPP being used in many engineering applications. This incorporation can be performed either by direct blending of the different components, filled polypropylenes [1-6] or blends [7,8], or by polymerization in the presence of fillers [9-11].

Copolymerization of propene with different α-olefin counits has been used as a route to modify iPP structure and properties [12-23]. Accordingly, outstanding performances have been reached, including high stiffness in homopolymers, excellent low-temperature impact strength in impact copolymers and excellent clarity and low melting point in random copolymers. Random copolymerization at an industrial scale has involved for long time incorporation of low counit contents, mainly ethylene, 1-butene or 1-hexene. Other comonomers as well as higher compositions of all these counits have been explored from a scientific standpoint. Those include, among others, 1-pentene [24-27] and 1-octene [28-30] as well as more scarcely counit of longer chains [18,29,31,32], like 1-tetradecene or 1-octadecene.

The inclusion of intermediate counit contents might lead to plastomers based polypropylenes. The "plastomer" term was referred in the late 90's to ethylene-α-olefin copolymers, with comonomer contents between 5 and 10 mol % and lower density than typical linear low density polyethylene, LLDPE, which exhibited the dual characteristic of plastic and elastomeric behavior and, then, a good balance between rigidity and elasticity [33]. Its market niche was primarily packaging since its superior sealability, excellent optics and appropriate oxygen transport behavior.

Propene-*co*-1-heptene copolymers (cPHp) have been barely referred in open literature. There are few investigations [34,35] that compare some aspects of their copolymerization kinetics and microstructure with those exhibited by others olefinic counits, but none investigations concerning either structural studies or properties evaluation in these cPHp copolymers. An article has been recently published aiming to learn if the trigonal δ form developed in random propylene copolymers with 1-pentene or 1-hexene at high comonomer compositions was able to be also generated in those 1-heptene based copolymers. This trigonal polymorph was not found at any content [36] probably due to its long side branches that cannot be accommodated into that lattice. Nevertheless, the evaluation of several physical characteristics turns out very interesting due to the lack of information about behavior exhibited by these copolymers.

Accordingly, the aim of this article consists of analyzing the mechanical response, transport and optical behavior as well as phase transitions exhibited by a set of propylene-1-heptene copolymers synthesized within a broad counit range. Some of these properties will be compared with those shown by plastomers based ethylene to determine the feasibility of using these new propylene copolymers in the packaging field.

6.3. Experimental

6.3.1. Materials

The synthesis procedure and the characterization of propylene copolymers with 1-heptene are described extensively elsewhere [36] The so-precipitated polymers were stirred overnight, filtrated, washed with ethanol (Aroca, 96%) and, finally, dried under vacuum at room temperature.

Molecular weights were determined by size exclusion chromatography (SEC), and compositions by carbon nuclear magnetic resonance, ^{13}C NMR. Table 1 shows the most representative SEC and ^{13}C NMR data for the different samples synthesized. Copolymers are named as cPHp followed by the comonomer content expressed as the closest integer number.

Specimens were obtained as films by compression molding in a Collin press between hot plates at temperature of 30 °C above the melting point, and using a pressure of 2.5 MPa for 3 min, and then quenched down to room temperature with circulating water. This thermal treatment was applied to simulate processing conditions imposed to industrial packaging films.

Table 1. Data from ^{13}C NMR, SEC and DSC characterization: comonomer content; average weight molecular weight (M_w); polydispersity (M_w/M_n); glass transition temperature (T_g); melting temperature (T_m); and crystallinity (f_c). The DSC magnitudes have been estimated from the first heating run. Last column refers to the value of visible transmittance (Vis T %) measured in the range from 400 to 800 nm.

Sample	1-heptene content (mol %)	M_w (g/mol)	M_w/M_n	T_g (°C)	T_m (°C)	f_c	Vis T %
iPP	0	140900	2.27	0	153	0.59	64
cPHp3	3.2	135300	2.05	-4	120	0.38	76
cPHp6	6.5	102700	2.05	-12	89	0.30	86
cPHp10	10.1	83400	2.43	-17	71	0.24	88
cPHp12	12.3	76900	2.05	-20	66	0.19	86
cPHp14	13.9	74000	2.04	-23	61	0.17	80
cPHp21	21.4	-	-	-28	-	0	-

6.3.2. Viscoelastic behavior

Dynamic mechanical relaxations were measured with a Polymer Laboratories MK II Dynamics Mechanical Thermal Analyzer, working in a tensile mode. The storage modulus, *E'*, loss modulus, *E"*, and the loss tangent, *tan* δ, of each sample were determined as function of temperature over the range from –150 to 150 °C at fixed frequencies of 3, 10, 30 and 50 Hz, and at a heating rate of 1.5 °C/min. Strips of 2.2 mm wide and 15 mm length were cut from the molded sheets.

6.3.3. Depth Sensing Indentation

Depth Sensing Indentation, DSI, experiments were performed at room temperature with a Shimadzu tester (model DUH211S) equipped with a Berkovich type diamond indenter. In all copolymers, at least 10 indentations were performed at different regions of the specimen surface.

The experimental measures were performed with the application of a load of 10 mN at a loading speed of 1.46 mN s^{-1}, and the maintenance of this constant load for 5 s. Finally, the release of the load was produced at an unloading speed equal to the one used along the loading stage.

Reduced elastic modulus, E_r, have initially been evaluated from the load and depth indentation curves by using the Oliver and Pharr method [37]. E_r is related to the indentation modulus, E_{IT}, and Poisson's ratio, v, of the specimen and the diamond indenter, E_i and v_i, as:

$$\frac{1}{E_r} = \frac{1-\nu^2}{E_{IT}} + \frac{1-\nu_i^2}{E_i} \qquad [1]$$

The Oliver and Pharr approach is an effective method to measure the elastic modulus and hardness in materials that undergo elastic–plastic behavior Nevertheless, this approach might not be adequate when determining the properties of viscoelastic solids and, occasionally, some corrections are required. Therefore, the results obtained in this present investigation have been checked to learn if any correction

should be applied, concluding that Oliver and Pharr method is completely fulfilled under the used experimental conditions.

6.3.4. Transport properties

Permeability measurements were performed by using a non-commercial experimental device that was developed in our laboratory. This device consists of a permeation cell with two chambers that are separated by the membrane, a thermostatic bath and a system for measuring pressure. The permeation cell is a stainless steel 47 mm filter holder (Millipore XX4404700) (effective area = 13.8 cm^2). Automated data collection was performed by absolute pressure sensors (MKS Baratron) and temperature sensors. Gas permeability of the specimens has been determined by means of diffusion experiments through an initially purged membrane. High vacuum (~10^{-4} mbar) was applied in both the high-pressure and low-pressure chambers separated by the film. After purging the system, a step variation of the pressure has been imposed on the high pressure side of the membrane ($p_H = p_0$ for time, $t > 0$) and the pressure on the low pressure side, p_L, has been monitored. Before each experiment, the leak curve was determined by measuring the variation of the pressure with time in the low-pressure chamber in vacuum and all membranes were degassed under vacuum overnight between runs. The experiments were carried out with oxygen, nitrogen and carbon dioxide at 1 bar of pressure and at several temperatures from 30 to 60 °C. The gases were supplied by Air Liquide: O_2 (purity 99.95), N_2 (purity 99.999) and CO_2 (purity 99.98).

6.3.5. Optical Properties

The transparency in the visible range (400–800 nm) of thin films, for 1-heptene copolymers, was determined with UV-Vis spectroscopy using a Perkin Elmer Lambda 35 spectrometer at a scan rate of 480 nm/min. Finally, all visible transmittance data have been normalized at 100 nm.

6.3.6. Calorimetric analysis

The calorimetric analysis was performed in a PerkinElmer DSC-7 calorimeter with a connection to a cooling system. The equipment was calibrated with different standards (indium, zinc and *n*-dodecane). Sample weights ranged from 2 to 5 mg. A heating rate of 10 °C/min was used for the different films. Besides the usual normalization to sample weight, the heat flows were also normalized to the scanning rate.

6.3.7. X-ray diffraction

Conventional wide-angle X-ray diffraction patterns were recorded in the reflection mode by using a Bruker D8 Advance diffractometer provided with a Goebel mirror and a PSD Vantec detector (from Bruker, Madison, Wisconsin). Cu Kα radiation (λ = 0.1542 nm) was used. The equipment was calibrated with different standards.

The nature of the thermal transitions was evaluated with real-time X-ray diffraction experiments (SAXS and WAXS) with synchrotron radiation on beamline BL11-NCD at ALBA (Cerdanyola del Vallés, Barcelona, Spain), at a fixed wavelength of 0.1 nm. Two detectors have been used: a Rayonix LX255-HS detector (with a pixel size of 40 µm), placed at about 19 cm from sample, and a tilt angle of around 30 degrees, for WAXS, and an ADSC 210 detector (with a pixel size of 102.4 µm), placed approximately at 300 cm from the position of the sample, for SAXS. The temperature control unit was a Linkam hot stage, connected to a cooling system of liquid nitrogen. The calibration of spacings was obtained by means of silver behenate and Cr_2O_3 standards. The initial 2D X-ray pictures were converted into 1D diffractograms, as function of the inverse scattering vector, $s = 1/d = 2 \sin \vartheta/\lambda$. Film samples of around 5 x 5 x 0.1 mm were employed in the synchrotron analysis.

6.4. Results and discussion

The use of a polymer for a given application requires not only showing specific properties for that precise purpose but also to exhibit a suitable mechanical performance. Therefore, knowledge of the viscoelastic response in a wide range of temperature is mandatory. Figure 1 shows the storage modulus, E', for polypropylene and the cPHp copolymers as function of temperature from subambient to high temperatures. E' is related to the elastic contribution of the complex modulus, i.e., to the rigidity of the polymeric material. It is seen that the values are clearly reduced from homopolymer to the copolymers. This decrease is more significant as comonomer composition is raised, as expected, and at temperatures higher than those where a large drop, ascribed to the relaxation related to the glass transition, takes place. Mobility of the macrochain is highly hindered below glass transition and the existing crystalline differences between distinct samples, as depicted in the inset of Figure 1, affect in a less extent than at temperatures above T_g. Those observed structural differences primarily concern the crystallinity degree, the type of crystalline lattice and the size and perfection of crystalline entities in the samples under study. Therefore, monoclinic crystallites (in a content of 0.57) are the crystalline polymorph for the homopolymer and the cPHp3 copolymer (whose crystallinity is 0.36), monoclinic crystals and mesomorphic entities (with an overall amount of 0.25 in a ratio of 0.09/016, respectively) for the cPHp6 copolymer and the mesomorphic form is the unique ordered modification developed in the copolymers cPHp10, cPHp12 and cPHp14. Values of 0.18, 0.15 and 0.12 are their respective degree of crystallinity estimated from the X ray profiles.

The iPP homopolymer shows the highest stiffness in the whole temperature interval while copolymers become progressively softer as 1-heptene content is increased since crystallinity reduction and variation in the other crystalline features.

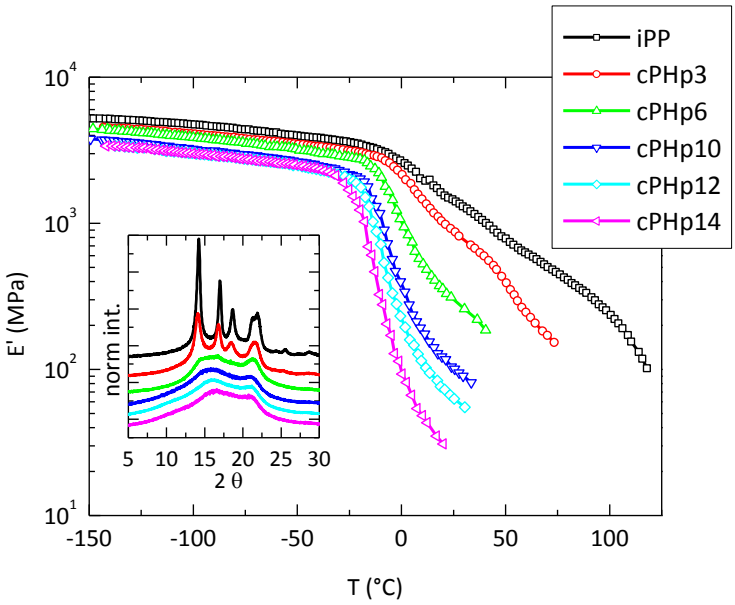

Figure 1. Temperature dependence of the storage modulus (real component of complex modulus) of the distinct specimens. Inset: Room temperature X ray profiles for the copolymers analyzed.

Identical conclusion is achieved from indentation measurements performed at room temperature. The elastic modulus as well as the hardness determined from those experiments display a decrease upon composition similar to the one found in other olefin copolymers [16,18,31,38,39]. Figure 2 shows the excellent agreement found between the values of storage modulus and the indentation moduli estimated for the different specimens. This good correlation has a considerable importance from a practical standpoint since indentation measurements can be used as a reliable non-destructive testing technique [40] requiring a rather small amount of material and representing its overall mechanical performance (additionally proving that the material is homogeneous).

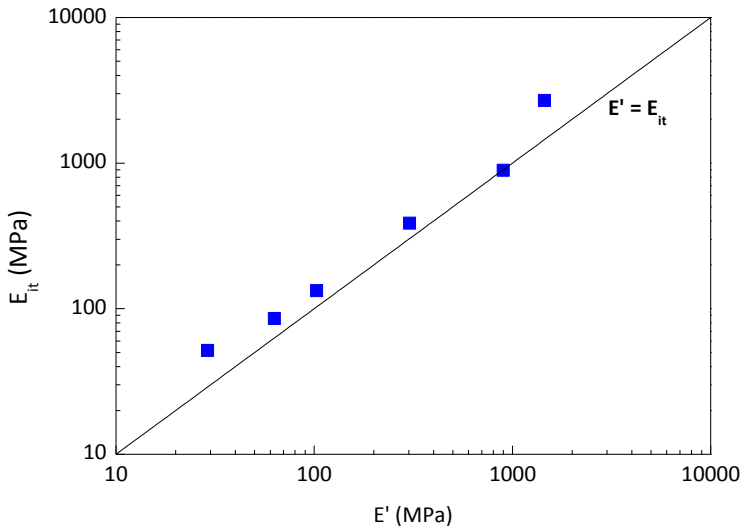

Figure 2. Indentation modulus, E_{it}, *vs.* storage modulus for the different samples analyzed.

Moreover, elastic modulus deduced from these indentation measurements changes upon crystalline details, and two distinct dependences, as shown in Figure 3, are observed as function of the amorphous content. Accordingly, the type of crystalline modification existing in the sample appears to have a significant effect and the reduction of amount of monoclinic crystallites decreases rigidity more considerably than the presence of mesomorphic entities does.

It should be commented, at this point, that storage modulus values described for plastomers based on copolymers of ethylene-1-octene [41,42] with 1-octene contents of 5.2 and 9.3 mol % are 65 MPa and 11 MPa, respectively. These specimens in the present study show values of 305 MPa and 105 MPa for those of analogous compositions, i.e., cPHp6 and cPHp10, respectively. Even, the copolymers with the higher contents, cPHp12 and cPHp14, exhibit values of storage modulus of 63 MPa and 29 MPa, respectively. Hence, the requirements of rigidity seem to be accomplished.

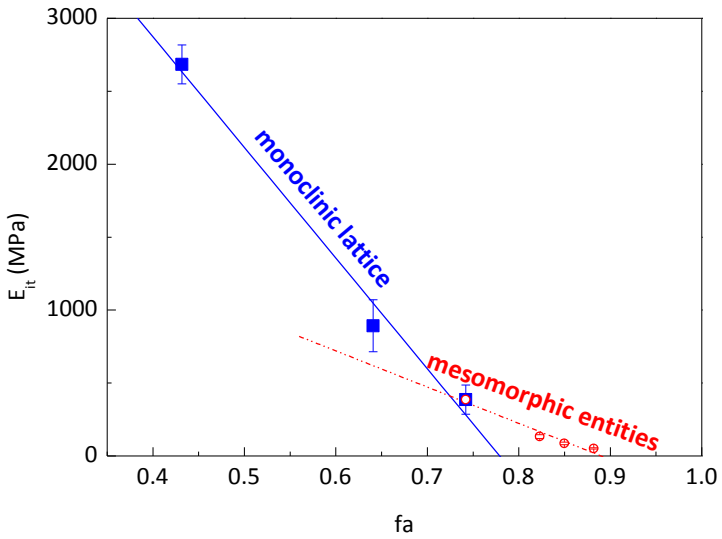

Figure 3. Dependence of indentation modulus on the amorphous fraction for the different a 1-heptene copolymers.

Dynamic mechanical thermal analysis also provides information about loss magnitudes, i.e., loss modulus and loss tangent, which are related to the part of energy dissipated along any molecular motion and to the mechanical damping, respectively. These two magnitudes are depicted in Figure 4 and allow learning about the relaxation mechanisms that can take place at a given temperature range. The dynamic mechanical spectrum of iPP as a function of temperature is well-known [43-45] iPP exhibits three relaxation mechanisms, labeled as γ, β and α in order of increasing temperature. The molecular cause behind each process corresponds to the local motions (methyl rotation around backbone) within the amorphous regions, the glass transition and movements within the iPP crystalline regions, respectively.

Figure 4 also displays several relaxations in the plots of loss magnitudes, tan □ and E", for these cPHp copolymers that are considerably dependent on counit content and crystalline features. The α relaxation at the highest temperature related to motions within the crystalline phase, especially to defect diffusion [46], is only evident

in the copolymer cPHp3. The incorporation of 1-heptene and the subsequent decrease in crystallinity leads to a considerable shift of the process to lower temperatures since the motion can take place just above glass transition. This relaxation disappears as comonomer content is further increased.

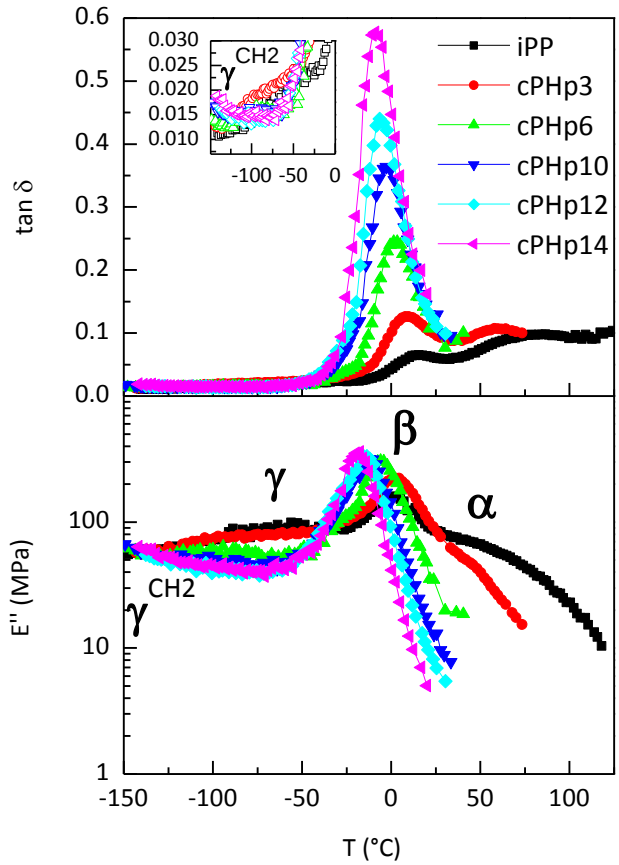

Figure 4. Temperature dependence of the loss tangent and imaginary component of complex modulus (upper and lower plots, respectively) of the distinct specimens.

The β relaxation, placed at around 15 °C in the homopolymer (tan δ plot), is ascribed to generalized motions of long chain segments that occur along the glass transition of the amorphous regions. The cooperative nature of this movement explains the great drop in the E′ magnitude found at this temperature range (see Figure 1). Its intensity in tan δ significantly rises as comonomer content does in the copolymer because of the increase in the amorphous fraction within the polymeric

material, as represented in Figure 5. Moreover, the location of the β relaxation also changes with composition, shifting down to lower temperatures with increasing comonomer content, because cooperative motions can occur easily as amount of ordered entities diminishes. Mobility is additionally enlarged, as deduced from Figure 5, at high contents because of the presence of mesomorphic entities instead of monoclinic crystallites.

It is interesting to compare these DMTA values regarding the β relaxation location, ascribed to the glass transition, with those reported in Table 1 and obtained from the T_g determined by DSC measurements. Both results exhibit identical dependence on amorphous content, although the DSC values are systematically, as expected, around 15 °C lower than those from DMTA because of experimental differences between the two techniques.

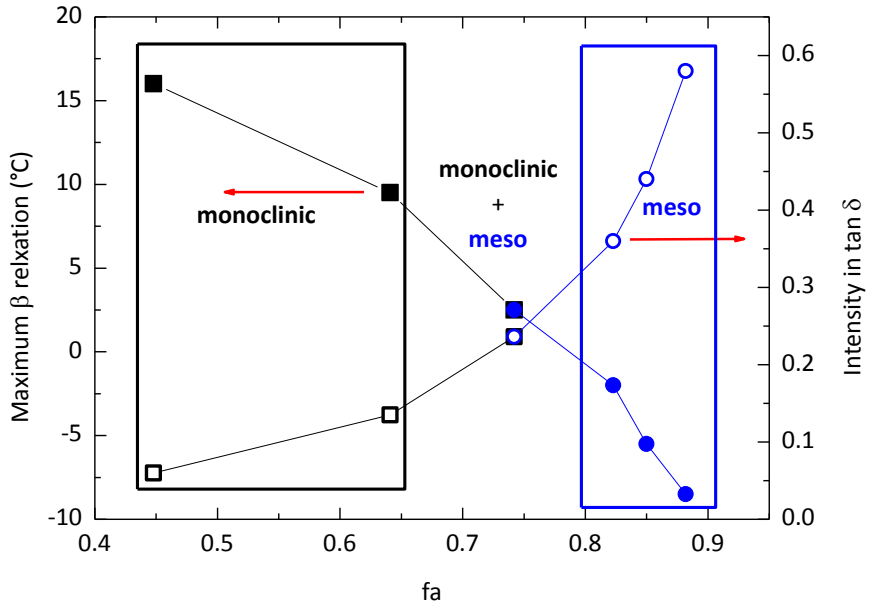

Figure 5. Dependence of location of β relaxation and its intensity upon amorphous fraction in the specimens under study.

The other γ relaxation process ascribed to rotational motions of methyl groups is observed in the copolymers at temperatures slightly lower than in the polypropylene homopolymer. Its intensity is now considerably reduced as comonomer

content increases. In fact, it is practically merged with other process appearing at even lower temperatures in the copolymers with the highest 1-heptene contents (cPHp10, cPHp12 and cPHp14). This overlapped relaxation has been already described at around -150 °C in other propylene based copolymers with intermediate and high comonomer contents of several alpha-olefins counits [29,31,38]. It has been named as γ^{CH2} because is molecular origin is related to the joint movements of chains containing three or more methylene units, *i.e.* its inherent cause is analogous to that responsible for the typical γ relaxation observed in polyethylene [47-49] (although now these methylene groups are located in the side chains). Therefore, its intensity is dependent upon counit content since as comonomer content increases there is a higher amount of methylene groups that can undergo and participate in this motion.

Good transport properties to gases are a requirement for feasible applicability of polymers in the packaging field. The permeation behavior of these 1-heptene copolymers has been evaluated for N_2, O_2 and CO_2 from the evolution of their gas pressures flowing through the corresponding polymeric membrane. The transport of gases through membranes is generally expressed in terms of the permeability, P. Experiments have been carried out at different temperatures although measurements were not possible to be performed at temperatures above 40 °C for copolymers with the highest comonomer contents since transformation from mesomorphic entities to monoclinic crystallites takes place at those temperatures, as will be commented below.

Figure 6 shows the permeability results to the distinct gases at 30 °C as a function of 1-heptene content. It is clearly seen that permeability increases as composition is raised. This feature is directly related to the overall mobility of the polymeric chains at a given material. As Figure 5 undoubtedly proved, copolymers with the highest 1-heptene compositions can undergo easily motions at 30 °C since their glass transition temperature is much far away from this temperature than in the case of copolymers with minor counit contents. In addition, mobility is also favored in those samples with mesomorphic entities and, accordingly, tortuosity of the path caused by

this ordered phase is diminished and the free-volume generated by the lateral chains is enlarged at the amorphous-crystal interfaces and within the amorphous regions as 1-heptene is raised. Accordingly, two dependences are observed in Figure 7 for the samples with and without monoclinic crystallites.

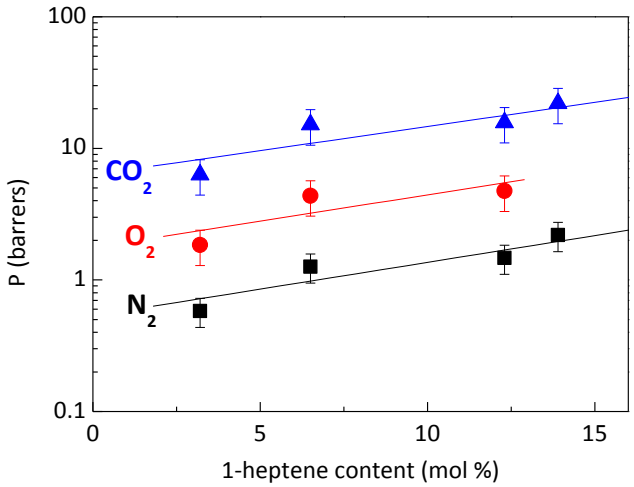

Figure 6. Variation of permeability at 30 °C with comonomer composition.

Figure 6 also displays that the highest permeability is found respect to CO_2, fact which comes from the size of the permeant molecules. Among various descriptions of the molecule sizes, the most applicable to transport phenomena is that called as "kinetic diameter" of molecules. This term is an indication of the smallest effective dimension in a given molecule. Literature reports on kinetic diameters for CO_2, O_2 and N_2 molecules. Although values estimated are slightly different, depending on the type of experiments used for their determination, all show that $CO_2 < O_2 < N_2$. The permeability values obtained in all of the samples are in agreement with variation of the kinetic diameter for the distinct gases evaluated.

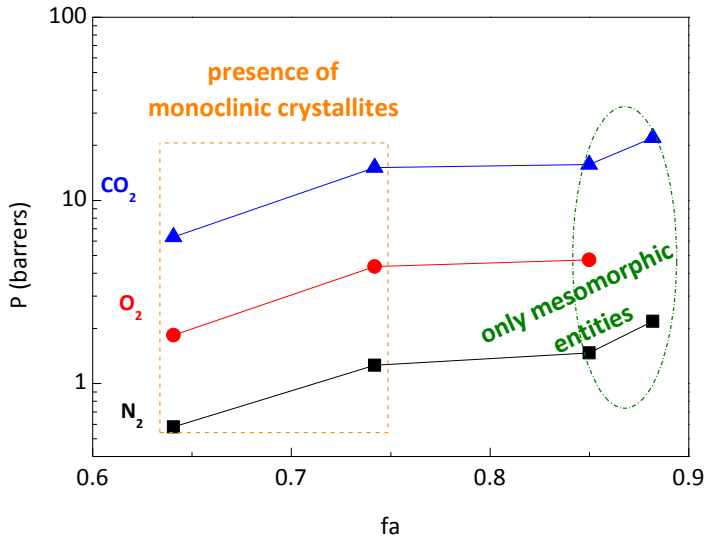

Figure 7. Dependence of permeability with amorphous fraction at 30 °C.

Moreover, Figure 6 also indicates that permeability dependence on composition at 30 °C is analogous for the different gases, i.e., N_2, O_2 and CO_2. This feature implies that selectivity does not noticeably change with this variable. In fact at this temperature, the average values of α (CO_2/O_2) and α (CO_2/N_2) selectivities are 3.4±0.1 and 11±1, respectively, for all the samples analyzed. This selectivity constancy upon counit content has been also described in copolymers based on ethylene [50]. On the other hand, these selectivity results are in the regular interval collected by Robeson [51].

On the other hand, the results show that permeability increases as function of temperature, as expected. The diffusive process through isotropic barriers is a thermally activated process, which obeys the Arrhenius expression:

$$D = D_0 \exp(-E_D/RT) \qquad [3]$$

where E_D is the activation energy of the diffusion and D_0 is a constant that is characteristic of the membrane-permeant system. The E_D values obtained for the different testing gases for the cPHp3 sample are 39 (± 2), 42 (± 13), and 43 (± 2) kJ/mol for O_2, N_2 and CO_2, respectively. All values are close to Van Krevelen results reported in

the literature [52]. The E_D values cannot be estimated for the rest of the samples because of occurrence of the mesomorphic to monoclinic transformation at temperatures just slightly above 40 °C, as will be discussed below.

Oxygen permeability value at 30 ºC for cPHp12 copolymer is 4.74 barrer. If it is compared with that exhibited by an ethylene-1-octene plastomer [53] with 9.3 mol % (17.5 barrer), it can be said that the copolymer under study is less permeable to oxygen, which can be a positive characteristic of some packaging applications in order to preserve the organoleptic properties of the products before their consumption.

Other feature that is highly recommended in that field is the transparency of films so that this characteristic has been determined from transmittance in the visible range for the different copolymers. The most transparent polymers are: poly(methyl methacrylate) with a 92 % of transmittance, polystyrene with a value around 90 % and poly(carbonate), whose transparency ranges from 80 to 90 %. As common feature all of them are completely amorphous. The copolymers under study are semicrystalline [15] (see also insert in Figure 1), although degree of ordering decreases as 1-heptene content increases (0.26, 0.18; 0.15, 0.12 for cPHp6, cPHp10, cPHp12 and cPHp14, respectively [36]), leading to the existence of a significant amorphous zone. The results show that the transmittance values observed are remarkably high at 6 mol % and 1-heptene contents above, as listed in Table 1. The processing that was used favors development of crystallites of low size and perfection since cooling stage takes place at very high rate. Consequently, even the iPP homopolymer exhibits a relatively high transmittance value, which is further increased because of incorporation of counits (as much as content is enlarged up to reach an almost constant value) and presence of mesomorphic entities at the high contents instead of the monoclinic crystals. Therefore, requirement of transparency is also accomplished by the materials under study.

The copolymers whose crystalline structure is based, partially or completely, on mesomorphic entities possess other very interesting characteristic. This consists in the order-order transition that occurs at around 50-70 °C depending on composition,

which involves the mesophase melting together with the further monoclinic recrystallization. This transition makes possible an expansion of range of temperature for a particular applicability, fact that can be considered very attractive.

This order-order transition is anticipated in the calorimetric curves represented in Figure 8. According to the X-ray results in the inset of Figure 1, it follows that under the thermal treatment used for preparing the film samples, the mesophase is obtained for comonomer contents above 6 mol%. Consequently, the mesophase-monoclinic transition is present for copolymers cPHp14, cPHp12, cPHp10 and cPHp6. On the contrary, only monoclinic crystals have been formed for samples cPHp3 and iPP.

The mesophase-monoclinic transition is much clearly observed in real-time variable-temperature experiments by using synchrotron radiation. Such experiments have been carried out on sample cPHp10. The corresponding diffractograms on its melting are shown in Figure 9, where the melting-recrystallization of the mesophase into monoclinic crystals (at around 50 °C) and the final melting of this monoclinic form at around 90 °C are well evident, both in the SAXS and in the WAXS channels.

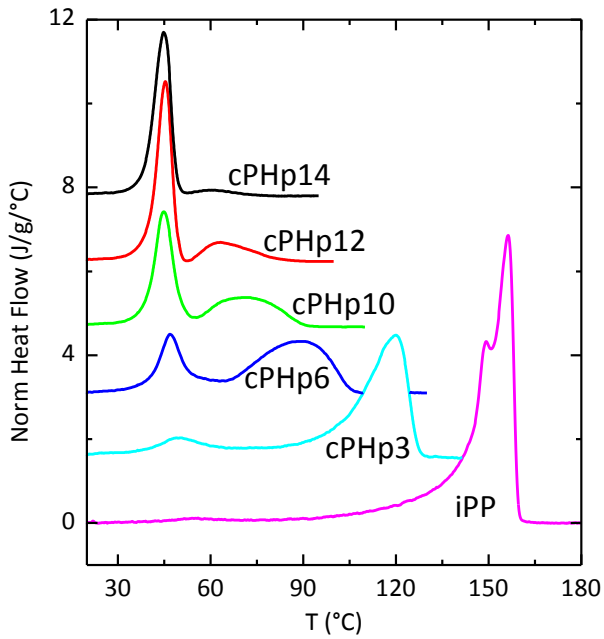

Figure 8. DSC melting curves for the different copolymers (heating rate: 10 °C/min).

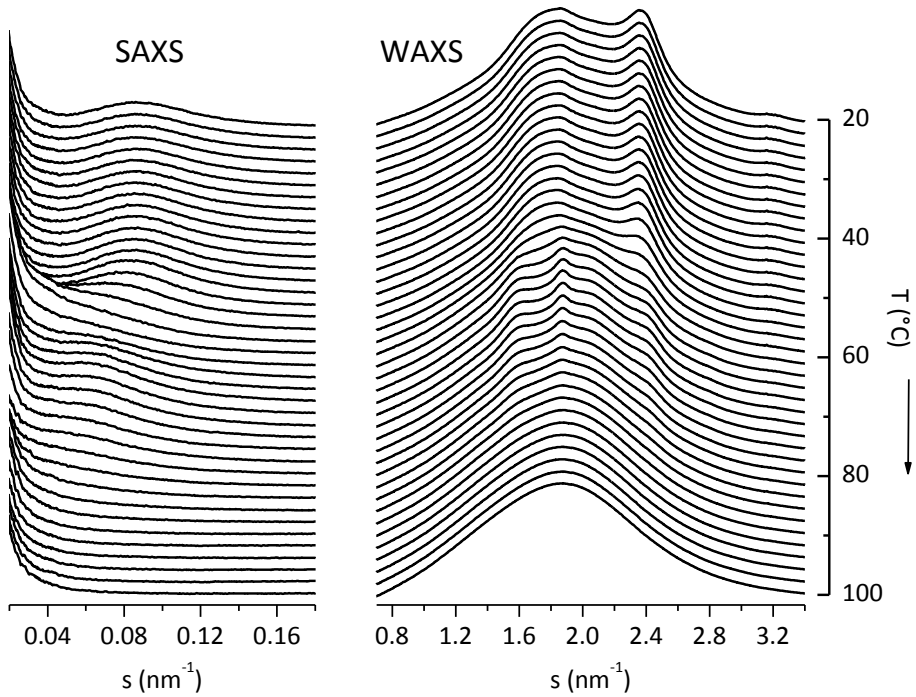

Figure 9. Variable-temperature SAXS and WAXS X-ray diagrams (acquired with synchrotron radiation) for cPHp10 on melting at 10 °C/min.

In addition to the elucidation of the phases involved in the different transitions, these synchrotron experiments also provide the corresponding amorphous (molten) profiles, so that it is possible to determine the ordered component and the degree of crystallinity (or degree of ordered structures, when the mesophase is present). It is necessary, however, to account for the temperature coefficient of the amorphous diagram and appropriately shifting it for each particular temperature [54-56].

Following such procedure with the real-time WAXS diagrams of Figure 9, the variation with temperature of exclusively the ordered component is shown in Figure 10, where the corresponding DSC melting curve is also depicted (red curve at the right of the figure). The two transitions, the melting-recrystallization of the mesophase into monoclinic crystals and the final melting of this monoclinic form, are now much better observed, and in perfect agreement with the DSC melting curve.

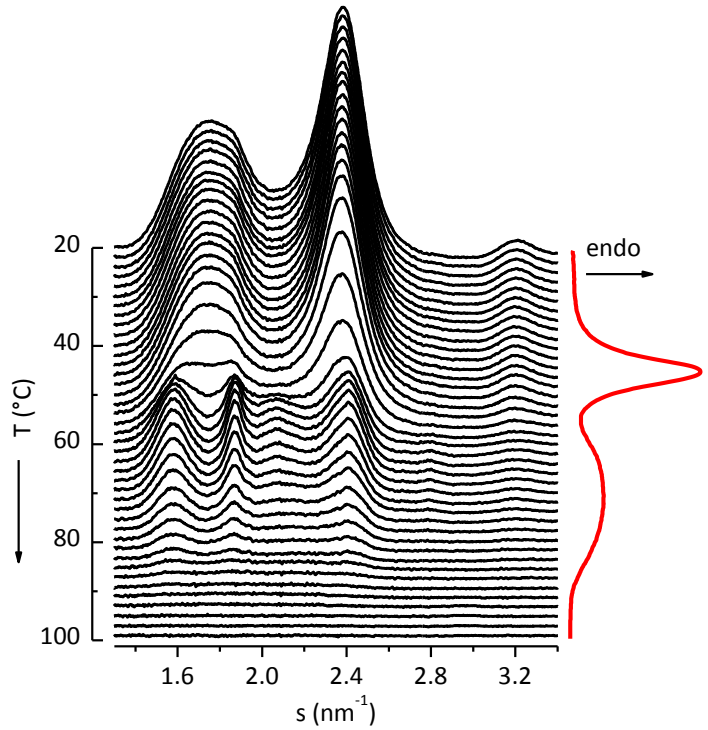

Figure 10. Variation with temperature of the ordered component in the real-time WAXS diagrams of Figure 8. The corresponding DSC melting curve is also shown (red curve at the right of the figure).

Incidentally, it seems that a very minor amount of monoclinic crystals are present in the initial sample, owing to the observation of a small, but appreciable, shoulder centered at around 1.9 nm^{-1}.

Additionally, the degree of ordered phases is implicit in the diffractograms of Figure 10, and the variation with temperature of that degree of ordered phases is shown in Figure 11. It can be observed, first, the modest degree of order (only around 0.17) in the initial sample. Interestingly, the melting-recrystallization of the mesophase into monoclinic crystals is only partial (at least at the employed heating rate, 10 °C/min) since only 0.06 of that 0.17 is recovered after such recrystallization.

And the final melting occurs at 90 °C, in perfect agreement with the DSC results.

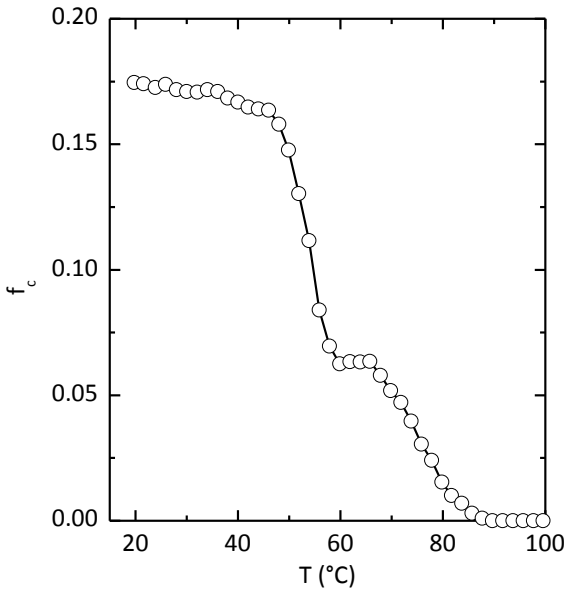

Figure 11. Variation with temperature of the degree of ordered phases for the real-time synchrotron experiment of cPHp10 on melting at 10 °C/min.

6.5. Conclusions

Poly(propylene-*co*-1-heptene) membranes in a wide 1-heptene content range have been analyzed. Monoclinic crystallites and mesomorphic entities are the only ordered structures that can be developed under the thermal history imposed during film preparation. The unique presence of one of them or the coexistence of both polymorphs is a key factor influencing the properties exhibited by the different copolymers, either those directly related to the crystalline morphology or to the amorphous regions. Concerning the former ones, a decrease of rigidity is observed with 1-heptene content, as expected, but its dependence on this variable is significantly superior when monoclinic lattice exists in the copolymer. On the contrary, that variation at those compositions where the mesomorphic form is generated becomes rather smooth.

Cooperative motions of long chain segments in the amorphous regions, i.e., glass transitions, show a different trend depending on crystalline polymorphs. Presence of the mesomorphic form imposes a less hindrance to those generalized movements.

On the other hand, an additional relaxation takes place in some of the copolymers. This process is caused by the movement of the methylene groups that are located in the side chains and, then, its intensity is increased as counit content is raised.

Evaluation of transport properties reveals that permeability dependence on composition is analogous for the different gases analyzed (N_2, O_2 and CO_2) at 30 °C. This feature implies that selectivity does not noticeably change with this variable.

Moreover, permeability trend also depends on the presence or lack of monoclinic crystallites. Permeability rises faster in specimens with mesomorphic entities because their mobility is also increases. The oxygen permeability is lowered compared with that observed in plastomers based ethylene. Then, copolymers under study are less permeable to oxygen, which can be a positive characteristic of some packaging applications in order to preserve the organoleptic properties of the products before their consumption.

The transition from mesophase to monoclinic recrystallization has been also studied by DSC, WAXS and SAXS experiments, since the temperature range for a particular applicability at those copolymers containing the mesomorphic form can be spread out because of that phase transformation. This melting-recrystallization from mesophase to monoclinic crystals is only partial (at least at the employed heating rate, 10 °C/min) and involves only one third of the initial ordered entities.

Summing up, these materials could be considered as plastomers based on propylene with a good mechanical performance, transparency and transport properties to different gases.

6.6. References

1. Kubacka, M.L. Cerrada, C. Serrano, M. Fernández-García, M. Ferrer, M. Fernández-García. J. Nanosci. Nanotech. 8 (6) (2008) 3241–3246.
2. M.L. Cerrada, C. Serrano, M. Sánchez-Chaves, M. Fernández-García, M.A. de Andrés, R.J. Riobóo, F. Fernández-Martín, A. Kubacka, M. Ferrer, M. Fernández-García. Environ. Sci. Techn. 43 (5) (2009) 1630–1634.
3. M. Gupta, Y. Lin, T. Deans, E. Baer, A. Hiltner, D.A. Schiraldi. Macromolecules 43 (9) (2010) 4230–4239.
4. X. Zhu, C. Melian, Q. Dou, K. Peter, D.E. Demco, M. Möller, D.V. Anokhin, J-M. Le Meins, D.A. Ivanov. Macromolecules 43 (14) (2010) 6067–6074.
5. Serrano, M.L. Cerrada, M. Fernández-García, J. Ressia, E.M. Vallés. Eur. Polym. J. 48 (3) (2012) 586–596.
6. J. Arranz-Andrés, E. Pérez, M.L. Cerrada. Sci. Adv. Mater. 5 (10) (2013) 1524–1532.
7. O. Prieto, J.M. Pereña, R. Benavente, M.L. Cerrada, E. Pérez. Macromol. Chem. Phys. 203 (12) (2002) 1844–1851.
8. Álvarez, A. Martínez-Gómez, E. Pérez, M.U. de la Orden, J.M. Urreaga. Polymer 48 (11) (2007) 3137–3147.
9. M.A. Milani, D. González, R. Quijada, N.R.S. Basso, M.L. Cerrada, D.S. Azambuja, G.B. Galland. Compos. Sci. Technol. 84 (2013) 1–7.
10. M.A. Milani, R. Quijada, N.R.S. Basso, A.P. Graebin, G.B. Galland. J. Polym. Sci., Part A: Polym. Chem. 50 (17) (2012) 3598–3605.
11. Wan, Z.J. Zhang, Y.J. Wang, H.P. Xing, Z.W. Jiang, T. Tang. Soft. Matter. 7 (2011) 5290–5299.
12. N. P. Cheremisinoff, M. Dekker. Handbook of Engineering Polymeric Materials, New York, 1997, p. 881.
13. R. Quijada, J.L. Guevara, G.B. Galland, F.M. Rabagliati, J.M. Lopez-Majada, Polymer 46 (5) (2005) 1567–1574.

14. R. Alamo, A. Ghosal, J. Chatterjee, K.L. Thompson. Polymer 46 (20) (2005) 8774–8789.

15. C. De Rosa, F. Auriemma, P. Corradini, O.Tarallo, S. Dello Iacono, E. Ciaccia, L. Resconi. J. Am. Chem. Soc. 128 (1) (2006) 80–81.

16. J.M. Lopez–Majada, H. Palza, J.L. Guevara, R. Quijada, M.C. Martinez, R. Benavente, J.M. Perena, E. Pérez, M.L. Cerrada. J. Polym. Sci., Polym. Phys. Ed. 44 (8) (2006) 1253–1267.

17. C. De Rosa, F. Aurienuna, O.R. De Ballesteros, L. Resconi, I. Carnurati. Chem. of Mater. 19 (21) (2007) 5122–5130.

18. H. Palza, J.M. Lopez-Majada, R. Quijada, J.M. Pereña, R. Benavente, E. Perez, M.L. Cerrada. Macromol. Chem. Phys. 209 (2008) 2259–2267.

19. K. Jeon, H. Palza, R. Quijada, R.G. Alamo. Polymer 50 (3) (2009) 832–844.

20. C. De Rosa, F. Auriemma, O.R. de Ballesteros, S. Dello Iacono, D. De Luca, L. Resconi. Cryst. Growth Des. 9 (1) (2009), 165–176.

21. Mileva, R. Androsch, D. Cavallo, G.C. Alfonso. Eur. Polym. J. 48 (6) (2012) 1082–1092.

22. K. Jeon, Y.L. Chiari, R.G. Alamo. Macromolecules 41 (1) (2008) 95–108.

23. C. De Rosa, F. Auriemma, P. Vollaro, L. Resconi, S. Guidotti, I. Camurati. Macromolecules 44 (3) (2011) 540–549.

24. B. Poon, M. Rogunova, A. Hiltner, E. Baer, S.P. Chum, A. Galeski, E. Piorkowska. Macromolecules 38 (4) (2005) 1232–1243.

25. B. Lotz, J. Ruan, A. Thierry, G.C. Alfonso, A. Hiltner, E. Baer, E. Piorkowska, A. Galeski. Macromolecules 39 (17) (2006) 5777–5781.

26. Pérez, M.L. Cerrada, R. Benavente, J.M. Gómez-Elvira. Macromol. Res. 19 (11) (2011), 1179–1185.

27. E. Pérez, J.M. Gómez-Elvira, R. Benavente, M.L. Cerrada. Macromolecules 45 (16) (2012), 6481–6490.

28. X. Li, Y. Mao, C. Burger, J. Che, B.S. Hsiao, R.R. Kulkarni, A.H. Tsou. Polymer 54 (17) (2013) 4545–4554.
29. M. J. Polo-Corpa, R. Benavente, T. Velilla, R. Quijada, E. Pérez, M.L. Cerrada. Eur. Polym. J. 46 (6) (2010) 1345–1354.
30. J. Arranz-Andres, R. Parrilla, M.L. Cerrada, E. Pérez. Macromolecules 46 (21) (2013), 8557–8568.
31. H. Palza, J.M. López–Majada, R. Quijada, R. Benavente, E. Pérez, M.L. Cerrada. Macromol. Chem. Phys. 206 (12) (2005) 1221–1230.
32. N. Djourelov, M. Misheva, C. Bas, D. Sillou, R. Benavente, E. Pérez, M.L. Cerrada. J. Polym. Sci.: Polym. Phys. 48 (18) (2010) 1994–2002.
33. T. Yu. Polym. Eng. Sci. 41 (4) (2001) 656–671.
34. U.M. Wahner, I. Tincul, D.J. Joubert, E.R. Sadiku, F. Forlini, S. Losio, I. Tritto, M.C. Sacchi. Macromol. Chem. Phys. 204 (14) (2003) 1738–1746.
35. M.C. Sacchi, F. Fortini, S. Losio, I. Tritto, G. Costa, P. Stagnaro, I. Tincu, U.M. Wahner. Macromol. Symp. 213 (1) (2004) 57–68.
36. A. García-Peñas, J. M. Gómez–Elvira, V. Lorenzo, E. Pérez, M. L. Cerrada, Eur. Polym. J. 64 (2015) 52–61.
37. W.C. Oliver, G.M. Pharr. J. Mater. Res. 7 (6) (1992) 1564–1583.
38. J. Arranz-Andrés, J.L. Guevara, T. Velilla, R. Quijada, R. Benavente, E. Pérez, M.L. Cerrada. Polymer 46 (26) (2005) 12287–12297.
39. C. Fonseca, J.M. Pereña, R. Benavente, M.L. Cerrada, A. Bello, E. Pérez. Polymer 36 (9) (1995) 1887–1892.
40. V. Lorenzo, J.M. Pereña. Curr. Trends. Polym. Sci. 4 (1999) 65–75.
41. M. L. Cerrada, R. Benavente, E. Pérez. Macromol. Chem. Phys. 202 (13) (2001) 2686–2695.
42. M. L. Cerrada, R. Benavente, E. Pérez. Macromol. Chem. Phys. 203 (4) (2002) 718–726.

43. N.G. McCrum, B.E. Read, G. Williams. Anelastic and Dielectric Effects in Solid Polymers; Dover, New York, 1991.

44. J. Arranz-Andrés, R. Benavente, B. Peña, E. Pérez, M.L. Cerrada. J. Polym. Sci. Polym. Phys. 40 (17) (2002) 1869–1880.

45. O. Prieto, J. M. Pereña, R. Benavente, E. Pérez, M.L. Cerrada. J. Polym. Sci. Polym. Phys. 41 (16) (2003) 1878–1888.

46. C. Jourdan, J.Y. Cavaille, J. Perez. J. Polym. Sci.: Part B: Polym. Phys. 27 (11) (1989) 2361–2384.

47. R.H. Boyd, S.M. Breitling. Macromolecules 7 (6) (1974) 855–862.

48. N.J. Heaton, R. Benavente, E. Pérez, A. Bello, J.M. Pereña.. Polymer 37 (17) (1996) 3791–3798.

49. M.L. Cerrada, R. Benavente, B. Peña, E. Pérez. Polymer 41 (15) (2000) 5957–5965.

50. M. F. Laguna, M. L. Cerrada, R. Benavente, E. Pérez, R. Quijada. J. Polym. Sci. Polym. Phys. 41 (18) (2003), 2174–2184.

51. L. M. Robeson. J. of Membr. Sci. 320(1–2) (2008) 390–400.

52. D.W. van Krevelen, Properties of Polymers: Their Correlation with Chemical Structure; Their Numerical Estimation and Prediction from Additive Group Contributions, third edition, Elsevier Scientific, Amsterdam, 1997.

53. M. F. Laguna, M.L. Cerrada, R. Benavente, E. Pérez. J. Polym. Sci. Polym. Phys. 42 (20) (2004) 3766–3774.

54. E. Pérez, M.L. Cerrada, R. Benavente, J.M. Gómez-Elvira. Macromol. Res. 19 (11) (2011) 1179–1185.

55. E. Pérez, J.M. Gómez-Elvira, R. Benavente, M.L. Cerrada. Macromolecules 45 (16) (2012) 6481–6490.

56. J. Arranz-Andres, R. Parrilla, M.L. Cerrada, E. Perez, Macromolecules 46 (21) (2013) 8557–8568.

CAPÍTULO 7

Trigonal δ form as a tool for tuning mechanical behavior in poly(propylene-*co*-1-pentene-*co*-1-heptene) terpolymers

Alberto García-Peñas, José M. Gómez-Elvira, Rosa Barranco-García,

Ernesto Pérez, María L. Cerrada

2015

7.1. Abstract

Terpolymers based on propylene with 1-pentene and 1-heptene as comonomeric units are satisfactorily synthesized containing distinct overall compositions in comonomers as well as three different 1-pentene/1-heptene ratios at a given composition. In addition to variation of composition and comonomer ratio on polymerization activity, intrinsic viscosity, and microstructural details, mechanical response has been preliminary checked. Rigidity related parameters, like Young´s modulus and yield stress, are primarily dependent on overall composition, but the comonomer ratio becomes a crucial variable at the terpolymers with a global counit contents higher than 10 mol %. This fact is ascribed to the capability or inability of developing the trigonal polymorph, depending on the counit that is in majority. Thus, crystallinity values in those terpolymers are considerably higher than the ones expected if only the 1-pentene units were incorporated into the trigonal crystals. This feature indicates that now 1-heptene is capable to be incorporated as defect into the trigonal lattice of these terpolymers, especially when 1-pentene is the major component. Consequently, the mechanical parameters are reflecting the different amounts in trigonal crystallinity.

7.2. Introduction

Isotactic polypropylene, iPP, is one of most versatile polymers currently produced at industrial level primarily because of its relatively low manufacturing cost and its rather attractive properties. These are intimately related to the amazing polymorphism shown by propylene based materials. Thus, depending on microstructural features, crystallization conditions and other factors like the use of specific nucleants, three different polymorphic modifications, α, β and γ, all sharing a three-fold conformation,[1-7] have been reported. In addition, fast quenching of iPP leads to a phase of intermediate or mesomorphic order,[1,2,8-10] which, on heating, undergoes a transformation into the α form.[11-14] The use of metallocene catalysts [15] involved an enormous advance in polymerization and copolymerization for polyolefins, in general, and for polypropylene in particular because of their great synthetic versatility. Then, the obtainment of PP with several tacticities (isotactic, atactic, syndiotactic, and hemiisotactic) is feasible by only changing the structure of catalyst.[16-18] Their single-site characteristics allow synthesizing polyolefins with narrow molecular weight distribution (polydispersities near two) and truly random copolymers with uniform intermolecular distribution of the comonomer content along the chains, the low polydispersity being maintained.[19-21] Then, the copolymers synthesized with metallocene catalysts are model-like materials to learn the effect of the comonomer content, or specifically the polymer microstructure, on the final properties of the material.

The option of synthesizing copolymers at high comonomer contents and homogeneous distribution prompted the discovery of a new trigonal form in copolymers of iPP with high contents of 1-hexene or 1-pentene as comonomers,[20,21,22-31] named as δ form. [31] In those articles, the trigonal δ polymorph is the only lattice obtained for comonomer contents above around 14 mol %, while different proportions of it with the α modification were found in the comonomer interval from around 8 to 13 mol %. At those intermediate contents, it

was established [29] that the mesomorphic form is also a competitor in the formation of this trigonal modification. This trigonal δ polymorph had been, then, exclusively attained using 1-hexene or 1-pentene as comonomers in propene based copolymers until 2013 year at which two different groups reported its formation in propylene terpolymers with both 1-pentene and 1-hexene as comonomeric units.[32,33]

Moreover, significant kinetic differences have been reported during the development of this δ lattice when using 1-hexene or 1-pentene as comonomers.[20,22,23,29,34] A very recent investigation [35] has described that the rate of formation of trigonal crystallites increases in blends of a miscible pair of propylene-1-hexene copolymers.

Some authors [23] proposed from the crystal structures obtained for 1-hexene based copolymers and the principle of density (entropy)-driven phase formation, that copolymers of propylene with olefins different from 1-hexene might crystallize in a similar trigonal form, the form I-type poly(1-butene) crystal structure, when the crystal density and the average composition of the copolymer moved toward those of poly(1-butene), if comonomer distribution was random. The crystallization of the trigonal form would be probably dependent on comonomer type, in such a way that in the case of shorter comonomer as, for instance, 1-pentene, it could be developed at higher comonomer concentrations and in the case of larger comonomers, as 1-heptene at lower comonomer contents. Nevertheless, our group has undoubtedly shown that trigonal polymorph is not developed in 1-heptene copolymers [36] synthesized in a broad composition interval up to 21 mol % and crystallized under different rates. The 1-heptene seems to be too long for being incorporated in a trigonal arrangement in spite of being randomly distributed along the macrochains. But what does it take place if some amount of 1-pentene counit is substituted in propylene-1-pentene copolymers by 1-heptene, i.e., if propylene-co-1-pentene-co-1-heptene terpolymers are obtained? Will the presence of 1-heptene allow the formation of trigonal polymorph in the resulting terpolymers? or will it be prevented?

The present investigation aims, therefore, to describe, for the first time in literature, the synthesis and a complete molecular characterization of these propylene-*co*-1-pentene-*co*-1-heptene terpolymers at different global compositions in comonomers (1-pentene or 1-heptene) and at three distinct 1-pentene/1-heptene ratios at a given total composition. Moreover, a preliminary examination of the different crystalline structures that are able to be developed at the different compositions will be checked as well as their impact in mechanical behavior because of its great importance in the final applicability of these unknown materials.

7.3. Experimental

7.3.1. Reagents and Materials

Toluene (Merck) and both comonomers, 1-pentene (Acros) and 1-heptene (TCI Tokyo Kasei), have been previously refluxed over sodium, distilled and kept under N_2 to avoid the presence of traces of water and oxygen. Both propylene (Praxair 2.5) and nitrogen (Conptse) were passed through oxygen-trap columns and molecular sieves before their use. The catalyst *rac*-dimethylsilylbis(1-indenyl) zirconium dichloride (Strem) and the cocatalyst methylaluminoxane (MAO) (10 wt.% solution in toluene, from Aldrich) were used as received. The activated catalyst was prepared by dissolving 15 mg of the metallocene in 3 mL of MAO solution. A volume of 0.313 mL containing $3.48 \cdot 10^{-6}$ moles of the active complex was used in each polymerization. Ethanol (Aroca, 96%) and HCl (VWR, 37%) were used for precipitation of the polymers.

7.3.2. Synthesis of the poly(propylene-*co*-1-pentene-*co*-1-heptene) terpolymers

The terpolymerization of propylene with 1-pentene and 1-heptene was carried out in a 500 mL Büchi glass ecoclave at -5 °C in toluene (250 mL) by using *rac*-dimethylsilylbis(1-indenyl)zirconium dichloride/MAO as catalyst/cocatalyst system ([Al]/[Zr] = 3,648). The initial propylene pressure was 0.40 bar, the catalyst amount $3.48 \cdot 10^{-6}$ moles and the starting comonomers/propylene molar ratio ranging from 0 to

0.935. The terpolymerization reaction was stopped by adding 5 mL of ethanol and enabling the unreacted propylene out from the reactor. The polymer was obtained as a powder by pouring the reaction batch on a mixture of ethanol/HCl (30:1). The precipitated was stirred thoroughly overnight, filtrated, washed again with ethanol and, afterwards, dried under vacuum at room temperature. Table 1 lists data for the polymerization of the iPP and the set of terpolymers synthetized at different overall compositions and at three 1-pentene/1-heptene ratios at a specific content. Terpolymers are referred as T followed by the global comonomer content and next the relative contents of 1-pentene (Pe) and 1-heptene (Hp).

Table 1. Data of Polymerization Runs

Sample	Composition* (mol %)	$(C_5+C_7)/C_3$ ** (mole ratio)	Yield (g)	Activity kg mol^{-1}(prop) mol^{-1} (cat)h^{-1})
iPP	0.0	0.000	1.287	4777
T4-75Pe-25Hp	3.8	0.187	1.268	3929
T4-50Pe-50Hp	4.0	0.187	0.850	2640
T4-25Pe-75Hp	3.2	0.179	1.408	5711
T6-75Pe-25Hp	6.4	0.357	3.241	14830
T6-50Pe-50Hp	6.0	0.357	2.745	10885
T6-25Pe-75Hp	6.7	0.374	2.594	10851
T10-75Pe-25Hp	11.3	0.714	3.630	13678
T10-50Pe-50Hp	10.1	0.714	1.371	5465
T10-25Pe-75Hp	10.5	0.714	2.939	13119
T13-75Pe-25Hp	12.8	0.893	3.557	-
T13-50Pe-50Hp	13.1	0.779	2.125	7679
T13-25Pe-75Hp	12.9	0.779	2.164	7207
T16-75Pe-25Hp	16.0	0.935	2.839	10497
T16-50Pe-50Hp	15.4	0.893	2.448	8828
T16-25Pe-75Hp	16.0	0.893	2.300	7390

* Total comonomer content

** Mole content of propylene in the reaction medium estimated by means of the relationship expressed by Villar and Ferreira [37] from a propylene pressure of 0.40 bar at –5 °C in a volume of 250 mL of toluene.

7.3.3. Film processing

Films of the different terpolymers were obtained by compression molding in a Collin press between hot plates, at 2.5 MPa for 3 min and a temperature of 30 °C above the melting point. They were subsequently cooled down to room temperature by a relatively rapid cooling between plates refrigerated with water (labeled as Q samples, cooling rate around 80 °C/min).

7.3.4. Size Exclusion Chromatography

Molecular weights were evaluated by size exclusion chromatography (SEC) in a Waters GPC/V 2000 equipment with both refractive index and viscosimeter detectors. A set of three columns of the PL Gel type (3 PL Gel 20 Φm Mixed A) was used with 1,2,4-trichlorobenzene as the solvent, at 145 °C and a flow rate of 1 mL/min. The system was calibrated with narrow molecular mass distribution standards of polystyrene.

7.3.5. Nuclear Magnetic Resonance Characterization

Composition in comonomers as well as tacticity of the terpolymers were determined by carbon nuclear magnetic resonance analysis, ^{13}C NMR, from a polymeric solution in 1,1,2,2-tetrachloroethane-*d*4 (70 mg/1 mL) at 80 °C, using an Innova 400 spectrometer (100 MHz). A minimum of 8000 scans were recorded with broad band proton decoupling, using an acquisition time of 1 s, a relaxation delay of 4 s and a pulse angle of 45°. The homopolymer and terpolymers at the lowest composition (around 4 mol%) were characterized in a Bruker Avance DPX-300 (75 MHz) spectrometer, from solution in 1,1,2,2-tetrachloroethane at 100 °C, using deuterated *o*-dichlorobenzene as an internal reference.

7.3.6. Calorimetric analysis

The calorimetric analysis was performed in a PerkinElmer DSC-7 calorimeter with a connection to a cooling system. The equipment was calibrated with different

standards (indium, zinc and *n*-dodecane). Sample weights ranged from 2 to 5 mg. A heating rate of 10 °C/min was used for the different films. Besides the usual normalization to sample weight, the heat flows were also normalized to the scanning rate.

7.3.7. Diffraction Profiles

Wide-Angle X-Ray Diffraction (WAXD) patterns were recorded in the reflection mode by using a Bruker D8 Advance diffractometer provided with a PSD Vantec detector (from Bruker, Madison, Wisconsin). Cu Kα radiation (λ = 0.1542 nm) was used, operating at 40 kV and 40 mA. The parallel beam optics was adjusted by a parabolic Göbel mirror with horizontal grazing incidence Soller slit of 0.12° and LiF monochromator. The equipment was calibrated with different standards. A step scanning mode was employed for the detector. The diffraction scans were collected with a 2θ step of 0.024° and 0.2 s per step.

7.3.8. Mechanical Behavior

Nominal stress-strain tests were performed at a temperature of 25 °C and a stretching rate of 10 mm/min in MTS Q-Test Elite dynamometer with a load of 100 N. Specimens for these experiments were punched out from the polymer films. The dimensions of these strips were 10 mm long, 2 mm wide and around 0.10 mm thick. At least, three different strips were stretched until fracture at a given specimen.

7.4. Results and discussion

Figure 1 shows the dependence of the molar mass on the global composition in counits for some of the propylene-based terpolymers synthesized. A remarkable decrease is observed as overall content is raised, this trend being also noticeable in other copolymers or terpolymers based on α-olefins.[36,38-40] Thus, the higher the comonomers composition is in the terpolymers, the lower the molecular weight is.

Figure 1 also shows that polydispersity for these terpolymers remains practically constant at around 2, as it is expected in metallocene synthesis.[38]

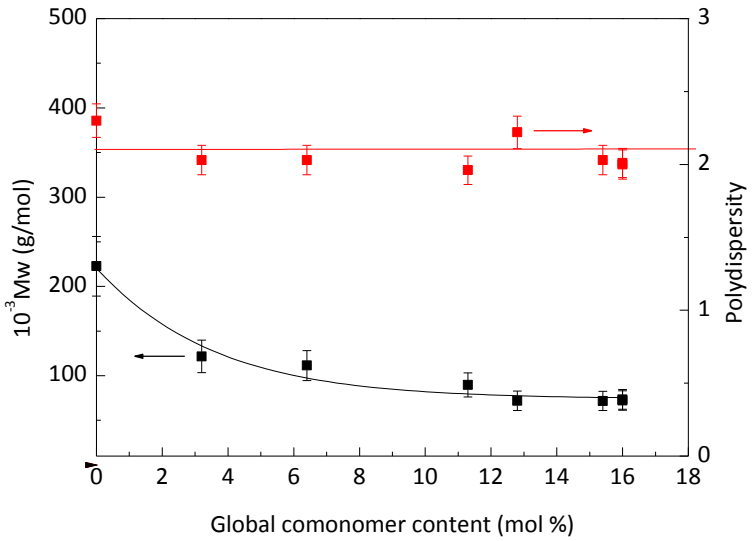

Figure 1. Weight-average molecular weight and polydispersity as function of global comonomers content for some of the different terpolymers.

Figure 2 depicts the variation of the catalyst activity with the molar feed ratio in toluene solution for the synthetized homopolymer and terpolymers. The apparent activity shows an initial increasing trend. This effect is attributed to the presence of comonomers, which has been set out in others works on the basis of different parameters:[41-47] the enhanced solubility of macrochains in the medium,[48] a larger chain transfer activity [49] and the modification of the active center quality.[39] At the highest molar feeding ratios, however, the activity undergoes an eventual decrease, in agreement with other materials synthesized by other authors.[47] The differences at a given molar feeding ratio should be considered inside the experimental error.

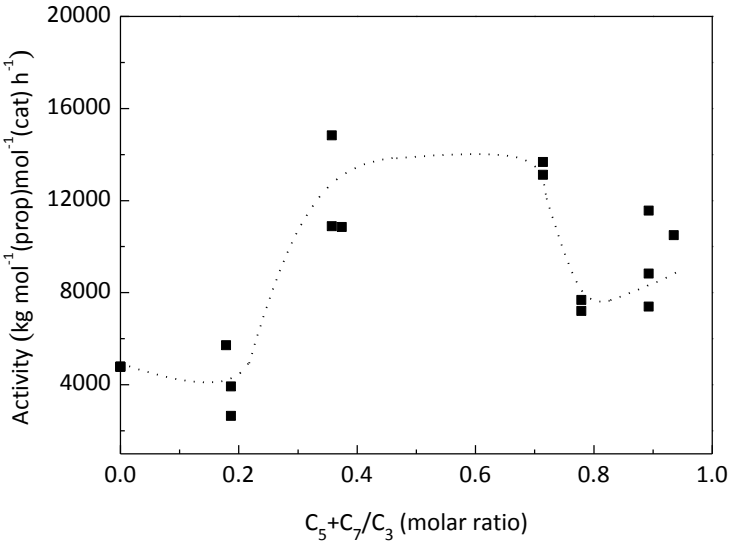

Figure 2. Variation of catalytic activity as a function of the global feed ratio in comonomers.

Figure 3 displays that the two comonomers units, 1-pentene and 1-heptene, exhibit roughly the same dependence on molar feed ratio contents at a specific ratio. That is, a ratio of 75, independently that comes from 1-pentene/1-heptene or vice versa varies rather analogously, and an identical feature is observed for the other two proportions: 50 (1-pentene): 50 (1-heptene) and 25 (1-pentene) : 25 (1-heptene). Then, this Figure seems to indicate intuitively that reactivity of both counits is very similar and there is not preference, at first approximation, in the insertion of both comonomers.

These results are in good agreement with those achieved from isotactic propylene-*co*-1-pentene-*co*-1-hexene terpolymers [50] where a thorough ^{13}C NMR analysis of the microstructure indicated the non-existence of preference from the catalyst to any of both counits, i.e., to 1-pentene and/or 1-hexene. In addition, that comprehensive microstructural evaluation showed suggests a random distribution of both comonomers into the chains.

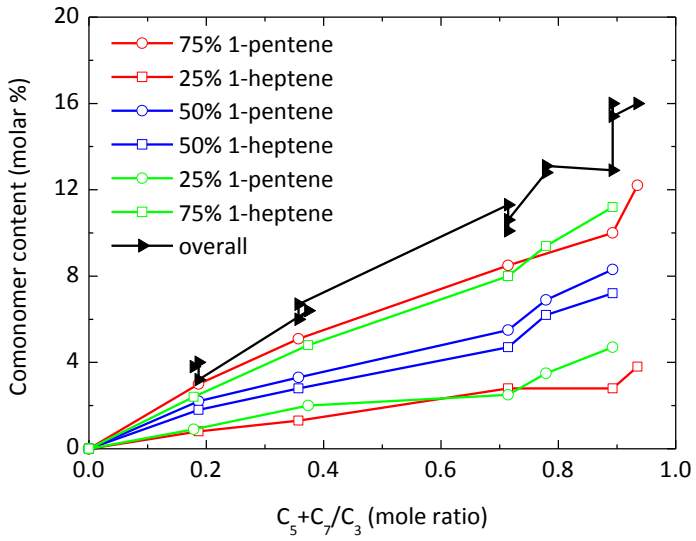

Figure 3. Dependence of the comonomer content on feeding composition found during the synthesis in toluene solution of the different terpolymers.

Identification and assignment of the characteristic ^{13}C NMR peaks for the distinct terpolymers under study are shown in Figure 4 and Table 2, respectively. The spectrum corresponds to the T16-75Pe-25Hp sample. Those signals can be undoubtedly assigned from the data reported in the literature associated with the analogous iPP, poly(1-pentene) and poly(1-heptene) homopolymers as well as from iPP copolymers based on both comonomers. [36,46,50-52] The different carbon nuclei have been named as P, Pe, Hp and X as belonging to propylene, 1-pentene, 1-heptene and unknown comonomer carbon nuclei (1-pentene or 1-heptene). In addition, superscript denotes the carbon position in the corresponding monomer, according to Scheme 1.

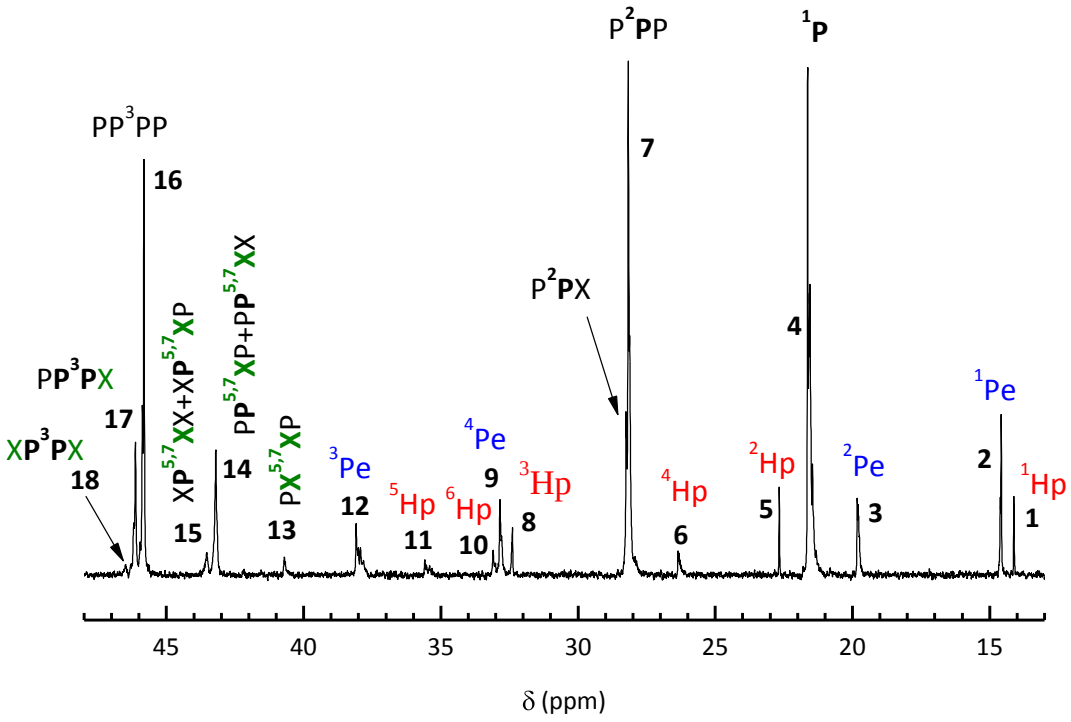

Figure 4. Identification of different carbon nucleus ^{13}C NMR spectra of T16-75Pe-25Hp obtained in 1,1,2,2-tetrachloroethane-*d4* at 80 °C.

Scheme 1. Numeration of carbons belonging to propylene (P), 1-pentene (Pe), and 1-heptene (Hp) in the polymer chain.

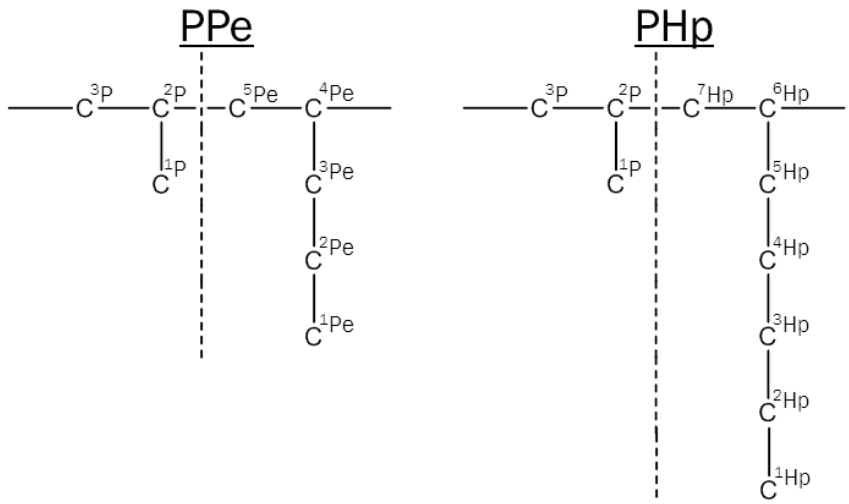

Table 2. Data of Polymerization Runs.

Peak	Assignment	Chemical Shift (ppm)
1	^{1}**Hp**	14.12
2	^{1}**Pe**	14.58
3	^{2}**Pe**	19.83
4	^{1}**P**	19.40-22.00
5	^{2}**Hp**	22.65
6	^{4}**Hp**	26.11-26.58
7	P^{2}**P**P+P^{2}**P**X	27.60-28.60
8	^{3}**Hp**	32.38
9	^{4}**Pe**	32.78-32.84
10	^{6}**Hp**	33.09-33.11
11	^{5}**Hp**	35.40-35.59
12	^{3}**Pe**	38.10
13	P**X**^{5,7}**X**P	40.72
14	P**P**^{5,7}**X**P+P**P**^{5,7}**X**X	43.22
15	X**P**^{5,7}**X**X+X**P**^{5,7}**X**P	43.54
16	P**P**^{3}**P**P	45.82
17	P**P**^{3}**PX**	46.15
18	X**P**^{3}**P**X	46.49

Both total and partial molar contents in comonomers are shown in Table 3. These results have been calculated from the relative intensities of the methyl signals of propylene (^{1}P), 1-pentene (^{1}Pe) and 1-heptene (^{1}Hp) in the ^{13}C NMR spectra (peaks 4, 2 and 1 respectively in Table 2). The so-obtained compositions of the terpolymers have been compared with those ones deduced from the methine carbon signals, and no appreciable differences have been found.

Table 3 also shows the propylene tacticity for the different terpolymers. The metallocene catalyst employed in this work leads only to the production of *mrrm* sequences as stereodefects. Although the side chain beta-methylene carbon of the 1-pentene unit (**^{2}Pe**, in Figure 4.) appears inside the region of syndiotactic methyls, this

signal overlaps with the absent *mrrr* misinsertion and not with the *mrrm* one, allowing an accurate measure of this propene misinsertion.

Table 3. Comonomer content and propylene tacticity for the different terpolymers.

Sample	Global comonomer			*mmmm*	*mmmr*	*rmmr*	*mmrr*	*mmrm + rmrr*	*mrmr*	*rrrr*	*mrrm*
	Global	Pe	Hp								
T4-75Pe-25Hp	3.8	3.0	0.8	92.4	1.5	0.1	1.5	0.3	0.0	0.0	0.4
T4-50Pe-50Hp	4.0	2.2	1.8	91.1	1.8	0.5	1.8	0.4	0.0	0.0	0.4
T4-25Pe-75Hp	3.2	0.9	2.3	93.4	1.7	0.1	1.3	0.1	0.0	0.0	0.2
T6-75Pe-25Hp	6.4	5.1	1.3	92.0	0.6	0.0	0.8	0.0	0.0	0.0	0.2
T6-50Pe-50Hp	6.0	3.2	2.8	92.0	0.7	0.0	0.9	0.0	0.0	0.0	0.4
T6-25Pe-75Hp	6.7	1.9	4.8	91.1	0.9	0.0	1.0	0.0	0.0	0.0	0.3
T10-75Pe-25Hp	11.3	8.5	2.8	86.4	1.6	0.0	0.5	0.0	0.0	0.0	0.2
T10-50Pe-50Hp	10.1	5.4	4.7	88.1	1.0	0.0	0.7	0.0	0.0	0.0	0.1
T10-25Pe-75Hp	10.5	2.5	8.0	86.7	1.8	0.0	1.0	0.0	0.0	0.0	0.0
T13-75Pe-25Hp	12.8	10.0	2.8	84.7	1.4	0.1	0.8	0.0	0.0	0.0	0.2
T13-50Pe-50Hp	13.1	6.9	6.2	85.1	1.0	0.0	0.5	0.0	0.0	0.0	0.3
T13-25Pe-75Hp	12.9	3.5	9.4	84.9	1.1	0.1	0.6	0.0	0.0	0.0	0.4
T16-75Pe-25Hp	16.0	12.2	3.8	80.8	2.1	0.6	0.5	0.0	0.0	0.0	0.0
T16-50Pe-50Hp	15.4	8.2	7.2	82.1	1.7	0.3	0.5	0.0	0.0	0.0	0.0
T16-25Pe-75Hp	16.0	4.7	11.3	82.5	1.4	0.0	0.1	0.0	0.0	0.0	0.0

The propylene tacticity has been estimated from the methyl region at the pentad level. It can be clearly seen in Table 3 the expected decrease in *mmmm* pentad. It is also noticeable that stereodefects tend to vanish at increasing comonomer contents, as it can be deduced from the evolution of the relative content of the *mmrr* pentads. Surprisingly, the content of the *mmmr* pentads increases. Nevertheless, this fact can be accounted for the growing presence of XPX units, whose ^{1}P ^{13}C NMR signal overlaps with that stereosequence.[53] A more detailed assignment

of the propylene methyl carbons in a T6 and a T16 specimen illustrates this fact in Figure 5.

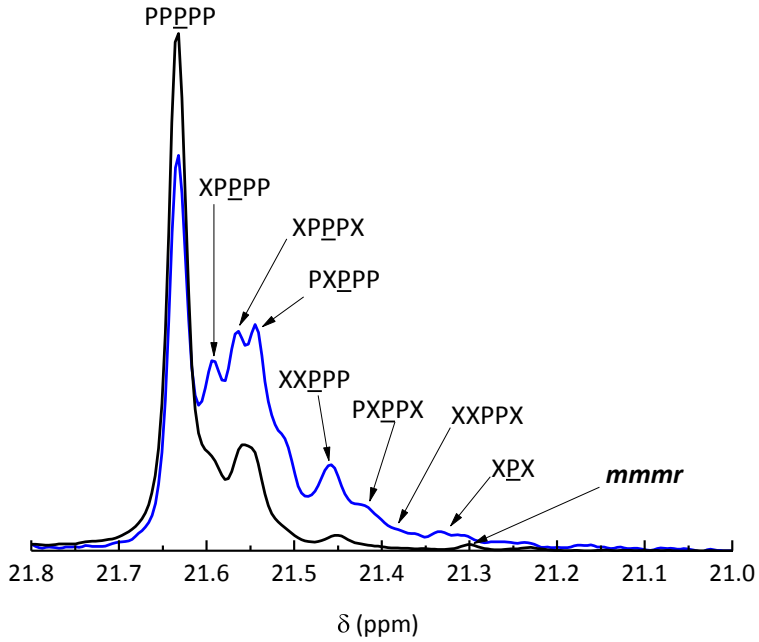

Figure 5. Methyl ^{13}C NMR spectra of T6-50Pe-50Hp and T16-75Pe-25Hp obtained in 1,1,2,2-tetrachloroethane-*d4* at 80 °C.

The composition distribution at the triad level is listed in Table 4. These materials do not lead to comonomer sequences longer than 2 units in the composition range studied and most of comonomers are present as isolated entities disrupting the polypropylene segments.[45,46,51,54] It is possible, however, to observe how the content of XX sequences grows up with the conversion. Only, the comonomer units are exclusively present as isolated units in the case of the T4 terpolymers. Methyl and methine carbons of propylene units in PPX triads appear at the same chemical shift regardless of the nature of the adjacent comonomer. In addition, main-chain methylene carbons in the middle of XX and PX diads (peaks 13, 14 and 15), as well as side branched methylenes of the comonomers, are not sensitive enough to the nature

of the adjacent X unit. Then, the distribution in composition can be only resolved in terms of XX diads.

Table 4. Relative content of triads and average propylene length, n_p.

Sample	PPP	PPX	XPX	PXP	XXP	XXX	[XXP]/[XXP]+[PXP] (x10^2)	n_p
T4-75Pe-25Hp	89.4	6.7	0.2	3.7	0.0	0.0	0.0	27
T4-50Pe-50Hp	88.9	7.1	0.2	3.8	0.0	0.0	0.0	26
T4-25Pe-75Hp	90.7	5.9	0.1	3.3	0.0	0.0	0.0	32
T6-75Pe-25Hp	80.9	11.5	0.8	5.6	1.2	0.0	17.6	14
T6-50Pe-50Hp	83.0	10.1	0.4	5.8	0.7	0.0	10.8	17
T6-25Pe-75Hp	81.2	11.3	0.5	6.4	0.6	0.0	8.6	15
T10-75Pe-25Hp	70.7	16.9	1.0	8.4	3.0	0.0	26.3	9
T10-50Pe-50Hp	71.7	16.3	1.3	7.9	2.7	0.0	25.5	9
T10-25Pe-75Hp	71.4	16.0	1.3	10.2	1.1	0.0	9.7	10
T13-75Pe-25Hp	66.7	18.6	1.3	10.2	3.2	0.0	23.9	8
T13-50Pe-50Hp	65.6	18.8	1.8	10.3	3.5	0.0	25.4	8
T13-25Pe-75Hp	66.4	17.8	1.7	11.2	2.8	0.0	20.0	8
T16-75Pe-25Hp	59.2	21.0	2.5	11.5	5.7	0.0	33.1	6
T16-50Pe-50Hp	60.5	20.4	2.6	12.2	4.4	0.0	26.5	7
T16-25Pe-75Hp	58.6	20.9	2.2	13.4	4.8	0.0	26.4	6

The distribution of the composition from the ^{13}C NMR spectra (Table 4) is then obtained at the triad level by using the following relationships:

$$[PPP] = K\cdot (I_7 - I_{14} - \tfrac{1}{2}\cdot I_{15})$$

$$[PPX] = K\cdot I_{14}$$

$$[XPX] = K\cdot \tfrac{1}{2}\cdot I_{15}$$

(The relationship [XPX] = ½· ([XPXP] + [XXPX]) is applied taking into consideration [55] that [XXPX] = 0)

$$[PXP] = K\cdot (I_1 + I_2 - 2\cdot I_{13})$$

$$[XXP] = K\cdot 2\cdot I_{13}$$

$$[XXX] = 0$$

where K is a normalization constant and I_n corresponds to the intensity of peak *n* tabulated in Table 2. It is immediately apparent that 1-pentene and 1-heptene units are mostly isolated and that the content of those ones belonging to XX diads grows from zero in T4 series up to more than 25% of the total composition in T16 series. Finally, a value of XPX triads denotes the presence of some isolated X units in alternating sequences (XPXP).

From the triad content, the average propylene length has been calculated according to the expression: [55]

$$n_p = ([PPP] + [PPX] + [XPX]) / ([XPX] + ½ \cdot [PPX])$$

It can be observed in Table 4 that the value of n_p changes from around 32 units in the T4 series to around 6 units in the T16 series. This important reduction will have, obviously, a deep influence on both the crystallinity and other crystalline-related characteristics, like crystal lattice and thickness. These morphological aspects will determine the whole spectrum of properties of these materials.

A comprehensive evaluation of physical properties has not been systematically performed in propylene based copolymers and/or terpolymers involving relatively long counits (1-pentene or larger) at intermediate or high comonomer contents (above around 8 mol %). Some tensile stress-strain curves have been only reported for propylene-1-hexene copolymers [20,25,82] and propylene-1-pentene-1-hexene terpolymers.[32] Poon et al.[20] reported yield stress values for propylene-1-hexene copolymers containing more than 10 mol% hexene higher than those shown in propylene-1-octene copolymers at similar counit contents because of new crystal form developed in the propylene-1-hexene copolymers. De Rosa et al.[25,28] described in propylene-1-hexene copolymers with increasing hexene concentration a reduction of values for the Young's modulus from nearly 300-350 MPa in the samples with 1.2 and 2.5 mol%, respectively, to nearly 40 MPa in the sample of 11.2 mol % and 13 MPa in a less isotactic specimen with 18 mol% (synthesized with other catalyst) the last two

ones with crystallinity of about 0.30. Authors indicated that those facts were consistent with the decrease of crystallinity of iPPHe samples with increasing hexene content. Parallel to the decrease of the elastic modulus, the values of the stress at yielding of those samples also strongly decreased with increasing hexene concentration.

Boragno et al.[32] reported for propylene-1-pentene-1-hexene terpolymers at high content of counits that the only possible competition was between the δ form and the mesomorphic structure; however, only the trigonal modification was developed at 20 °C. Alternatively, the samples exhibited very low strength due to the low crystallinity of the terpolymers, therefore, notwithstanding the very small thickness of the lamellae of the δ form crystallites. Stresses were not then capable to destroy the original structure even in proximity of sample's rupture.

Figure 6 shows the stress-strain behavior exhibited by the iPP homopolymer and these terpolymers at the different global contents of counits and the distinct ratios at a specific overall composition. It is clearly noticeable for the 75Pe:25Hp set that tensile stretching takes place through a cold drawing process where the linear dependence of stress on strain is evident at the beginning; later on, neck formation occurs followed by its propagation along the strip and, finally, at high elongations, strain hardening is initiated. As expected, iPP homopolymer exhibits the highest elastic modulus and yield stress together with the lowest breaking deformation because of its rigid and relatively fragile mechanical response. An increase in composition, T4-75Pe-25Hp terpolymer, leads to a significant reduction in mechanical parameters related to the stiffness, *i.e.*, modulus and yield stress while final elongation rises. The decreasing trend in Young's modulus and stress at yielding is further seen for T6-75Pe-25Hp and T10-75Pe-25Hp terpolymers. Nevertheless, T13-75Pe-25Hp shows very similar parameters to those found in the T10-75Pe-25Hp specimen and, finally, T16-75Pe-25Hp exhibits values for both mechanical magnitudes higher than those achieved in either T10-75Pe-25Hp or T13-75Pe-25Hp. Then, the average Young's modulus obtained is 155 MPa and 7.4 MPa for yield stress, as can be evidently deduced from

Figure 7. Deformability is extremely large (strain superior to 500 %) when the global comonomer content is higher than 4 mol %. These mechanical values are much larger than those reported for other authors at comparable contents in spite the molecular weights of those materials were considerably higher. These greater parameters might be associated with the fact that literature provides information on propylene-1-hexene copolymers while the major counit is the 1-pentene in these terpolymers.

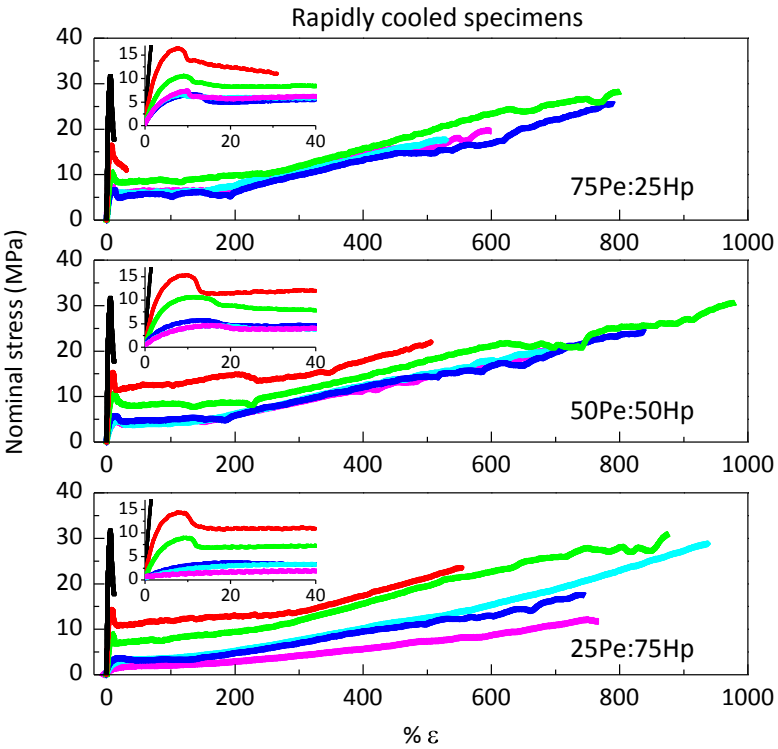

Figure 6. Stress-strain curves for the homopolymer (black symbols) and the terpolymers at different counits ratios for a specific overall composition and at the distinct total contents: T4 (red symbols); T6 (green symbols); T10 (blue symbols); T13 (cyan symbols); T16 (magenta symbols).

The behavior observed in the terpolymers at the 50Pe:50Hp ratio is rather similar to the one just described for the 75Pe:25Hp terpolymers. Variation in the mechanical parameters between the T10-50Pe-50Hp and T13-50Pe-50Hp specimens is now slightly greater. At the lowest global contents, values are rather similar to those

found for the previous 75Pe:25Hp ratio and differences become more important at global contents higher than 10 mol%.

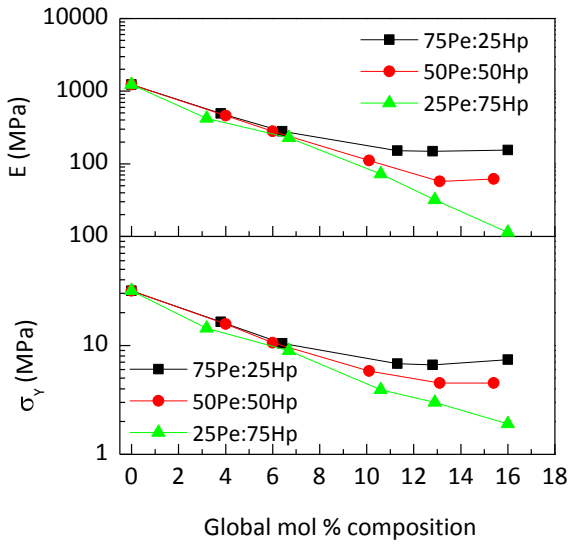

Figure 7. Dependence of Young's modulus and yield stress on global composition for the iPP homopolymer and the different terpolymers.

The 25Pe:75Hp terpolymeric set shows a linear decreasing dependence of modulus and stress at yielding on global content. In addition, it can be also observed a transition from a cold drawing process with necking formation at low counits contents to a homogenous deformation process corroborating that these terpolymers at the highest overall compositions are much softer than those with 75Pe:25Hp and 50Pe:50Hp ratios. Nevertheless, the values reached for the T16-75Pe-25Hp specimen are 11.3 MPa and 1.9 MPa for the elastic modulus and yield stress, respectively.

Then, mechanical response shows two distinct regimes: the one including T4 and T6 terpolymers, which is practically independent of 1-pentene:1-heptene ratios and shows an almost linear variation with global composition; and, the second region that involves the highest overall contents T10, T13 and T16 terpolymers. Here, ratio is a key variable since different dependences are observed. At the 75Pe:25Hp proportion, the T16-75Pe-25Hp sample shows modulus and yield stress higher than

those in the T13-75Pe-25Hpspecimen. At the 50Pe:50Hp proportion, the T16-50Pe-50Hp terpolymer exhibits a higher stiffness and same stress at yielding than the T13-50Pe-50Hp sample; and, at a ratio of 25Pe:75Hp, a linear decrease of both mechanical parameters is seen on global composition. The knowledge of the crystalline details is absolutely required to understand this different mechanical behavior.

Figure 8 shows the X ray profiles at room temperature for the distinct terpolymers. A very interesting polymorphic behavior is observed in these samples, whose films have been prepared by a rapid cooling from the molten state. The variation of the crystalline lattices with the overall content in comonomers is clearly noticeable. Thus, T4-75Pe-25Hp, T4-50Pe-50Hp and T4-25Pe-75Hp terpolymers (and the homopolymer) exhibit the diffractions that characterize the monoclinic α lattice. There is not evidence of the (117) reflection stemming from the orthorhombic cell, most probably because of the high cooling rate used during the film processing.

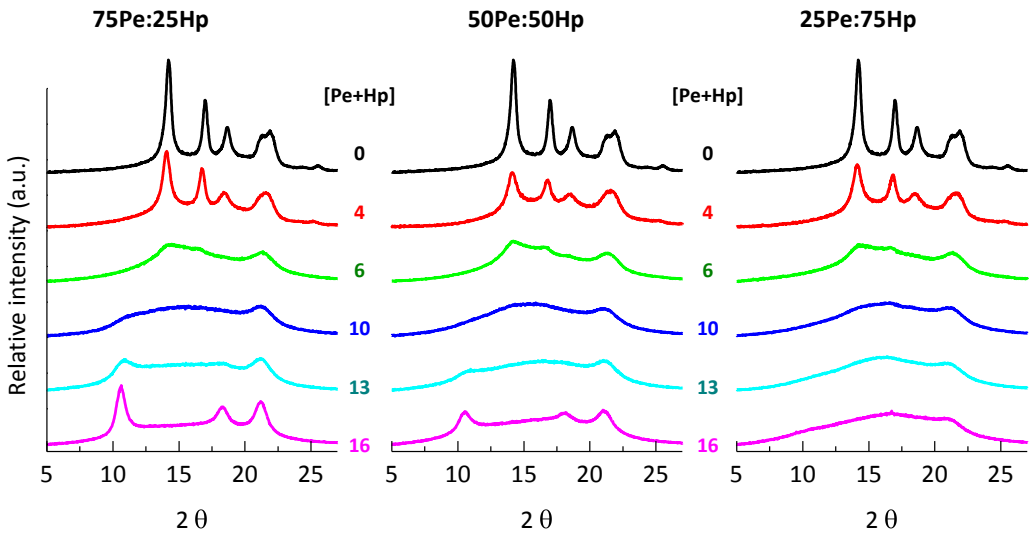

Figure 8. X ray profiles at room temperature for the iPP homopolymer and the different terpolymers at different overall composition and distinct 1-pentene:1-heptene ratios.

The increase of composition in both comonomers, T6-75Pe-25Hp, T6-50Pe-50Hp and T6-25Pe-75Hp terpolymers, leads to the development of a minor amount of defective monoclinic crystallites in addition to a majority of mesomorphic entities. The

situation is somehow different in the T10 terpolymers, where the macromolecular chains are mostly ordered into mesomorphic entities. It should be mentioned that the diffraction characteristic of the trigonal δ form, located at around 10.5°, starts to be evident in the T10-75Pe-25Hp sample.

A competition between the trigonal polymorph and the mesomorphic phase is also observed for the T13 series, but clearly dependent on the ratio of comonomers: thus, the trigonal form is predominant in T13-75Pe-25Hp terpolymer, while only the mesophase is present in the case of the T13-25Pe-75Hp specimen.

If overall composition is still enlarged, a higher amount of the trigonal lattices is achieved for the T16-75Pe-25Hp and T16-50Pe-50Hp terpolymers. Consequently, the trigonal form can be developed in these terpolymers even if crystallization takes place under these not very favorable conditions. At this point, it should be recalled that propylene copolymers with 1-heptene are not able to generate the trigonal form [36]. Nevertheless, the T16-50Pe-50Hp terpolymer exhibits a substantial amount of trigonal polymorph even though its 1-pentene content is only 8.3 mol % (see Table 3), not enough to account for the observed crystallinity in trigonal modification. Thus, Figure 9a shows the variation of the trigonal crystallinity on composition in 1-pentene alone compared with literature data on poly(propylene-*co*-1-pentene) copolymers . [31,34] Since trigonal modification is accompanied, in most cases, by considerable amount of mesophase with overlapping diffractions, the trigonal content has been estimated by integrating the [110] trigonal peak and multiplying by 3.

It is evident from Figure 9a that the terpolymers exhibit a considerably higher crystallinity than the one expected if only the 1-pentene units were incorporated into the trigonal crystals. In fact, if the variation is expressed as function of the global composition (Figure 9b) it can be observed that the Tx-75Pe-25Hp follows a trend rather similar to that found for poly(propylene-*co*-1-pentene) copolymers. The other two series (Tx-50Pe-50Hp and Tx-25Pe-75Hp), however, display a considerably and increasing deviation of the 1-pentene copolymers (yet with a higher trigonal content than the one due to 1-pentene alone, as deduced from Figure 9a).

It is concluded, therefore, that 1-heptene is capable to be incorporated into the trigonal lattice of these terpolymers, especially when 1-pentene is the mayor component.

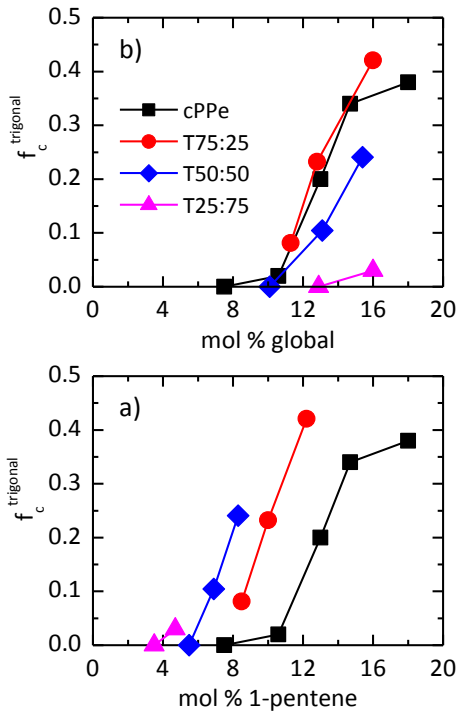

Figure 9. Dependence of the trigonal crystallinity with: a) the composition in 1-pentene, and b) the global composition, for the different terpolymers (circles: Tx-75Pe-25Hp; diamonds: Tx-50Pe-50Hp; triangles: Tx-25Pe-75Hp) compared with literature data on 1-pentene copolymers [31,34] (squares).

The overall degree of crystallinity, f_c, can be estimated from the diffractograms in Figure 8, if the one related to the amorphous component is known at a particular composition. Since variable-temperature X-ray diffraction experiments have been performed for these specimens (results under analysis), the amorphous diffractogram is known. Then, following the procedure reported before for poly(propylene-*co*-1-pentene) and poly(propylene-*co*-1-heptene) copolymers, [34,36] the variation of the overall crystallinity with composition is shown in Figure 10. As can be observed, dependence of crystallinity on global content of counits is very analogous to that

found from the mechanical parameters. This feature indicates that trigonal δ form can be used as a valuable tool for tuning mechanical behavior in these poly(propylene-*co*-1-pentene-*co*-1-heptene) terpolymers.

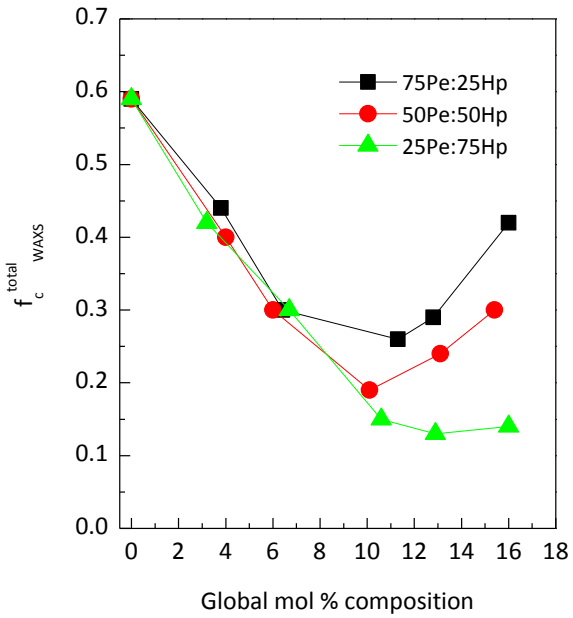

Figure 10. Dependence of overall crystallinity on global composition for the iPP homopolymer and the different terpolymers.

7.5. Conclusions

Poly(propylene-*co*-1-pentene-*co*-1-heptene) terpolymers have been synthesized for the first time in literature at different global compositions in comonomers and three 1-pentene/1-heptene ratios at a given composition. Molecular weight decreases as counits content increases and isotacticity is reduced with comonomer content. Moreover, the relationship between comonomer content, estimated from ^{13}C NMR, and feeding composition clearly indicates that reactivity is very similar for both counits and there is not any preference in their insertion in the resulting macrochains.

The modulus and yield stress exhibit two different trends depending on the global composition in specimens prepared by a rapid cooling from the molten state. At low overall contents, their values are changing with composition but rather independent of comonomer ratio. On the contrary, at composition of 10 mol % or higher ones these mechanical parameters are strongly dependent on 1-pentene / 1-heptene proportion. These two tendencies are ascribed to the crystalline structures able to be developed at different global compositions and distinct ratios. If total comonomer content is low enough, the three terpolymers at a specific composition show similar polymorphs or competence between them. However, differences are rather significant at composition of 10 mol % or higher: the trigonal form can be developed in these terpolymers in spite of propylene-*co*-1-heptene copolymers were unable to generate this lattice at similar compositions. In fact, crystallinity values in those terpolymers are considerably higher than the ones expected if only the 1-pentene units were incorporated into the trigonal crystals, especially for 75Pe:25Hp and 50Pe:50Hp ratios. This feature indicates that now 1-heptene is capable to be incorporated as defect into the trigonal lattice of these terpolymers, particularly when 1-pentene is the major component. Consequently, the mechanical parameters are reflecting the different amounts in trigonal crystallinity.

7.6. References

1. Bruckner, S.; Meille, S.V.; Petraccone, V.; Pirozzi, B. Prog. Polym. Sci. 1991, 16, 361.
2. Phillips, P.J.; Mezghani, K. The Polymeric Materials Encyclopedia, J.C. Salamone, Ed. 1996, CRC Press, Boca Raton, 6637.
3. Natta, G.; Corradini, P. Nuovo Cimento Suppl. 1960, 15, 40.
4. Turner-Jones, A.; Aizlewood, J.M.; Beckett, D.R. Makromol. Chem. 1964, 75, 134.
5. Bruckner, S.; Meille, S.V. Nature 1989, 340, 455.
6. Varga, J. J. Mater. Sci. 1992, 27, 2557.

7. Meille, S.V.; Ferro, D.R.; Bruckner, S.; Lovinger, A.J.; Padden, F.J. Macromolecules 1994, 27, 2615.
8. Lotz, B.; Wittmann, J.C.; Lovinger, A.J. Polymer 1996, 37, 4979.
9. Slichter, W.P.; Mandell, E.R. J. Appl. Phys. 1958, 29, 1438.
10. Grebowicz, J.; Lau, S.F.; Wunderlich, B. J. Polym. Sci., Polym. Symp. 1984, 19.
11. Vittoria, V. J. Macromol. Sci., Phys. 1989, B28, 489.
12. O'Kane, W.J.; Young, R.J.; Ryan, A.J.; Bras, W.; Derbyshire, G.E.; Mant, G.R. Polymer 1994, 35, 1352.
13. Arranz-Andres, J.; Benavente, R.; Perez, E.; Cerrada, M.L. Polym. J. 2003, 35, 766.
14. Pérez, E.; Gómez-Elvira, J.M.; Benavente, R.; Cerrada, M.L. Macromolecules 2012, 45, 6481–6490.
15. Sinn, H.; Kaminsky, W.; Vollmer, H.J., Woldt, R. Angew. Chem. Int. Ed. 1980, 19, 390.
16. Ewen, J.A.; Jones, R.L.; Razavi, A.; Ferrara, J.D. J. Am. Chem. Soc. 1988, 110, 6255.
17. Brintzinger, H.H.; Fischer, D.; Mulhaupt, R.; Rieger, B.; Waymouth, R.M. Angew. Chem. Int. Ed. 1995, 34, 1143.
18. Mansel, S.; Perez, E.; Benavente, R.; Perena, J.M.; Bello, A.; Roll, W.; Kirsten, R.; Beck, S.; Brintzinger, H.H. Macromol. Chem. Phys. 1999, 200, 1292.
19. Mulhaupt, R. Macromol. Chem. Phys. 2003, 204, 289.
20. Poon, B.; Rogunova, M.; Hiltner, A.; Baer, E.; Chum, S.P.; Galeski, A.; Piorkowska, E. Macromolecules 2005, 38, 1232.
21. De Rosa, C.; Auriemma, F.; Talarico, G.; de Ballesteros, O.R. Macromolecules 2007, 40, 8531.
22. Lotz, B.; Ruan, J.; Thierry, A.; Alfonso, G.C.; Hiltner, A.; Baer, E.; Piorkowska, E.; Galeski, V.; Macromolecules 2006, 39, 5777.

23. C. De Rosa, S. Dello Iacono, F. Auriemma, E. Ciaccia, and L. Resconi, Macromolecules, 39, 6098 (2006).
24. C. De Rosa, F. Auriemma, P. Corradini, O. Tarallo, S. Dello Iacono, E. Ciaccia, and L. Resconi, J. Am. Chem. Soc., 128, 80 (2006).
25. De Rosa, C.; Auriemma, F.; De Ballesteros, O.R.; Resconi, L.; Camurati, I. Chem. Mater. 2007, 19, 5122.
26. De Rosa, C.; Auriemma, F.; De Ballesteros, O.R.; De Luca, D.; Resconi, L. Macromolecules 2008, 41, 2172.
27. Keon, J.; Palza, H.; Quijada, R.; Alamo, R.G. Polymer 2009, 50, 832.
28. De Rosa, C.; Auriemma, F.; de Ballesteros, O.R.; Dello Iacono, S.; De Luca, D.; Resconi, L. Cryst. Growth Des. 2009, 9, 165.
29. Cerrada, M.L.; Polo-Corpa, M.J.; Benavente, R.; Pérez, E.; Velilla, T.; Quijada, R. Macromolecules 2009, 42, 702.
30. Stagnaro, P.; Costa, G.; Trefiletti, V.; Canetti, M.; Forlini, F.; Alfonso, G.C. Macromol. Chem. Phys. 2006, 207, 2128.
31. Stagnaro, P.; Boragno, L.; Canetti, M.; Forlini, F.; Azzurri, F.; Alfonso, G.C. Polymer 2009, 50, 5242.
32. Boragno, L.; Stagnaro, P.; Forlini, F.; Azzurri, F.; Alfonso, G.C. Polymer 2013, 54, 1656-1662.
33. García-Peñas, A.; Gómez-Elvira J.M.; Pérez, E.; Cerrada, M.L. J. Polym. Sci., Part A: Polym. Chem. 2013, 51, 3251–3259.
34. Pérez, E.; Cerrada, M.L.; Benavente, R.; Gómez-Elvira J.M. Macromol. Res. 2011, 19, 1179-1185.
35. Janani, H.; Álamo R.G. Polymer 2015, 64, 163-175.
36. García-Peñas, A.; Gómez-Elvira, J.M.; Lorenzo, V.; Pérez, E.; Cerrada, M.L. Eur. Polym. J. 2015, 64, 52–61.
37. Villar, M. A.; Ferreira, M. L. J. Polym. Sci. Part A: Polym. Chem. 2001, 39, 1136–1148.

38. Boragno, L.; Stagnaro, P.; Forlini, F.; Azzurri, F.; Alfonso, G.C. Polymer 2013, 54, 1656-1662.
39. Heiland, K.; Kaminsky, W. Makromol. Chem. 1992, 193, 601.
40. Quijada, R. Macromol. Chem. Phys. 1996, 197, 3091.
41. Kaminsky, W.; Hahnsen, H. In Advances in Polyolefins, R. B. Seymour, T. Cheng, Eds., Plenum Press: New York, 1987, 361–371.
42. Akimoto, A.; Yano, A. In Metallocene-Based Polyolefins, J. Scheirs, W. Kaminsky Eds., John Wiley & Sons, Chichester, 2000, 287–308.
43. Tsutsui, T.; Kashiwa, T. Polym. Commun. 1988, 29, 180–183.
44. Chien, J. C. W.; Nozaki, T. J. Polym. Sci. Part A: Polym. Chem. 1993, 31, 227–237.
45. Da Silva, M. A.; Galland, G. B. J. Polym. Sci. Part A: Polym. Chem. 2008, 46, 947–957.
46. Forlini, F.; Tritto, I.; Locatelli, P.; Sacchi, M. C.; Piemontesi, F. Macromol. Chem. Phys. 2000, 201, 401–408.
47. Quijada, R. Macromol. Chem. Phys. 1996, 197, 3091–3098.
48. Herrmann, H. F.; Böhm, L. L. Polym. Commun. 1991, 32, 58–61.
49. Koivumäki, J.; Seppälä, J. V. Macromolecules 1993, 26, 5535–5538.
50. García-Peñas, A.; Gómez-Elvira, J.M.; Pérez, E.; Cerrada, M.L. J. Polymer Sci. Polymer Chem. 2013, 51, 3251-3259.
51. U.M. Wahner, I. Tincul, D.J. Joubert, E.R. Sadiku, F. Forlini, S. Losio, I. Tritto, M.C. Sacchi, Macromol. Chem. Phys. 2003, 204, 1738.
52. Sacchi, M.C.; Fortini, F.; Losio, S.; Tritto, I.; Costa, G.; Stagnaro, P.; Tincu, I.; Wahner, U.M. Macromol. Symp. 2004, 213:57-68.
53. Sachi, M.C.; Forlini, F.; Losio, S.; Tritto, I.; Wahner, U.M.; Tincul, I.; Joubert, D.J.; Sadiku, E.S. Macromolecules 2003, 204, 1643-1652.
54. Escher, F.F.N.; Galland, G.B. J. Polym. Sci. Part A: Polym. Chem. 2004, 42, 2474.

55. Randall, JC. J. Macromol. Sci. –Rev. in Macromol. Chem. Phys. 1989, C29, 201–317.

CAPÍTULO 8

Microstructure and thermal stability in metallocene iPP-materials: 1-pentene and 1-hexene copolymers

Alberto García-Peñas, María L. Cerrada, José M. Gómez-Elvira and Ernesto Pérez.

2015

8.1. Abstract

Two series of co-poly-α-olefins, 1-pentene and 1-hexene-co-polypropylene samples, have been synthesized via metallocene catalysis up to comonomer contents around 14 mol %. The pyrolysis behaviour of these iPP-rich copolymers has been studied and compared with the corresponding thermal response of the referential iPP homopolymer. Dynamic TGA analysis at different heating rates have been carried out in order to evaluate kinetic changes, all along the weight loss interval, either through the Friedman's method or through a pseudo-first order model. A thorough characterization of chain microstructure has allowed screening chain features, which are likely involved in the existence of a low E_{act} initial stage. Namely, oxidation degree, molecular weight and comonomer composition have been considered. Changes encountered in the pyrolysis kinetics have been found to be consistent with differences in chain flexibility, as the parameter which seems to rationalize the influence of all chain characteristics together.

8.2. Introduction

The emergence of metallocene catalysis has made it possible the production of tailor made polyolefins, not available from Ziegler-Natta catalysts [1-4]. Actually, a large variety of iPP grades in composition can be prepared by inserting alpha-olefins in a random and uniform fashion up to really high contents.

These new copolymers are expected to have a growing impact on the production of iPP-based thermoplastics, as they offer an actual way for widening even more the performance spectrum of these materials. The reason for this perspective not only lies in the fact that low α-olefin contents allows the crystalline fraction to be changed, but also in the fact that the quality of crystals can be modulated. On this matter, much effort has been made to study the modifications undergone by the iPP crystalline phase, as a consequence of inserting α-alkene units [5-16].

It is well known that a major drawback of iPP-based materials is the fact that, very small contents of anomalous structures are enough to cause severe property deterioration. Therefore, the study of thermal stability in every new PP-based family arises as an essential starting point, from which end use applications can be assessed.

This thermal performance study is also gaining importance at present from the sustainable production point of view. Actually, an increasingly diversification of grades, e.g. in composition, could imply a new scenario in mechanical recycling and recovery technologies used, weather it substantially modify the parameters driving such processes. The possibility to apply chemical recycling, as an interesting method to reduce plastic waste and saving raw materials [17], makes it worth studying the kinetics features of pyrolysis in PP-based materials.

To the best of our knowledge, there is no any study at present focusing on the behaviour of propylene copolymers with α-olefins under pyrolytic conditions. Only some punctual results have been reported, within the context of some studies about oxidative degradation of ethylene-co-α-olefins copolymers [18,19]. On the one hand,

Tincul et al report a positive effect of the branch length on the thermal stability in a series of polyethylene copolymers with even carbon number α-olefins, as it is measured by TGA. On the other, Corrales et al have been reasonably associated the slight thermal stability decreasing found in polyethylene copolymers with either 1-hexene or 1-octadecene, to the introduction of tertiary carbons, which are well known to favour the hydrogen abstraction step and then, the C-C splitting process. In the iPP copolymer case with either 1-pentene or 1-hexene, the microstructural factors likely to be considered as potentially influential in the thermal stability are branching degree, i.e. comonomer content, branch length (three or four carbon long), molecular weight and finally, the content of anomalous groups. On account of the fact that these factors can influence the thermal performance in opposite directions, a study is required in order to find out which is the final resulting effect.

A preliminary TGA study on the thermal stability of 1-pentene and 1-hexene-co-polypropylene, up to 14 mol% in comonomer content under anaerobic conditions, is presented in this work.

8.3. Experimental

8.3.1. Synthesis and sample preparation

The synthesis of iPP and PP copolymers was carried out via metallocene catalysis. Propylene (Praxair 2.5) and nitrogen (Contse) gases were purified by flowing through oxygen-trap columns and molecular sieves before use. Oxygen and water free solvent and comonomers were got by refluxing over sodium and further distillation under Nitrogen.

The copolymerizations of propylene with 1-pentene (Acros) and 1-hexene (Acros) were performed in a 500 mL Büchi glass ecoclave at -5 °C in 250 mL of toluene (Merck) for 30 min by using *rac*-dimethylsilylbis(1-indenyl) zirconium dichloride (Strem)/MAO (MAO-Aldrich, 10 wt% solution in toluene) as the catalyst/cocatalyst system ([Al]/[Zr] = 3648). The initial propylene pressure was 0.40 bar and the catalyst amount was

$1.39 \cdot 10^{-6}$ mol. The copolymerization reaction was stopped by adding 5 mL of ethanol (Aroca, 96%) and enabling the unreacted propylene out from the reactor. The polymer was obtained by pouring the reaction batch on a mixture of ethanol/HCl (30:1). The precipitated solid was stirred thoroughly overnight, filtrated, washed again with ethanol and, afterwards, dried under vacuum at room temperature.

The homopolymer and copolymer series are respectively referred as PP, PPEN and PHEX, followed by the total content of comonomer in the case of the copolymer samples. Thus, for example, PHEX9.6 stands for a copolymer containing 9.6 mol % of global 1-hexene content. The samples considered in this study cover a conversion range up to 14 mol % and are shown in Table 1.

Table 1. Composition, SEC and DSC data of Metallocene iPP materials.

Sample	Comonomer	Composition (mol %)	Mn	Mw	Mw/Mn	Tm (°C)
PP	homopolymer	0.0	96900	222700	2.3	154
PPEN4.4	1-pentene	4.4	63300	151500	2.4	116
PPEN8.4	1-pentene	8.4	-	-	-	91
PPEN9.8	1-pentene	9.8	39600	98000	2.5	85
PPEN14.1	1-pentene	14.1	23600	74300	3.1	71
PHEX4.7	1-hexene	4.7	68900	142900	2.1	112
PHEX6.1	1-hexene	6.1	-	-	-	102
PHEX9.6	1-hexene	9.6	45900	95400	2.1	79
PHEX14.2	1-hexene	14.2	-	-	-	49

All samples were processed by compression-molding in a Collin 200x200 press, at 20 °C over the corresponding melting temperature, and 25 bar during 3 min. Final films were obtained by cooling the molten samples at room temperature and pressing between water refrigerated plates at the same pressure.

8.3.2. Size exclusion chromatography and viscosimetry

The molecular weights of the iPP sample and some of the 1-pentene and 1-hexene copolymers were evaluated by size exclusion chromatography (SEC) in a Waters GPC/V 2000 equipment with both refractive index and viscosimeter detectors. A set of three columns of the PL Gel type was used with 1,2,4-trichlorobenzene as the solvent. The

equipment was calibrated with narrow molecular mass distribution standards of polystyrene. The measurements are shown in Table 1.

An indirect assessment of the molecular weight evolution with conversion was also performed by measuring the intrinsic viscosity in stabilized decaline (1g/L of Irganox 1010), at 135 °C.

8.3.3. NMR characterization

Compositional and configurational chain microstructure of samples was analyzed by means of the ^{13}C NMR spectroscopy. The spectra were obtained from 1,1,2,2-tetrachloroethane-d_4 (70 mg/1 mL) at 80 °C, using an Inova 400 spectrometer (100 MHz). In the case of the PP and low conversion copolymer samples, the ^{13}C NMR spectra were obtained from 1,2,4-trichlorebenzene solutions in a Bruker Avance DPX-300 (75 MHz) at 100 °C, using deuterated *o*-dichlorobenzene as an internal reference. A minimum of 8000 scans were recorded with broad band proton decoupling and using an acquisition time of 1 s, a relaxation delay of 4 s, and a pulse angle of 45°.

The molar content in 1-pentene and 1-hexene for the different copolymers was estimated from the relative intensities of the comonomer and propylene methyl signals in the ^{13}C NMR spectra. The so-obtained composition of the copolymers was compared with that one calculated from the methine carbons, but no significant differences were found. Finally, the propylene tacticity was estimated from the methyl region at the pentad level.

8.3.4. DSC characterization

A preliminary DSC analysis was performed by using a Perkin-Elmer DSC-7 calorimeter connected to a cooling system and calibrated with different standards. The sample weight was around 2 mg.

The purified samples were heated from - 45 °C to 220 °C at a heating rate of 10 °C/min and then cooled to - 45 °C at the same rate. Finally, a second cycle was carried out with the same procedure. The values of Tm, shown in table 1, were taken

respectively from the maximum of the peaks corresponding to these transitions in the second scan.

8.3.5. FTIR characterization

The FTIR spectra of all samples were recorded from prepared films, by performing 10 scans in a Perkin Elmer Spectrum One, in the 4000 to 450 cm^{-1} range, at a resolution of 2 cm^{-1}. The spectra were normalized by taking the intensity of the 2722 cm^{-1} band as a reference.

8.3.6. Dinamic TGA analysis

The pyrolysis of the samples in the film state was carried out by running dynamic thermal gravimetric analysis (TGA). Measurements were carried out from 40 °C up to 550 °C in a Thermal Analysis TGA-Q-500 device. The samples were 4 mm disc of approximately 2 mg cut from the film with a calibrate die. Constant heating rates of 2, 5, 10 and 20 °C/min under a 90 mL/min flow of Nitrogen were used.

8.4. Results and discussion

8.4.1. Molecular weights

Molecular weight is well-known to play a role in the thermal stability of polyolefins. Actually, its influence under oxidative conditions has been studied for long in iPP based materials. In the case of the solid state, the effect of molar mass is mainly related to the influence on the crystalline degree, which is ultimately the parameter controlling the oxygen accessibility to the chains. On the contrary, the role played by chain length in the pyrolysis of the iPP, has not been considered. On this matter, some preliminary results [20] show that the Mw evolution itself could be a factor contributing to the E_{act} variation in the pyrolysis of a high-Mw-iPP with conversion. For this reason we considered convenient to take into account the distinctive molar masses of the specimens here studied.

Molar mass and intrinsic viscosity have been found to be magnitudes directly related. As a matter of fact, molecular weights obtained for three 1-pentene copolymers (PPEN4.4, PPEN9.8 and PPEN14.1) and two 1-hexene copolymers (PHEX4.7 and PHEX9.6) and intrinsic viscosity values present the same trend, as it is possible to appreciate in Figure 1. In this figure it is apparent, on the one hand, that molar masses of propylene-based copolymers decrease remarkably upon addition of α-olefins in the feeding and, on the other, that this trend is not sensitive to the comonomer nature, as for it turns out to be unique in the composition range studied. Consequently, the intrinsic viscosity can be used as a suitable parameter to compare molar molecular weights of the copolymer samples.

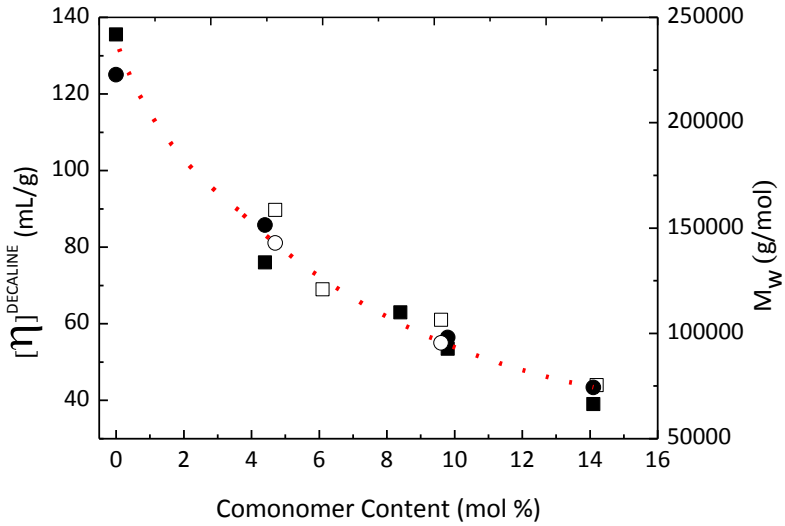

Figure 1. Variations of the intrinsic viscosity in decaline at 135°C and SEC weight-average molecular weights, as a function of the global comonomer content. Viscosity: (■) 1-pentene-copolymers; (□) 1-hexene copolymers. SEC: (●) 1-pentene-copolymers; (○)1-hexene copolymers.

8.4.2. Chemical defects FTIR analysis

FTIR spectroscopy is a suitable technique to characterize the microstructure of iPP and iPP-based polyolefins. It has been traditionally used to monitor the progress of the oxidative degradation in the polymer by means of the carbonyl index [21,22]. It

can be assumed that air oxidizes the samples during the molten processing leading, this way, to the production of different kinds of groups, namely, ketones, acids, esters and hydroperoxides.

It is very important to control carbonyl group and hydroperoxide contents due to their roles as main initiators in the UV and thermo-oxidative degradation of polypropylene [23,24].

Figure 2 shows the two FTIR spectral windows which are worth considering from the stability point of view. The first one covers the 1550-2000 cm^{-1} wave number range, where stretching modes of carbonyl groups appear, as well as stretching modes of –C=C- groups [25,26]. The second one is located from 3250 to 3550 cm^{-1} and corresponds to the OH stretching modes of hydroperoxides [22].

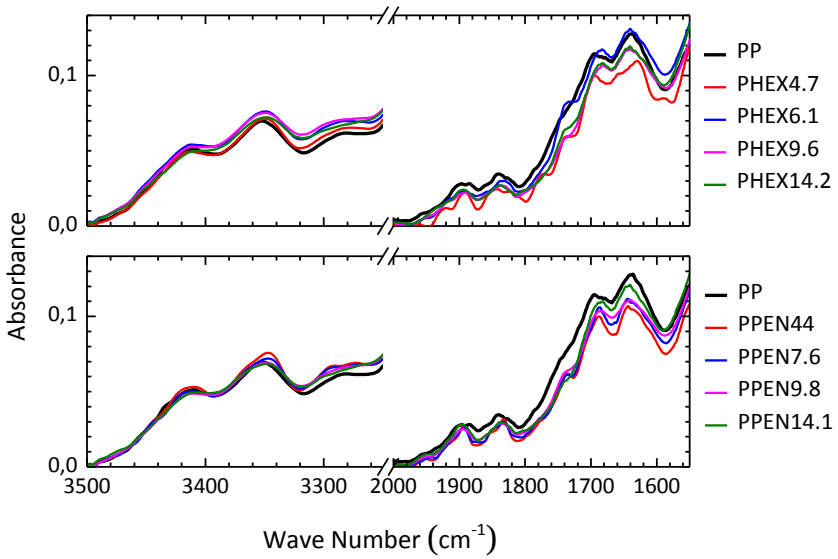

Figure 2. Normalized FTIR data corresponding to ROOH and CO windows for iPP, PPEN and PHEX samples.

The comparison of either CO or hydroperoxide contents of 1-pentene and 1-hexene copolymers series with respect of the corresponding ones in the iPP case shows that, although 1-hexene copolymers seem to be slightly more oxidized than 1-pentene copolymers, no big differences exist and all of them can be considered to

present similar oxidation degrees. This difference cannot be really connected with other factors than little variations in processing.

8.4.3. Melting temperature

DSC experiments have shown the typical melting behavior of iPP-based polymers and thermal changes encountered can be directly linked to molecular weight and microstructure [27].

Actually, the higher the comonomer content, the shorter the propylene average length and, consequently, the lower the melting point is (Table 1).

8.4.4. Microstructure ^{13}C NMR analysis

Figure 3 displays as an example the ^{13}C-NMR spectra of the isotactic polypropylene, and two copolymers with around 10 mol % comonomer content. The identification of the signals has been made according to literature [16,28] and they have been identified by using the nomenclature shown in Scheme 1.

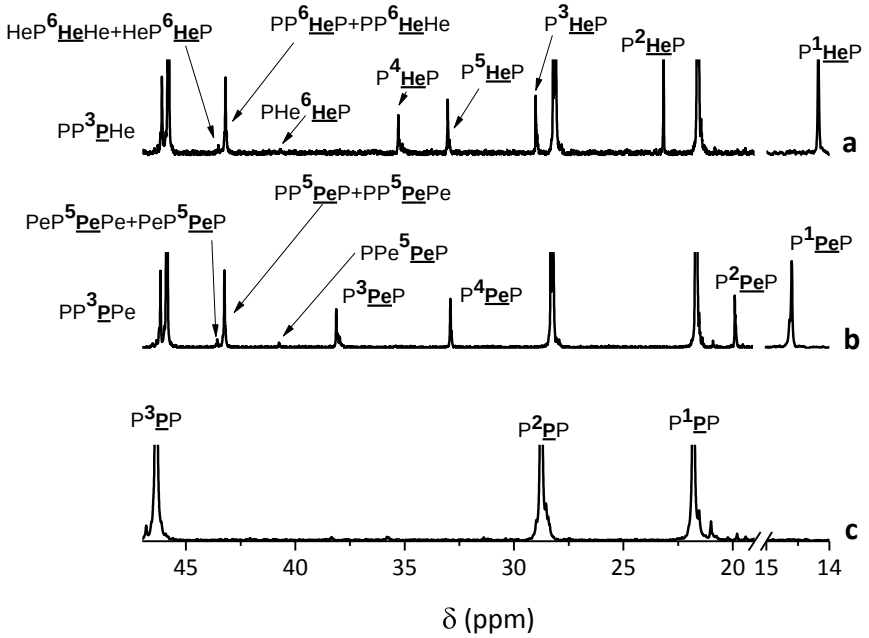

Figure 3. ^{13}C NMR spectra of PHEX9.6 (a), PPEN9.8 (b) and iPP (c).

The different carbon nuclei have been named as P, Pe and He as belonging to propylene, 1-pentene and 1-hexene, respectively. In addition, a superscript denotes the carbon position in the corresponding monomer, according to Scheme 1, is also used.

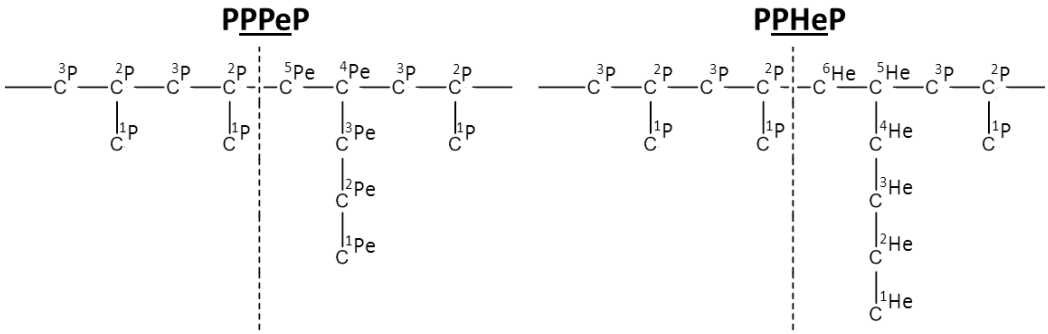

Scheme 1. Numeration of carbons belonging to propylene (P), 1-pentene (Pe) and 1-hexene (He) units in the polymer chain.

The quantitative analysis of microstructures in configuration and composition has been performed according to the criteria reported elsewhere [16]. The corresponding results are collected in Tables 2 and 3 at the triad and the pentad levels respectively.

Table 2. Relative content of triads in composition and average propylene length (n_p).

Sample	PPP	PPPe	PePPe	PPeP	PePeP	PePePe	[PePeP]/ [PPeP+PePeP] (x10^2)	n_p
PPEN4.4	86.9	8.0	0.1	5.0	0.0	0.0	0.0	23
PPEN8.4	77.9	12.5	0.8	8.2	0.6	0.0	7.4	13
PPEN9.8	73.2	15.3	1.2	8.3	2.0	0.0	19.2	10
PPEN14.1	65.3	18.8	1.4	10.4	4.1	0.0	28.6	8
Sample	**PPP**	**PPHe**	**HePHe**	**PHeP**	**HeHeP**	**HeHeHe**	**[HeHeP]/ [PHeP+HeHeP] (x10^2)**	**n_p**
PHEX4.7	86.9	8.1	0.1	4.9	0.0	0.0	0.0	23
PHEX6.1	82.8	11.2	0.0	6.0	0.0	0.0	0.0	17
PHEX9.6	73.8	15.1	0.8	8.8	1.5	0.0	14.7	11
PHEX14.2	61.3	21.0	2.2	10.6	4.9	0.0	31.5	7

The most important result from this analysis is the evidence of a similar evolution of the microstructure both in composition and in configuration for the two series of copolymers. In particular, shorter and shorter propylene sequences linked either by isolated comonomer units or by an increasing amount of comonomer diads, are produced when the comonomer content increases. In all cases, the propylene average sequence given in Table 2 is really a representative microstructural parameter because of the random insertion of the comonomers [16].

Table 3. Relative content of propylene tactic sequences at the pentad level.

Sample	*mmmm*	*mmmr*	*rmmr*	*mmrr*	*mmrm + rmrr*	*rmrm*	*rrrr*	*rrrm*	*mrrm*
PP	90.3	5.2	0.9	3.1	0.8	0.0	0.0	0.0	0.6
PPEN4.4	92.1	1.9	0.0	1.1	0.1	0.0	0.0	0.0	0.4
PPEN8.4	89.8	0.9	0.0	0.9	0.0	0.0	0.0	0.0	0.0
PPEN9.8	88.0	1.5	0.0	0.7	0.0	0.0	0.0	0.0	0.0
PPEN14.1	81.6	3.8	0.0	0.5	0.0	0.0	0.0	0.0	0.0
PHEX4.7	92.0	1.6	0.0	1.3	0.2	0.0	0.0	0.0	0.2
PHEX6.1	90.0	1.0	0.0	2.4	0.0	0.0	0.0	0.0	0.5
PHEX9.6	88.8	1.2	0.0	0.4	0.0	0.0	0.0	0.0	0.0
PHEX14.2	82.5	2.2	0.0	1.1	0.0	0.0	0.0	0.0	0.0

On the basis of this analysis, an enhanced flexibility of copolymers chains is expected with regard to the iPP homopolymer, where the distinctive rigidity conferred by longer isotactic sequences is only distorted by a small content of stereo and regioerrors. On this matter, the above-mentioned changes in Tm, all along the conversion range under study, serves as a support of this assertion. Such a change in

the global flexibility of chains is a factor which should be considered, among others, to set out the thermal stability of these iPP-based materials.

8.4.5. Thermogravimetrical analysis

Dynamic TGA analysis of the copolymers has been carried out at four heating rates under Nitrogen. The weight loss curves obtained correspond to single step processes, as it is expected for typical pyrolysis of polyolefins, iPP and propylene rich copolymers in our case. Representative TGA curves for two samples at different rates are shown in Figure 4. In particular, those of the iPP and PPEN14.1 samples have been chosen. In this figure it is also indicated the criterion used to assess the onset temperature (T_{onset}), which is usually associated to initial pyrolysis processes. In our experiments, a simple checking of the corresponding W_{onset} shows that such parameter is, in fact, associated to stages surrounding a 22 weight loss percent (Figure 5).

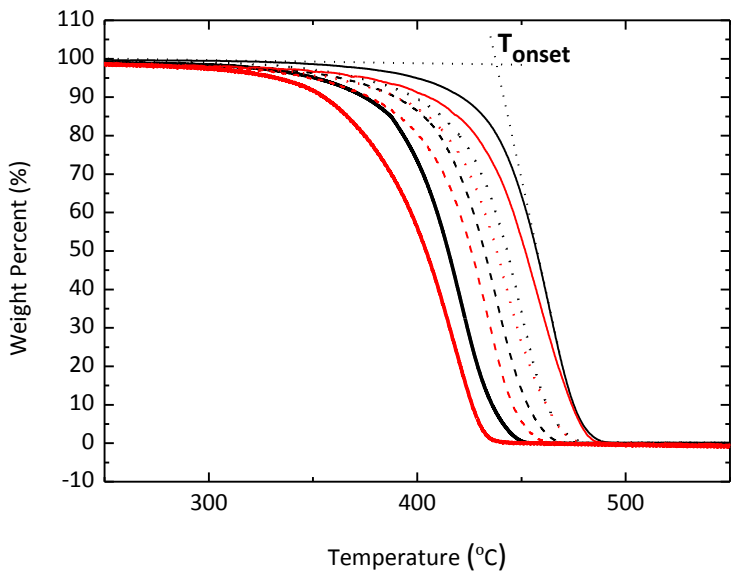

Figure 4. Comparison of TGA thermograms for iPP (black) and PPEN14.1 (red) at heating rates of 2 (thick line), 5 (dash), 10 (dot) and 20 ° C/min (thin line).

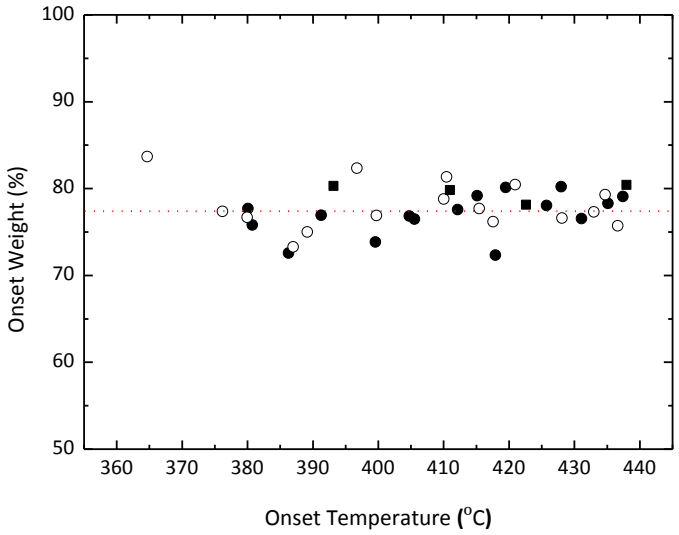

Figure 5. Onset weight loss versus onset temperature for isotactic polypropylene (■), 1-pentene copolymers (●) and 1-hexene copolymers (○).

As it is well-known, the shift of T_{onset} when increasing the heating rate is due to the shorter time necessary for the sample to reach a given temperature [29]. It is apparent that weight loss curves of PPEN14.1 are shifted to lower temperatures with respect to the iPP case. That is to say that the thermal stability of samples with such a comonomer content is significantly reduced, as it is discussed below in more detail.

The corresponding derivative curves (DTG) are shown in Figure 6. They really confirm the existence of one single process, whose maximum (T_{peak}) serves also as a characteristic parameter for assessing relative stabilities of iPP and its copolymers at advanced degradation stages.

The variations of both T_{onset} and T_{peak} with the comonomer content are shown in Figures 7 and 8 respectively. Even though T_{onset} and T_{peak} allow tracking the process at very different stages, both parameters seem to vary in the same way with compositions. Actually, these two references seem to undergone a net decreasing on going towards higher comonomer contents. Additionally, it is also remarkable that this

reduction of the thermal performance starts at conversions over 4 mol %, a value which shows the same thermal stability than the parent homopolymer.

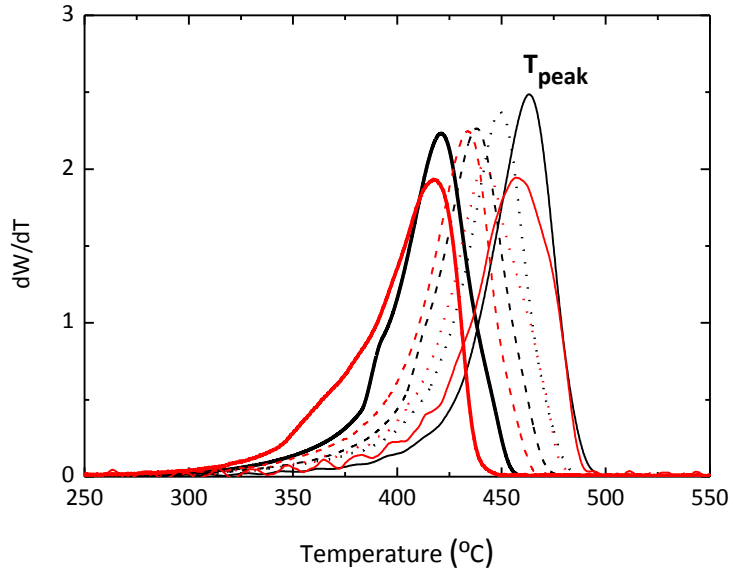

Figure 6. Comparison of DTG curves for iPP (black) and PPEN14.1 (red) at heating rates of 2 (thick line), 5 (dash), 10 (dot) and, 20 ° C/min (thin line).

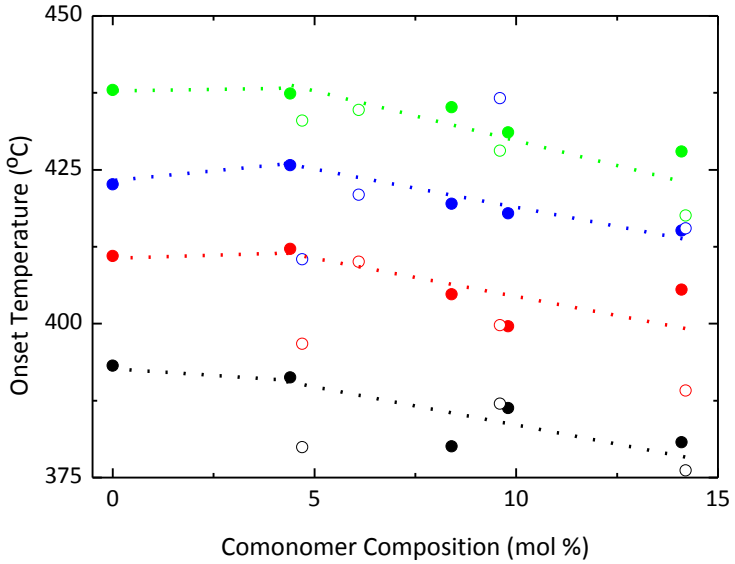

Figure 7. T_{onset} versus comonomer content for isotactic polypropylene (●), 1-pentene copolymers (●) and 1-hexene copolymers (○), at heating rates of 2 (black), 5 (red), 10 (blue) and 20 ° C/min (green).

This temperature lowering must be the result of changes undergone by apparent kinetic parameters, featuring the emission of volatiles. Consequently, the measurement of apparent activation energy and pre-exponential factor (E_{act} and A) is mandatory, so as to know whether chain microstructure has a real role in pyrolysis.

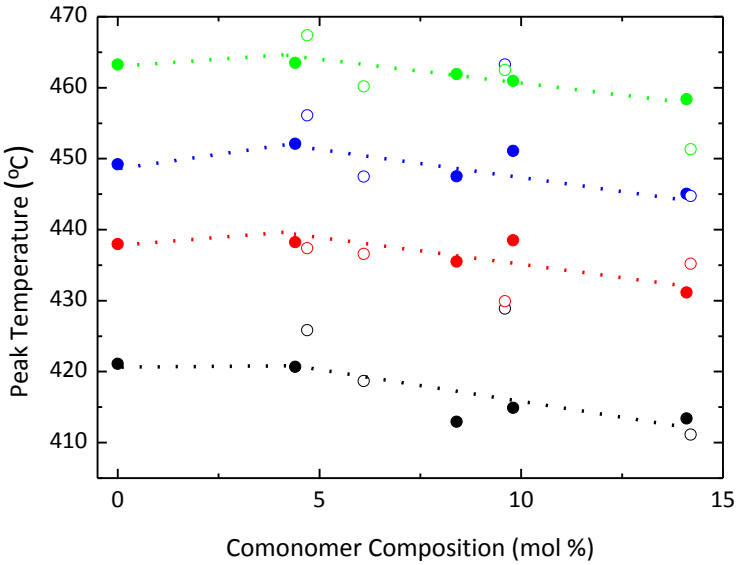

Figure 8. T_{peak} versus molar comonomer content for isotactic polypropylene (●), 1-pentene copolymers (●) and 1-hexene copolymers (○), at heating rates of 2 (black), 5 (red), 10 (blue) and, 20 ° C/min (green).

It can be assumed that the pyrolysis mechanism of ours copolymers is that one describing the emission of volatiles in the PP case, under the same conditions. The process is accepted to take place through several steps which imply the scission of main chain C-C bonds, as the most energy demanding one, and the intra-molecular transposition of hydrogen to produce mid-chain radicals. These mid-chain radicals eventually yield through β-scission end alkenes and saturated hydrocarbons as volatiles and, thereby, similar ending groups (terminal vinylidene and n-propyl) in the polymeric residue [30]. The former step is consequently thought to contribute the most to the apparent E_{act} of the whole process and, provided that no change in the

mechanism occurs, any variation in that magnitude would mainly reflect a change in the nature of the split C-C bond.

The E_{act} variation with pyrolysis progress has been tracked for every specimen by running the Friedman´s procedure, which is a multiple heating rate and model-independent method [31]. The results shown in Figure 9 reveal the well-known fact that E_{act} of the PP pyrolysis quickly builds-up in the first stage of the process [29,32]. A similar behavior is also somewhat appreciated in the copolymer series and has been attributed to the presence of "weak points", among which anomalous oxygen containing groups would be included [29]. Some previous work has in fact evidenced that anomalous structures, e.g. carbonyl containing groups, are involved at the very beginning of the pyrolysis, but also that some very few regular C-C bonds would be selectively involved [20].

The variation of E_{act} has been also checked to occur by applying the method proposed by Chan et al. [29]. This model assumes the order of reaction to be one and implies the use of expression 1 for every single heating rate.

$$\ln\left[\frac{\left(-\frac{dW}{dt}\right)}{W}\right] = \ln A - \frac{E_{act}}{R \cdot T} \qquad [1]$$

This function is displayed in plot 10 for the iPP and the 1-pentene copolymers, at 20 °C/min as an example. The figure shows two well-defined linear correlations in every sample, whose slopes and independent terms yield apparent E_{act} and A values respectively, for each individual kinetic stage, henceforth referred to as 1 and 2 regions. Table 4 collects these values.

It is then clear that the initial region I is related with both low E_{act} and low A processes ($E_{act}1$, A1), and that the subsequent final stage (region II) is featured by upper E_{act} as well as higher A ones ($E_{act}2$, A2).

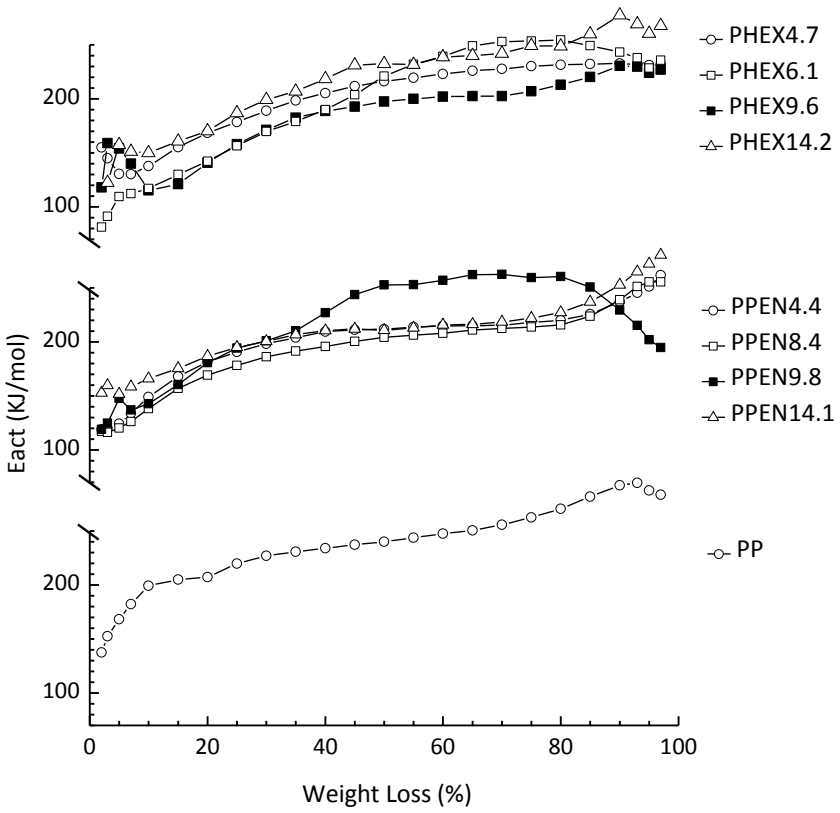

Figure 9. Variation of the apparent activation energy as a function of the weight loss percent, obtained using the Friedman's method for the different polymers synthetized.

The representation of both E_{act} against comonomer composition in Figure 11 makes evident two important facts. While the second stage $E_{act}2$ is roughly constant, the lower $E_{act}1$ characterizing initial processes increases from comonomer contents over 4 mol %. Actually, their values eventually approach those ones of the second stage level at higher comonomer contents. These trends seem clear in spite of the large dispersion of data, especially in $E_{act}2$ values. Nevertheless, it must be taken into account that Figure 11 displays the whole set of E_{act} values whatever the heating rate may be.

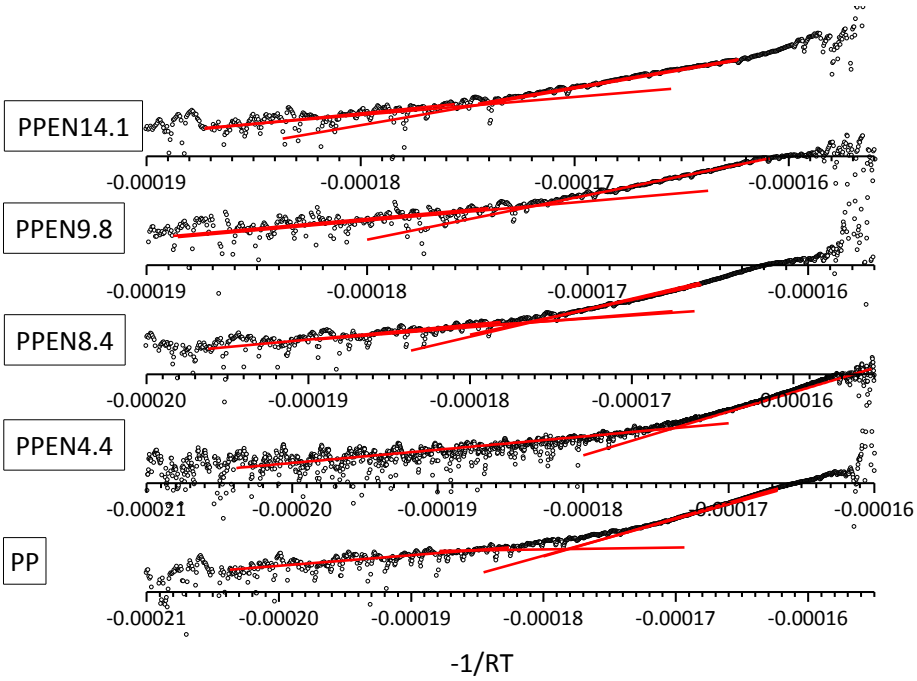

Figure 10. Variation of Ln[(-dW/dt)/W] versus -1/RT at 20°C/min for the iPP and the PPEN series.

At this point of the discussion, the global decreasing of both T_{onset} and T_{peak} (Figures 7 and 8) can be explained on the basis of initial stages associated to higher and higher A values, as long as the insertion of comonomer increases or, in other words, initial stages associated to very likely C-C scissions, which necessarily promote the emission of low molecular weight species against simple macrochain breaking.

Among the factors which are expected to justify the existence of a low $E_{act}1$ pyrolysis stage, oxidation degree has been considered to be the main one. As a matter of fact, oxygen containing functions have been found to be involved in the very beginning of the pyrolysis, namely at temperature below 200 °C when the weight loss has not started yet [20]. However, differences in chain oxygen content are not able to predict the growing path observed for $E_{act}1$ in Figure 11, since all specimens have been shown to present similar oxidized species by means of FTIR spectroscopy, both qualitatively and quantitatively.

Changes in apparent activation energy could be linked with other factors, such as molecular weight and microstructure. As far as the former is concerned, two opposite effects can be considered as arising from the conversion dependent molecular weight decreasing (Figure 1).

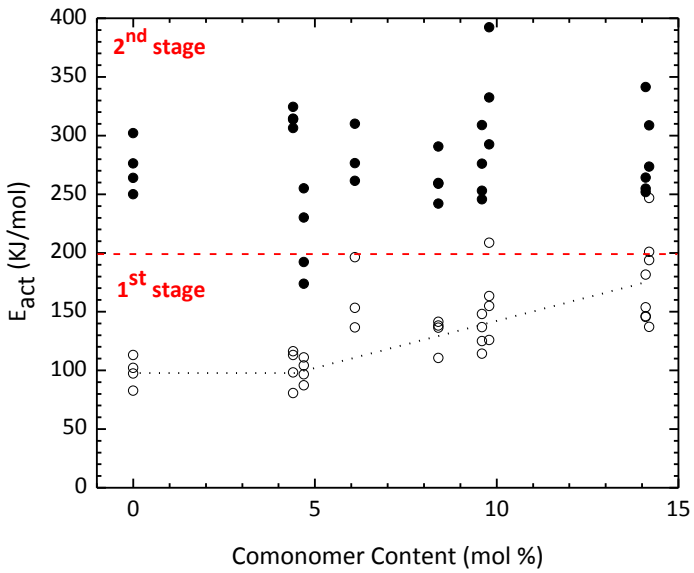

Figure 11. Variation of the apparent activation energies, as they were calculated from the pseudo-first order model, with the comonomer content for all samples and all heating rates. First stage $E_{act}1$ values (○), second stage $E_{act}2$ values (●).

On the one hand, the increasingly content of chain-end groups with comonomer conversion could be thought to contribute to low E_{act} processes, but the $E_{act}1$ trend shown in Figure 11 contradicts such assumption. In fact, $E_{act}1$ increases as long as molecular weight decreases. On the other hand, some previous results on the pyrolysis of a high molecular weight iPP point indeed to flexibility as a main factor driving the apparent E_{act} of the process [20]. In the samples under study, chain flexibility is enhanced by increasing comonomer insertion as well as by the molecular weight decreasing. These changes are expected to promote the removing of specific intrachain interactions, e.g. angular and torsional stresses, which have been proposed to cause certain regular C-C bonds to behave as weak points in longer [33] and more rigid PP-rich chains.

Table 4. Apparent activation energy (E_{act}) and pre-exponential factor (A) values for the two pyrolysis stages in every sample, as they were calculated through the pseudo-first order model [29].

Sample	v2				v5				v10				v20			
	$E_{act}1$ (KJ/mol)	LnA1	$E_{act}2$ (KJ/mol)	LnA2	$E_{act}1$ (KJ/mol)	LnA1	$E_{act}2$ (KJ/mol)	LnA2	$E_{act}1$ (KJ/mol)	LnA1	$E_{act}2$ (KJ/mol))	LnA2	$E_{act}1$ (KJ/mol)	LnA1	$E_{act}2$ (KJ/mol)	LnA2
PP	113.1	16.1	249.8	41.2	101.9	14.4	264.0	43.4	97.2	13.9	276.1	45.5	82.7	11.1	302.0	49.7
PPEN4.4	116.1	17.2	313.7	52.6	113.0	16.6	314.3	52.2	80.5	10.7	306.4	50.6	98.1	14.1	324.4	53.5
PPEN8.4	138.1	21.6	242.0	40.3	141.3	22.1	290.6	48.4	136.2	21.0	259.4	42.8	110.4	16.6	258.9	42.5
PPEN9.8	208.7	34.2	684.6	115.7	163.1	26.4	392.1	65.7	154.7	24.8	332.4	54.9	125.8	19.7	292.5	48.3
PPEN14.1	181.4	29.7	341.4	59.0	153.6	24.3	264.2	41.2	146.1	23.1	254.7	42.2	145.5	23.1	251.8	41.4
PHEX4.7	110.9	16.3	230.0	37.6	104.0	15.1	192.3	31.2	87.2	12.2	173.8	28.0	96.4	14.3	254.9	41.6
PHEX6.1	196.4	32.1	436.3	73.3	--	--	261.3	43.1	153.3	24.0	276.6	45.5	136.6	21.2	310.1	51.1
PHEX9.6	136.7	30.4	276.1	45.6	124.8	19.3	245.6	40.8	147.9	22.6	308.9	50.2	114.2	17.7	252.9	41.4
PHEX14.2	246.8	41.6	550.2	93.5	200.9	33.2	849.6	142.4	193.9	31.6	308.6	51.4	136.9	22.1	273.4	45.7

Finally, microstructure is another parameter related with chain mobility. It is a well-known fact that characteristic Tm in iPP copolymers drops on increasing the comonomer content, as it has been shown in Table 1. This is a phenomenon directly linked to the random distribution of comonomer units, which play as interruptions of propylene sequences. As a certain check of the influence of changes in flexibility derived from microstructure in composition, over the first stage apparent $E_{act}1$, Figure 12 shows the evolutions of $E_{act}1$ values for every copolymer sample, against the relative content of comonomer containing triads (PXP, PPX, XXP, XPX), where X is indistinctly 1-pentene and 1-hexene. In this case $E_{act}1$ corresponds to an average value from those ones obtained at the different heating rates and the trends are roughly linear in all cases. These dependences are proposed to be associated with the increasingly flexibility of chains.

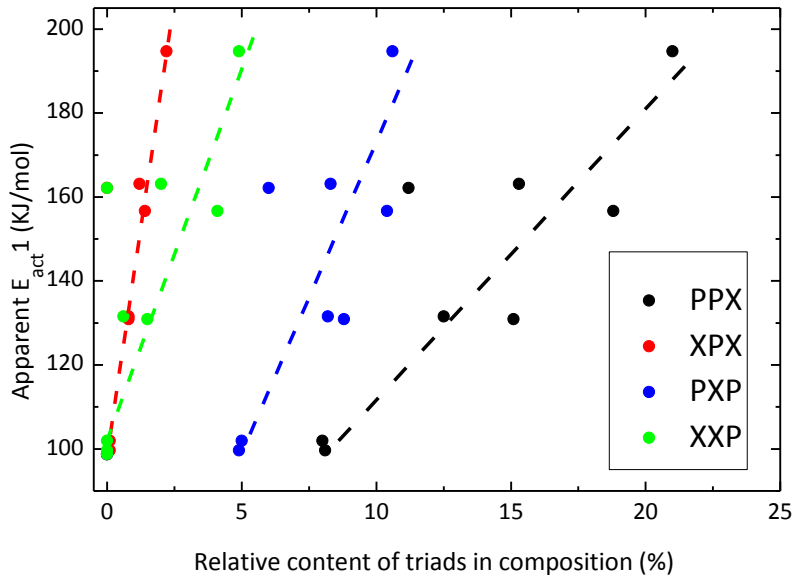

Figure 12. Variation of average $E_{act}1$ values as a function of the relative content of comonomer containing triads.

Such a hypothesis can be differently checked by choosing the propylene average length as the parameter, against which the above mentioned average $E_{act}1$ can be plotted. The result is shown in Figure 13 and describes an exponential-like $E_{act}1$ increment for propylene average lengths below 20 units. In the case of the iPP homopolymer, the isotactic average length (n_{iso}= 52) has been taken as the referential value.

Even though these results are not conclusive, they do show that all factors determining chain flexibility must be taken into account, in order to give a consistent explanation on the variation of the apparent E_{act}, characterizing the first step of the iPP-based copolymer pyrolysis.

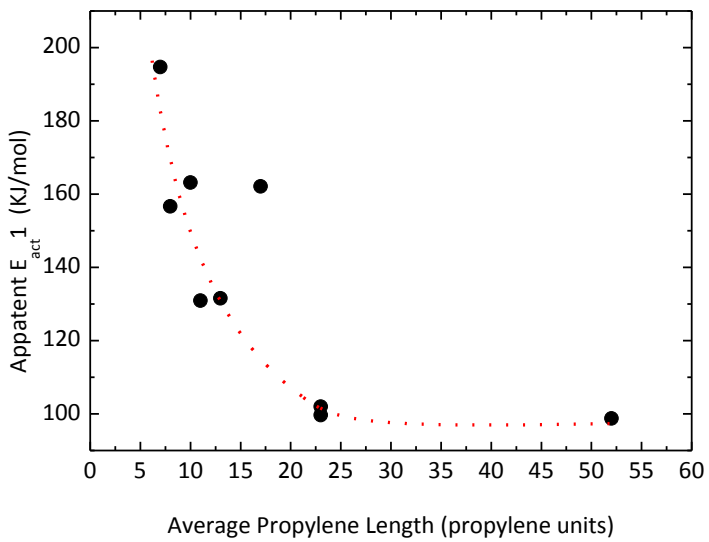

Figure 13. Variation of the apparent average $E_{act}1$ as a function of the average propylene length.

8.5. Conclusions

Metallocene catalysis has been used to prepare two series of random *co*-α-olefin-*co*-polypropylene samples in a controlled fashion. Their microstructures have been found to be different enough to study the influence of several chain features on the pyrolysis kinetics.

The analysis of pyrolysis kinetics has been performed by means of dynamic TGA runs, either through the isoconversional Friedman´s method or by running the pseudo-first order model proposed by Chan et al. Any of the treatments revealed the existence of an increasingly trend for the apparent activation energy, as far as the process progresses. Results obtained from the latter are particularly enlightening as for they evidence two well-defined kinetic stages. First, there exists an initial period associated to low E_{act} and A values which, nevertheless, level up from comonomer contents over 4 mol% to almost reach the threshold of the second stage. Finally, a subsequent second kinetic stage runs at higher and roughly constant E_{act} and A values.

Even though oxygen-containing groups are indeed weak points, where chain scission is supposed to be promoted, their similar quality and content in all samples cannot justify differences observed in the first stage low apparent E_{act}.

On account of the fact that, molecular weight and composition are found to consistently vary with the initial E_{act}, their influence on chain flexibility is proposed to drive the kinetic features of the pyrolysis.

8.6. References

1. Spaleck W, Kueber F, Winter A, Rohrmann J, Bachmann B, Antberg M, Dolle V, Paulus E. The Influence of Aromatic Substituents on the Polymerization Behavior of Bridged Zirconocene Catalysts. Organometallics 1994; 13: 954-963.
2. Mise T, Miya S, Yamazaki H. Excellent stereoregular isotactic polymerizations of propylene with C2-symmetric silylene-bridged metallocene catalysts. Chem Lett 1989; 10: 1853-1856.

3. Razavi A, Atwood J. Isospecific propylene polymerization with unbridged Group 4 metallocenes. J Am Chem Soc 1993; 115: 7529-7530.
4. Kaminsky W. Highly active metallocene catalysts for olefin polymerization. J Chem Soc, Dalton Trans 1998: 1413-1418.
5. Karger-Kocsis J. Polypropylene: Structure, Blends and Composites 1. London, GB; Chapman & Hall; 1995.
6. Benavente, R., Pereña, J., Bello, A., Pérez E, Locatelli P, Fan Z, Zucchi D. Thermal and viscoelastic behaviour of copolymers of propene and 1-hexene. Polym Bull 1996; 36: 249-256.
7. Arranz-Andrés J, Guevara J, Velilla T, Quijada R, Benavente R, Pérez E, Cerrada M. Syndiotactic polypropylene and its copolymers with alpha-olefins. Effect of composition and length of comonomer. Polymer 2005; 46: 12287-12297.
8. Arnold M, Henschke O, Knorr J. Copolymerization of propene and higher α-olefins with the metallocene catalyst Et[Ind]2HfCl2/methylaluminoxane. Macromol Chem Phys 1996; 197: 563-573.
9. Halász L, Belina K, Vorster O, Juhász P. Rheological, thermal and crystallisation properties of ethylene, propylene and α-olefin copolymers. II Thermal and crystallisation properties. Plastics, Rubber and Composites 2004; 5: 205-211.
10. Jeon K, Palza H., Quijada R, Alamo R. Effect of comonomer type on the crystallization kinetics and crystalline structure of random isotactic propylene 1-alkene copolymers. Polymer 2009; 50: 832-844.
11. Palza H, López-Majada J, Quijada R, Pereña J, Benavente R, Pérez E, Cerrada M. Comonomer Length Influence on the Structure and Mechanical Response of Metallocenic Polypropylenic Materials. Macromol Chem Phys 2008; 209: 2259-2267.
12. De Rosa C, Auriemma F, Corradini P, Tarallo O, Iacon S, Ciaccia E, Resconi L. Crystal Structure of the Trigonal Form of Isotactic Polypropylene as an Example of Density-Driven Polymer Structure. J Am Chem Soc 2006; 128: 80-81.

13. Lotz B, Ruan J, Thierry A, Alfonso G, Hiltner A, Baer E, Piorkowska E, Galeski A. A Structure of Copolymers of Propene and Hexene Isomorphous to Isotactic Poly(1-butene) Form I. Macromolecules 2006; 39: 5777-5781.
14. Guidetti G, Busi P, Giulianelli I, Zannetti R. Structure-properties relationships in some random copolymers of propylene. Eur Polym J 1983; 19: 757-759.
15. Hong S, Seo Y. Crystallization of a Polypropylene Terpolymer Made by a Ziegler−Natta Catalyst: Formation of γ-phase. J Phys Chem B 2007; 111: 3571-3575.
16. García-Peñas A, Gómez-Elvira J, Pérez E, Cerrada M. Isotactic poly(propylene-co -1-pentene- co -1-hexene) terpolymers: Synthesis, molecular characterization, and evidence of the trigonal polymorph. J Polym Sci Part A: Polym Chem 2013; 51: 3251-3259.
17. Miskolczy N, Bartha L, Deak GY, Jover B, Chemical recycling of waste polyethylene and polypropylene. Petroleum and Coal 2003; 45:125-130.
18. Corrales T, Escudero M, Quijada R, Catalina F, Abrusci C. A chemiluminescence study on termal and photostbility of ethylene/α-olefin copolymers synthesized with rac-Et(Ind)2ZrCl2/MAO catalyst system. Eur Polym J 2009; 45: 2708-2716.
19. Tincul J, Thakally V, Govender T. Degradation of polyolefins prepared with Fischer-Tropsch derived olefins. Macromol Symp 2005; 225: 179-189.
20. Gomez-Elvira JM, Benavente R, Martínez MC, Correlation between chain microstructure and activation energy in the pyrolysis of a high molecular weight isotactic polypropylene. Polym Deg Stab 2015; 117: 46-57.
21. Philippart JL, Sinturel C, Gardette JL. Influence of light intensity on the photooxidation of polypropylene. Polym Degrad Stab 1997; 58: 261e8.
22. Gugumus F. Thermooxidative degradation of polyolefins in the solid state: part 1. Experimental kinetics of functional group formation. Polym Deg Stab 1996; 52: 131e44.

23. Allen NS, Recent advances in the photo-oxidation and stabilization of polymers. Chem Soc Rev 1986;15:373-404
24. Heacock J, Mallory F, Gay F. Photodegradation of polyethylene film. J Polym Sci Part A-1 1968; 6: 2921-2934.
25. Philippart JL, Sinturel C, Arnaud R, Gardette JL. Influence of exposure parameters on the mechanism of photooxidation of polypropylene. Polym Deg Stab 1999; 64: 213-25.
26. Lacoste J, Vaillant D, Carlsson DJ. Gamma-, photo, and thermally initiated oxidation of isotactic polypropylene. J Polym Sci Part A Polym Chem 1993; 31: 715-22.
27. Arranz-Andrés J, Peña B, Benavente R, Pérez E, Cerrada M. Influence of isotacticity and molecular weight on the properties of metallocenic isotactic polypropylene. Eur Pol J 2007; 43: 2357-2370.
28. García-Peñas, A., Gómez-Elvira, J., Pérez, E., & Cerrada, M. (2014). Microstructure of metallocene isotactic propylene- co -1-pentene- co -1-hexene terpolymers. J Polym Sci Part A: Polym Chem 2014; 52: 2537-2547.
29. Chan JH, Balke ST. The thermal degradation kinetics of polypropylene: part III. Thermogravimetric analyses. Polym Deg Stab 1997;57:135e49.
30. Sawaguchi T, Ikemura T, Seno M. Preparation of a,u-Diisopropenyloligopropylene by thermal degradation of isotactic polypropylene. Macromolecules 1995;28:7973e8.
31. Friedman H. Kinetics of thermal degradation of char-forming plastic from thermogravimetry. Application to a phenolic plastic. J Polym Sci C 1964;C6:183e95.
32. Peterson JD, Vyazovkin S, Wight CA. Kinetics of the thermal and thermooxidative degradation of polystyrene, polyethylene and poly(propylene). Macromol Chem Com 2001;202:775-84.

33. Stoliarov SI, Lyon RE, Nyden MR. A reactive molecular dynamics model of thermal decomposition in polymers. II. polyisobutylene. Polymer 2004;45:8613-21.

CONCLUSIONES

Los hitos y conclusiones más significativos obtenidos del presente trabajo de investigación, que recoge esta Memoria de Tesis Doctoral, se detallan a continuación:

1.- Se ha llevado a cabo la síntesis satisfactoria de diversas arquitecturas de polipropileno con diferentes alfa-olefinas como unidades comonómeras, algunas de ellas nunca descritas en la literatura hasta el presente. Se han preparado en un amplio intervalo de composiciones, obteniendo una diversidad considerable de **copolímeros** de propileno-*co*-1-penteno, propileno-*co*-1-hexeno y propileno-*co*-1-hepteno, y una gran variedad de **terpolímeros** de propileno-*co*-1-penteno-*co*-1-hexeno y propileno-*co*-1-penteno-*co*-1-hepteno, en los que además de la composición global se ha variado adicionalmente el ratio entre comonómeros, habiéndose seleccionado tres diferentes. Asimismo, se han sintetizado los diferentes **homopolímeros** de partida, es decir: polipropileno isotáctico, poli-1-penteno, poli-1-hexeno y poli-1-hepteno.

2.- Los diferentes materiales de base propilénica presentan, en general, **pesos moleculares suficientemente elevados** para garantizar una correcta prestación mecánica, y una **polidispersidad** en torno a **2** que indica la estrecha distribución de pesos moleculares característica de los materiales polímeros obtenidos con catalizadores metalocenos. La elucidación de sus características moleculares ha permitido conocer el grado de **isotacticidad** de los materiales, además de su **composición**.

3.- El estudio detallado de la **microestructura,** particularizado para los terpolímeros propileno-*co*-1-penteno-*co*-1-hexeno, y sus correspondientes copolímeros de propileno-*co*-1-penteno y propileno-*co*-1-hexeno, ha revelado que la incorporación del comonómero de ambas counidades se produce de manera similar, y que la variación del peso molecular parece depender exclusivamente del contenido global en comonómero. Por otro lado, el cálculo de los **ratios de reactividad** a través de los métodos propuestos por Finemman-Ross y Kelen-Tudos, si bien ajustan

razonablemente el diagrama de composición/alimentación del terpolímero estudiado, en el intervalo de conversiones analizado, no son capaces de predecir la distribución experimental de la composición. Por el contrario, los valores obtenidos a partir del análisis ^{13}C-NMR sí permiten predecir dicha distribución. El producto de las relaciones de reactividad que se obtiene utilizando este último método es muy próximo a la unidad, lo que permite concluir que estos materiales presentan una distribución al **azar** de las unidades monoméricas a lo largo de las cadenas poliméricas. Estos resultados sugieren un mismo tipo de incorporación para el resto de familias sintetizadas como consecuencia de la similitud de las características moleculares encontradas para todas y cada una de las restantes cadenas macromoleculares.

4.- Las diversas arquitecturas de propileno preparadas presentan un **comportamiento polimórfico** muy interesante y múltiple en función de las condiciones de cristalización, del contenido en comonómeros, y, además para los terpolímeros, del ratio entre ambas co-unidades implicadas.

5.- El nuevo **polimorfo trigonal** se había descrito hasta la fecha exclusivamente en copolímeros de propileno-*co*-1-penteno y propileno-*co*-1-hexeno. Sin embargo, esta estructura cristalina ha sido dilucidada también para los **terpolímeros** de **propileno-*co*-1-penteno-*co*-1-hexeno** y **propileno-*co*-1-penteno-*co*-1-hepteno** a elevados contenidos en comonómeros, independientemente del tratamiento térmico aplicado. Asimismo, la velocidad de cristalización de esta forma trigonal está estrechamente relacionada con el ratio entre comonómeros, habiéndose observado que el 1-hexeno ralentiza la aparición del nuevo polimorfo en comparación al 1-penteno.

6.- La incorporación de 1-hepteno como comonómero ha resultado especialmente interesante. En los **copolímeros propileno-*co*-1-hepteno**, sintetizados en un amplio intervalo de composiciones y preparados en muy diversas condiciones de cristalización, **no** es **posible generar** la nueva **entidad** cristalina **trigonal** en ninguna

circunstancia. Por el contrario, los **terpolímeros propileno-*co*-1-penteno-*co*-1-hepteno** exhiben un **contenido** en fase **trigonal** mucho más **elevado** que el esperado si sólo el 1-penteno participara en la formación de dicho polimorfo. Esto demuestra que el **1-hepteno** es **capaz de incorporarse** en la **celdilla trigonal** cuando el 1-penteno está también presente, sobre todo a altos valores del ratio 1-penteno / 1-hepteno.

7.- La estructura mesomórfica se genera en todas y cada una de las familias sintetizadas, en un intervalo de composición y condiciones de cristalización específicas. En particular, la formación de la **mesofase** en los copolímeros de propileno-*co*-1-hepteno requiere unas **velocidades** de enfriamiento **menores** con el **aumento** del contenido en **comonómero**, circunstancia que resulta muy interesante. Además, esta **modificación** entra en **competencia directa** con la forma **monoclínica**, excepto para elevados contenidos en co-unidades donde la aparición de esta última aparece muy restringida.

8.- El estudio de las diferentes estructuras cristalinas generadas, así como de las variaciones del grado de cristalinidad en función de la **longitud del comonómero** empleado ha puesto de manifiesto que las unidades de mayor longitud requieren de un **mayor tiempo de acoplamiento** de las cadenas. Por ello, el uso de **counidades** más **largas**, como el 1-hepteno, induce **velocidades** de cristalización más **lentas**, a elevados contenidos en comonómeros, favoreciendo las cristalizaciones en frío, así como menores temperaturas de fusión.

9.- Diversas **propiedades** de interés se han examinado para la posible aplicabilidad de estos materiales. Estas **propiedades**, además de **variar** muy significativamente con la **composición**, dependen también en gran medida de la **estructura cristalina** generada, es decir, del interesante y variado polimorfismo que presentan estos materiales.

10.- La **rigidez** en los **copolímeros de propileno-*co*-1-hepteno** está estrechamente ligada al **contenido** en comonómero. Por otra parte, su **comportamiento mecánico** está también muy **condicionado** por el tratamiento térmico y, por tanto, por las **diferentes estructuras cristalinas** que pueden generarse. La presencia de la **celdilla monoclínica** conduce a **polímeros** más **rígidos** frente a la mayor **deformabilidad** exhibida por los que desarrollan la **fase mesomórfica**.

11.- Las propiedades de transporte de gases se han evaluado también en estos copolímeros. De este estudio se ha deducido una clara **dependencia** entre la **permeabilidad** y el **contenido en comonómero**, con tendencias análogas para el N_2, O_2 y CO_2. Además, los materiales con mayor contenido en la **fase mesomórfica** muestran valores más altos de **permeabilidad** debido a la **mayor** movilidad de estas entidades.

12.- El examen de las propiedades ópticas ha puesto de manifiesto que los valores de **transmitancia** exhibidos en la región visible por estos copolímeros de propileno-*co*-1-hepteno son **elevados**, por encima del 80 % para algunas de las composiciones sintetizadas. Esta **transparencia** es tanto función de la **cristalinidad** como de la **proporción de estructuras** cristalinas (en el caso de que haya coexistencia entre varias), de modo que se ha observado que los cristalitos **monoclínicos** conducen a valores **inferiores** de la transmitancia en la región visible que los correspondientes **mesomórficos**.

13.- Diversos **parámetros mecánicos** se han evaluado también en **terpolímeros de propileno-*co*-1-penteno-*co*-1-hepteno**, demostrando igualmente que el conocimiento de la **estructura cristalina** es **fundamental** para entender el comportamiento mecánico.

14.- La **estabilidad térmica** de los **copolímeros propileno-*co*-1-penteno** y **propileno-*co*-1-hexeno** se ha analizado con cierto detalle. El análisis cinético de la degradación

en **ausencia de oxígeno** ha revelado la existencia de **dos etapas cinéticas**: una **inicial** caracterizada por un valor de la **energía** de activación aparente relativamente **bajo** que aumenta con el contenido en comonómero, y una **segunda** etapa que presenta **valores elevados** y constantes de la energía de activación aparente, independientemente de la composición del copolímero. Es de destacar que la variación de los valores de la **energía** de activación aparente asociados a la **primera etapa** no se puede justificar en base al contenido en oxígeno en los diferentes materiales y, por ello, se puede pensar en el hecho de que dicha variación **se relaciona** con los cambios de **flexibilidad** que experimentan las cadenas como consecuencia del avance del proceso de pirolisis.

15.- Como **conclusión general**, las propiedades de los diversos materiales estudiados han resultado ser muy sensibles tanto a la cristalinidad total como a la naturaleza de las diversas fases presentes, lo que ha permitido obtener materiales polímeros en un extenso espectro de propiedades, que se pueden modular a voluntad en un amplio intervalo.

The most important assumptions and conclusions obtained from the present research work and collected in this PhD Thesis, are the following:

1.- Synthesis of different propylene architectures with various alpha-olefins as comonomer units has been carried out satisfactorily. Some of them have been never described in the literature up to date. They have been prepared in a broad range of compositions and, consequently, a great diversity of propylene-*co*-1-pentene, propylene-*co*-1-hexene, and propylene-*co*-1-heptene **copolymers** as well as a large variety of propylene-*co*-1-pentene-*co*-1-hexene and propylene-*co*-1-pentene-*co*-1-heptene **terpolymers** have been obtained. Besides the global composition, ratio between comonomers has been additionally varied, selecting three different values. Moreover, the corresponding **homopolymers** have been also synthesized, i.e., isotactic polypropylene, poly-1-pentene, poly-1-hexene and poly-1-heptene.

2.- The different propylene-based materials exhibit **molecular weights sufficiently high** to guarantee a proper mechanical performance, and **polydispersity** values around 2, indicating narrow molecular weight distributions. The elucidation of their molecular features has allowed determining the **isotacticity** degree of these materials, and also their **composition**.

3. – A detailed **microstructure** study, focused on propylene-*co*-1-pentene-*co*-1-hexene terpolymers and their corresponding propylene-*co*-1-pentene and propylene-*co*-1-hexene copolymers, has revealed that incorporation of both comonomers takes place in a similar way, and that molecular weight variations seem to depend exclusively on global comonomer content. On the other hand, estimations of the **reactivity ratios**, through Finenmman-Ross and Kelen-Tudos methods, are not able to predict the experimental distribution of composition, although they adjust the composition/feeding diagram of the different terpolymers in the range of conversions analyzed. On the contrary, the values attained from ^{13}C-NMR analysis allow predicting

the experimental distribution. The product of reactivity ratios obtained with the latter method is very close to unity, which allows concluding that these materials present a **random** distribution of monomeric units along the polymeric chains. These results suggest an analogous type of counit incorporation for the other synthetized families since the similar molecular features showed by all these macromolecular chains.

4.- The different propylene architectures synthesized exhibit a very interesting and rich **polymorphic behavior**, as function of crystallization conditions, content in comonomers, and, in the case for terpolymers, ratio between both counits.

5.- The new **trigonal polymorph** had been exclusively described up to now in propylene-*co*-1-pentene and propylene-*co*-1-hexene copolymers. However, this crystalline structure has been observed also in this work for **terpolymers of propylene-*co*-1-pentene-*co*-1-hexene and propylene-*co*-1-pentene-*co*-1-heptene** with high comonomer contents, independently of the thermal history applied. Moreover, crystallization rate of this trigonal form is closely related to ratio between comonomers. Therefore, development of the new polymorph slows down as 1-hexene is increased in the corresponding terpolymers of propylene-*co*-1-pentene-*co*-1-hexene.

6.- Incorporation of 1-heptene, as comonomer, has turned out of special interest. **Propylene-*co*-1-heptene copolymers** have been synthesized in a broad range of compositions, and prepared under different crystallization conditions. They **are not able** to generate the new **trigonal crystalline lattice** under any circumstance. On the contrary, **propylene-*co*-1-pentene-*co*-1-heptene terpolymers** exhibit a trigonal content higher than that expected if only 1-pentene would participate in their formation. This fact proves that **1-heptene is able to be incorporated** itself in the trigonal modification when 1-pentene is also present, especially for high ratios between 1-pentene/1-heptene.

7.- The mesomorphic structure is generated in all these polymeric materials,at a specific range of composition and crystallization conditions. In particular, **mesophase** formation in propylene-*co*-1-heptene copolymers **requires lower cooling rates as comonomer content rises**. Moreover, this mesomorphic modification is in **direct competition** with the **monoclinic** form, except at high counit contents where monoclinic crystallites are very restricted.

8.- The study on the different crystalline structures developed as well as the crystalline degree variations as function of the **length of the comonomer** employed, has pointed out that the longer counits require **greater times for an ordered** chain **arrangement**. Thus, the use of comonomer as long as **1-heptene** leads to **slower crystallization rates**, at high comonomer contents, favoring cold crystallizations as well as lower melting points.

9.- Different **properties** of interest have been examined to evaluate the applicability of these materials. These **properties**, besides **varying** rather significantly with **composition**, also depend very much on the **crystalline structure** generated, i.e., on the interesting and varied polymorphism presented by these materials.

10.- R**igidity** in **propylene-*co*-1-heptene copolymers** is closely related to the **comonomer content**. On the other hand, their **mechanical behavior** is also significantly affected by the thermal history applied and, consequently, by the **different crystalline structures** that can be generated. Presence of the **monoclinic** cell leads to **stiffer** polymeric materials, in contrast to the higher **deformability** exhibited by those specimens containing **mesomorphic** entities.

11.- Gas transport properties have been also evaluated in these copolymers. Their evaluation shows a clear dependence between **permeability** and **comonomer content**, with analogous variations for N_2, O_2 and CO_2. In addition, the materials with higher **mesomorphic** content show greater **permeability** values owing to the **higher mobility** of these entities.

12.- Analysis of optical properties has shown that **transmittance** values exhibited in the visible range for propylene-*co*-1-heptene copolymers are **high**, above 80 % for some of the synthesized compositions. This **transparency** is a function of both **crystallinity** and **ratio between the different crystalline structures** (in the case of coexistence between entities), so that it has been observed that **monoclinic** crystals lead to values of transmittance in the visible range **lower** than those obtained when the **mesomorphic** entities are present.

13.- Different **mechanical parameters** have been evaluated in **propylene-*co*-1-pentene-*co*-1-heptene terpolymers**. It has been also deduced that knowledge of **crystalline structure is essential** to understand the mechanical behavior.

14.- **Thermal stability** of **propylene-*co*-1-pentene and propylene-*co*-1-hexene copolymers** has been examined in detail. The kinetic analysis of degradation **in absence of oxygen** has revealed the existence of **two kinetic stages**: an initial one characterized by a low apparent activation energy that increases with the comonomer content, and a second step that presents higher and constant values of apparent activation energies, independently of the copolymer composition. It is worthy of mentioning that variation of apparent activation energies associated with the first stage cannot be justified based on the oxygen content in the different materials, and, thus, it could be deduced that this dependence is related to changes of **flexibility** undergone by the chains as consequence of the progress in the pyrolysis process .

15.- As **general conclusion**, properties of the different materials have turned out very sensitive both to the **global crystallinity** and to the **nature of the existing phases**. This fact allows obtaining polymeric materials in a **broad range of properties**, which can be greatly **tailored** and modulated depending on their final requirements.

ANEXOS

ANEXO I. Listado de Publicaciones

1. **Isotactic poly(propylene-*co*-1-pentene-*co*-1-hexene) terpolymers: Synthesis, molecular characterization, and evidence of the trigonal polymorph.** Alberto García-Peñas, José M. Gómez-Elvira, Ernesto Pérez, María L. Cerrada. *J. Polym. Sci. Polym Chem.* **51**, 3251–3259 (2013)
2. **Microstructure of metallocene isotactic propylene-co-1-pentene-co-1-hexene terpolymers.** Alberto García-Peñas, José M. Gómez-Elvira, Ernesto Pérez, María L. Cerrada. *J. Polym. Sci. Polym Chem.* **52**, 2537-2547 (2014)
3. **Synthesis, molecular characterization, evaluation of polymorphic behavior and indentation response in isotactic poly(propylene-co-1-heptene) copolymers.** Alberto García-Peñas, José M. Gómez-Elvira, Ernesto Pérez, Vicente Lorenzo, María L. Cerrada. *Eur. Polym. J.* **64**, 52–61 (2015)
4. **Microstructure and Thermal Stability in Metallocene iPP-materials: 1-Pentene and 1-Hexene Copolymers.** Alberto García-Peñas, Ernesto Pérez, María L. Cerrada, José M. Gómez-Elvira. (Enviado)
5. **Mesophase features in isotactic poly(propylene-co-1-heptene) copolymers.** Alberto García-Peñas, José M. Gómez-Elvira, María U. de la Orden, María L. Cerrada. (Enviado)
6. **Poly(propylene-co-1-heptene) copolymers: Dependence of their mechanical and transport properties on monoclinic and/or mesomorphic polymorphs.** Alberto García-Peñas, José M. Gómez-Elvira, Vicente Lorenzo, Ernesto Pérez, María L. Cerrada. (Enviado)
7. **Trigonal δ form as a tool for tuning mechanical behavior in poly(propylene-co-1-pentene-co-1-heptene) terpolymers.** Alberto García-Peñas, José M. Gómez-Elvira, Rosa Barranco-García, Ernesto Pérez, María L. Cerrada. (Enviado)

ANEXO II. Congresos y Seminarios

1. **A. García-Peñas**, M.L. Cerrada, J.M. Gómez-Elvira, E. Pérez. Polimorfismo en terpolímeros de propileno con 1-hexeno y 1-penteno. Congreso de Jóvenes Investigadores en Polímeros JIP 2012. Islantilla. Abril 2012. (Oral)
2. **A. García-Peñas**, M.L. Cerrada, J.M. Gómez-Elvira, E. Pérez. Presentación del proyecto de tesis: Estructuras mesomórficas en arquitecturas de polipropileno: síntesis, competencia con otros polimorfos y propiedades. XXXIII Reunión de Electroquímica de la Real Sociedad Española de Química. Miraflores. Junio 2012. (Oral)
3. **Alberto García-Peñas**, José M Gómez-Elvira, Ernesto Pérez, María L. Cerrada. Terpolímeros poli(propileno-co-1-penteno-co-1-hexeno): elucidación de sus estructuras polimorfas. XXXIV Reunión Bienal de la Real Sociedad Española de Física, 23º Encuentro Ibérico para la enseñanza de la Física, Valencia, España. 15-19 de julio de 2013. (Oral)
4. **Alberto García-Peñas**, José M Gómez-Elvira, Ernesto Pérez, María L. Cerrada. Polymorphic Behavior in isotactic Poly(propylene-co-1-pentene-co-1-hexene) Terpolymers. The 44th IUPAC World Chemistry Congress, IUPAC2013, Istanbul, Turkey. 11-16 August 2013. (Oral)
5. E. Pérez, M. L. Cerrada, **A. García-Peñas**, J. Arranz-Andrés, J. M. Gómez-Elvira, A. Bello, R. Benavente, J. M. Pereña and A. Svensson. SYNCHROTRON STUDIES OF MESOPHASES IN POLYMERIC SYSTEMS, Barcelona, Spain. 3-6 September 2013. (Oral)
6. **García-Peñas A.**, Gómez-Elvira J.M., Pérez E., Cerrada M.L. Microstructure and Thermal Stability in Metallocene iPP-materials: Terpolymers with Alpha-olefins. 1st International Conference in Polymers with special Focus in Early Stage Researchers, POLYMAR2013. Barcelona, España. 3-7 November 2013 (Oral)
7. **García-Peñas A.**, Gómez-Elvira J.M., Pérez E., Cerrada M.L. Isotactic Poly(propylene-co-1-pentene-co-1-hexene) Terpolymers and their Crystalline Polymorphs. 1st

International Conference in Polymers with special Focus in Early Stage Researchers, POLYMAR2013. Barcelona, España. 3-7 November 2013 (Oral)

8. **A. García-Peñas**, J.M. Gómez-Elvira, V. Lorenzo, E. Pérez, M.L. Cerrada. Polimorfismo en copolímeros isotácticos de propileno con 1-hepteno. GEP 2014, Girona 7 al 10 Sep. 2014 (Oral)
9. V. Lorenzo, **A. García-Peñas**, J.M. Gómez-Elvira, E. Pérez, M.L. Cerrada. Respuesta a la indentación de copolímeros isotácticos de propileno-co-1-hepteno. GEP 2014, Girona 7 al 10 Sep. 2014. (Oral)
10. Charla divulgativa. Gruppenseminar AK Wilhelm. 19.09.2014. Heidelberg (Alemania). "Mesomorphic structures in polypropylene architectures" (40 min.). Invitación: Prof. Dr. Manfred Wilhelm.
11. **A. García-Peñas**, J.M. Gómez-Elvira, E. Pérez, M.L. Cerrada. DSC study of polymorphism in isotactica poly(propylene-*co*-1-heptene) copolymers. MEDICTA 2015. Mediterranean Conference on Thermal Analysis and Calorimetry. Gerona. 17-19 June 2015. (Poster)
12. **A. García-Peñas**, J.M. Gómez-Elvira, E. Pérez, M.L. Cerrada. Trigonal lattice in isotactic poly(propylene-*co*-1-pentene-*co*-1-Hexene) terpolymers: elucidation and Competition with other polymorphs. MEDICTA 2015. Mediterranean Conference on Thermal Analysis and Calorimetry. Gerona. 17-19 June 2015. (Oral)
13. **A. García-Peñas**, J.M. Gómez-Elvira, E. Pérez, M.L. Cerrada. The trigonal cell crystallization in isotactic poly(propylene-*co*-1-pentene-*co*-1-hexene) terpolymers and their competition with other polymorphs. Synchlight2015. Campinas (Brasil) 14th July 2015. (Poster)